OPTIMAL PROCESS DESIGN FOR COUPLED CO_2 SEQUESTRATION AND ENHANCED GAS RECOVERY IN CARBONATE RESERVOIRS

A Dissertation

by

UCHENNA ODI ODI

Submitted to the Office of Graduate and Professional Studies of
Texas A&M University
in partial fulfillment of the requirements for the degree of

DOCTOR OF PHILOSOPHY

Chair of Committee,	Anuj Gupta
Committee Members,	Robert H. Lane
	Maria A. Barrufet
	Christine Ehlig-Economides
	Hadi Nasrabadi
Head of Department,	Dan Hill

December 2013

Major Subject: Petroleum Engineering

ABSTRACT

Increasing energy demand combined with public concern for the environment obligates the oil industry to supply oil and natural gas to the public while minimizing the carbon footprint due to its activities. Today, fossil fuels are essential in meeting the global energy needs, but have the undesirable outcome of producing carbon dioxide. Carbon dioxide (CO_2) injection in reservoirs is an appealing Enhanced Oil/Gas Recovery method for increasing hydrocarbon production by using the miscible interactions between hydrocarbon and carbon dioxide. Carbon dioxide flooding is beneficial to the environment and to petroleum producers, since it can store carbon dioxide while increasing oil and natural gas production. A practical challenge in combining CO_2 Sequestration with Enhanced Gas Recovery (EGR) is determining the optimal process parameters that maximize the project value.

This research describes the development of a procedure to determine the best process conditions for the CO_2 EGR and Sequestration process. Analysis includes experimental work that illustrates that CO_2 is able to reduce the dew point pressure of wet gas fluids and that reservoir fluid phase changes can be indicated by changes in total fluid compressiblity. In addition, compositional simulation illustrates that CO_2 improves condensate and natural gas recovery. Studies show that the ideal reservoir management strategy for CO_2 EGR is to set the CO_2 injectors' bottom hole pressure to the initial reservoir pressure. An economic model is developed that illustrates the capital investment necessary for the CO_2 EGR and Sequestration process for different capture

technologies and levels of captured CO_2 impurity. This economic model is utilized in conjunction with an optimization algorithm to illustrate the potential profitability of the CO_2 EGR and Sequestration project. To illustrate the economic risk associated with CO_2 EGR and Sequestration project, probabilistic analysis is used to illustrate scenarios where the technology is successful.

This work is applicable to carbonate wet gas reservoirs that have significant gas production problems associated with condensate blockage. This work is also useful in modeling the economics associated with CO_2 EGR and CO_2 Sequestration. The strategy developed in this work is applicable to designing process conditions that correspond to optimal CO_2 EGR and optimal CO_2 Sequestration.

DEDICATION

I dedicate this to my family and to God in Jesus Christ.

ACKNOWLEDGEMENTS

There have been many people who have influenced me during my six years at Texas A&M. I would first like to thank Dr. Lane for supporting and encouraging me. I would also like to thank Dr. Gupta for inviting me to do my PhD under him. I would like to also thank everyone that believed in me during this entire process.

TABLE OF CONTENTS

Page

Page

LIST OF FIGURES

Page

Page

Page

Page

Page

Page

LIST OF TABLES

Page

Page

1 INTRODUCTION

The International Energy Agency (IEA) has estimated the potential global storage capacity of depleted oil/gas fields to be 900 Gigatonnes (IEA Energy Technology Essentials, 2006). In addition to this, many countries such as the United States (Carbon Dioxide Information Analysis, 2012b) and Qatar (Carbon Dioxide Information Analysis, 2012a) produce CO_2 emissions (illustrated by Figure 1) as a byproduct of industries in their respective countries.

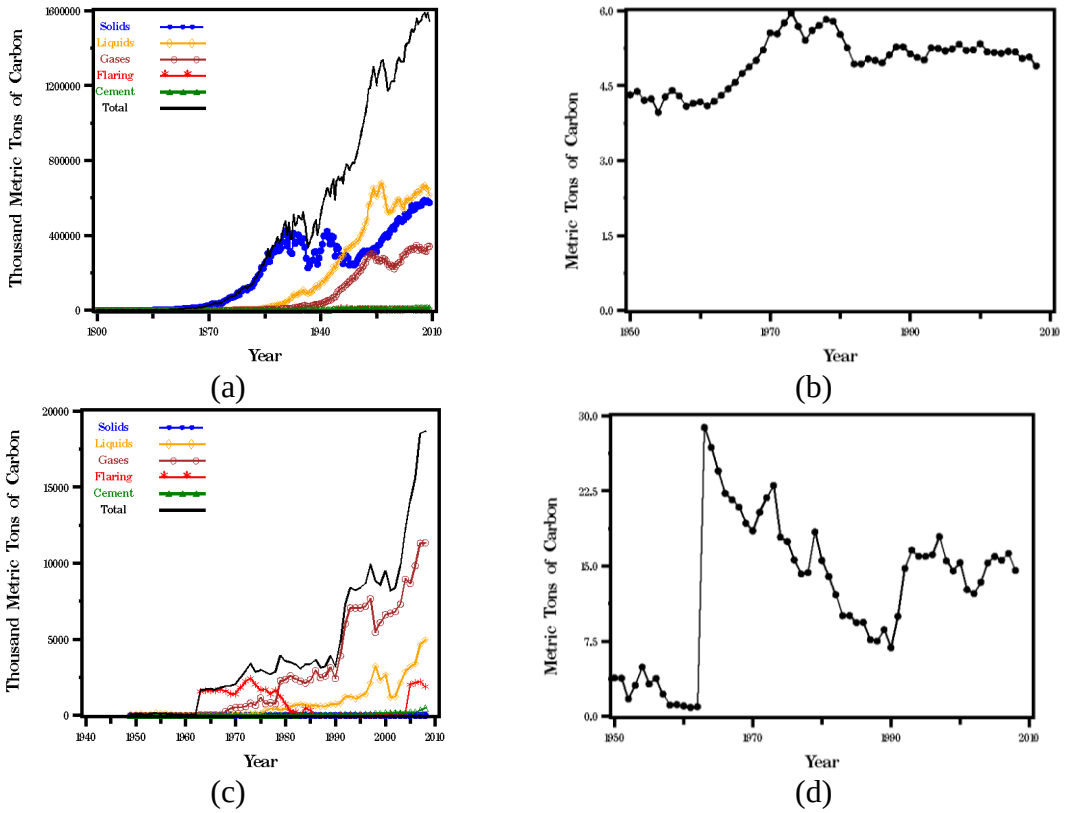

Figure 1: Categorized and Per Capita CO_2 emissions (a) United States Categorized (b) United States Per Capita (c) Qatar Categorized (d) Qatar Per Capita

A proposed solution for improving hydrocarbon recovery while reducing CO_2 emissions is a process termed "CO_2 EGR and Sequestration". This process is beneficial because it provides capacity to store CO_2 while enhancing gas recovery. Combining CO_2 Sequestration and EGR creates a complex process as some of the CO_2 injected into the reservoir for Sequestration is produced during EGR. Figure 2 illustrates the injection of CO_2 and the subsequent production of gas, evaporated condensate and CO_2.

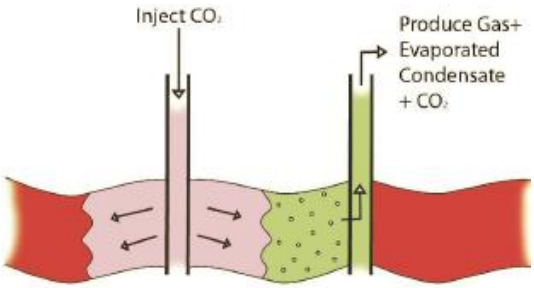

Figure 2: CO_2 Sequestration and EGR (Gupta, 2010)

This research investigates integration of CO_2 Sequestration and EGR processes by implementing a strategy that ensures optimal CO_2 storage and gas recovery. The challenge to this strategy is making CO_2 EGR and Sequestration profitable. This notion is addressed in this work and the overall CO_2 EGR and Sequestration process that can make hydrocarbon recovery profitable while storing CO_2 is illustrated in Figure 3. The challenge of CO_2 EGR and Sequestration is determining the ideal process conditions.

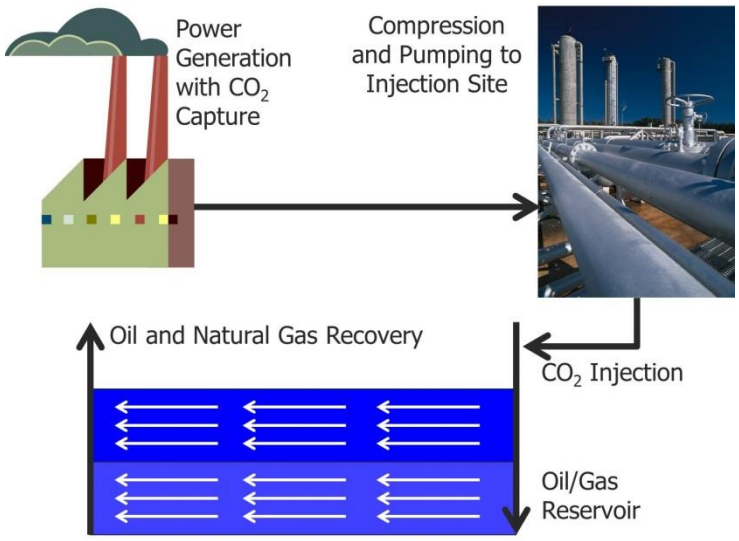

Figure 3: Overall CO_2 EGR and Sequestration Process Description

The overall objective of this work is to develop a strategy for determining the optimal process conditions for CO_2 Sequestration coupled with EGR. Optimal conditions are defined as maximizing hydrocarbon recovery and CO_2 storage for a gas reservoir in order to maximize the economic value of the project. Many gas fields experience condensate blockage in the near wellbore region due to production below the dew point pressure. Condensate blockage limits the flow of gas in gas reservoirs and thus hampers the economic value of the project. Injecting CO_2 into the condensate bank can remove the condensate blockage and thus improve the gas production but it requires adequate understanding of condensate blockage and its interaction with CO_2.

Accomplishing this requires a fundamental understanding of the pressure, volume, and temperature (PVT) interactions between gas condensate and CO_2. Discerning these PVT interactions and accurate modeling of their mechanisms is necessary in order to establish the optimum conditions for the transfer of condensate to

the vapor phase. Maximizing this transfer helps achieve optimal EGR. In addition to the PVT interactions inherent in CO_2 mixing with condensate, the geochemical interactions between CO_2 and carbonate matrix will be considered using a compositional simulator. The PVT interactions of condensate with CO_2 have been studied experimentally and theoretically using an equation of state. A simulation model that models necessary mechanisms is used along with an optimization algorithm that maximizes an objective function corresponding to the economic value of the CO_2 Sequestration and CO_2 EGR process.

2 LITERATURE REVIEW

In order to understand the state-of-the-art related to combined CO_2 Sequestration and EGR, a literature review of topics including CO_2 core flooding, CO_2 injection in aquifers, experimental design optimization, and hydrocarbon interaction with CO_2 is conducted. Theory of hydrocarbon interaction with CO_2 provides critical analysis of the PVT relationships between CO_2 and condensate blockage. Diagnosis and removal of near wellbore condensate blockage is critical in ensuring reservoir flow conditions for optimal CO_2 Sequestration and EGR. Each of these topics represents an approach that needs to be considered in designing the optimum process for CO_2 Sequestration and EGR.

Mamora *et al.* (2002) studied the possibility of enhanced gas recovery from depleted gas reservoirs. They modeled and performed core flood studies of CO_2 displacing methane in a carbonate porous medium. In their analysis, they were able to calculate the dispersion coefficients of the floods using a convection-dispersion model and a history match of experimental data. The authors determined the range of the coefficient of dispersion to be 0.01 to 0.12 cm^2/min, which is relatively small. They concluded that the displacements were an efficient process which resulted in recovery of 73%-87% of the original gas in place (OGIP). They predicted that this could translate into production of unrecoverable gas reserves by improving the sweep efficiency and repressurization of depleted gas fields. A limitation of their approach is that they did not consider geochemical reactions, which are expected to affect the flow of CO_2 in

carbonate reservoir. These reactions can consume some of the available CO_2 and therefore need to be included in the overall analysis of CO_2 transport in reservoir rocks. Nevertheless, the authors demonstrated a suitable experimental method for determining the coefficient of dispersion. Their analysis method would be beneficial for studying the physical response for coupled CO_2 Sequestration and EGR.

Shamshiri and Jafarpour (2010) reported on optimal CO_2 injection conditions that maximize sweep efficiency in aquifer systems for CO_2 Sequestration. These authors introduce a new method to optimize flooding sweep efficiency in geologic formations with heterogeneous properties (for water floods). The authors applied a modified version of this method to maximize the storage capacity of aquifers for CO_2 Sequestration. The main idea centered on delaying CO_2 breakthrough times. They did this by using pseudo production wells to optimize the sweep efficiency. The purpose of the pseudo wells was to estimate the arrival time of CO_2 and its fractional production rate such that the injection schedule could be altered to enhance the contact time between fresh brine and injected CO_2 plume. This in turn enhanced the residual and solubility trapping. Shamshiri and Jafarpour's approach did not consider detailed geochemical interactions of the reservoir but instead relied solely on adjusting the CO_2 injection rate until the system's goal was maximized. Shamshiri and Jafarpour's approach does have the potential to be applied reliably in systems involving complex interactions with different phases. For example, in a condensate, water, gas, and carbonate mineral system; the interactions between CO_2 and each phase must be accounted for. Factors such as miscibility between the CO_2 and the condensate phase

can be fully addressed in Shamshiri and Jafarpour's optimization approach because miscibility is controlled by pressure, temperature, and the concentrations of CO_2 and condensate. All of these factors could be considered for cases involving complex interactions. Nevertheless, Shamshiri and Jafarpour's approach is suitable for aquifers with negligible geochemical interactions; lessons can be learned from the application of pseudo wells and the mathematical treatment of the optimization solution.

Ghomian *et al.* (2010) proposed optimization of enhanced oil recovery and CO_2 Sequestration processes using an experimental design approach that took into considerations several factors. They noted that for coupled CO_2 enhanced oil recovery and CO_2 Sequestration, there are competing interests. These interests are maximizing oil recovery and maximizing the amount of CO_2 stored in the reservoir. Both depended on a large number of parameters and strategies. These researchers postulated that a very large number of simulations are required to understand the different strategies for each reservoir. Design parameters selected for their study are: well spacing, different injection and productions schemes, various well control techniques, and different mobility control methods. The authors used fractional factorial design and D-optimal methods to study the effect of these parameters. To reduce effort needed for optimization, very often fractional factorial design is used carefully selecting subsets of the experimental runs of a full factorial design. Full factorial experiments are designs consisting of two or more factors, each with discrete possible values or "levels", and whose experimental units take on all possible combinations of theses levels across all such factors. D-optimality seeks to maximize the determinant of the information matrix

of the design. The authors used fractional factorial design (for sandstones) and D-optimal method (for carbonates) to simultaneously optimize revenue and amount of CO_2 stored. Some of the parameters that were considered are: produced gas oil ratio, well spacing, production and injection well types, and injection scheme which included water alternating gas (WAG) or continuous CO_2. In doing this, the authors considered compression costs and injection constraints. Table 1 and 2 represent the flood design variables used for their experiments.

Table 1: Optimization Scenarios for Flood Design Variables in Carbonate Reservoirs (Ghomian *et. al*, 2010).

Objectives	Optimizing Profit ($/bbl) & CO_2 Storage	Maximizing only CO_2 Storage
A: Produced GOR, SCF/STB	31000	40000
B: Production well type	Vertical	Vertical
C: Injection well type	Vertical	Vertical
D: Production well constraint	BHP	BHP
E: Injection well constraint	BHP	BHP
F: Injection scheme	WAG	Continuous CO_2
G: Average field permeability (md)	50	5
H: Kv/Kh	.1	1
J: Well spacing, acre	45	65
CO_2 Saturation, fraction	0.29	0.44
Profit, $/bbl	23	21

Table 2: Optimization Scenarios for Flood Design Variables in Sandstone Reservoirs (Ghomian *et. al*, 2010).

Objectives	Optimizing Profit ($/bbl) & CO_2 Storage	Maximizing only CO_2 Storage
A: Production well type	Vertical	Vertical
B: Injection well type	Horizontal	Horizontal
C: Production well constraint	Rate	Rate
D: Injection well constraint	BHP	BHP
E: Recycling	Yes (re-inject)	Yes (re-inject)
F: Produced GOR, SCF/STB	50000	50000
G: Shut-In/Open strategy	Yes	Yes
H: Injection scheme	WAG	Continuous CO_2
J: Well spacing, acre	50	90
CO_2 Saturation, fraction	0.22	0.34
Profit, $/bbl	17.7	3.8

The authors' analysis concluded that carbonate reservoirs typical of the Permian Basin are better candidates for coupled CO_2 Enhanced Oil Recovery and Sequestration projects. Gulf Coast sandstone reservoirs did not perform as well as the Permian Basin carbonate reservoirs. The main critique of the authors' work is that they did not explain why their analysis yielded better results for carbonate reservoirs. Analysis must be included that concentrates on the phase interactions caused by the presence of CO_2. One possible reason that the carbonate reservoirs yielded better results is because of the solubility and mineral trapping caused by the geochemical reactions. From a reservoir

management perspective, Ghomian *et al.* approach is suitable for cases involving a large number of parameters but can potentially be improved in accuracy by including the rock-fluid interactions and phase interactions for coupled CO_2 Enhanced Oil Recovery and Sequestration.

From literature it can be seen that researchers have approached the issue of CO_2 Sequestration and EGR from different viewpoints. In order to optimize the storage of CO_2 while optimizing the recovery of condensate and natural gas, it is important to understand the hydrocarbon interaction with CO_2. As stated before, wet gas reservoirs have a tendency to experience condensate blockage due to production below the dew point pressure. Condensate blockage occurs when there is a dramatic increase in oil saturation in the near wellbore region which causes a decrease in gas relative permeability and thus leads to decreased gas productivity which can severely hamper optimal EGR. It has been reported in literature that condensate blockage in the near wellbore region can create a radius of damage that acts like a skin (Muskat, 1981 and Fetkovich, 1973). CO_2 can be used to remove this condensate blockage skin. The removal of condensate blockage skin is made possible by CO_2's ability to reduce the saturation pressure of oil/gas systems. One example of this phenomenon was reported by Monger *et al.* (1981) in their Appalachian crude oil system that the crude oil aromaticity correlated with improved hydrocarbon extraction into a CO_2 rich phase. In addition to these observations, Monger *et al.* noted that CO_2 has the ability to lower miscibility pressure for paraffin fluids that do not contain suitable amounts of aromatic content. This holds great promise because wet gas/condensate reservoirs usually contain

lighter end hydrocarbons that can be extracted by using CO_2. The approach outlined in this work illustrates that CO_2 has the capacity to lower the saturation pressure of gas and condensate systems so as to force the near wellbore region liquids into the gas phase. The following chapter describes the constant composition expansion (CCE) experiments conducted in this study with a sample gas system with increasing amounts of CO_2. Results demonstrate CO_2's ability to reduce the dew point pressure of the sample reservoir gas.

As a general strategy, once the evidence of CO_2 reducing the dew point of the wet gas condensate system is established, a genetic algorithm variant is utilized to determine the optimal injection configuration that maximizes the NPV of the CO_2 EGR and CO_2 Sequestration process. Genetic algorithm is a stochastic optimization method that is able to search for the global minimum or maximum of an objective function.

3 LAB STUDIES OF DEW POINTS AS A FUNCTION OF CO_2

Condensation is a critical factor in determining the performance of wet gas reservoirs. Condensation in the near wellbore region can lead to a dramatic reduction in gas flow rate due to a reduction in effective permeability to gas. Gas relative permeability reduction in the near wellbore region is caused by an increase in liquid saturation due to condensation. This can be observed by studying a typical gas relative permeability relationship as illustrated in Figure 4. In a gas condensate system, a small reduction of gas phase saturation can correspond to an exponential decrease in gas relative permeability. Figure 4 illustrates that as the liquid saturation increases, and the gas phase decreases from the maximum saturation value, there is a dramatic decrease in its relative permeability.

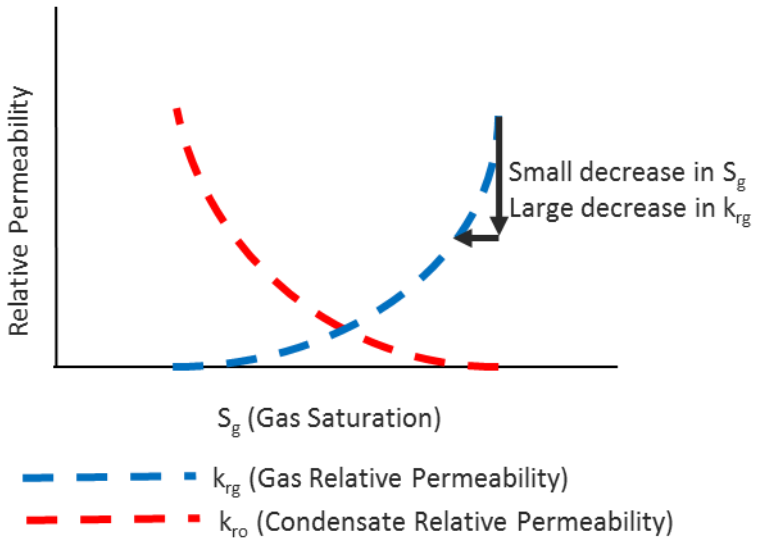

Figure 4: Relative Permeability Relationship between Gas and Condensate Phase

In wet gas reservoirs, increase in liquid saturation, which is the primary reason for reduction of gas relative permeability, is caused when the bottom hole pressure drops below the dew point pressure. Gas reservoir operators often allow this in absence of accurate values for dew point pressure or in order to maintain economic gas production rates from the wells. In order to accurately identify minimum pressure levels that must be maintained in a gas reservoir, dew point pressure measurements can be conducted using a representative sample of the reservoir fluid in a PVT apparatus. For a wet gas reservoir, PVT experiments and analysis are needed to measure the dew point pressure at the known reservoir temperature. The simplest conventional method of determining the dew point pressure of a hydrocarbon gas mixture is a visual test that requires collection of a representative wet gas sample at reservoir conditions and testing it in a PVT cell chamber with a glass window. During the dew-point experiment, the sample is first equilibrated at the initial reservoir conditions of pressure and temperature and then, starting from a high pressure gas phase, it is gradually depressurized in the PVT cell to observe physical changes through the glass window into the cell. The first instant of condensation, seen as slight clouding of the window, is referred to as the dew point pressure for the sample. The limitation of this method is that the observation of condensation is subjective and can contribute to erroneous estimation of dew point pressure leading to inaccurate wet gas characterization.

Another method of dew point measurement involves using the acoustic signature of the sample fluid. The acoustic method relies on acoustic theory which states that the acoustic response is proportional to the velocity of signal through the fluid (Sivaraman *et*

al., 1997). To determine the dew point using the acoustic method requires using an apparatus that is capable of transmitting an acoustic signal through a reservoir fluid and receiving and analyzing the signal that transmits through the reservoir fluid. The travel time and alteration in signal during transit through the reservoir fluid is used to characterize the physical phase of the reservoir fluid. Determination of the dew point pressure using this method requires performing a constant composition expansion test similar to the visual method. The first instance of a liquid signature in the vibrational response during this test is defined as the dew point pressure. The limitation of this method is that it still requires the visual method to validate the estimated dew point. Thus, any PVT apparatus that is designed to implement the acoustic method must have a window cell to ensure accuracy, in addition to the equipment that can transmit and receive the acoustic signal. The capital investment needed for the acoustic method can be significantly higher than for the standard PVT cell used for the visual method.

Potsch *et al*. (1996) presented a method to determine the dew point pressure graphically. Their method involved using the real gas equation of state to calculate the total moles in the reservoir fluid sample for several measurements of pressure above the dew point pressure. They proposed that below the dew point pressure, condensation will cause the calculated moles in the gas phase to be different from the actual number of moles. They proposed that the first instance from the deviation from the true amount of moles indicates dew point pressure. Their work may be in error because the real gas equation of state is not valid for fluids near the saturation pressure as indicated by their plots of the calculated molar quantity changing with pressure above dew point pressure.

For a valid method, the calculated amount of moles would have remained constant because of the conservation of mass in the PVT cell (no mass exits or leaves the PVT cell). Potsch *et al.*'s attempt to characterize the dew point pressure appears to be theoretically inaccurate.

The method proposed in this work is based on tracking changes in compressibility to pinpoint dew point pressure measurements in wet gas fluid samples. Using this method, this work demonstrates the potential of using CO_2 to lower the dew point pressure as a solution to condensate blockage. Comparisons with Peng Robinson equation of state are used to validate the approach illustrated in this work.

3.1 Saturation Pressure Theory

Dew point pressure can be described as the pressure at which a gas starts condensing into a liquid phase. Pressure and temperature phase diagrams are generally used to describe bubble points and dew points as functions of pressure and temperature. For example, Figure 5 illustrates a pressure and temperature phase diagram for a wet gas. The dew-point line, the curve that is to the right of the critical point can be used to describe the variation of dew point pressure with temperatures.

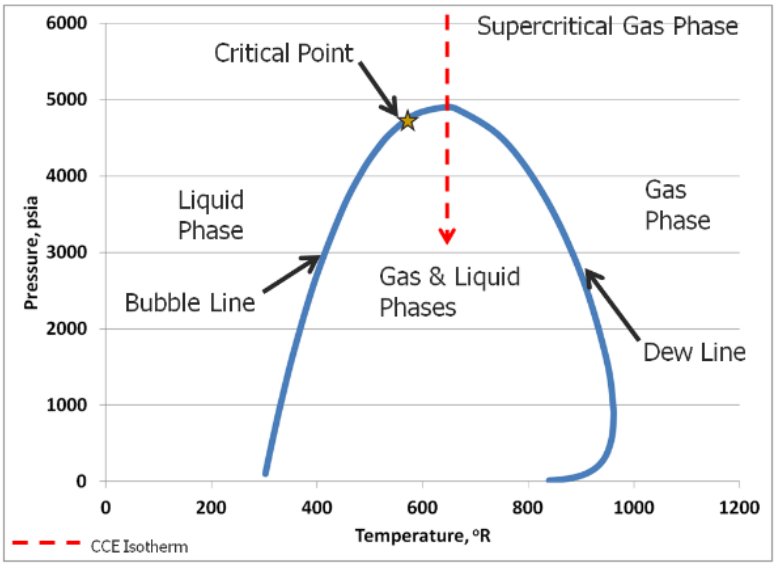

Figure 5: Pressure and Temperature Diagram for Wet Gas/Condensate with CCE Isotherm

When analyzing the results of constant composition expansion (CCE) experiment, a general test used to estimate bubble and dew points using the visual method, it is important to understand the thermodynamic changes that occur to the reservoir fluid during phase change. Determination of bubble points using the graphical method based on CCE tests is made possible by the large differences between the compressibility of liquid phase and the less dense gas phase.

Determination of phase changes involved in the transition from the gas phase to the liquid phase is much more difficult due to indistinguishable slope changes. Such is the case when looking at dew points of gas condensates. This can be illustrated by considering an isotherm in the pressure and temperature phase diagram of an example wet gas/condensate as illustrated by Figure 5. Starting from the super critical gas region, as the pressure drops isothermally, there is an expansion of the system volume as the wet

gas/condensate transitions from the supercritical region to the gas region and finally past the dew line. When the wet gas undergoes decompression there is a gradual change in the total compressibility of the reservoir fluid. This gradual change is not as distinct as the change observed in black oils. The reason behind this difference in phenomenon can be determined by observing the mathematical definition of isothermal compressibility. This can be understood by considering the total isothermal compressibility of a reservoir fluid inside the PVT cell described by the following equation.

$$c_T = -\frac{1}{V_t}\left(\frac{\partial V_t}{\partial p}\right) \quad \textbf{(1)}$$

Where c_T is the total isothermal compressibility, V_t is the total volume of the fluid mixture in the PVT cell, and p is the pressure of the fluid. For black oils above the bubble line, the total isothermal compressibility represents the compressibility of the liquid phase. This contrasts with wet gases, in that above the dew line the total isothermal compressibility represents the compressibility of the supercritical phase. Below the bubble line and dew line, the total compressibility can be derived using material balance between the gas and liquid phases that exists in all stages of the CCE. This material balance based compressibility can be derived by first defining the total volume at all stages of the CCE. This is seen in the following expression.

$$V_t = V_G + V_L \quad \textbf{(2)}$$

V_G and V_L represent the gas and liquid volumes respectively. The total mass, m_t, is the sum of the mass of each phase which is expressed in the following expression.

$$m_t = m_G + m_L \quad \textbf{(3)}$$

The parameters m_G and m_L represent the gas and liquid masses respectively. During the CCE, the total mass is constant. Therefore, when differentiating the total mass with respect to pressure results in the following expression.

$$0 = \frac{\partial m_G}{\partial p} + \frac{\partial m_L}{\partial p} \quad \textbf{(4)}$$

The volumes of each phase can be put in terms of density and mass using the following expressions.

$$V_G = \frac{m_G}{\rho_G} \quad \textbf{(5)}$$

$$V_L = \frac{m_L}{\rho_L} \quad \textbf{(6)}$$

The parameters ρ_G and ρ_L represent the gas and liquid densities respectively. Combining the previous expressions with the total volume equation, results in the following relationship for the total volume.

$$V_t = \frac{m_G}{\rho_G} + \frac{m_L}{\rho_L} \quad \textbf{(7)}$$

To determine the material balance total compressibility requires differentiating the previous expression with respect to pressure. Which results in the following expression.

$$\frac{\partial V_t}{\partial p} = -\frac{m_G}{{\rho_G}^2}\frac{\partial \rho_G}{\partial p} + \frac{1}{\rho_G}\frac{\partial m_G}{\partial p} - \frac{m_L}{{\rho_L}^2}\frac{\partial \rho_L}{\partial p} + \frac{1}{\rho_L}\frac{\partial m_L}{\partial p} \quad \textbf{(8)}$$

This expression can be further simplified by incorporating the expression that contains the differentiated mass balance which is the following expression.

$$\frac{\partial m_L}{\partial p} = -\frac{\partial m_G}{\partial p} \tag{9}$$

Substitution of the preceding expression into the differentiated total volume expression results in the following relationship.

$$\frac{\partial V_t}{\partial p} = -\frac{m_G}{{\rho_G}^2}\frac{\partial \rho_G}{\partial p} + \frac{1}{\rho_G}\frac{\partial m_G}{\partial p} - \frac{m_L}{{\rho_L}^2}\frac{\partial \rho_L}{\partial p} - \frac{1}{\rho_L}\frac{\partial m_G}{\partial p} \tag{10}$$

The differentiated total volume can be further simplified by using the relationship between density, mass, and volume. The result of this simplification is seen here.

$$\frac{\partial V_t}{\partial p} = -\frac{V_G}{\rho_G}\frac{\partial \rho_G}{\partial p} + \frac{1}{\rho_G}\frac{\partial m_G}{\partial p} - \frac{V_L}{\rho_L}\frac{\partial \rho_L}{\partial p} - \frac{1}{\rho_L}\frac{\partial m_G}{\partial p} \tag{11}$$

The differentiated total volume can be further simplified by using the definition of gas compressibility, c_G, and oil compressibility, c_L, which are defined in the following expressions.

$$c_G = \frac{1}{\rho_G}\left(\frac{\partial \rho_G}{\partial p}\right) \tag{12}$$

$$c_L = \frac{1}{\rho_L}\left(\frac{\partial \rho_L}{\partial p}\right) \tag{13}$$

The differentiated total volume can now be expressed as the following relation.

$$\frac{\partial V_t}{\partial p} = -V_G c_G + \frac{1}{\rho_G}\frac{\partial m_G}{\partial p} - V_L c_L - \frac{1}{\rho_L}\frac{\partial m_G}{\partial p} \tag{14}$$

The differentiated total volume can be further simplified by using dm_g/dp as the common factor.

$$\frac{\partial V_t}{\partial p} = -V_G c_G - V_L c_L + \left(\frac{1}{\rho_G} - \frac{1}{\rho_L}\right)\frac{\partial m_G}{\partial p} \quad \textbf{(15)}$$

The differentiated total volume can now be substituted into the total compressibility expression.

$$c_T = -\frac{1}{V_t}\left[-V_G c_G - V_L c_L + \left(\frac{1}{\rho_G} - \frac{1}{\rho_L}\right)\left(\frac{\partial m_G}{\partial p}\right)\right] \quad \textbf{(16)}$$

The $1/V_t$ factor can then be distributed to each term.

$$c_T = \frac{V_G}{V_t} c_G + \frac{V_L}{V_t} c_L + \frac{1}{V_t}\left(\frac{1}{\rho_L} - \frac{1}{\rho_G}\right)\left(\frac{\partial m_G}{\partial p}\right) \quad \textbf{(17)}$$

Using the definition of oil volume fraction ($f_L = V_L/V_t$) and gas volume fraction ($f_G = V_G/V_t$) the final derived form of the total compressibility for all stages of compression is represented in the following expression for the PVT cell.

$$c_T = c_G f_G + c_L f_L + \frac{1}{V_t}\left(\frac{1}{\rho_L} - \frac{1}{\rho_G}\right)\left(\frac{\partial m_G}{\partial p}\right) \quad \textbf{(18)}$$

The mass balance total compressibility expression has important implications at saturation pressure and in the two phase region depending on the fluid. For example, consider black oil bubble points. Above the bubble point pressure, black oils have small approximately constant compressibility (McCain, 1990). At and below the bubble point the black oil exhibits large increases total compressibility. This is because, the gas released from the black oil at or below the bubble point is extremely compressible. Additionally, gas density is generally smaller than liquid density. Combining these observations with the fact that black oil CCEs have a negative dm_G/dp for changes in pressure, it is evident that at the bubble point black oils experience sharp increases in

total compressibility as illustrated in Figure 6. This increase is caused by the product of the $(1/\rho_L - 1/\rho_G)$ which is negative and the dm_G/dp term which is also negative (caused by the increased gas mass for decreasing pressures associated with typical black oils).

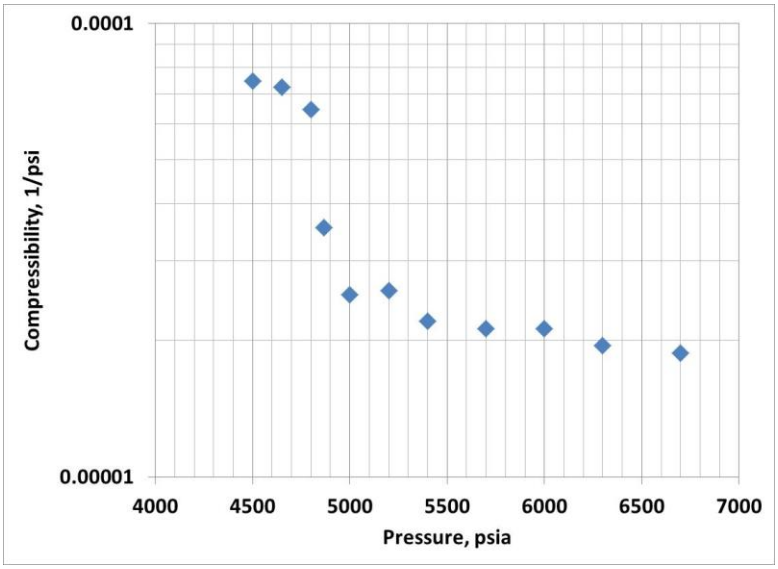

Figure 6: CCE of Example 34.9 API Black Oil at 260 ^{o}F (Bubble Point at 4866 psia) that Illustrates Sharp Compressibility Contrast at the Bubble Point (Barrufet, 2013)

The behavior of a condensate contrasts from a black oil. At above the dew point the condensate exists as a supercritical fluid. Supercritical fluid has approximately larger compressibilities of a gas above the dew point pressure. At and below the dew point pressure the supercritical portion partitions into a wet gas with some liquid dropout. This gas below the dew point pressure has compressibility slightly larger than the supercritical fluid. In addition to this, the liquid condensate that drops out of the wet gas exhibits initial large increases of liquid saturation at the dew point, followed by

decrease in liquid saturation as the pressure decreases below the upper dew point. This observation can be seen in Figure 7 for the sample wet gas.

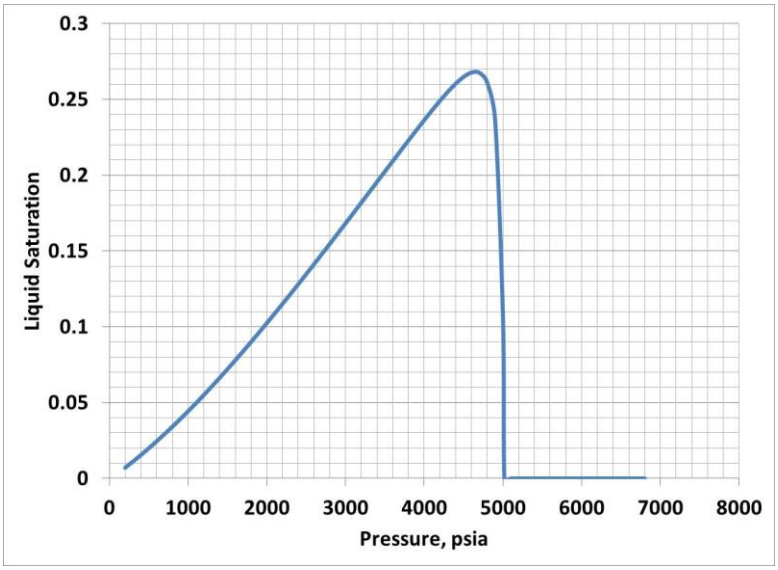

Figure 7: Liquid Saturation for Wet Gas/Condensate System During CCE (Retrograde Behavior)

The liquid saturation decreases because lighter components vaporize out of the liquid phase leaving heavier components behind to make up the majority of the liquid phase. The evidence is seen in Figure 8 which indicates an increase in liquid density as the pressure drops.

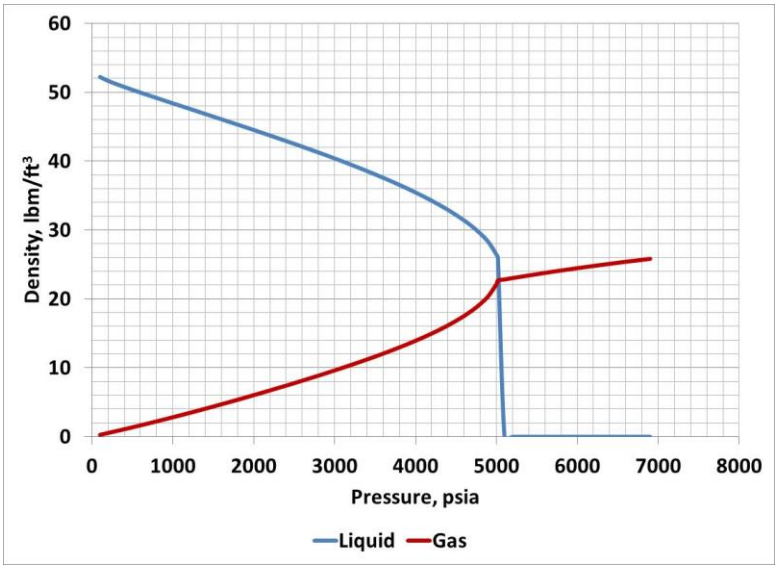

Figure 8: Density for Wet Gas/Condensate System During CCE

For gas condensates, the liquid density increases corresponding to the liquid phase becoming richer in heaver components. Figure 8 illustrates a negative $d\rho/dp$ relationship. A consequence of this is that the liquid compressibility, represented by $c_L=(1/p)*d\rho/dp$, results in a negative value. For gas condensates, these liquid compressibilities are necessary in maintaining the material balance detailed in total compressibility equation. This material balance is essential because it is one of the reasons why total compressibility does not change sharply. Combining this observation with the fact that gas condensate CCEs have a positive dm_G/dp as the pressure reduces towards the dew point, it is evident that at the dew point pressure gas condensates experience gradual increases in total compressibility (when compared to black oils). This speed of increase in total compressibility is less than for the black oil because of the product of $(1/\rho_L-1/\rho_G)$ which is negative and the dm_G/dp term which is positive (caused by the decreased gas mass for decreasing pressures at the dew point). Therefore, the

product, $(1/\rho_L - 1/\rho_G)^* dm_G/dp$ is negative at the dew point and thus is one of the factors that reduces the inflection seen in the total compressibility plot. To illustrate this, the simulated gas compressibility and total compressibility for the sample wet gas are illustrated in Figure 9.

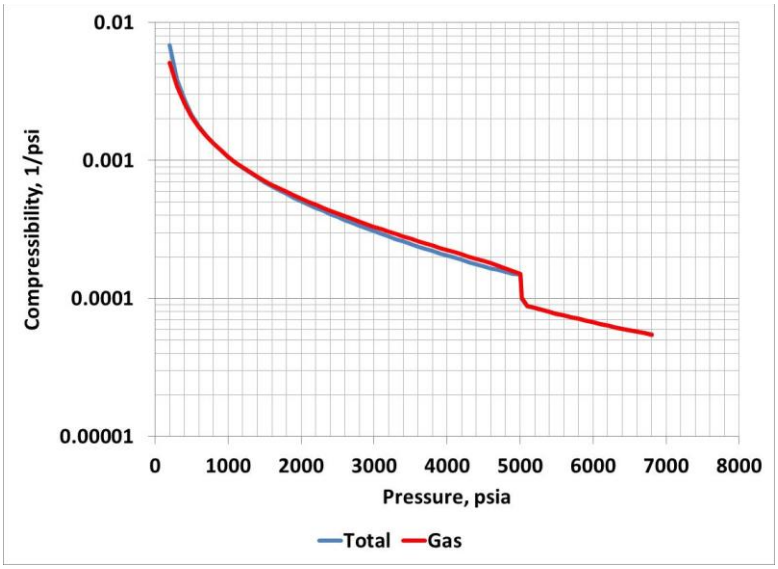

Figure 9: Comparison between Simulated Total Compressibility and Simulated Gas Compressibility of Wet Gas Sample

It can be seen that the total and gas compressibilities track one another below the dew point (5018 psia) and eventually deviate from one another at pressures less than the dew point. At the dew point the gas compressibility is slightly larger than the total compressibility. This difference occurs because of the negative product $(1/\rho_L - 1/\rho_G)^* dm_G/dp$ and the negative oil compressibility which are a result of the retrograde behavior of the gas condensate. In addition to this, the impact of the oil compressibility is tempered by the low oil volume fraction at the dew point pressure. Similarly, the impact

of the $1/\rho_L$-$1/\rho_G$)* dm_G/dp term is tempered by the total volume (i.e. the $1/V_t$ factor). A summary of the impact of each term is listed in Table 3.

Table 3: Total Compressibility Components at Saturation Pressures (Sign Change and Total Compressibility Response)

	$c_G f_G$	$c_L f_L$	$\left(\frac{1}{\rho_L}-\frac{1}{\rho_G}\right)\left(\frac{\partial m_G}{\partial p}\right)$	Total Compressibility response
Bubble Point	"positive"	"positive"	"positive"	Sharp Increase
Dew Point	"positive"	"negative"	"negative"	Gradual Increase

Determining the increase in the total compressibility with pressure is the main premise of the method used in this work. For both black oils and gas condensates the total compressibility increases at the saturation point. It can be seen that before the saturation pressure the total compressibility is linear with respect to pressure on a semi log plot. An example of this is illustrated in Figure 10 for a wet gas. When the total compressibility deviates from the linear compressibility behavior during the CCE process, it is theorized that this is the dew point pressure. The general procedure to use compressibility for determining saturation points involves completing the following tasks.

1. Use the CCE experimental data (pressure and volume data) to calculate the central difference approximation of the compressibility as indicted in Equation 1.
2. Create a plot of the calculated compressibility versus the experimental pressure of the CCE experiment.

3. Starting from the highest pressure of the compressibility versus pressure plot locate the first linear line and draw a line through it.
4. Find the nearest linear line next to the first linear line and draw a line through it.
5. The intersection between the first and second linear line is the observed saturation point (dew point for gas condensates; bubble point for black oils).

As an example of this novel analysis, consider the typical wet gas/condensate system. Its total compressibility plot can be seen in Figure 10. Using the previously described compressibility analysis, it can be seen that the dew point of this fluid at 200^{o}F is 5000 psia which matches with the Peng Robinson approximation of 5018 psia.

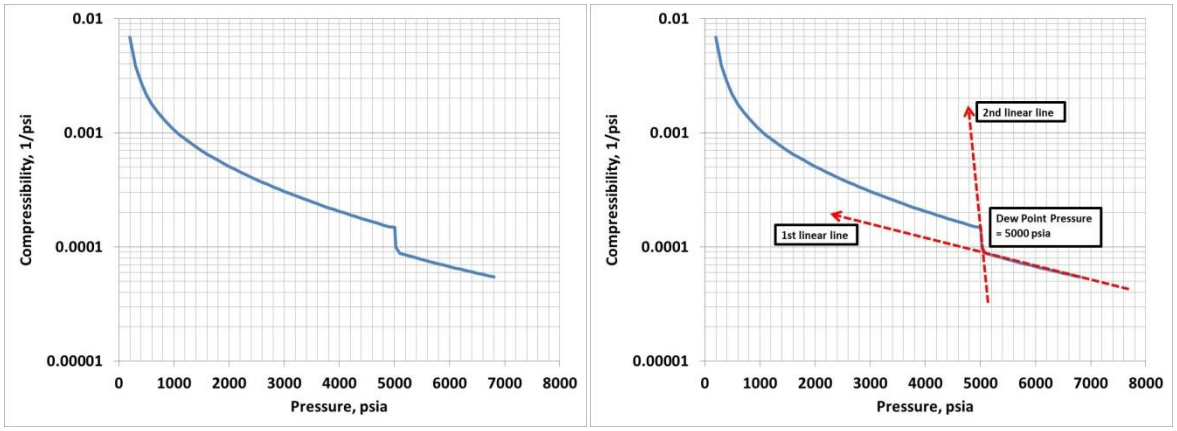

(a) (b)

Figure 10: Wet Gas/Condensate Sample Dew Point Determination (a) Compressibility Before Analysis (b) Compressibility After Analysis

This example was based on a Peng Robinson equation of state analysis for the example wet gas/condensate fluid described earlier. This same analysis is applied to experimental wet gas/condensate fluids.

3.2 Experimental Design

To test the new dew point determination method several condensate mixtures were created. These condensate mixtures include a base condensate mixture with a 1% molar composition of CO_2. The other condensate mixtures contained 10% and 15% molar concentrations of CO_2. The base condensate mixture components can be seen in Table 4. Critical properties were based on values reported in literature. Acentric factor values were obtained from Winnick (1997) and Poling *et. al* (2001). Density values were obtained from the American Petroleum Institute's Components-data (2008). The purpose of using these condensate mixtures was to understand the effect of adding CO_2 to the base concentration and to also illustrate the methodology of the new dew point determination method.

Table 4: Base Composition for Experimental Studies

Component	Composition, mol %	Molecular Weight	Critical Temperature, ^{o}R	Critical Pressure, psia	Acentric factor	Liquid Density (60 ^{o}F), lb/gal
Methane	83	16.04	343	667	.007	2.5
Carbon Dioxide	1	44.01	547.4	1069.5	.225	6.82
Ethane	4	30.07	549.6	706.6	.099	2.97
Propane	3	44.1	665.7	616.1	.153	4.227
Octane	3	114.23	1043.9	422.8	.398	5.894
Dodecane	6	170.34	1215.6	315.3	.576	6.276

To load, mix, and observe the hydrocarbon phase transitions of the proposed condensate mixtures, a pressure, volume, and temperature (PVT) system (illustrated in

Figure 11) was used. As an example of the process used to create and transfer a mixed condensate, consider the base condensate in Table 4. To calculate the necessary molar amounts of each component requires determination of the volumetric amount of each component at ambient conditions. At atmospheric pressure and room temperature the only components that are in the liquid phase are octane and dodecane. The volumetric amount of these liquid components can be found by using the following equation.

$$V_i = \frac{MW_i y_i n_t}{\rho_i} \tag{19}$$

Where V_i is the i^{th} liquid component's feed liquid volume, ρ_i is the i^{th} liquid component's density at standard conditions, MW_i is the i^{th} liquid component's molecular weight, and y_i is the i^{th} component's mole fraction in the gas condensate mixture.

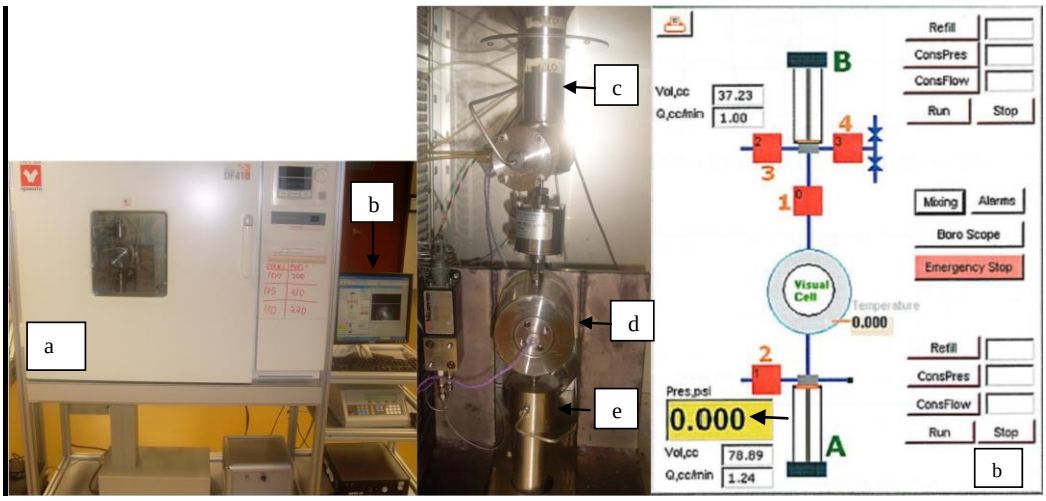

Figure 11: PVT System for Dew Point Measurement (a) Oven (b) Computer Data Gathering Equipment (c) Top Pump B (d) PVT Visual Cell (e) Bottom Pump A

The remaining components in the condensate mixture are gases at standard conditions. To feed the required number of moles of each gas component into the PVT

system requires loading the gas components at a target pressure and corresponding volume. Setting the volume of each gas is much easier to control than pressure, therefore the loading pressure of each gas component was determined using the Virial equation of state. The following steps can be used to determine the feed pressure of a component using the Virial equation of state.

1. Select a working pressure of the component, P_i, and loading volume of the component, V_i.
2. For the component, determine the reduced pressure, P_r, and reduced temperature, T_r.

$$T_r = \frac{T}{T_c} \quad \textbf{(20)}$$

$$P_r = \frac{P}{P_c} \quad \textbf{(21)}$$

Where T_c and P_c are the critical temperature and critical pressure of the component.

3. Calculate the Virial coefficients (Winnick, 1997) using the following equations.

$$B^{(0)} = 0.083 - 0.422T_r^{-1.6} \quad \textbf{(22)}$$

$$B^{(1)} = 0.139 - 0.172T_r^{-4.2} \quad \textbf{(23)}$$

$$B_r = B^{(0)} + \omega B^{(1)} \quad \textbf{(24)}$$

Where ω is the acentric factor of the component.

4. Calculate the compressibility factor of the component, z_i.

$$z_i = 1 + \frac{B_r P_r}{T_r} \quad \textbf{(25)}$$

5. Recalculate the working pressure, P_i, using the real gas law.

$$P_i = \frac{z_i y_i n_t RT}{V_i} \quad \textbf{(26)}$$

6. Repeat steps 2-5 using the calculated P_i from step 5. Iterate until the value of P_i converges.

The procedure to calculate the feed pressure of each component is based on the Virial equation state and assumes that the reduced pressure and reduced temperature are within the low density region. This region corresponds to a reduced temperature and reduced pressure relationship that results in reduced temperatures greater than approximately $T_r = .436P_r + 0.6$ (Winnick, 1997). This approach is quantified by later comparison to the Peng Robinson equation of state which can be more tedious to model without the appropriate software.

Once the feed liquid quantities and feed gas components are calculated it is important to ensure that the total mixture can reach system pressures larger than the expected dew point pressure of the condensate system. This is important because the CCE experiments are begun at pressures much larger than the dew point pressure. Using this assumption, values of the compressibility factor were calculated using an empirical version of the Standing correlation described by Cronquist (2001) which is dependent on the pseudo critical properties of the mixed condensate. The pseudo critical temperature and pressure were calculated using a correlation by Piper *et al* (1993) which accounts for reservoir impurities such as nitrogen, hydrogen sulfide, and carbon dioxide. As an

example of this process, consider the base condensate listed in Table 4. The phase diagram of this condensate is illustrated in Figure 12.

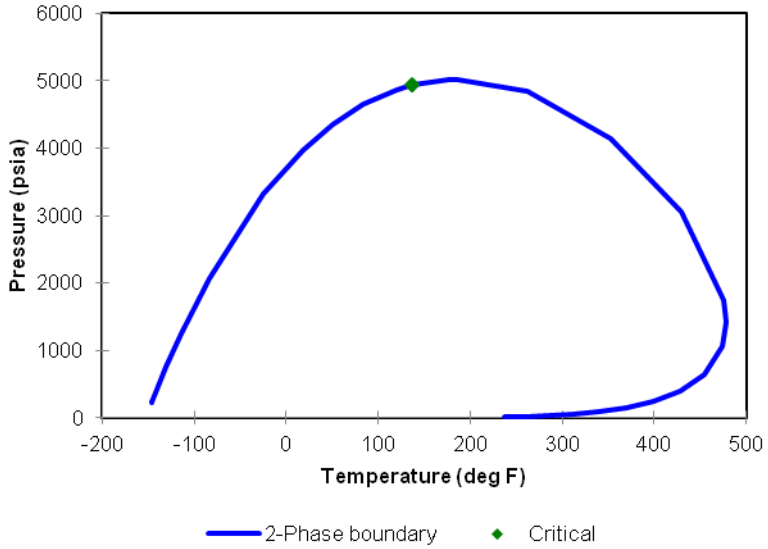

Figure 12: Pressure-Temperature Phase Diagram for Base Condensate

From the phase diagram, it can be seen that for a CCE experiment at 200°F, the dew point pressure is approximately 5000 psia. Therefore, at 200°F the initial pressure of the system is set to 6000 psia which is greater than the dew point pressure. Using this and the volume of the PVT cell it is possible to calculate the total amount of moles that will ensure that the PVT cell reaches the initial starting pressure. These steps are listed here.

1. Calculate the gas specific gravity, γ_g, of the gas condensate sample.

$$\gamma_g = \frac{\sum_i^6 y_i MW_i}{29} \tag{27}$$

2. Calculate the pseudo critical temperature, T_{pc}, and pseudo critical pressure,

P_{pc}, using Piper *et al*. (1993) correlation. Assume a pressure larger than the dew point pressure, P_t, and a temperature, T_t, used for the CCE experiments.

$$J = \eta_0 + \sum_{f=1}^{3} \eta_f y_f \left(\frac{T_c}{P_c} \right)_f + \eta_4 \gamma_g + \eta_5 \gamma_g^{\,2} \quad \textbf{(28)}$$

$$K = \beta_0 + \sum_{f=1}^{3} \beta_f y_f \left(\frac{T_c}{\sqrt{P_c}} \right)_f + \beta_4 \gamma_g + \beta_5 \gamma_g^{\,2} \quad \textbf{(29)}$$

$$T_{pc} = \frac{K^2}{J} \quad \textbf{(30)}$$

$$P_{pc} = \frac{T_{pc}}{J} \quad \textbf{(31)}$$

The parameter, *f*, corresponds to the reservoir fluid impurities in the following order H_2S, CO_2, and N_2. Values for η_f and β_f are shown in Table 5.

Table 5: Piper *et al* (1993) Parameters for Pseudo Critical Temperature Pressure Calculation

f	η_f	β_f
0	1.1582E-01	3.8216E+00
1	-4.5820E-01	-6.5340E-02
2	-9.0348E-01	-4.2113E-01
3	-6.6026E-01	-9.1249E-01
4	7.0729E-01	1.7438E+01
5	-9.9397E-02	-3.2191E+00

3. Calculate the compressibility factor, z_t, of the condensate sample at the expected experimental conditions above the dew point pressure using the Standing correlation (Cronquist, 2001).

$$T_{pr} = \frac{T_t}{T_{pc}} \quad \textbf{(32)}$$

$$P_{pr} = \frac{P_t}{P_{pc}} \quad \textbf{(33)}$$

$$A = 1.39\left(T_{pr} - 0.92\right)^{0.5} - 0.36T_{pr} - 0.101 \quad \textbf{(34)}$$

$$B = \left(0.62 - 0.23T_{pr}\right)P_{pr} + \left[\frac{0.066}{T_{pr} - 0.86} - 0.037\right]P_{pr}{}^{2} + \frac{0.32P_{pr}{}^{6}}{10^{9}\left(T_{pr} - 1\right)} \quad \textbf{(35)}$$

$$C = 0.132 - .32\log T_{pr} \quad \textbf{(36)}$$

$$D = 10^{-\left(0.3106 - .49T_{pr} + 0.1824T_{pr}{}^{2}\right)} \quad \textbf{(37)}$$

$$z_t = A + \left(1 - A\right)e^{B} + CP_{pr}{}^{D} \quad \textbf{(38)}$$

4. Recalculate the pressure of the cell at the CCE conditions using the expanded volume of the cell, V_t, and the real gas law.

$$P_t = \frac{z_t n_t R T_t}{V_t} \quad \textbf{(39)}$$

5. Repeat steps 3-4 using the calculated P_t from step 4. Keep doing this until the difference between each iterative P_t is minimized.

The preceding procedure is dependent on the total amount of moles, n_t, in the PVT cell which is also a necessary component in the calculation of the volumetric amount of liquid needed and the calculation of the loading pressure for the gas components. Therefore, any changes made to the total amount of moles in the preceding procedure have to be followed by recalculations of liquid volumes and gas component loading pressures (at specified loading volumes). As example of these considerations,

consider the base condensate mixture in Table 4. For a CCE experiment at 200 ^{o}F (660 ^{o}R) for a PVT cell with 18 cm^3 volume (with a value of 100 cm^3 out of a possible 200 cm^3 of additional adjustable volume used for compression and expansion) the calculation of the necessary parameters are listed in Table 6 and Table 7.

Table 6: Calculated Liquid Volumes for Base Case

Component	Feed State	V_i, cc
Methane	gas	n/a
Carbon Dioxide	gas	n/a
Ethane	gas	n/a
Propane	gas	n/a
Octane	liquid	6.64
Dodecane	liquid	18.6

Table 7: Gas Calculations for Loading Pressures, P_i, Using Specified Loading Volumes, V_i, for Base Case

Component	P_i guess, psia	T_r	P_r	$B^{(0)}$	$B^{(1)}$	B_r	z_i	V_i, cc	P_i calculated, psia
Methane	2698	1.55	0.718	-0.13	0.111	-0.13	0.6687	100	2698
Carbon Dioxide	48	0.968	0.144	-0.36	-0.0580	-0.37	0.983	100	48
Ethane	176	0.964	0.202	-0.36	-0.0613	-0.37	0.9044	100	176
Propane	125	0.796	0.124	-0.52	-0.309	-0.57	0.8547	100	125
Octane	n/a	n/a	n/a	n/a	n/a	n/a	n/a	n/a	n/a
Dodecane	n/a	n/a	n/a	n/a	n/a	n/a	n/a	n/a	n/a

The Peng Robinson equation of state was used to check the accuracy of the loading pressure calculation. This was done by calculating the Peng Robinson estimate of the loading volume. This was accomplished by using the molar amounts of the

gaseous component, the calculated loading pressure from Table 7, and a feed temperature of 70^{o}F. This Peng Robinson check is illustrated in Table 8 and shows approximate agreement with the Virial equation of state.

Table 8: Peng Robinson Check of Loading Pressures by Comparing Virial Equation of State and Calculated Volume versus Peng Robinson Calculated Volume.

Component	Feed State	V_i, cc	*Molar amount, gmols*	P_i calculated, psia	*Vi, Peng Robinson estimate, cc*
Methane	gas	100	1.136	2698	118
Carbon Dioxide	gas	100	0.01369	48	99
Ethane	gas	100	.05477	176	98
Propane	gas	100	0.04108	125	97
Octane	liquid	n/a	n/a	n/a	n/a
Dodecane	liquid	n/a	n/a	n/a	n/a

Table 9: Parameters Used to Calculate .003 Total lbmol Needed to Reach 6000 psig at 200^{o}F (Volume Used for Calculation is 118 cc). Peng Robinson Estimate is .003368 lbmol

γ_q	1.03
J	0.736
K	18.3
T_{pc}, ^{o}R	457
P_{pc}, *psi*	621
T_{pr}	1.16
P_{pr}	9.67
A	0.163
B	20.5
C	0.111
D	0.972
z_t	1.17
P_t, *psig*	6000

The total amount of moles needed to bring the system to 6000 psig was found to be 0.003 lbmol. This quantity is verified because it can be used to calculate the 6000 psig desired pressure at 200 ^{o}F and 118 cc of available volume (Table 9). This quantity is also verified by the Peng Robinson equation of state that determined that the molar volume of the experimental wet gas fluid was 1.237 ft^3/lbmol. This corresponds to a Peng Robinson estimate of .003368 lbmole which is comparable to the amount determined using the Standing correlation. This quantity was also found to satisfy the procedure of determining the gas loading pressures (Table 7) and the required liquid volumes (Table 6).

3.3 Experimental Results

Dew points were determined for the synthetically designed condensate mixtures by observing changes in compressibility from constant composition expansion experiments and verified by equation of state models such as Peng Robinson equation of state. Peng Robinson equation of state was calculated using the Winprop Phase Property Program (2011). As an example of the process of using the compressibility to determine the dew point pressure, consider the 15% CO_2 case at 200 ^{o}F. Its CCE isotherm (Figure 13) illustrates the pressure volume relationship for this fluid. The total compressibility of this fluid was calculated for each pressure point (Figure 14) using a central finite difference version of the total compressibility.

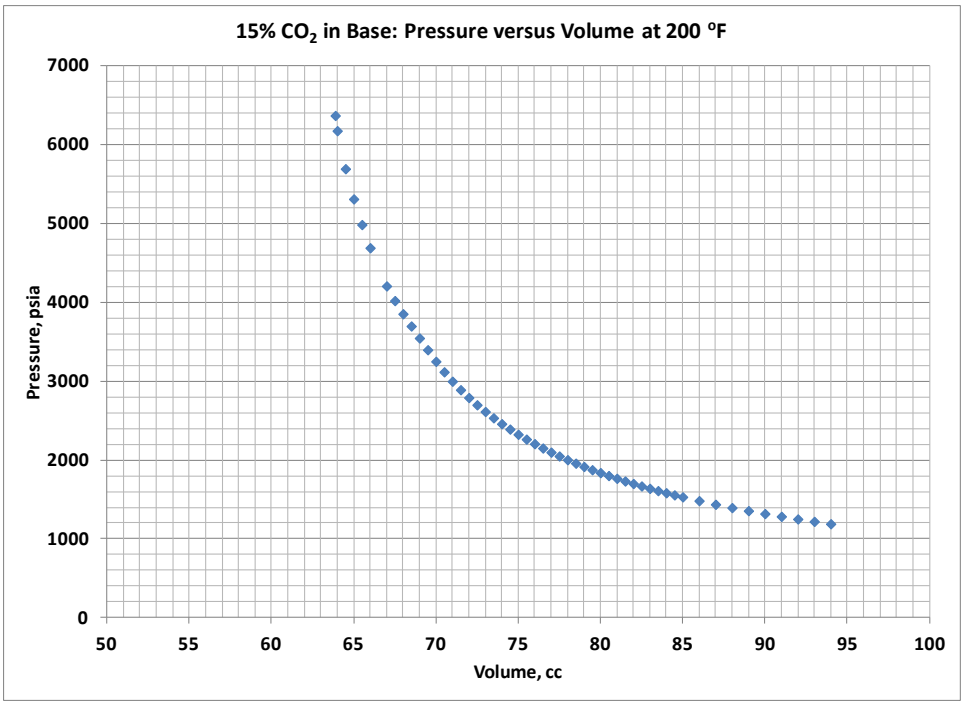

Figure 13: CCE Isotherm for 15% CO_2 in Base Case at 200 °F

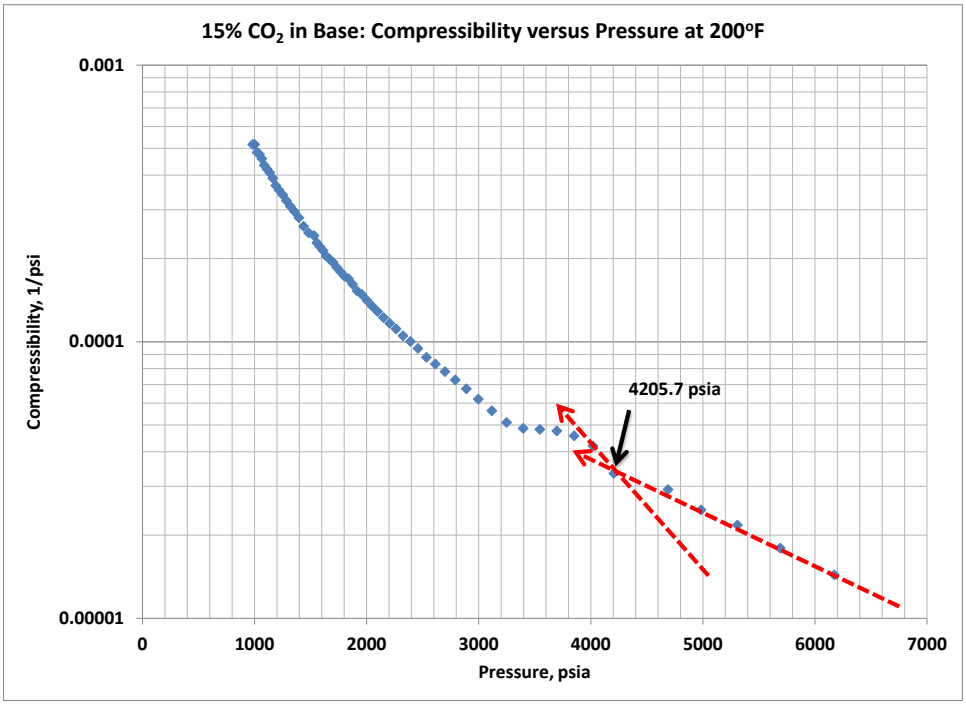

Figure 14: Dew Points Determination Using Compressibility Versus Pressure Plot for 15% CO_2 in Base Case at 200 °F

Figure 14 illustrates a substantial increase in the compressibility at approximately 4200 psia. This large increase is attributed to the first instance of liquid saturation in the PVT cell. According to the proposed procedure a sudden rise in compressibility is an indication of dew point pressure. Using this large rise in compressibility, the dew point pressure for the 15% CO_2 case is approximately 4200 psia.

The compressibility methodology was applied to the Base case, 10% CO_2 case, and the15% CO_2 case. Results of the dew point measurement of each case can be seen in Table 10 and Figure 15. Plots of the matched experimental data for each case superimposed on the Peng Robinson theoretical data and the Ideal gas approximation are shown in Figure 16.

Table 10: Comparison of Dew Point Measurements at 200^{o}F

	Experimental	Theoretical (Peng Robinson)	% absolute Error
Base Case	5627	5018	12
10% CO_2 in Base	3703	4641	20
15% CO_2 in Base	4206	4438	5

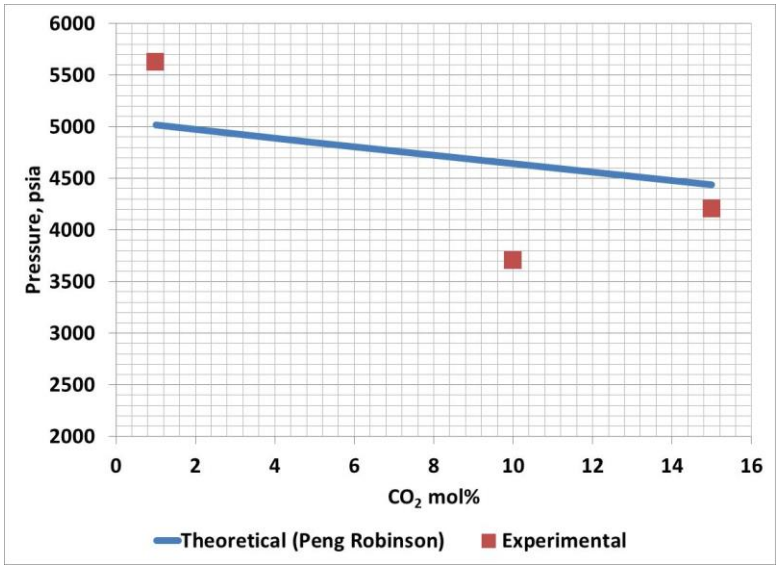

(a)

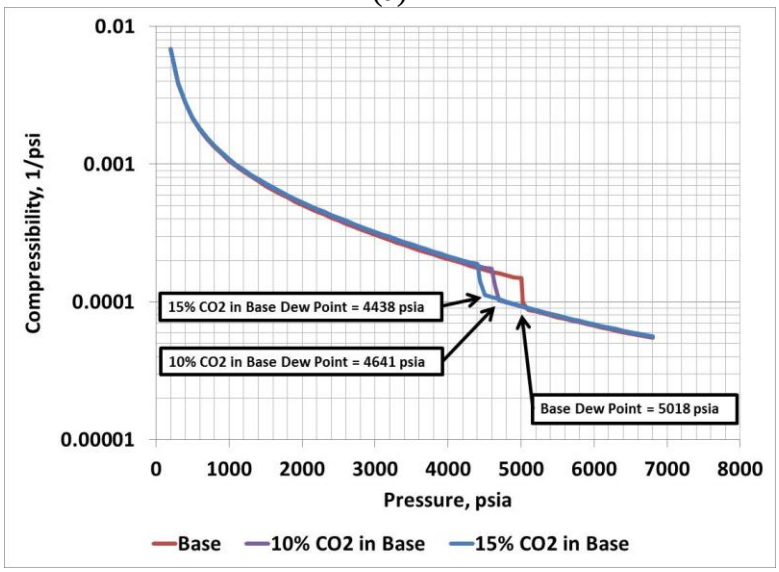

(b)

Figure 15: Dew Point Comparison as Function of CO_2 Concentration in Base Composition at 200°F (a) Experimental Versus Theoretical Comparison (b) Theoretical Compressibility Indicating Dew Point Pressures

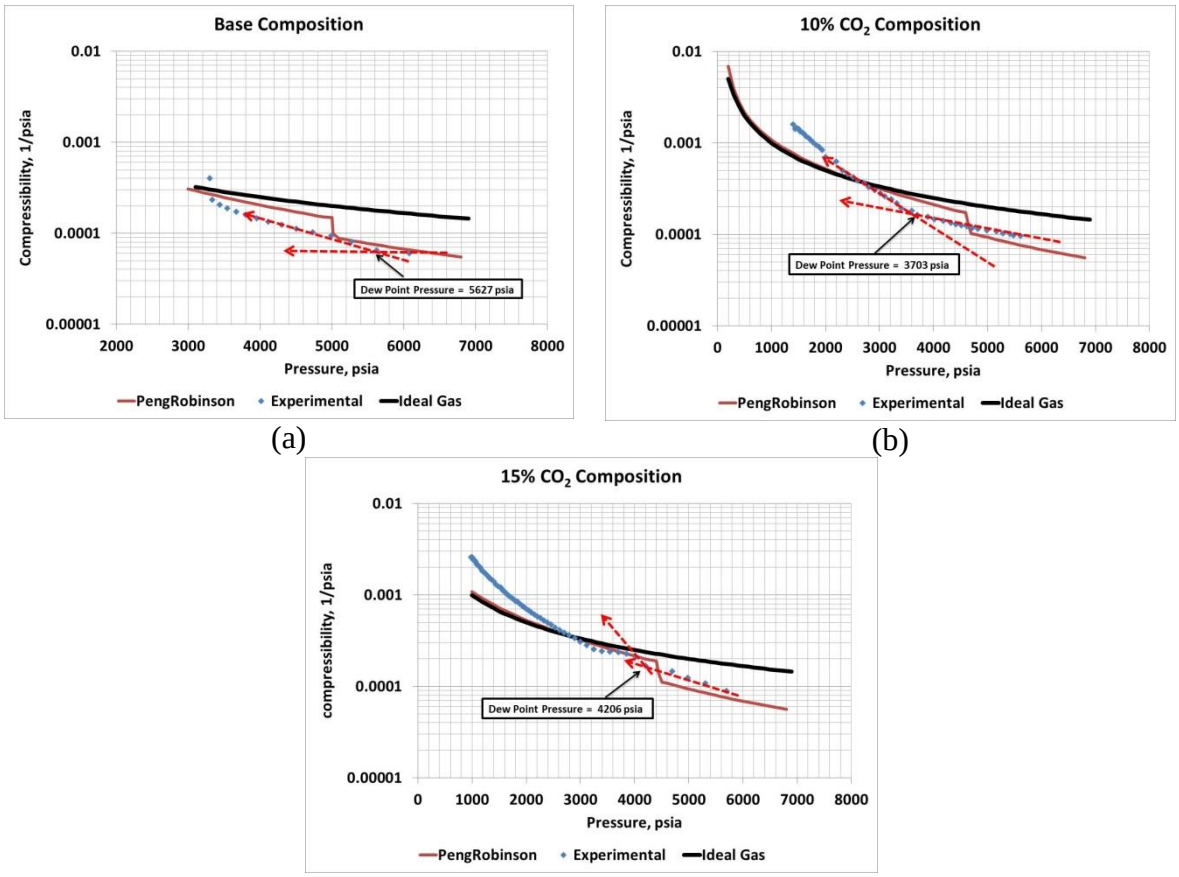

Figure 16: Match Experimental Data and Theoretical Data Comparison (a) Base Case (b) 10% CO_2 in Base (c) 15% CO_2 in Base

When comparing the theoretical dew point pressure among each case at 200 ^{o}F it can be seen that CO_2 has the unique ability to reduce the dew point pressure. The experimental results show some deviation from the theoretical observation which is attributed to preparing the wet gas samples and running the experiments. Nonetheless it is observed that CO_2 theoretically reduces the dew point pressure of wet gas/condensate fluids. This is observed in Figure 15 and Figure 17 which is a plot of the relative volume (PVT cell volume divided by the cell volume at the dew point).

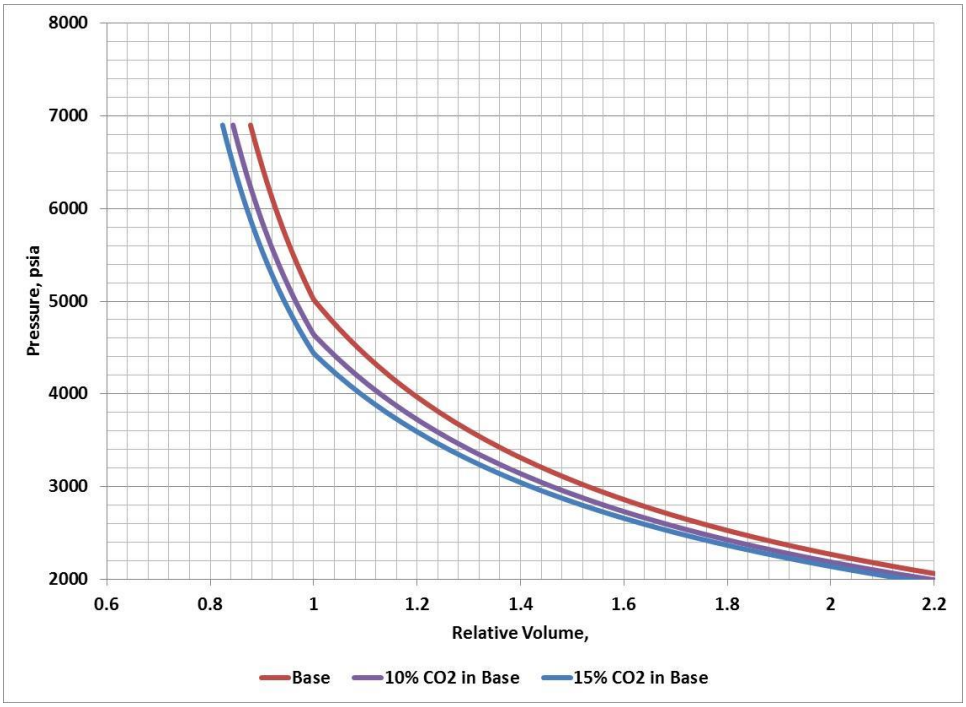

Figure 17: Theoretical Relative Volume of Base Condensate as Function of CO_2 at 200^{o}F

The relative volume plot in Figure 17 indicates that CO_2 decreases the corresponding pressures observed during CCE. In addition to this, the overall phase diagram of the gas condensate illustrates that the phase envelope decreases as a function of CO_2 concentration. This is conveyed in Figure 18. These results can be explained by analyzing previous studies of CO_2 with hydrocarbon systems. Monger *et al.* (1981) were able to illustrate in their Appalachian crude oil system that the crude oil aromaticity correlated with improved hydrocarbon extraction into a CO_2 rich phase. In addition to this, Monger *et al.* observed that CO_2 has the ability to lower miscible pressures for paraffin fluids that do not contain large amount of aromatic content. In terms of gas condensate systems, this means that the lighter end hydrocarbons partition into the CO_2

rich phase. This is beneficial because the CO_2 rich phase is a supercritical gas in typical reservoir conditions which implies that CO_2 lowers the hydrocarbon mixtures dew point pressure.

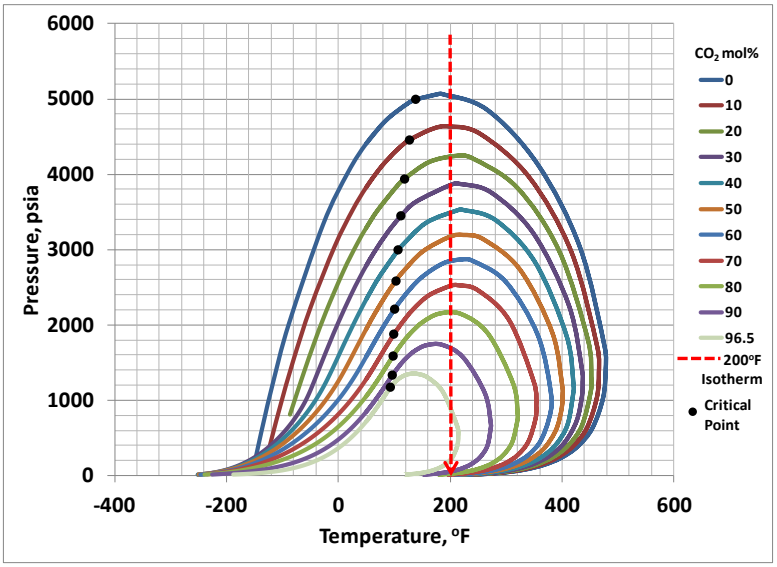

(a)

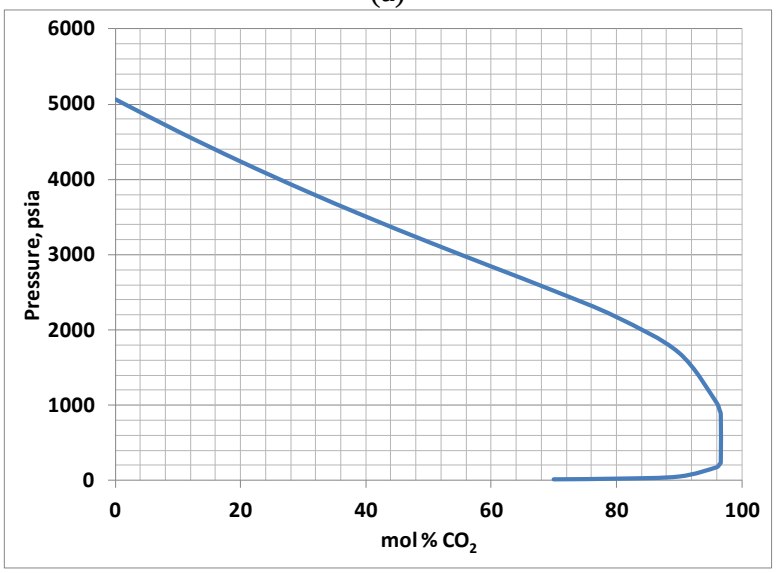

(b)

Figure 18: Peng Robinson Phase Envelope of Gas Condensate as Function of CO_2 Concentration (a) Pressure Temperature Phase Envelope (b) Pressure Composition Phase Envelope at 200 °F

In terms of liquid compressibility, the Peng Robinson approximation of the liquid saturation during CCE (Figure 19) gives an indication that there is less liquid dropout occurring as the amount of CO_2 increases. In regards to production from gas condensate reservoirs, this is beneficial because this shows that increasing the CO_2 concentration can decrease the maximum amount of liquid saturation that can occur in the reservoir.

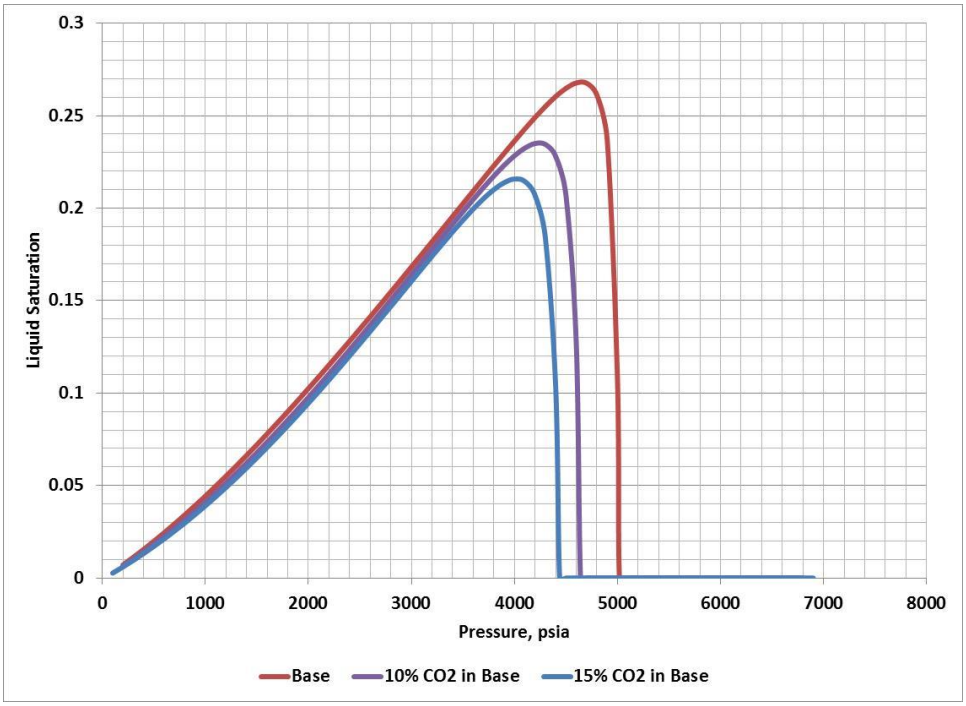

Figure 19: Peng Robinson Liquid Saturation of Base Condensate as Function of CO_2 at 200°F

3.4 Thermodynamic Justification of Using CO_2

CO_2 injection into condensate banks has a theoretical justification. Consider a wet gas above the dew point and a wet gas below the dew point. Gibbs free energy is a

thermodynamic property that describes thermodynamic equilibrium. For a mixture the change in Gibbs free energy is the following (Winnick, 1997):

$$dG = -SdT + VdP + \sum_i \mu_i dn_i \quad \textbf{(40)}$$

Where G is the Gibbs free energy, S is the entropy, V is the volume, P is the pressure, T is the temperature, n is moles, μ_i is the chemical potential of component i. The chemical potential of component i is the rate of change of Gibbs free energy when moles are added at constant T and P at its current phase. At equilibrium between the liquid (subscript l) and vapor (subscript v) phases the change in Gibbs free energies are equal.

$$\left[-SdT + VdP + \sum_i \mu_i dn_i\right]_l = \left[-SdT + VdP + \sum_i \mu_i dn_i\right]_v \quad \textbf{(41)}$$

In addition to this the chemical potentials of each component in the mixture are equal at equilibrium and the transport of each species is equal therefore the expression can be reduced further.

$$\left[-SdT + VdP\right]_l = \left[-SdT + VdP\right]_v \quad \textbf{(42)}$$

$$(V_l - V_v)dP = (S_l - S_v)dT \quad \textbf{(43)}$$

$$\frac{dP}{dT} = \frac{dS}{dV} \quad \textbf{(44)}$$

From the previous expression the right side's numerator and denominator can be divided by the total number of moles, n, of the system. This leaves the expression to be a function of molar entropy, *s*, and molar volume, *v*.

$$\frac{dP}{dT} = \frac{\frac{\Delta S}{n}}{\frac{\Delta V}{n}} = \frac{\Delta s}{\Delta v} \quad \textbf{(45)}$$

The previous expression can be reduced to a useful form by using the definition of Gibbs free energy which is the expression, $\Delta g = \Delta h - T\Delta s$, where Δh is the change in enthalpy. At equilibrium the difference in free energy between the two phases is 0 therefore the change in molar entropy of the system is $\Delta s = \Delta h/T$. This reduces the previous expression into the following form.

$$\frac{dP}{dT} = \frac{\Delta h}{T\Delta v} \quad \textbf{(46)}$$

The previous expression is known as the Clapeyron relation and it has been used to model the vapor pressure as a function of temperature for pure components. It is unique idea to apply this relationship to a mixture. To do this requires defining the Δv term. This term can be defined as the change in volume between the liquid and vapor phases. Precisely, this change in molar volume can be expressed as $\Delta v = v_v - v_l$. Assuming ideal gas behavior, the vapor molar volume can be expressed as $v_v = RT/P$ where R is the ideal gas constant. Substituting this definition of v_v and assuming that the liquid molar volume is approximately 0, the previous expression can be expressed as the following expression.

$$\frac{dP}{dT} = \frac{P\Delta h}{RT^2} \quad \textbf{(47)}$$

The previous expression is the Clausius-Clapeyron relationship (Winnick, 1997). Solving for the enthalpy term leaves the following expression.

$$\Delta h_{condensation} = -RT \ln P_{dew} \quad \textbf{(48)}$$

Where P_{dew} is the dew point of the wet gas and $\Delta h_{condensation}$ is the heat of enthalpy due to condensation.

The impact of the heat of condensation expression can be understood by considering a wet gas that has been studied in literature and that will be used for the rest of this work. This fluid description can be seen in Table 11.

Table 11: Composition for Compositional Simulation (Whitson et al., 2005)

Component	z_i, mol%	Molecular Weight	T_c, R	P_c, psia	Accentric Factor	Vshift	T_b, °R	SG	Zc (Visc)	Pchor
N2	3.349	28.01	227.2	492.8	0.037	0.0009	139.4	0.2724	0.2918	59.1
CO_2	1.755	44.01	547.4	1069.5	0.225	0.2175	333.3	0.751	0.2743	80
H2S	0.529	34.08	672.1	1300	0.09	0.1015	382.4	0.8085	0.2829	80.1
C1	83.265	16.04	343	667	0.011	0.0025	201.6	0.1398	0.2862	71
C2	5.158	30.07	549.6	706.6	0.099	0.0589	332.7	0.3101	0.2792	111
C3	1.907	44.1	665.7	616.1	0.152	0.0908	416.2	0.499	0.2763	151
iC4	0.409	58.12	734.1	527.9	0.186	0.1095	471.1	0.5726	0.282	188.8
nC4	0.699	58.12	765.2	550.6	0.2	0.1103	491.1	0.5925	0.2739	191
iC5	0.28	72.15	828.7	490.4	0.229	0.0977	542.4	0.6312	0.2723	227.4
nC5	0.28	72.15	845.5	488.8	0.252	0.1195	557	0.6375	0.2684	231
C6	0.39	82.32	924.2	491.3	0.2373	0.1341	606.2	0.7036	0.2703	232.6
C7	0.486	95.36	988.3	457.2	0.2714	0.1429	658.7	0.7367	0.265	263.9
C8	0.361	108.77	1043.9	422.8	0.3094	0.1522	707.5	0.7594	0.2652	296.1
C9	0.266	121.9	1094.1	390	0.35	0.1697	754	0.7761	0.2654	327.6
C10	0.201	134.78	1138.6	361.7	0.39	0.1862	796.9	0.7896	0.2655	358.5
C11	0.153	147.59	1178.9	337	0.4295	0.2018	836.8	0.8009	0.2657	389.2
C12	0.116	160.3	1215.6	315.3	0.4684	0.2165	874.3	0.8107	0.2658	419.7
C13	0.089	172.91	1249.4	296.3	0.5067	0.2302	909.5	0.8193	0.266	450
C14	0.068	185.42	1280.6	279.4	0.5444	0.243	942.7	0.827	0.2661	480
C15	0.052	197.82	1309.5	264.5	0.5814	0.2548	973.9	0.834	0.2662	509.8
C16	0.04	210.11	1336.3	251.1	0.6178	0.2657	1003.4	0.8404	0.2664	539.3
C17-19	0.073	233.39	1383.1	229.3	0.6857	0.2843	1055.8	0.8513	0.2666	595.1
C20-29	0.063	299.51	1493.7	184.6	0.8712	0.3239	1183.8	0.8764	0.2672	753.8
C30+	0.012	477.34	1616.9	167.6	1.0411	0.1154	1309.7	0.9215	0.2677	1180.6

Adding CO_2 to this wet gas shrinks the phase envelope and thus the dew point pressure for a corresponding reservoir temperature as indicated by Figure 20.

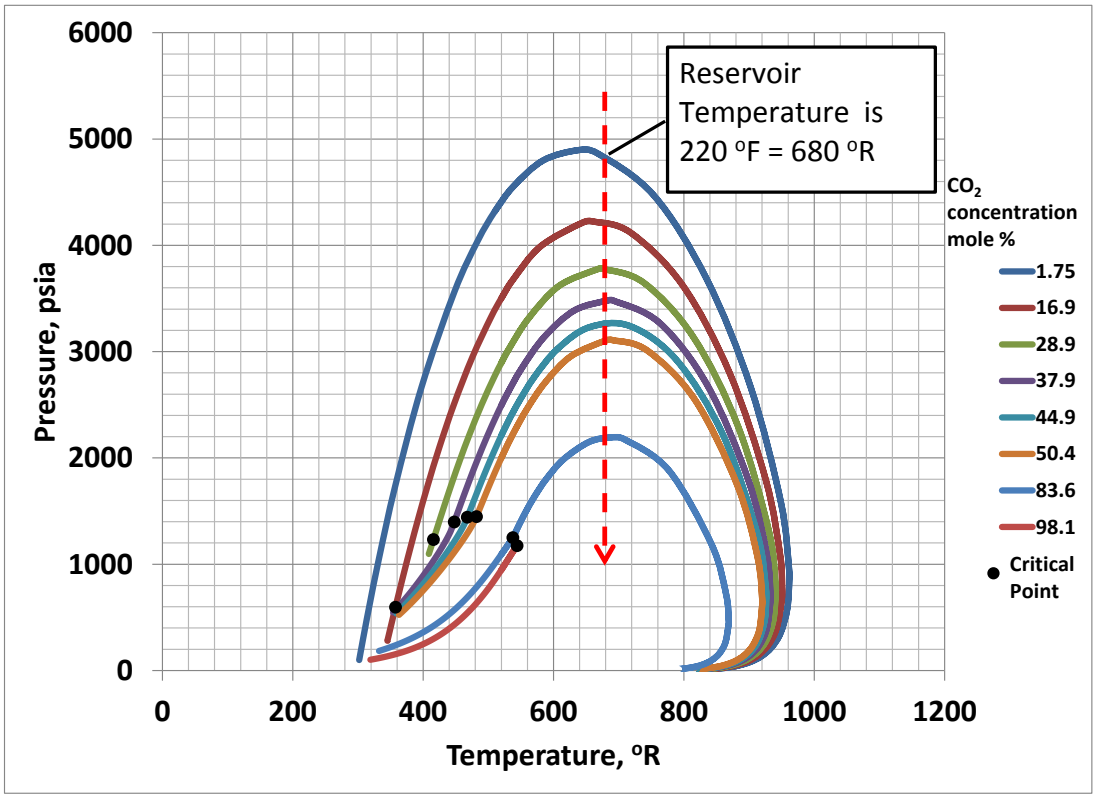

Figure 20: Phase Envelope of Sample Wet Gas Composition Used for Compositional Simulation as Function of CO_2 Concentration

The dew point pressure of each phase envelope (listed in Table 12) can be obtained using the Peng Robinson equation of state. From there, the enthalpy of condensation can be calculated. The enthalpy of condensation is illustrated in Figure 21.

Table 12: Dew Point of Sample Wet Gas Used for Compositional Simulation as Function of CO_2 Concentration at 220°F

mol % CO_2	Dew Point Pressure, psia
2	4837
17	4212
29	3778
38	3482
45	3266
50	3102
84	2190

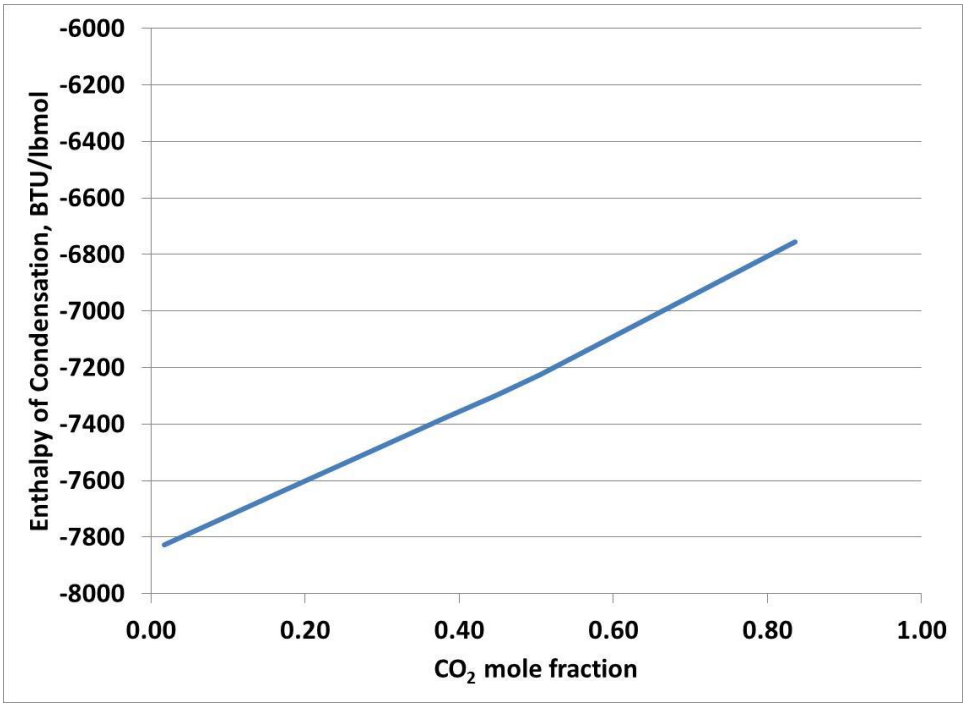

Figure 21: Enthalpy of Condensation of Sample Wet Gas Used for Compositional Simulation as Function of CO_2 Concentration at 220°F

The heat of condensation is a measure of the heat released in bringing a fluid from the gas phase to the liquid phase. An increase in the enthalpy of condensation corresponds to a gas having difficulty in condensing to a liquid. In the context of CO_2's

interaction with wet gases, the increase in CO_2 concentration results in wet gas fluid having a greater difficulty of having liquid dropout. This concept is illustrated in Figure 21 and is the thermodynamic justification of injecting CO_2 to remove condensate blocking and for CO_2 EGR.

The lab experimental study illustrates the potential of CO_2 reducing the dew point of reservoir fluids. This chapter illustrated the PVT nature of CO_2 with gas condensates. The next chapter deals with modeling the geochemistry inherent in the compositional simulations in this work.

4 CARBONATE GEOCHEMISTRY AND THE INFLUENCE OF CO_2

The purpose of this chapter is to elucidate the geochemical system used for the compositional simulations. Injecting CO_2 into carbonate formations can cause dissolution or precipitation of mineral depending on the geochemical status of the carbonate formation. Consider the standard aqueous and mineral equilibrium reactions that can occur when CO_2 interacts with carbonate (represented by calcite). The aqueous reactions (listed in Table 13) in conjunction with the mineral reaction (listed in Table 14) give an indication of the geochemical equilibrium that exists when CO_2 interacts with the carbonate (calcite or $CaCO_3$) matrix (Nghiem *et al*., 2004). All equilibrium rate constants and solubility rate constants are referenced at 25 ^oC.

Table 13: Aqueous Reactions

Aqueous Reactions	Log Equilibrium Rate Constant
1. $H_2O \leftrightarrow H^+ + OH^-$	Log K_{A1} = -13.2631
2. $CO_2(aq) + H_2O \leftrightarrow H^+ + HCO_3^-$	Log K_{A2} = -6.3221
3. $CO_2(aq) + H_2O \leftrightarrow 2H^+ + CO_3^{2-}$	Log K_{A3} = -16.5563

Table 14: Mineral Reactions

Mineral Reactions	Solubility Rate Constant
1. $CaCO_3 + H^+ \leftrightarrow Ca^{2+} + HCO_3^-$	Log K_{SP1}= 1.36

To deduce the total reaction requires assuming chemical equilibrium and that the reactions occur simultaneously (Laidler *et al.*, 2003). The overall reaction can be determined by summing all the reactions as seen in Table 15. This chemical reaction is an equilibrium reaction that has the capacity to cause dissolution of the carbonate matrix which is indicated by the creation of aqueous ions or the mineralization of calcite. The net reaction depends on the amount of CO_2 that is injected into the carbonate matrix.

Table 15: Carbonate Geochemical Reaction

Total Reaction	Total Equilibrium Constant
1. $CaCO_3 + 2CO_2(aq) + 3H_2O \leftrightarrow 3H^+ + OH^- + 2HCO_3^- + Ca^{2+} + CO_3^{2-}$	$K_{EQ} = K_{A1}K_{A2}K_{A3}K_{SP1}$

Assuming that there are vast amounts of calcite in the carbonate matrix (when compared to CO_2 and H_2O) the forward reaction indicates that CO_2 is the limiting reagent. When the required stoichiometric amount of CO_2 exceeds the required stoichiometric amount of the aqueous ions than dissolution of the carbonate matrix will occur. When the required stoichiometric amount of CO_2 is less than the required stoichiometric amount of the aqueous ions than mineralization of the carbonate matrix will occur. These rules are melded into the compositional simulator used in this work. In terms of initial conditions, Table 16 illustrates the initial composition of the water phase in all subsequent compositional reservoir simulations.

Table 16: Aqueous Component Properties

Component	Initial Concentration (Molality)	Molecular Weight
H^+	10^{-7}	1.0079
Ca^{2+}	$9.12x10^{-5}$	40.08
OH^-	$5.46x10^{-7}$	17.0073
HCO^{3-}	$1.17x10^{-5}$	61.0171
CO_3^{2-}	$2.49x10^{-2}$	60.0092

Moreover, these geochemical considerations and mass transfer between all the components in the oil and gas phases are modeled using a Sigmund diffusion algorithm that is incorporated into the compositional simulator (CMG, 2011b). Mass dispersion between CO_2 and the aqueous phase was set to $2x10^{-5}$ cm^2/s (Nghiem *et al*., 2004). For all subsequent compositional simulations the previous geochemical, diffusion, and solubility considerations are utilized in the compositional simulator. The next section gives an overview on the production aspects associated with CO_2 Huff-n-Puff and EGR.

5 CONDENSATE BLOCKAGE AND THE INFLUENCE OF CO_2

Wet gas reservoirs have a tendency to experience condensate blockage due to production below the dew point pressure. When this condensate blockage occurs there is an increase in oil saturation in the near wellbore which causes a decrease in gas relative permeability and thus leads to decreased gas productivity. CO_2 injection is proposed to reduce this condensate blockage and thus increase gas productivity. To understand the impact of CO_2 on condensate it is important to consider the ways that others have quantified condensate blockage.

Muskat quantified this condensate blockage by developing a model that estimates the radius of the condensate blockage as a function of time, gas rate, and reservoir fluid and rock properties (Muskat, 1981). Fetkovich later used Muskat's results to create a rate and time dependent condensate blockage skin factor for use in the gas inflow performance relationship (Fetkovich, 1973). The drawback to Fetkovich and Muskat's work is that the inflow performance relationship that describes the gas flow did not account for the pressure gradient that exists from the wellbore to the reservoir's boundaries. For a compressible fluid like gas, the pressure gradient causes changes in fluid properties such as density, relative permeability, and viscosity. However, others directly or indirectly attempted to address this problem by using a pseudo integral approach. The pseudo pressure integral approach uses the relative permeability, the densities, and the viscosities of each phase evaluated over a pressure range to quantify changes in phase saturation and composition. O'Dell and Miller (1967) were the first to

present gas inflow performance relationship that used a pseudo pressure function to describe changes in saturation. Their approach however was only valid for pressures above the dew point and was inaccurate when the flowing composition deviated from the original composition. Their approach was also very limiting when there was significant condensation in the near wellbore region.

Jones and Raghavan (1988) were able to perform compositional simulations that accurately modeled the depletion of a gas condensate reservoir below the dew point pressure. The only problem with their approach was that compositional simulation was necessary in order to determine compositions and saturations that are a requirement in evaluating the two phase pseudo pressure integral. Fevang and Whitson (1995) improved the approach of Jones and Raghavan by subdividing the two phase pseudo pressure integral into three components that represented three characteristic zones for condensate blockage. They were able to evaluate these zones by using the instantaneous producing well stream composition and PVT data taken from the well stream. Specifically, Fevang and Whitson derived a pseudo-steady state inflow performance relationship for gas condensate flow. The two phase pseudo pressure integral for gas condensate flow is described in the following expression.

$$\Delta m = \int_{p_{wf}}^{p} \left(\frac{k_{ro}}{B_o \mu_o} R_s + \frac{k_{rg}}{B_g \mu_g} \right) dp \qquad \textbf{(49)}$$

Where k_{ro} is the oil relative permeability, k_{rg} is the gas relative permeability, B_o is the oil formation volume factor, B_g is the gas formation volume factor, μ_g is the gas viscosity, μ_o is the oil viscosity, R_s is the solution GOR. Fevang and Whitson showed that their

expression matched well with simulation. The only drawback to their approach is that condensate blockage is not quantified as skin. Fevang and Whitson incorporated condensate blockage into their derived pseudo pressure expression (Fevang and Whitson, 1995). Therefore, it is difficult to access the severity of condensate blockage using Fevang and Whitson's pseudo pressure because the effect due to condensate blockage is incorporated into the pseudo pressure expression.

To better account for the severity of condensate blockage, Xu and Lee (1999) successfully showed that a single phase analogy can be used to describe gas flow in gas condensate reservoirs. To account for liquid dropout, Xu and Lee used a two zone analogy to describe condensate blockage. These zones, illustrated in Figure 22 (adapted from Xu and Lee), consist of a condensate blockage zone which includes a mechanical damage zone (spans radially from r_w to r_s) and the area that has liquids dropping out (spans radially from r_w to r_c).

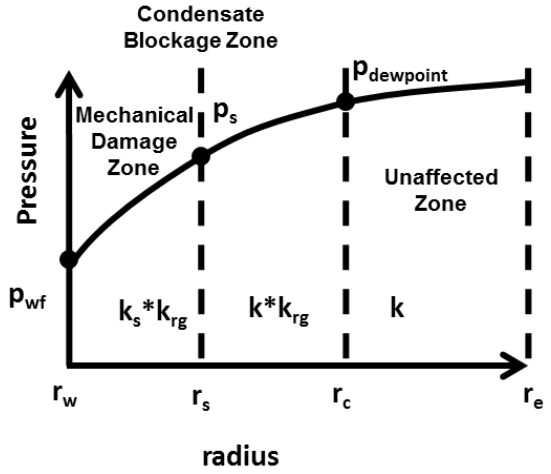

Figure 22: Two Zone Condensate Blockage Analogy

The mechanical damage area accounts for damage due to the reservoir's natural permeability. In this region the permeability is k_s while the reservoirs natural permeability is k. The condensate dropout region consists of reduction to the ideal gas relative permeability. This condensate blockage gas relative permeability is k_{rg}. The unaffected zone does not have liquids dropping out. The permeability to gas in the mechanical damage zone is k_s*k_{rg}. The permeability to gas in the region between r_s and r_c is $k*k_{rg}$. The permeability to gas in the unaffected zone is k since there is no liquid drop out occurring in this zone. Taking into consideration the dry gas analogy presented by Xu and Lee (1999) the pseudo steady state inflow performance relationship (in field units) for a single phase gas is the following expression (Economides *et al.*, 1994).

$$q_g = \frac{kh\Delta m}{1424T\left[\ln\left(\frac{r_e}{r_w}\right) - 0.75 + s_t\right]} \quad \textbf{(50)}$$

Where q_g is the gas flow rate in field units, k is permeability, h is the net pay, r_e is drainage radius, r_w is wellbore radius, T is the temperature in Rankin, and s_t is the total skin factor. The pseudo pressure integral for the single phase gas is the following expression.

$$\Delta m = 2\int_{p_{wf}}^{p}\left(\frac{p}{z_g\mu_g}\right)dp \quad \textbf{(51)}$$

Where z_g is the gas compressibility factor. Xu and Lee then demonstrated that the total skin that exists due to production below the dew point pressure using a single phase analogy can be represented by the following expression (Xu and Lee, 1999).

$$s_t = \frac{s_m}{k_{rg}} + s_c \tag{52}$$

Where s_m is the total mechanical skin, k_{rg} is the gas relative permeability in the condensate blockage zone, and s_c is the condensate blockage skin.

$$s_c = \frac{1}{k_{rg}}\left(1 - k_{rg}\right)\ln\frac{r_c}{r_w} \tag{53}$$

In this work, the condensate blockage skin is used to quantify the impact of injecting CO_2 into the reservoir. To understand the impact of removing condensate blockage from the near wellbore region the dimensionless productivity is derived by first defining the productivity for a well undergoing condensate blockage. This expression, which incorporates the expression for pseudo steady state gas inflow performance relationship and the total skin expression is seen here as the following relation.

$$J_0 = \frac{kh}{1424T\left[\ln\left(\frac{r_e}{r_w}\right) - 0.75 + \frac{s_m}{k_{rg}} + \frac{1}{k_{rg}}\left(1 - k_{rg}\right)\ln\frac{r_c}{r_w}\right]} \tag{54}$$

The productivity assuming total removal of condensate blockage can be determined by removing the condensate blockage expression from the productivity relationship describing condensate blockage. The productivity assuming complete removal of condensate blockage can be seen in the following equation.

$$J = \frac{kh}{1424T\left[\ln\left(\frac{r_e}{r_w}\right) - 0.75 + \frac{s_m}{k_{rg}}\right]} \tag{55}$$

The productivity ratio that describes the factor of improvement due to removing condensate blockage can be expressed as $J_D=J/J_0$. This expression is seen here.

$$J_D = \frac{\ln\left(\frac{r_e}{r_w}\right) - 0.75 + \frac{s_m}{k_{rg}} + \frac{1}{k_{rg}}\left(1-k_{rg}\right)\ln\frac{r_c}{r_w}}{\ln\left(\frac{r_e}{r_w}\right) - 0.75 + \frac{s_m}{k_{rg}}} \tag{56}$$

The productivity ratio is a good indicator of the expected productivity improvement if the condensate blockage is removed. For example, consider a reservoir experiencing condensate blockage with no mechanical damage (s_m). If the original relative permeability in the condensate blockage zone is $k_{rg}=0.1$ and the dimensionless drainage radius is $r_e/r_w=10^6$ then the expected increase in productivity if the condensate blockage zone comprises 40% of the drainage radius is approximately 9.9. Which means that if the condensate blockage is removed then the well can expect a factor of 9.9 improvement in its productivity. This logic is summarized in Figure 23, which is a plot of the productivity ratio for different cases of gas relative permeability, condensate blockage radius, and dimensionless drainage radius.

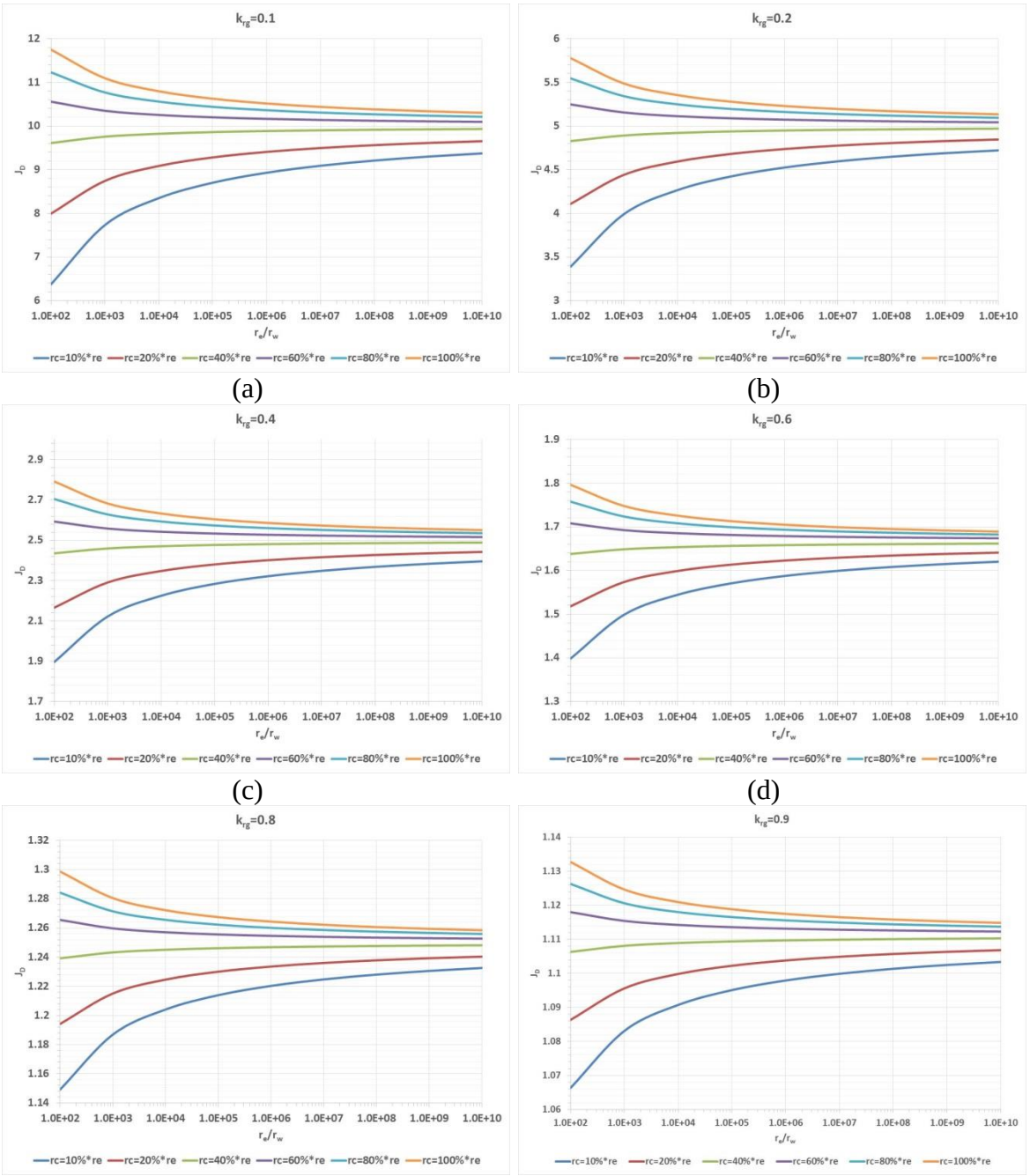

(a) (b)

(c) (d)

(e) (f)

Figure 23: Productivity Ratio Which Indicates Increases in Gas Productivity After Removal of Condensate Blockage as a Function of Gas Relative Permeability in the Condensate Blockage Zone, Condensate Blockage Radius, and Dimensionless Drainage Radius (a) k_{rg}=.1, (b) k_{rg}=0.2, (c) k_{rg}=0.4, (d) k_{rg}=0.6, (e) k_{rg}=0.8, (f) k_{rg}=0.9

From the productivity ratio illustrated in Figure 23, it is evident that increases in productivity occur in situations in which gas relative permeability in the condensate blockage zone is low and condensate blockage radius is large. This fundamental concept is essential in the overall theme of this work which is to use CO_2 to remove condensate blockage and thus improve gas productivity.

As previously mentioned, the main drawback to the pseudo pressure integral approach is that condensate blockage is not quantified as damage skin with respect to gas flow potential. The pseudo pressure integral approach quantifies the condensate blockage effect into a pressure expression but this expression does not explicitly describe the extent of the reduction of gas production below the dew point pressure nor does it give the radial distance over which this reduction due to liquid drop out occurs. Furthermore, CO_2 Huff-n-Puff and CO_2 EGR cause large changes to the original fluid composition of the reservoir. A pseudo pressure approach relies on a black oil representation of the reservoirs fluid properties (formation volume factor, solution gas ratio, and etc.) This black oil representation is inadequate for modeling CO_2-Huff-n-Puff and CO_2 EGR because of the large compositional changes that occur in the reservoir during these processes. This causes a problem because pseudo pressure is the primary component in well test analysis. Because of this limitation, compositional simulation is used to model condensate blockage and property profile plots (in conjunction with single phase analogy) are used to calculate condensate blockage skin.

One obvious advantage compositional simulation has over the pseudo pressure integral approach is that it is able to incorporate complex grid systems such as carbonate

reservoirs with different levels of deliverability. The appearance of condensate in the near wellbore region can be strongly dependent on the permeability and net pay of each layer. For varying permeability and net pays, liquid drop out can occur depending on the mobility of each wet gas component. Therefore, compositional simulation becomes a very powerful tool in modeling the compositional changes inherent in the CO_2 Huff-n-Puff and CO_2 EGR process. To model these changes, simulation studies were conducted on wet gas systems to discern the development of condensate in the reservoir and the subsequent removal using CO_2. For this study, a wet gas composition represented Table 11 (Whitson *et al.*, 2005) was used. To illustrate the potential of using CO_2 with regards to gas condensate systems the gas composition illustrated by Table 11 was simulated with different concentrations of CO_2. The net result of these simulations indicates the advantageous changes that occur with the phase envelope. At 220 ^{o}F (680 ^{o}R) and pressures above the saturation line for 1.75 mole % CO_2 (base concentration for the wet get sample) the phase envelope indicates that the sample is in the gas phase (Figure 20). As the reservoir pressure declines, the production engineer is forced to lower the bottom hole pressure so as to maintain economic production. Eventually the bottom hole pressure is lowered below the saturation line (for the base CO_2 concentration). As a result of this, the wet gas sample goes into the two phase region which corresponds to liquids dropping out and forming condensate in the near wellbore region. This results in condensate blockage and a severe reduction in gas relative permeability. To vaporize this condensate, the CO_2 concentration can be increased which results in a reduction of the saturation pressure at a given reservoir temperature as indicated by Figure 20.

During the process of increasing the CO_2 concentration in the near wellbore region the reservoir pressure simultaneously increases due to the act of injecting additional CO_2 volume to the reservoir. The simultaneous actions of lowering the dew point pressure while pressurizing the reservoir allows the reservoir fluid to remain in a single gaseous phase. This is the theoretical advantage of injecting CO_2 into condensate banks.

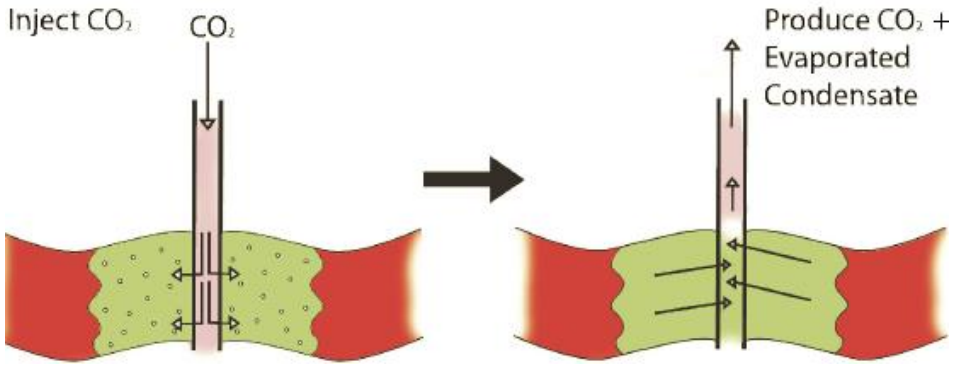

Figure 24: CO_2 Huff-n-Puff (Gupta, 2010)

To take advantage of the CO_2 interaction with condensate banks, a reservoir undergoing depletion is modeled using the fluid described in Table 11. After this study, CO_2 Huff-n-Puff (illustrated in Figure 24) is simulated to illustrate the benefits of injecting CO_2 into the condensate blockage zone. These studies use a simple radial model representing the carbonate reservoir system. Relative permeability curves used for the simulation studies are listed in Figure 25.

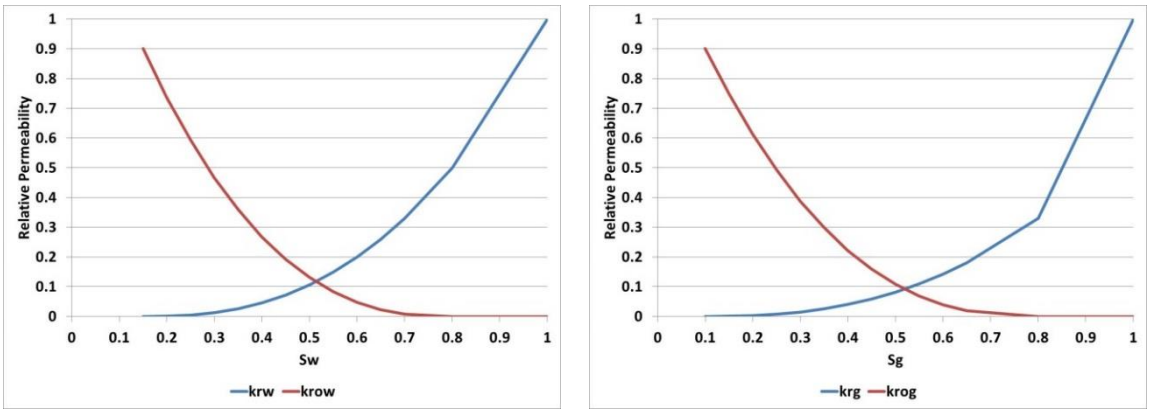

(a) (b)

Figure 25: (a) Water Saturation (S_w) Versus Water Relative Permeability (k_{rw}) and Oil Relative Permeability (k_{row}) (b) Gas Saturation (S_g) Versus Gas Relative Permeability (k_{rg}) and Oil Relative Permeability (k_{rog}).

5.1 CO_2 Huff-n-Puff Simulation

It has been illustrated that carbonate reservoirs containing wet gas have a tendency of having liquids drop. This creates a zone of condensate blockage in the near well bore region that restricts gas flow. These zones are necessary for maintaining target gas production rates but, can contribute to condensate blockage in the near wellbore region. To remedy this, CO_2 Huff-n-Puff can be applied to remove condensate blockage from the near wellbore region using miscible interactions between CO_2 and the condensed hydrocarbon phase. To study the feasibility of this process, simulations were conducted to model the condensation of hydrocarbon liquid in the near-wellbore region and its subsequent removal by CO_2. These simulations were conducted using the GEM Advanced Compositional and GHG Reservoir Simulator (2011). The simulations model a 40 acre carbonate field using a radial grid model (illustrated in Figure 26) with properties listed in Table 17.

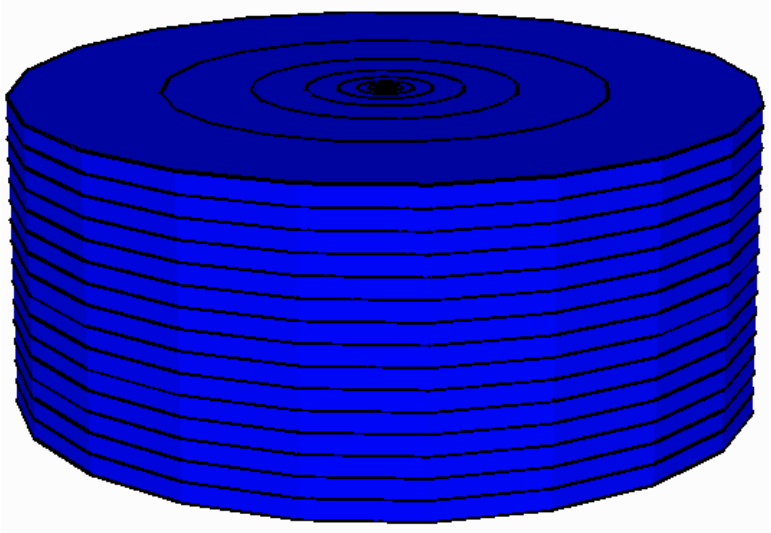

Figure 26: Simulation Grid for CO_2 Huff-n-Puff Study

Table 17: Simulation Grid Properties for CO_2 Huff-n-Puff Study

Surface Area	40 Acres	**Reservoir Temperature**	220 ^{o}F
Gridding of Radial Model	15 x 1 x 15	**Rock Compressibility**	5.00E-06 psi^{-1}
Radial grid blocks, ft	0.2223, 0.3729, 0.6255, 1.0493, 1.7603, 2.9529, 4.9536, 8.3098, 13.9399, 23.3844, 39.2280, 65.8058, 110.3908, 185.1831, 310.6490	**Depth to top of formation**	9600 ft
Angular grid blocks, degrees	360	**Initial Pressure**	5300 psia
Vertical grid blocks	43 ft	**Initial Water Saturation**	15%
Porosity	20%	**Critical Gas Saturation**	15%
Permeability	1 md	**Pay Zone**	645 ft
CO_2 Injector Constraint	.7 psi/ft of pay	**Producer Minimum Bottom Hole Pressure**	1000 psia

The reservoir was produced under primary depletion using a target gas production rate of 10 MMSCF/Day for 20 years (year 2011 to 2031) and the minimum bottomhole pressure limit of 1000 psi. The separator conditions used for the simulation study are listed in Table 18. Results of the simulation studies, shown in Figure 27, reveal that the target production rate could be maintained for about 5 years after which it declined exponentially.

During this phase, the condensate production and condensate gas ratio declined indicating condensate dropout in the near-wellbore region. This also coincided with the bottomhole pressure dropping below the dew-point pressure of the reservoir fluid, as shown in Figure 27. The dew point pressure of the selected fluid system at the reservoir temperature of 220 ^{o}F is approximately 4800 psia. The carbonate reservoir produced at below the dew point pressure through the end of the production history.

Table 18: Separator Conditions for CO2 Huff-n-Puff Simulation Study

Separator	1	2	3
Pressure	1000 PSIA	350 PSIA	14.7 PSIA
Temperature	80 ^{o}F	70 ^{o}F	60 ^{o}F

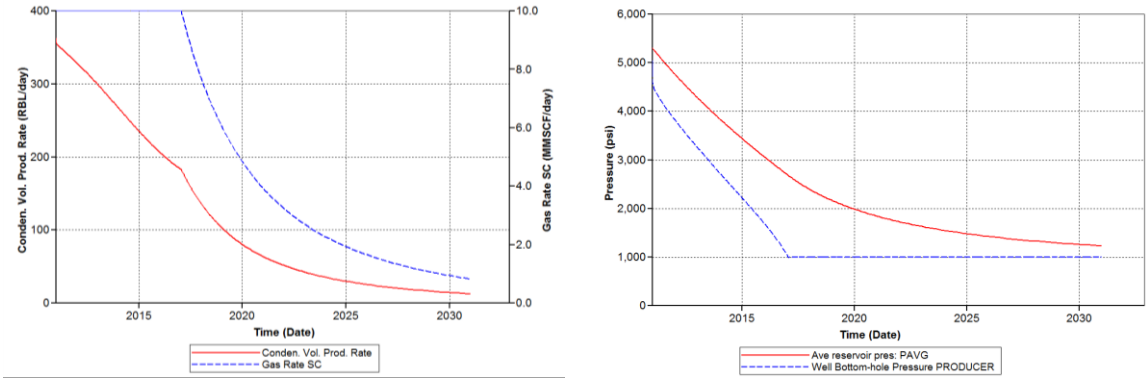

(a) (b)

Figure 27: Primary Depletion of CO_2 Huff-n-Puff Study Reservoir (a) Production Decline (b) Average Reservoir Pressure and Bottom Hole Pressure (Dew Point Pressure is 4800 psia)

Figure 28 and Figure 29 show the oil saturation, gas saturation, and gas relative permeability profile in the near wellbore region of high deliverability zone, resulting from primary depletion with the reservoir subject to pressures significantly below the dew-point of the reservoir fluid. It is clearly seen that condensate bank development resulting from production below the dew-point pressure reduced permeability to gas by about 40% in the near-wellbore region. This condensation extends deep into the reservoir and leads to an equivalent reduction in gas saturation and reduction in gas relative permeability. Figure 28 shows a reduction in gas saturation in the near well bore region from the original value of 85% at the start of the production to 76% after 10 years of production. This miniscule reduction in gas saturation reduces gas relative permeability near-wellbore from 0.5 to 0.28, which is a dramatic reduction of about 44%. Such a reduction can seriously reduce gas and condensate production. The low gas relative permeability would correspondingly reduce gas production. The depletion

study of the CO_2 Huff-n-Puff reservoir shows the importance of improving the gas relative permeability in wet gas systems. CO_2 can be used for this purpose.

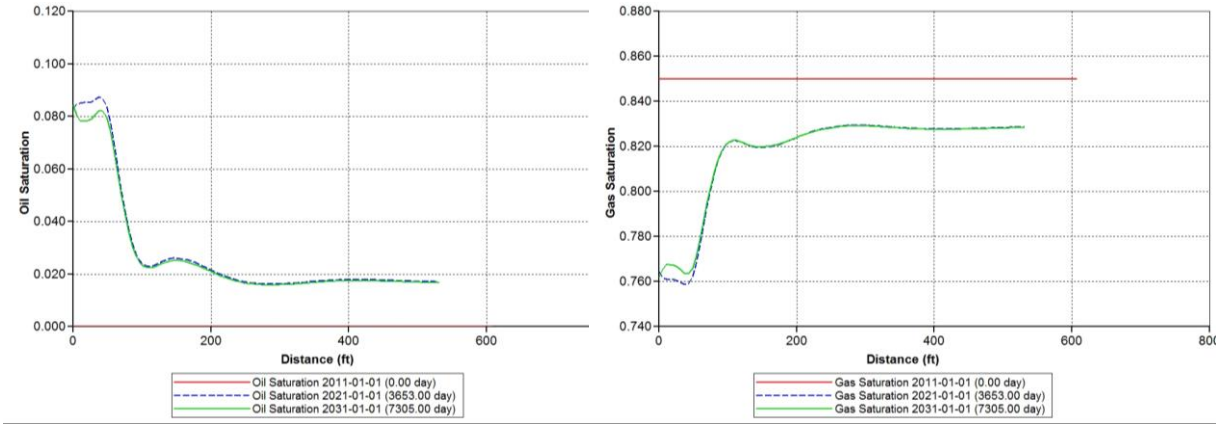

(a) (b)

Figure 28: Depletion Profile Plots (a) Oil Saturation (b) Gas Saturation

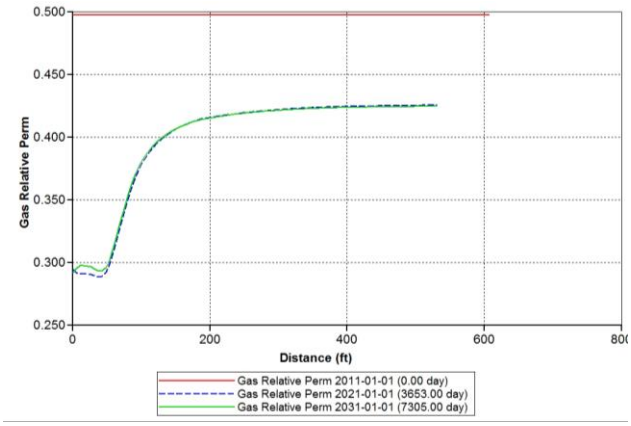

Figure 29: Depletion Gas Relative Permeability Profile Plot

From the profiles shown in Figure 28 and Figure 29, it can be deduced that the appearance of the condensate phase increases over time and hampers the mobility of the gas phase. To remedy this, CO_2 Huff-n-Puff can be implemented for the reduction of

condensate saturation and restoration of gas permeability and gas production. To investigate the potential benefits, CO_2 Huff-n-Puff was applied using the schedule shown in Table 19. The well schedule consists of a gas production period where the well has a target gas production rate of 10 MMSCF/Day. During this primary depletion period, the reservoir pressure is expected to fall below the dew point pressure leading to condensate banking in the near-wellbore region. In order to remove the condensate phase, CO_2 is injected and the well is shut-in to allow time for mass transfer between the condensate/gas and CO_2. This interaction lowers the dew point pressure. Afterwards, production is resumed after the shut-in period to ensure that the condensate bank is removed and gas relatively permeability is improved.

Table 19: CO_2 Huff-n-Puff Well Schedule

Well Event	Well Event Date (Duration)
Gas Production (10 MMSCF/Day)	1/1/2011 to 1/1/2021 (10 years)
CO_2 Injection (10 MMSCF/Day)	1/1/2021 to 3/1/2021 (2 months)
Shut-in Period	3/1/2021 to 6/1/2021 (3 months)
Gas Production (10 MMSCF/Day)	6/1/2021 to 1/1/2031 (9 years and 7 months)

Injection of CO_2 is expected to serve two purposes: (a) miscible interaction with the condensate phase to reduce the dew point pressure of the oil/gas phase, and, (b) re-pressurization of the reservoir so that the pressure is raised above the dew point in the near-wellbore region. These two phenomena are expected to help remove the condensate bank from the reservoir. Reduction of dew-point on mixing of reservoir

gas/condensate with CO_2 is illustrated in Figure 20, which shows relevant portion of the phase envelopes for mixtures of a representative gas/condensate with increasing concentration of CO_2.

As the concentration of CO_2 increases in the gas/condensate system the dew-point pressure is lowered. For example, at a reservoir temperature of 220°F, dew point pressure is around 4800 psia for a mixture with 1.75 mole percent of CO_2 but drops to about 2200 psia when the mole percent of CO_2 is 83.7 mole percent CO_2.

The second benefit of CO_2 injection is to raise the reservoir pressure above the dew point pressure. This can be defined as re-pressurizing the reservoir above a CO_2-concentration-controlled dew point pressure. This phenomenon is investigated by simulating the response of the reservoir for varying injection rates of CO_2 during the two month long "Huff" part of the process. Increasing injection rates lead to increasing the total amount of CO_2 introduced into the reservoir, to larger concentrations of CO_2 in the reservoir, and to larger increases in reservoir pressure, as shown in Figure 31. This trend is beneficial because, as the concentration of CO_2 in the reservoir increases, the dew point pressure reduced according to Figure 20. The dew point reduction trend illustrated by Figure 20 can be further simplified by using Figure 30, which quantitatively illustrates the CO_2 composition necessary to lower the dew point pressure of the wet gas sample.

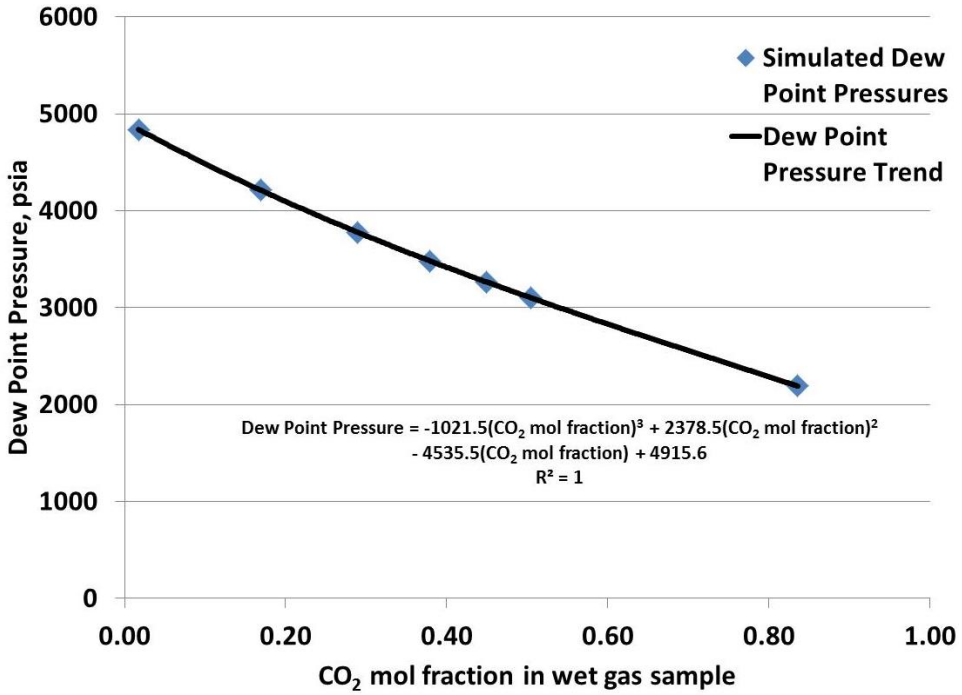

Figure 30: Trend Line of Dew Point Pressure of Wet Gas Sample as Function of CO_2 Composition

In addition to this beneficial trend of CO_2 reducing the dew point pressure of the wet gas sample, the added CO_2 volume raises the reservoir pressure above the CO_2-concentration-controlled dew point pressure. Therefore, increasing the volume of injected CO_2 can force the system to stay above the dew point pressure. Simulation results shown in Figure 31 suggest that increasing the amount of CO_2 injected leads to delayed condensate production decline.

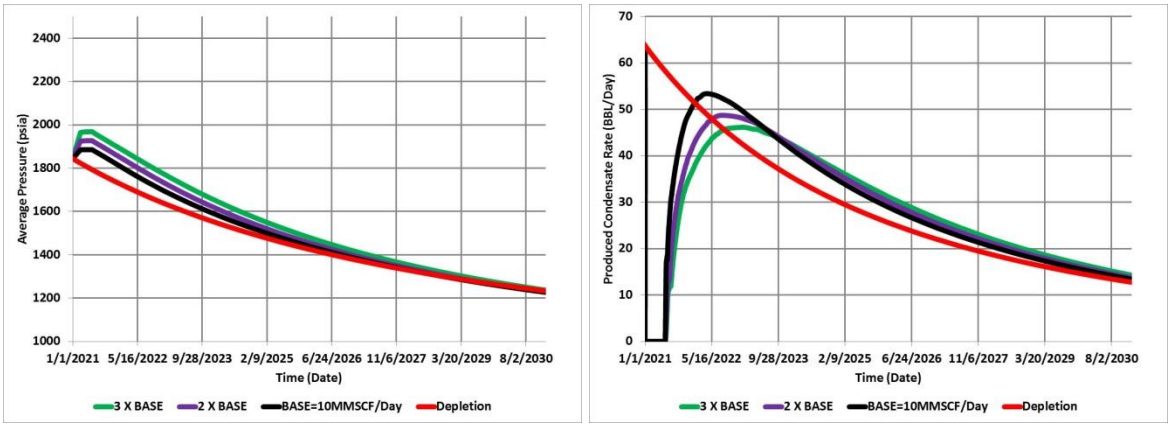

(a) (b)

Figure 31: Pressure Increase Response After CO_2 Injection (a) Average Pressure (b) Condensate Production

Figure 31 also shows that increasing the CO_2 injection rate/amount prolongs the plateau condensate production rate. This observation suggests opportunity for the optimization of Huff-n-puff and Enhanced gas Recovery process. Any hydrocarbon liquids condensing in the reservoir can potentially be vaporized into the gas phase with suitable process design that takes into consideration the economic impact of injecting CO_2 and separating it from the produced gas stream. This is illustrated in Figure 31 and Figure 32 which show that the condensate and gas production rates increase as the CO_2 injection rate/amount increases.

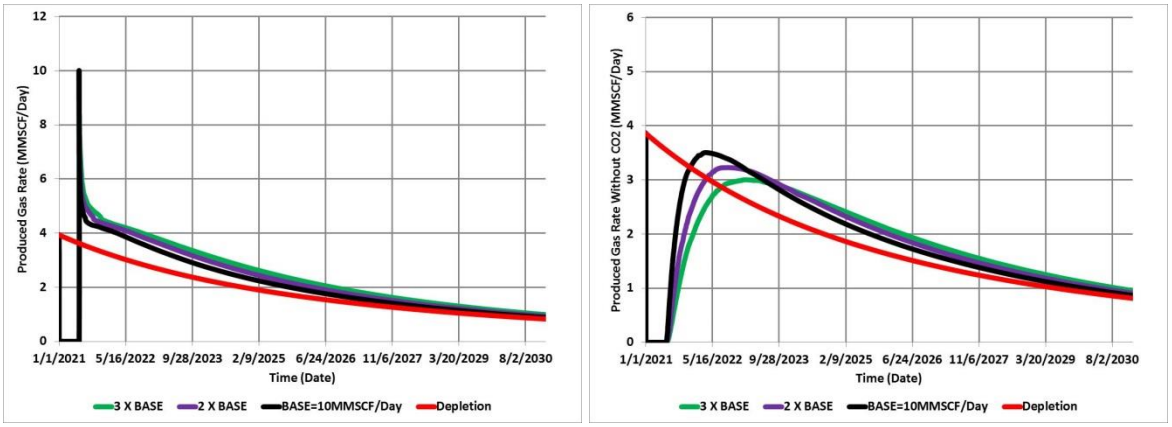

(a) (b)

Figure 32: Gas Production Response After CO_2 Injection (a) Gas Production with CO_2 in Produced Stream (b) Gas Production without CO_2 in Produced Stream.

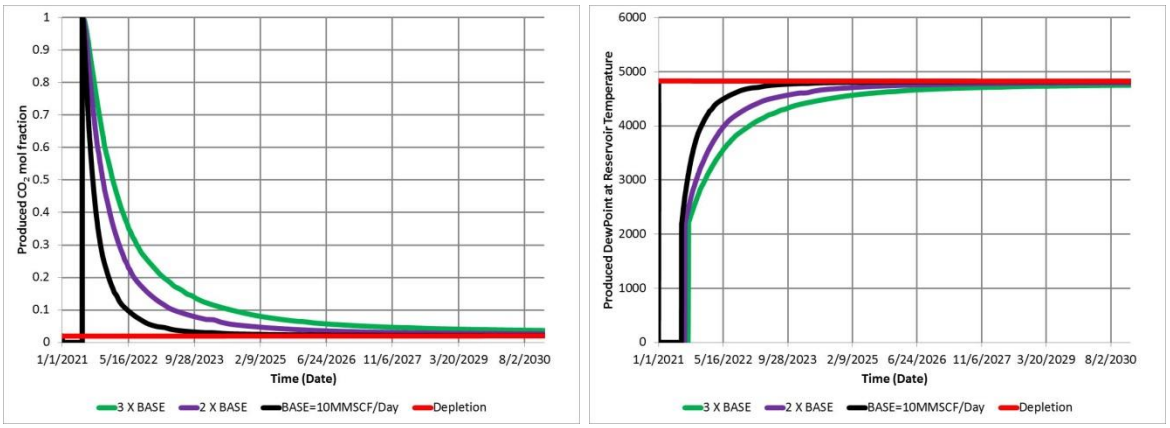

(a) (b)

Figure 33: Produced CO_2 composition and Produced Dew Point Pressure (a) CO_2 Composition (b) Dew Point Pressure

In order to understand the role played by improving the gas mobility, it is important to investigate the oil saturation and gas relative permeability radial profiles after the CO_2 Huff-n-puff treatment. Figure 34 and Figure 35 show profiles of CO_2 concentration, oil saturation, and, gas relative permeability, six months after CO_2 injection and shut-in period. Figure 34 and Figure 35 show that as the injection

rate/amount of CO_2 increases, CO_2 concentration increases, oil saturation is reduced, and the relative permeability to gas is increased. This profile improvement occurs because of the increased in CO_2 concentration in the reservoir. Increasing the CO_2 concentration lowers the dew point pressure of reservoir fluids, as suggested by simulation results shown in Figure 20. Lowering the dew point pressure resulted in re-vaporization of condensed hydrocarbon liquids which, in turn, lowered the oil saturation in the reservoir and increased gas relative permeability.

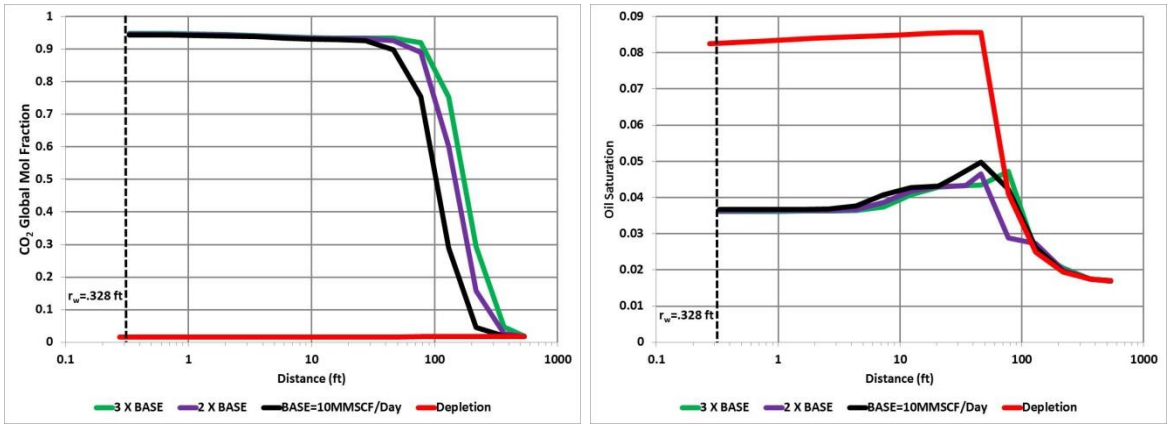

(a) (b)

Figure 34: Profile Plot 6 months After CO_2 Injection (a) CO_2 Concentration (b) Oil Saturation

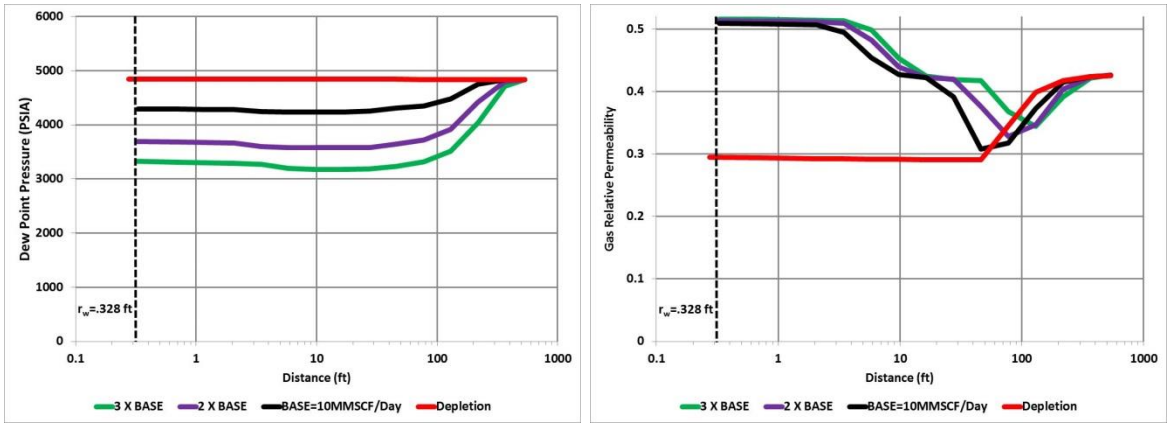

(a) (b)

Figure 35: Profile Plot 6 Months After CO_2 Injection (a) Dew Point Pressure (b) Gas Relative Permeability

This observation is supported also by analysis of the shut in period after CO_2 injection into the reservoir. Using the single phase analogy, the skin factor can be calculated using the condensate blockage radius illustrated by the oil saturation profile plot and the average relative permeability in the condensate blockage zone. For this work the condensate blockage radius is the point where the oil saturation is greater than zero. This is the extent that condensate blockage affects the relative permeability. During the shut in period, the CO_2 mixed with condensate and resulted in a condensate blockage radius of 536 ft.

Table 20: Condensate Blockage Skin Calculation

	condensate blockage zone radius, ft	average relative permeability	condensate blockage skin
Depletion	536	0.329	15.1
BASE=10MMSCF/Day	536	0.432	9.72
2 X BASE	536	0.442	9.35
3 X BASE	536	0.449	9.08

It is evident that CO_2 improves the gas relative permeability in the condensate blockage zone. It reduces the condensate blockage skin for all cases of injection. There is a distinct trend (demonstrated by Table 20) that shows that the condensate blockage skin is reduced as the CO_2 injection rate is increased. It has been illustrated that CO_2 is able reduce condensate blockage skin. Further analysis involves optimization of CO_2 EGR and Sequestration and is illustrated in subsequent chapters regarding the process design and optimization of the CO_2 EGR and Sequestration process.

6 CO_2 EGR AND SEQUESTRATION PROCESS DESCRIPTION

The CO_2 EGR and CO_2 Sequestration process involves using CO_2 to reduce condensate banks while storing CO_2. To bring CO_2 EGR and CO_2 Sequestration into an economic reality it is important to consider the primary components in the process. This can be done by considering the different stages of this process which are capture, transportation, injection, and production of CO_2.

To consider CO_2 EGR and CO_2 Sequestration consider the process flow diagram illustrated by Figure 36. From this diagram it can be seen that CO_2 originates from the power generation and CO_2 capture process indicated by the Power Generation with CO_2 Capture block. In this process, power is generated from a combustion process which results in a flue gas stream. This flue gas stream is then stripped of CO_2 and dehydrated. In this work, four power generation coupled with CO_2 capture technologies are considered. Specifically they are Post-combustion Capture from Coal-fired Power Generation by Amines (CFGA), Pre-combustion CO_2 Capture from Integrated Gasification Combined Cycles (IGCC), Oxy-combustion CO_2 Capture from Pulverized Coal Power Generation (OPC), and Post-combustion CO_2 Capture from Natural Gas Combined Cycles (NGCC).

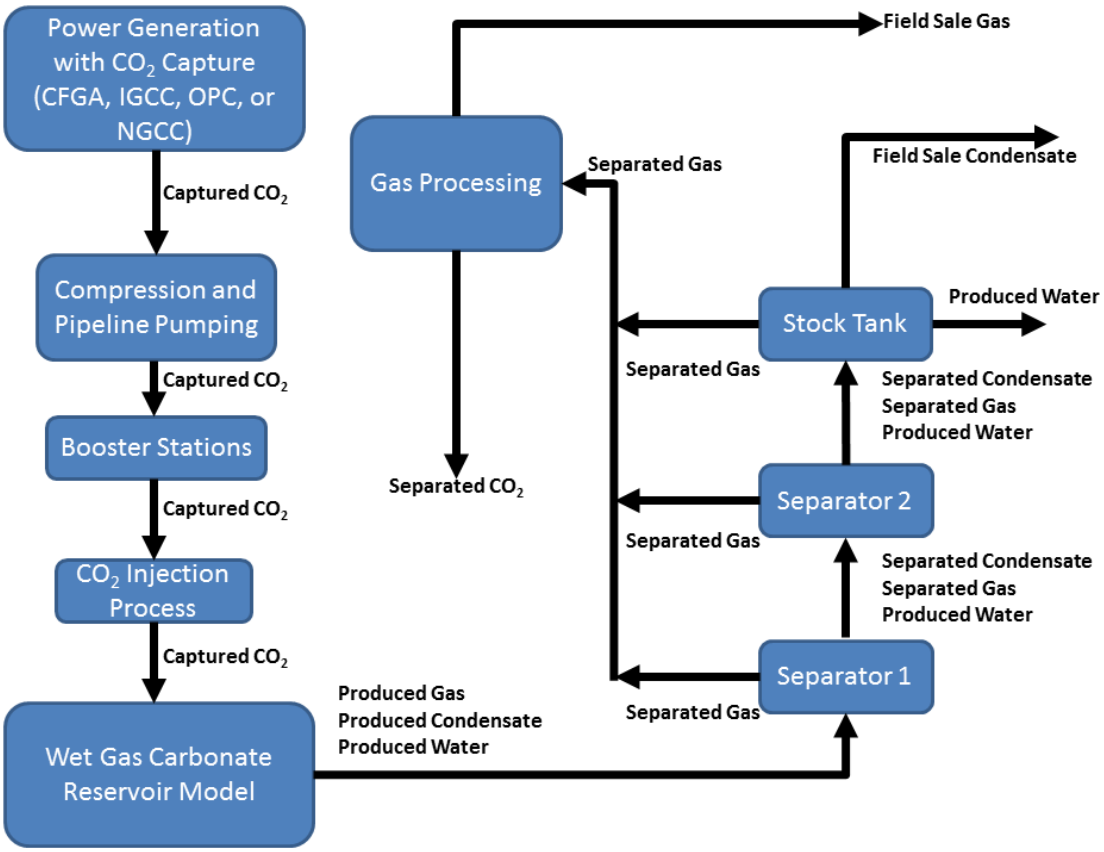

Figure 36: CO_2 EGR and CO_2 Sequestration Process Flow Diagram

CFGA captures CO_2 from the flue gases by using a liquid solvent (usually mono-ethanolamine) to strip the CO_2 from the nitrogen rich flue gas stream. A simple process diagram of this process can be seen in Figure 37 in the post combustion process description. For the case of CFGA, CO_2 is generated by the combustion of coal in the presence of air. This combustion process generates power, heat, and a resultant flue gas (approximately 3-15% CO_2 by volume) stream. This flue gas stream is stripped using mono-ethanolamine and the resultant CO_2 rich stream is compressed and dehydrated for transport for EOR, EGR, and or CO_2 Sequestration (IPCC, 2005).

IGCC, illustrated in Figure 37 in the pre-combustion process description, captures CO_2 with a process which involves the creation of synthesis gas. Synthesis gas is created by combining a primary combustible fuel with steam and air or oxygen which then reacts to form and produce a gas stream consisting of carbon monoxide and hydrogen. CO_2 is generated by reaction of this carbon monoxide combined with steam in a second reactor (results in a stream of 15% to 60% CO_2 by volume). CO_2 and hydrogen, the products of this reaction, can then be separated into two separate streams. From this point CO_2 is compressed and dehydrated for transport for EOR, EGR, and or CO_2 Sequestration while the hydrogen is used as extra fuel in generating power (IPCC, 2005).

OPC, illustrated in Figure 37 in the Oxyfuel process description, captures CO_2 by first using oxygen instead of air in the combustion of a pulverized coal. The result of this combustion is a flue gas stream consisting of water vapor and CO_2 (80% by volume). The resultant CO_2 is then dehydrated and compressed for EOR, EGR, and or CO_2 Sequestration (IPCC, 2005). OPC requires near pure oxygen which can be obtained from upstream separation of oxygen from air.

NGCC is similar to CFGA. Instead of using coal as the primary fuel, NGCC uses natural gas as the primary fuel. From there it follows a process similar to CFGA which results in the compression and dehydration for transport for EOR, EGR, and or CO_2 Sequestration.

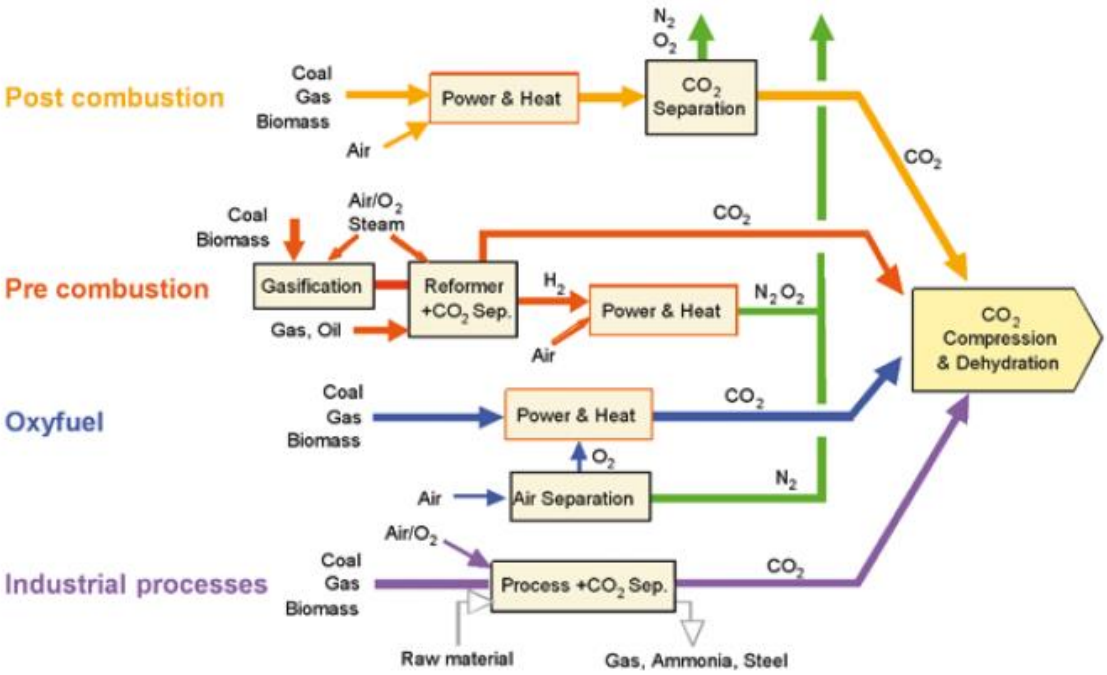

Figure 37: Overview of CO_2 Capture Processes (IPCC, 2005)

After the CO_2 is captured and dehydrated it is compressed and pumped through a pipeline network to an injection site. This process is represented in Figure 36 by the Compression and Pipeline Pumping block. Also, depending on the distance from the CO_2 capture site booster stations (represented by the Booster Station block) are needed to insure that the captured CO_2 is able to maintain pressures consistent with the super-critical or liquid phase. Once the captured CO_2 reaches the injection site it is injected into the carbonate reservoir. This process is represented by the CO_2 Injection Process and Wet Gas Carbonate Reservoir Model blocks in Figure 36. Following the process streams indicated by Figure 36, some of the CO_2 is produced back along with condensate, water, and other gases. From there it undergoes separation through 3 stages (represented by Separator 1, Separator 2, and Stock Tank). Each subsequent pass

through the separator process results in more gas produced and transferred to gas processing. Each subsequent pass through the separator process also produces condensates until it reaches the final stage of sale condensate. The gas separated during the separation stage undergoes more separation in the gas processing stage where sour gas such as CO_2 is separated from sale gas.

The primary focus of this work is to get a fundamental understanding on the subsurface phenomenon of CO_2 interaction with the many components in the hydrocarbon carbonate reservoir but it is important to understand the basics in getting captured CO_2 to a stage of injection. To understand this process an economic model is constructed that simulates the economics of capturing, compressing, pumping, injection, and storing CO_2. This economic model is necessary for the characterization and optimization of the CO_2 EGR and CO_2 Sequestration Process.

7 CO_2 EGR AND SEQUESTRATION ECONOMIC MODEL

The economic model used for the CO_2 EGR and Sequestration process describes the economics associated with the capture, compression, pumping, injection, recycle, and storage of CO_2 for the combined CO_2 EGR and Sequestration process. The calculation procedure for this model follows some of the guidelines proposed by others (Algharaib and Abu Al-Soof, 2008). In addition to this there are notable reports already completed like the International Energy Agency's "Cost and Performance of CO_2 Capture from Power Generation" that give an overview of the potential parameters associated with capturing CO_2 from different forms of power generation (Finkenrath, 2011). The economic model's primary purpose is to give reasonable estimates of the capital expense associated with the CO_2 Enhanced Gas Recovery and Sequestration process. The economic model considers four current CO_2 capture technologies from power generation which are CFGA, IGCC, NGCC, and OPC. It also considers CO_2 impurities of 2 mol%N_2, 4 mol%N_2, 6 mol%N_2, 8 mol%N_2, and 10 mol%N_2. This analysis requires the use of robust reliable thermodynamic simulator that can characterize CO_2 in the midst of impurities. Because of this, the NIST Standard Reference Database was used with a Peng Robinson equation of state (Lemmon *et al.*, 2010). In addition to this, unit conversions between captured CO_2 mass and captured CO_2 volume was done using a correlation by Barrufet *et al.* (2010). The economic model consists of five modules which are a Capturing Cost Module, Compression Cost

Module, Transportation Cost Module, and Storage Cost Module, and Injection Cost Module.

7.1 Capturing Cost Module

The Capturing Cost module purpose is to determine the economics of capturing CO_2 from power generation. It uses a methodology proposed by David (2000). The Capturing Cost module uses four different power generation technologies which are Post-combustion CO_2 capture from Coal-fired Power Generation by Amines (CFGA), Pre-combustion CO_2 Capture from Integrated Gasification Combined Cycles (IGCC), Oxy-combustion CO_2 Capture from Pulverized Coal Power Generation (OPC), and Post-combustion CO_2 Capture from Natural Gas Combined Cycles (NGCC). The economic data for these processes was found in documents from the IEA (Finkenrath, 2011). A summary of this data for the different power generation technologies can be seen in Table 21.

Table 21: CO_2 Capture from Power Generation Economics for CFGA, IGCC, OPC, and NGCC (Finkenrath, 2011)

	CFGA	IGCC	OPC	NGCC
Net Power output without capture, MW	582	633	566	528
Net Power output with capture, MW	545	546	543	461
Net efficiency without capture, LHV %	41.4	41.4	41.6	56.6
Net efficiency with capture, LHV %	30.9	33.1	31.9	48.4
CO_2 emissions without capture, kg/MWh	820	793	825	370
CO_2 emissions with capture, kg/MWh	111	115	59	55
Capital cost without capture, USD/kW	1899	2356	1931	925
Capital cost with capture, USD/kW	3135	3166	3153	1541
Relative decrease in net efficiency, %	25	20	23	15
LCOE without capture, USD/MWh	66	75	62	77
LCOE with capture, USD/MWh	107	104	102	102
Cost of CO_2 avoided, USD/tCO_2	58	43	52	80

To calculate capture cost per amount of CO_2 requires first determining the cost of generating power with and without CO_2 capture. The following expression can be used calculate the cost of generating power without CO_2 (David, 2000).

$$COE = A_c + B_c \quad \textbf{(57)}$$

Where A_c is the capital cost without CO_2 capturing facilities in \$/kWh and B_c is the fuel and operational cost to generate 1-kWh without CO_2 capturing facilities in \$/kWh. The following expression can be used to calculate the cost of generating power with CO_2 (David, 2000).

$$COEW = D_c + E_c \quad \textbf{(58)}$$

Where D_c is the capital cost with CO_2 capturing facilities in \$/kWh and E_c is the fuel and operational cost to generate 1-kWh with CO_2 capturing facilities in \$/kWh. The capture

cost per amount of CO_2 captured can be calculated using COEW and COE and the following expression (David, 2000).

$$C_{cap} = \frac{[COEW - COE]}{G_c} \quad \textbf{(59)}$$

Where G_c is the tones of CO_2 emitted per 1 –kWh of electricity generated in tones/kWh and C_{cap} is the capture cost per amount of CO_2 captured. Using the above expressions and Table 21 the following values were calculated for the different capture technologies.

Table 22: CO2 Capture Values for CFGA, IGCC, OPC, and NGCC

	CFGA	IGCC	OPC	NGCC
Cost of Generating Power without CO_2 capture, \$/kWh	1899	2356	1931	925
Cost of Generating Power with CO_2 capture, \$/kWh	3135	3166	3153	1541
Capture Cost per amount CO_2 captured, \$/MSCF	0.59	0.37	1.09	0.59
Capture Cost per amount CO_2 captured, \$/tonne	11.14	7.04	20.71	11.20
Capital Cost of Capture Facility, MM\$	1709	1729	1712	710

The annualized facility cost can be calculated based on the values determined in Table 22. The annual facility cost can determined using the following equation.

$$C_{capfacility} = \frac{CAPEX_{capfacility}}{t_{dep}} \quad \textbf{(60)}$$

Where $CAPEX_{capfacility}$ is the capital cost of the capture facility and t_{dep} is the total length of the project. The annual capital capture cost is one component of the overall costs of the CO_2 EGR and Sequestration project. The next module deals with determining the cost of compressing the CO_2 after capture.

7.2 Compression Cost Module

The Compression Cost Module's purpose is to determine the economics associated with compressing and pumping the captured CO_2 to the injection site. It follows the approach outlined by McCollum and Ogden (2006). To begin, it is assumed that the captured CO_2 from power generation is captured at .1 MPa (approximately 1 atm) and 289K (60 ^{o}F). At this stage the captured CO_2 is in the gas phase and therefor requires a compressor to compress it to the liquid or supercritical phase for pumping to the injection site. According to McCollum and Ogden, 15 MPa (2176 psia) is a suitable pressure for pipeline transport to the injection site. To reach this pressure for pure CO_2 requires first compressing from the inlet pressure of .1MPa to a cut off pressure that brings the captured CO_2 to the liquid or super critical phase (at 60^{o}F). To do this McCollum and Ogden recommended that this be done in 5 stages of compression starting with the inlet .1MPa pressure. Using this assumption the compression ratio of each stage, *CR*, can be determined using the following expression (McCollum and Ogden, 2006).

$$CR = \left(\frac{P_{cut-off}}{P_{initial}} \right)^{1/N_{stage}} \quad \textbf{(61)}$$

Where $P_{cut\text{-}off}$ is the cut off pressure of the captured CO_2 at 289K (60^{o}F), $P_{initial}$ is the inlet pressure into the compressor (.1 MPa), and N_{stage} is the number of stages used for compression. The cut off pressure and the compression ratio of each stage of the different impurities of captured CO_2 can be seen in Table 23.

Table 23: Cut-off Pressure and Compression Ratio for Different CO_2 Impurities

mol fraction CO_2 in N2	Pinitial, Mpa	Pcut-off, Mpa	Pcut-off, psia	Cut-off Phase	CR
1	0.1	5.16	748	supercritical	2.20
0.98	0.1	5.36	777	liquid	2.22
0.96	0.1	5.56	807	liquid	2.23
0.94	0.1	5.80	841	liquid	2.25
0.92	0.1	6.06	879	liquid	2.27
0.9	0.1	6.32	917	liquid	2.29

Using the following expression, the compression ratio calculation can then be used to calculate the power requirement, $W_{s,i}$, for the i^{th} stage of compression (McCollum and Ogden, 2006).

$$W_{s,i} = \left(\frac{1000}{24 \cdot 3600}\right)\left(\frac{mZ_{sc}RT_{in}}{M_{sc}\eta_{is}}\right)\left(\frac{k_{sc}}{k_{sc}-1}\right)\left[(CR)^{\frac{k_{sc}-1}{k_{sc}}}-1\right] \quad \textbf{(62)}$$

Where m is the mass rate of captured CO_2 in tonnes/day, R is the ideal gas constant of 8.314 J/mol*K, T_{in} is the inlet temperature to the compressor which is 289K (60 ^oF), M_{sc} is the molecular weight of the captured CO_2, η_{is} is the isentropic efficiency of the compressor set a .75 for this work, Z_{sc} is the compressibility factor for the captured CO_2, and k_{sc} is the ratio of the specific heat at constant pressure to the specific heat at constant volume for each individual stage. Using the methodology endorsed by McCollum and Ogden, the parameters k_{sc} and Z_{sc} are evaluated at the temperature of the compressor (set to 356K or 181^oF) and the average pressure between the inlet and outlet pressure of the compressor. The calculation of the compressor power per tonne of captured CO_2 injected per day as a functiuon of CO2 captured composition can be seen in Tables 24 through Table 29.

Table 24: Compressor Power Requirement Per Stage for 100 mol% CO_2 at Compressor Temperature of 356 K

Stage	Inlet Pressure , MPa	Outlet Pressure, MPa	Average Pressure, MPa	Z_{sc}	k_{sc}	W_{si}/m, kW/tonne/day
1	0.1	0.24	0.17	0.99534	1.2708	0.719
2	0.24	0.56	0.4	0.98901	1.2783	0.716
3	0.56	1.32	0.94	0.974	1.2969	0.708
4	1.32	3.12	2.22	0.93761	1.3478	0.690
5	3.12	5.16	4.14	0.88075	1.447	0.662

Table 25: Compressor Power Requirement Per Stage for 98 mol% CO_2 and 2 mol% N_2 at Compressor Temperature of 356 K

Stage	Inlet Pressure , MPa	Outlet Pressure, MPa	Average Pressure, MPa	Z_{sc}	k_{sc}	W_{si}/m, kW/tonne/day
1	0.1	0.24	0.17	0.99546	1.2725	0.737
2	0.24	0.56	0.4	0.98929	1.2799	0.734
3	0.56	1.32	0.94	0.97469	1.2983	0.727
4	1.32	3.12	2.22	0.9394	1.3481	0.708
5	3.12	5.36	4.24	0.88153	1.4499	0.679

Table 26: Compressor Power Requirement Per Stagefor 96 mol% CO_2 and 4 mol% N_2 at Compressor Temperature of 356 K

Stage	Inlet Pressure , MPa	Outlet Pressure, MPa	Average Pressure, MPa	Z_{sc}	k_{sc}	W_{si}/m, kW/tonne/day
1	0.1	0.24	0.17	0.99558	1.2743	0.756
2	0.24	0.56	0.4	0.98958	1.2816	0.753
3	0.56	1.32	0.94	0.97539	1.2996	0.745
4	1.32	3.12	2.22	0.94118	1.3483	0.727
5	3.12	5.56	4.34	0.88249	1.4525	0.697

Table 27: Compressor Power Requirement Per Stage for 94 mol% CO_2 and 6 mol% N_2 at Compressor Temperature of 356 K

Stage	Inlet Pressure , MPa	Outlet Pressure, MPa	Average Pressure, MPa	Z_{sc}	k_{sc}	W_{si}/m, kW/tonne/day
1	0.1	0.24	0.17	0.9957	1.276	0.775
2	0.24	0.56	0.4	0.98986	1.2832	0.772
3	0.56	1.32	0.94	0.97608	1.301	0.765
4	1.32	3.12	2.22	0.94295	1.3486	0.747
5	3.12	5.80	4.46	0.88324	1.4557	0.716

Table 28: Compressor Power Requirement Per Stage for 92 mol% CO_2 and 8 mol% N_2 at Compressor Temperature of 356 K

Stage	Inlet Pressure , MPa	Outlet Pressure, MPa	Average Pressure, MPa	Z_{sc}	k_{sc}	W_{si}/m, kW/tonne/day
1	0.1	0.24	0.17	0.99582	1.2778	0.796
2	0.24	0.56	0.4	0.99015	1.2849	0.793
3	0.56	1.32	0.94	0.97678	1.3024	0.786
4	1.32	3.12	2.22	0.94472	1.349	0.769
5	3.12	6.06	4.59	0.88381	1.4594	0.737

Table 29: Compressor Power Requirement Per Stage for 90 mol% CO_2 and 10 mol% N_2 at Compressor Temperature of 356 K

Stage	Inlet Pressure , MPa	Outlet Pressure, MPa	Average Pressure, MPa	Z_{sc}	k_{sc}	W_{si}/m, kW/tonne/day
1	0.1	0.24	0.17	0.99594	1.2797	0.818
2	0.24	0.56	0.4	0.99044	1.2866	0.815
3	0.56	1.32	0.94	0.97748	1.3038	0.808
4	1.32	3.12	2.22	0.94647	1.3493	0.791
5	3.12	6.32	4.72	0.8846	1.4628	0.758

The total compressor power, $W_{s\text{-}total}$, can be determined by assuming the compressor power for each stage by using the following expression (McCollum and Ogden, 2006).

$$W_{s-total} = \sum_{i=1}^{N_{stage}} W_{s,i} \quad \textbf{(63)}$$

The total compressor work as a function of captured CO_2 composition is illustrated in Figure 38.

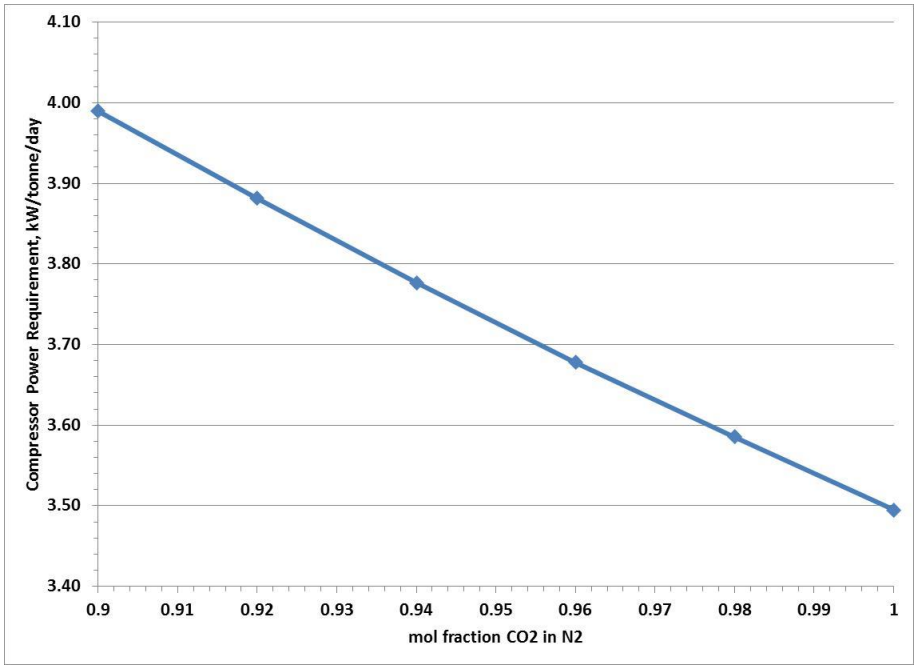

Figure 38: Compressor Power Requirement as Function of CO_2 Composition in Captured CO_2

To calculate the corresponding cost associated with pumping the captured CO_2 requires first determining the number of parallel compressor trains. The CO_2 flows into these compressor trains in parallel and the required power for each train is 100/Ntrain % of the flow/power, where N_{train} represents the number of compressor trains. In addition to this it is assumed that each compressor train is rated at 40,000 kW. Using this assumption the number of compressor trains needed as a function of the total compressor

work is $N_{train}=W_{s\text{-}total}/40000$. The mass rate through each compressor train, m_{train} in kg/s, can then be calculated using the following expression (McCollum and Ogden, 2006).

$$m_{train} = \frac{1000 \cdot m}{24 \cdot 3600 \cdot N_{train}} \tag{64}$$

The total capital cost in USD for each compressor can then be calculated using the following expression from McCollum and Ogden (2006).

$$C_{comp} = m_{train} N_{train} \left[\left(0.13 \times 10^6\right)\left(m_{train}{}^{-0.71}\right) + \left(1.40 \times 10^6\right)\left(m_{train}{}^{-0.60}\right) \ln\left(\frac{P_{cut-off}}{P_{initial}}\right) \right] \tag{65}$$

The required cost per kW can be determined by dividing the compressor cost by the total compressor power requirement. The result of this calculation can be seen in Figure 39.

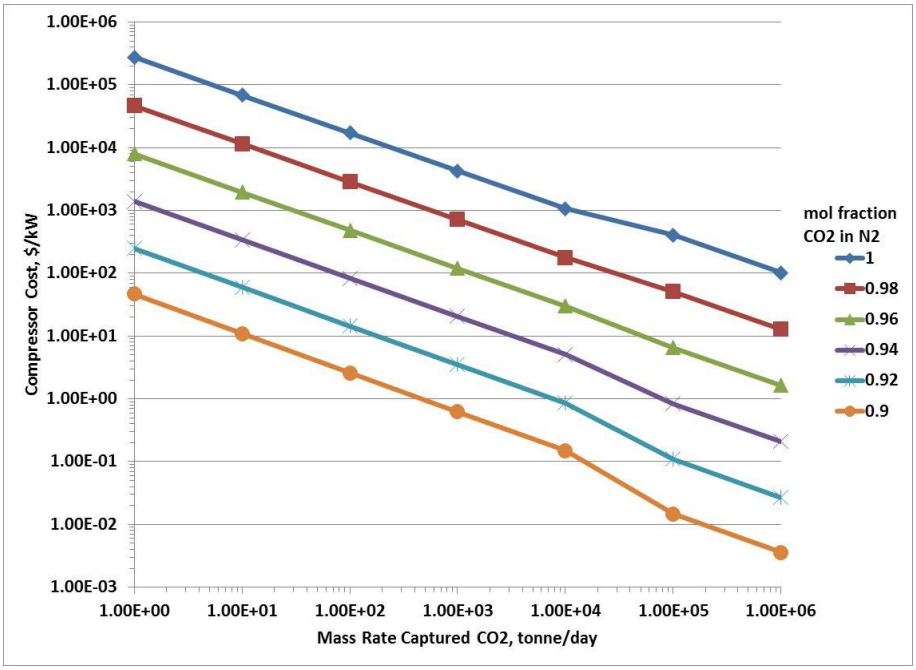

Figure 39: Compressor Cost for Different Captured CO_2 Impurities

The pumping power, W_p in kW/tonne/day, required to boost the compressed captured CO_2 to the injection site can be found using the following expression (McCollum and Ogden, 2006).

$$W_p = \left(\frac{1000 \cdot 10}{24 \cdot 3600}\right)\left[\frac{m\left(P_{final} - P_{cut-off}\right)}{\rho_p \eta_p}\right] \quad \textbf{(66)}$$

Where P_{final} is the injection pressure at the injection site, η_p is the efficiency of the pump, and ρ_p is the density of the captured CO_2 evaluated at 356 K (181 F) and at the average pressure between $P_{cut\text{-}off}$ and P_{final}. To determine the pumps capital cost, C_{pump}, requires using the pumping power expression and the following equation adapted from McCollum and Ogden (2006).

$$C_{pump} = \left(1.11 \times 10^6\right)\left(\frac{W_p}{1000}\right) + 0.07 \times 10^6 \quad \textbf{(67)}$$

The required cost per kW can be determined by dividing the pump cost by the total pumping power requirement. The result of this calculation can be seen in Figure 40.

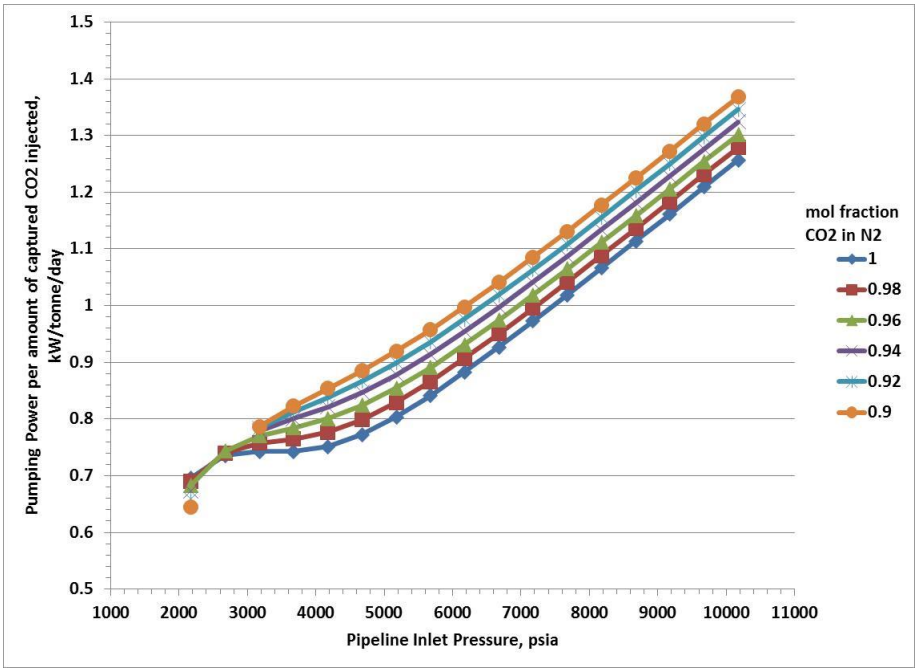

Figure 40: Pumping Cost for Different Captured CO_2 Impurities

The total annualized capital cost of the compressor and pump can be determined by first summing the compression and pump costs and then dividing the total by the project's depreciation time. This procedure can be seen in the following expressions (McCollum and Ogden, 2006).

$$CAP_{c-p} = C_{comp} + C_{pump} \quad \textbf{(68)}$$

$$CAPEX_{c-p} = \frac{CAP_{c-p}}{t_{dep}} \quad \textbf{(69)}$$

The total annualized capital cost of the compressor and pump at a pipeline inlet pressure of 2175 psia can be seen in Figure 41 for different CO_2 impurities.

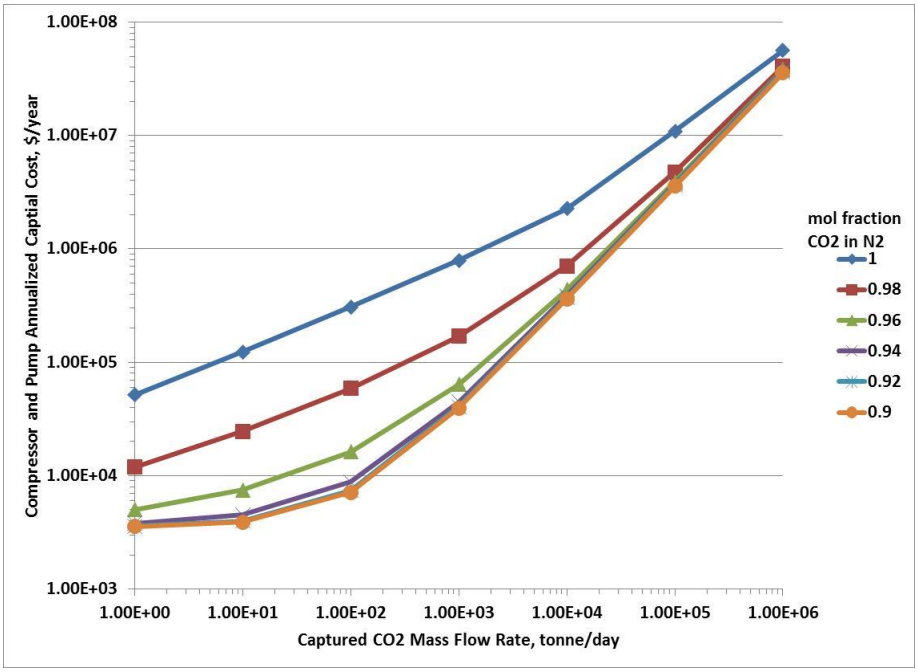

Figure 41: Compressor and Pump Annualized Capital Cost at 2175 psia

The annual cost of electricity is dependent on the cost of electricity, P_e, provided by the CO_2 capture by power generation plant. These costs are listed in Table 22. The annual electricity cost of compressing and pumping can be determined using the values listed in Table 22 and the following expression (McCollum and Ogden, 2006).

$$E_{c-p} = \left(W_{s-total} + W_p\right) P_e C_F \quad \textbf{(70)}$$

Where C_F represents the capacity factor for the compressor and pumps (0.8 for this work). The annual cost of electricity illustrated in Figure 42 for different CO_2 impurities and different capture technologies.

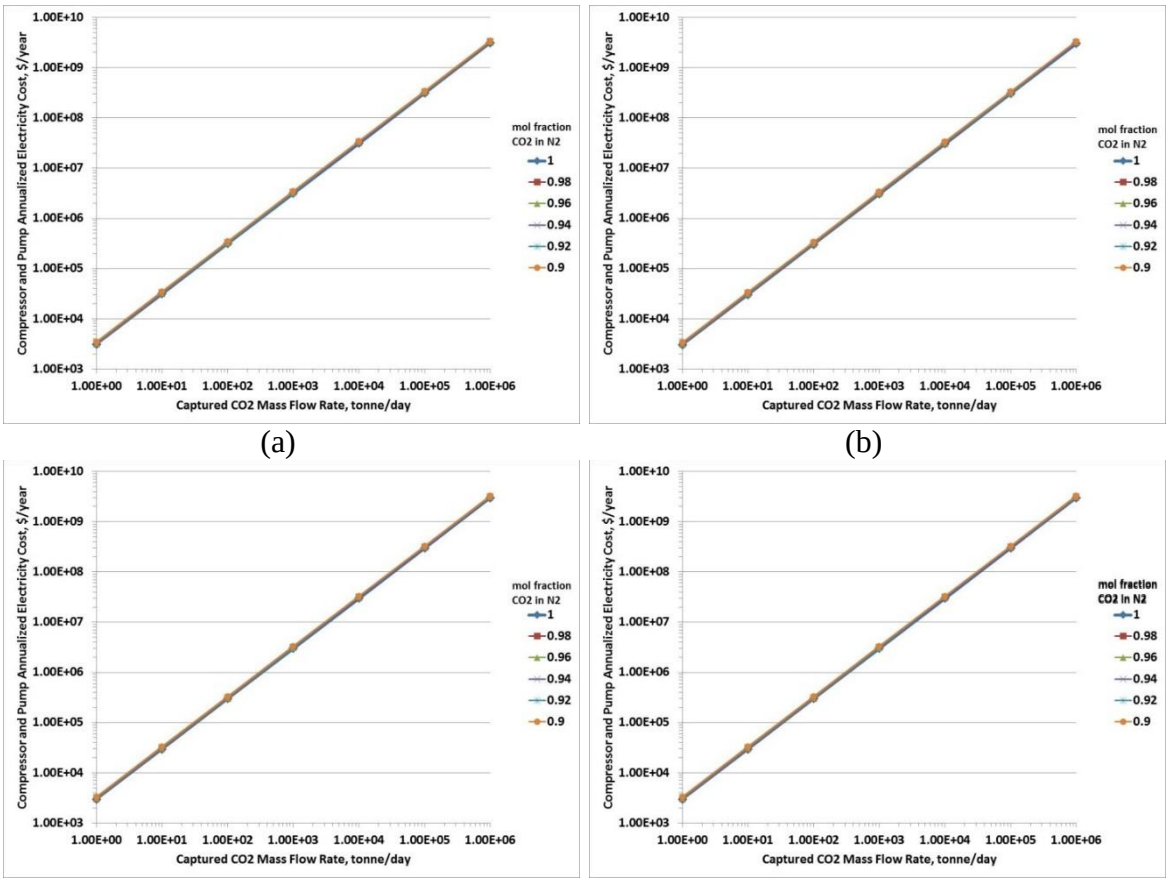

Figure 42: Compressor and Pump Annualized Electricity Costs at 2175 psia Pumping Pressure (a) CFGA, (b) IGCC, (c) OPC, (d) NGCC

These plots illustrate that CO_2 impurity does not have a significant impact on compressor and pump annualized electricity cost. The compressor and pump operating expense can be determined using the following expression, where C_{CCF} is the capital cost factor of the pump and compressor (0.04 for this work) (McCollum and Ogden, 2006).

$$OPEX_{c-p} = C_{CCF} CAP_{c-p} + E_{c-p} \quad \textbf{(71)}$$

The compressor and pump operating expense for each capture technology (assumes that pump is rated up to 2175 psia) is illustrated in Figure 43 as a function of capture rate and CO_2 impurity.

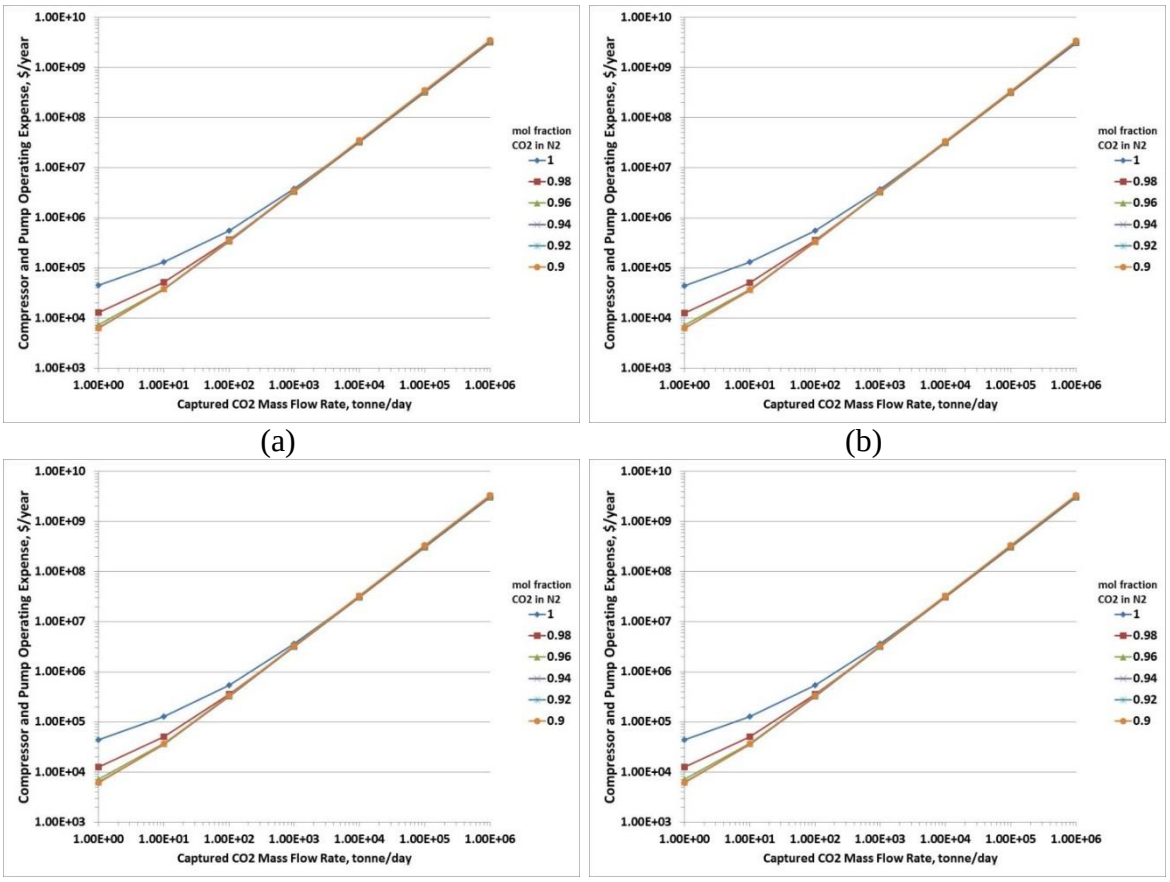

Figure 43: Compressor and Pump Operating Expense at 2175 psia Rating (a) CFGA, (b) IGCC, (c) OPC, (d) NGCC

The compressor and pump annual expense, C_{c-p}, can be determined using the following expression (McCollum and Ogden, 2006).

$$C_{c-p} = CAPEX_{c-p} + OPEX_{c-p} \quad \textbf{(72)}$$

The compressor and pump annual expense for each capture technology (assumes that pump is rated up to 2175 psia) is illustrated in Figure 44 as a function of capture rate and CO_2 composition.

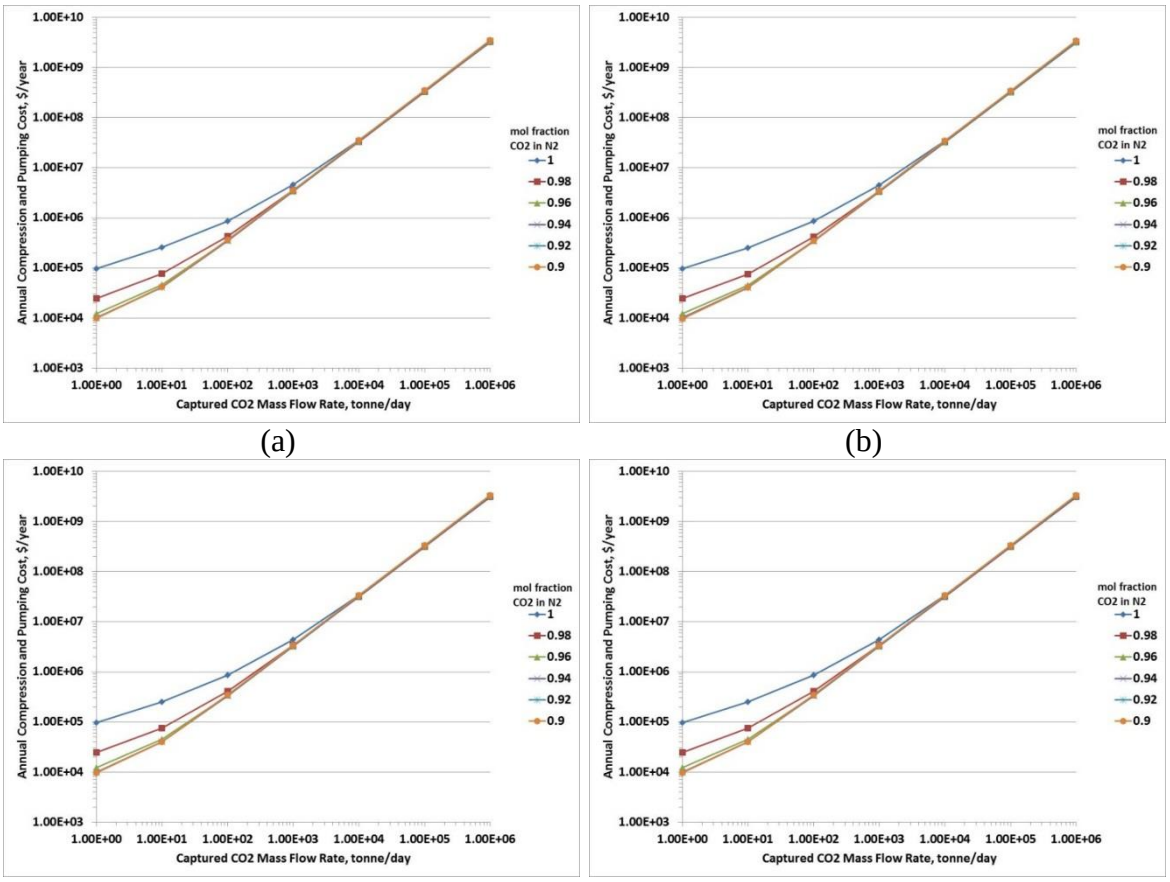

Figure 44: Compressor and Pump Annualized Cost at 2175 psia Rating (a) CFGA, (b) IGCC, (c) OPC, (d) NGCC

The compressor and pump annual expense for each capture technology was fitted using a third order polynomial expression of the following form.

$$C_{c-p} = a_{c-p}m^3 + b_{c-p}m^2 + c_{c-p}m + d_{c-p} \quad \textbf{(73)}$$

Where m is in tonnes/day and $a_{c\text{-}p}$, $b_{c\text{-}p}$, $c_{c\text{-}p}$, $d_{c\text{-}p}$ are regression coefficients. The regression parameters for the compressor and pump annual expense for each capture technology (assumes that pump is rated up to 2175 psia) are listed in Tables 30 through Table 33 as a function of pressure and CO_2 composition.

Table 30: CFGA Regression Coefficients for Compressor and Pump Annualized Costs

mol fraction CO_2 in N_2	$a_{c\text{-}p}$	$b_{c\text{-}p}$	$c_{c\text{-}p}$	$d_{c\text{-}p}$	R^2
1	2.00E-09	-2.20E-03	3532.9	448655	1.00
0.98	4.00E-10	-4.00E-04	3330.7	82254	1.00
0.96	7.00E-11	-8.00E-05	3348.4	19449	1.00
0.94	1.00E-11	-2.00E-05	3405.5	8608	1.00
0.92	3.00E-12	-3.00E-06	3470.8	6713.2	1.00
0.9	5.00E-13	-5.00E-07	3539.6	6376	1.00

Table 31: IGCC Regression Coefficients for Compressor and Pump Annualized Costs

mol fraction CO_2 in N_2	$a_{c\text{-}p}$	$b_{c\text{-}p}$	$c_{c\text{-}p}$	$d_{c\text{-}p}$	R^2
1	2.00E-09	-2.20E-03	3444.8	448655	1.00
0.98	4.00E-10	-4.00E-04	3240.8	82254	1.00
0.96	7.00E-11	-8.00E-05	3256.7	19449	1.00
0.94	1.00E-11	-2.00E-05	3312	8608	1.00
0.92	3.00E-12	-3.00E-06	3375.3	6713.2	1.00
0.9	5.00E-13	-5.00E-07	3442.2	6376	1.00

Table 32: OPC Regression Coefficients for Compressor and Pump Annualized Costs

mol fraction CO_2 in N_2	a_{c-p}	b_{c-p}	c_{c-p}	d_{c-p}	R^2
1	2.00E-09	-2.20E-03	3386	448655	1.00
0.98	4.00E-10	-4.00E-04	3180.9	82254	1.00
0.96	7.00E-11	-8.00E-05	3195.6	19449	1.00
0.94	1.00E-11	-2.00E-05	3249.6	8608	1.00
0.92	3.00E-12	-3.00E-06	3311.7	6713.2	1.00
0.9	5.00E-13	-5.00E-07	3377.2	6376	1.00

Table 33: NGCC Regression Coefficients for Compressor and Pump Annualized Costs

mol fraction CO_2 in N_2	a_{c-p}	b_{c-p}	c_{c-p}	d_{c-p}	R^2
1	2.00E-09	-2.20E-03	3386	448655	1.00
0.98	4.00E-10	-4.00E-04	3180.9	82254	1.00
0.96	7.00E-11	-8.00E-05	3195.6	19449	1.00
0.94	1.00E-11	-2.00E-05	3249.6	8608	1.00
0.92	3.00E-12	-3.00E-06	3311.7	6713.2	1.00
0.9	5.00E-13	-5.00E-07	3377.2	6376	1.00

7.3 Transportation Cost Module

The purpose of the transportation Cost Module is estimating the annual cost associated with offshore and onshore pipeline costs. It requires first determining the pipeline diameter and then using existing correlations for offshore and pipeline costs as a function of diameter and injection rate.

An iterative procedure was used to determine the pipeline diameter. This procedure, proposed by Heddle *et al*. (2003), requires guessing an initial diameter and knowing the pressure drop per unit length. The initial guess is improved by recalculating the diameter assuming turbulent flow. The diameter guess is used to

calculate the Reynolds number which is expressed by the following relation (Heddle *et al*., 2003).

$$\mathrm{Re} = \frac{4m}{\pi \mu_{pipe} D_{pipe}} \tag{74}$$

Where D_{pipe} is the diameter, m is the mass flow rate of the captured CO_2, and μ_{pipe} is the viscosity of the captured CO_2 evaluated at the pumping temperature (356K) and average pressure between the cut-off pressure and final pumping pressure. The Reynolds number is then used to calculate the fanning friction factor assuming turbulent flow. To determine the fanning friction factor, ff, the Chen equation (Economides *et al*, 1994) was used. This expression can be seen in the following equation.

$$\frac{1}{\sqrt{ff}} = -4\log\left\{\frac{\varepsilon}{3.7065} - \frac{5.0452}{N_{\mathrm{Re}}}\log\left[\frac{\varepsilon^{1.1098}}{2.8257} + \left(\frac{7.149}{\mathrm{Re}}\right)^{0.8981}\right]\right\} \tag{75}$$

Where ε is the pipeline roughness factor set to .00015 (Heddle *et al*., 2003). The diameter can be recalculated by using an expression from Heddle *et al*. (2003) that combines the equations for pressure drop and head loss. This expression can be seen here.

$$D_{pipe}^{\ 5} = \frac{32\, ff m^2}{\pi^2 \rho_{pipe}(\Delta P / \Delta L)} \tag{76}$$

Where ρ_{pipe} is the density of the captured CO_2 evaluated at the pumping temperature (356K) and average pressure between the cut-off pressure and final pumping pressure, ΔP is the pressure difference between the final pumping pressure and cut-off pressure, and ΔL is the pipeline distance between the CO_2 capture site and the CO_2 injection site.

For this work 500 km was the assumed distance between the capture site and the CO_2 injection site. Using the procedure proposed by Heddle *et al*. (2003) for the determination of the pipeline diameter, the pipe line diameter as a function of maximum CO_2 throughput and CO_2 composition can be seen in Figure 45.

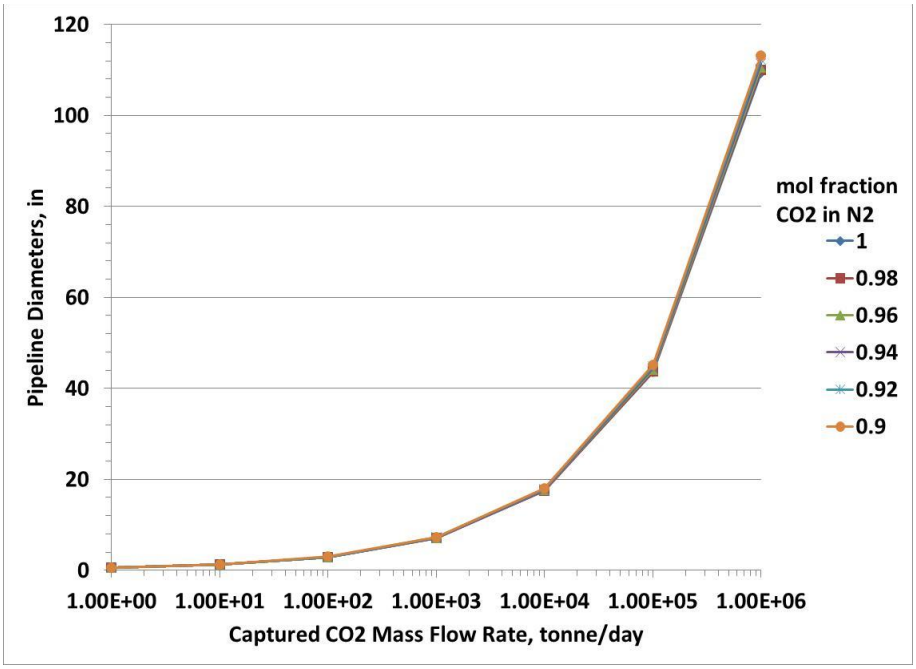

Figure 45: Pipeline Diameter as Function of Maximum CO_2 Injection Rate and CO_2 Composition

From the above figure it can be seen that CO_2 composition does not have a significant impact on the determination of adequate diameters but the capture rate of CO_2 does have an exponential impact on the required pipeline diameter.

Existing correlations where used to estimate the capital investment and operational expense for the pipeline system. The first correlation used corresponds to

the capital investment for the pipeline. This correlation is the following expression (IEA Greenhouse Gas R&D Programme, 2005).

$$InvPipe = C_{\varepsilon-\$}\left(C_1\Delta L + C_2 + \left(C_3\Delta L - C_4\right)D_{pipe} + \left(C_5\Delta L - C_6\right)D_{pipe}{}^2\right)T_F * 10^6 \qquad \textbf{(77)}$$

Where T_F is a terrain factor corresponding to the type terrain where the CO_2 EGR and Sequestration is taking place (set to 1.1 which is the value that corresponds to a stony desert) and $C_{\varepsilon\text{-}\$}$ is currency conversion factor from euro to US dollars (1.29 USD per Euro). The other constants depend on whether the pipeline is offshore or onshore. These constants are listed in Table 34. Figure 46 illustrates the pipeline investment as function of CO_2 capture rate and CO_2 impurity.

Table 34: Correlation Constants for Onshore and Offshore Pipeline System's Capital Cost (IEA Greenhouse Gas R&D Programme, 2005)

	C_1	C_2	C_3	C_4	C_5	C_6
Onshore	0.057	1.8663	0.00129	0	0.000486	0.000007
Offshore	0.4048	4.6936	0.00153	0.0113	0.000511	0.000204

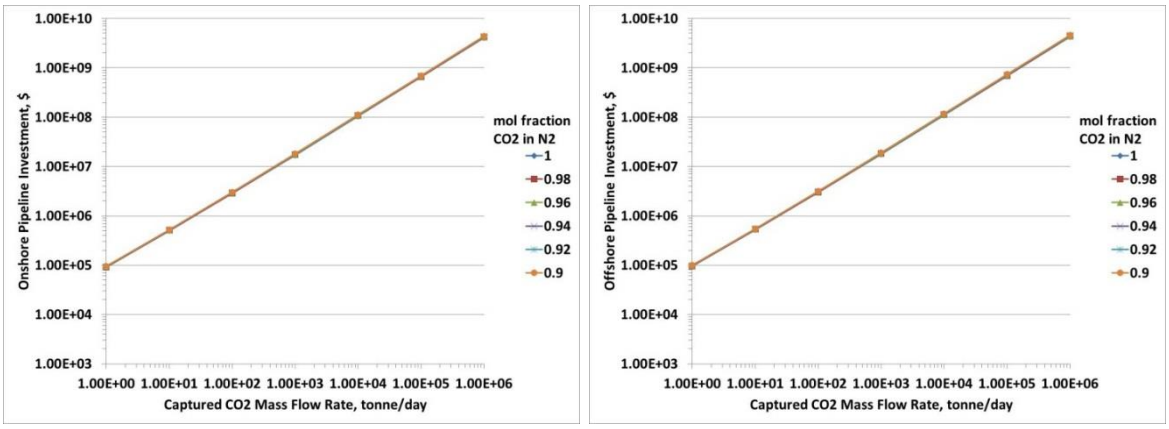

(a) (b)

Figure 46: Pipeline Investment as Function of Capture CO_2 Mass Flow Rate and CO_2 Composition (a) Onshore (b) Offshore

As part of the pipeline system, booster stations are necessary to repressurize the CO_2 as it loses superficial velocity due to friction hampering its flow. It is assumed that booster stations exist every 200 km according to the recommendation by the IEA Greenhouse Gas R&D Programme (2005). The investment correlation for booster stations for onshore and offshore pipeline is expressed in the relationship (IEA Greenhouse Gas R&D Programme, 2005).

$$InvBS = C_{\varepsilon-\$} InvBS_{norm} \Delta L \quad \textbf{(78)}$$

$InvBS_{norm}$ represents the normalized investment for the booster stations (35000 €/km for onshore and 70000 €/km for offshore). The total capital expense for the pipeline system is the sum of the pipeline investment and the booster station investment. This is expressed in the following expression (IEA Greenhouse Gas R&D Programme, 2005).

$$CAPEX_{trans} = InvPipe + InvBS \quad \textbf{(79)}$$

Using the various correlations the onshore and offshore capital expense for CO_2 EGR and Sequestration project can be seen as a function of captured CO_2 mass flow rate. Notice that the CO_2 impurity does not impact the cost of the pipeline system. However the offshore and onshore cost, shown in Figure 47, clearly shows that offshore planning is generally more expensive.

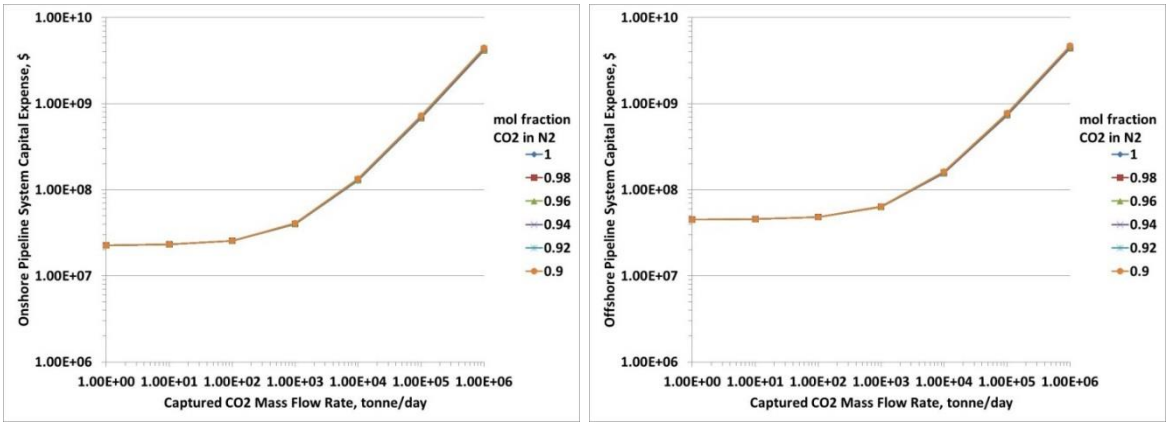

(a) (b)

Figure 47: Total Capital Expense for the Pipeline System (500 km Pipeline) as Function of Captured CO_2 Mass Flow Rate and CO_2 Composition (a) Onshore (b) Offshore

To operate the pipeline system requires additional investment beyond the capital investment. An IEA correlation was used to calculate operational expense of the pipeline system (M. Algharaib and Al-Soof, 2008). This listed correlation is expressed in the following relationship and illustrated in Figure 48.

$$OPEX_{trans} = -260102.59 + 1734.19\Delta L + 41673.43D_{pipe} \quad \textbf{(80)}$$

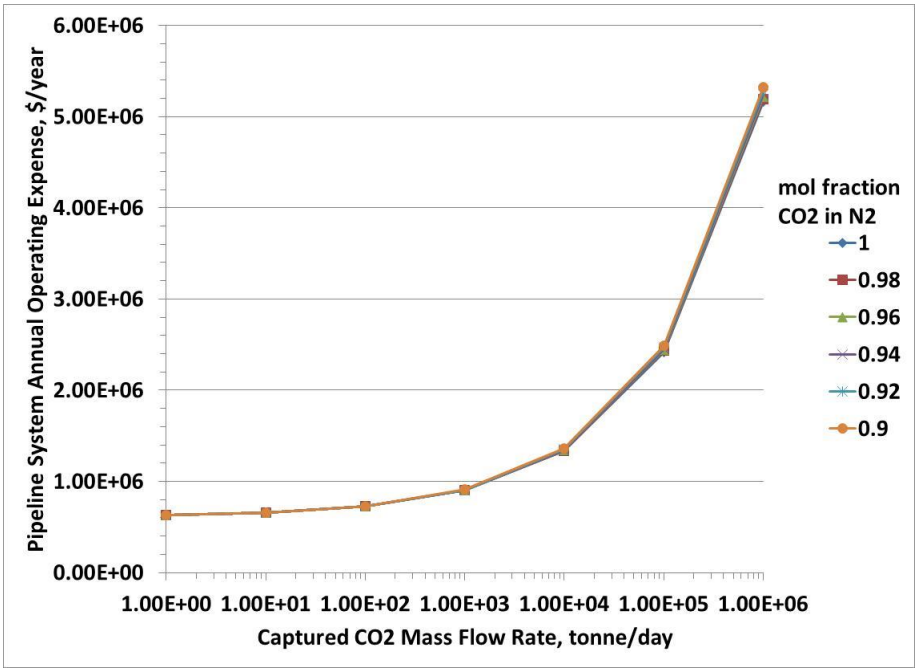

Figure 48: Pipeline System Operating Expense (500 km Pipeline) as Function of Captured CO_2 Mass Flow Rate

Assuming that the pipeline system's capital cost is annualized over the projects life (20 years) the annual expenditures for the pipeline system is expressed as the following expression (M. Algharaib and Al-Soof, 2008).

$$C_{trans} = \frac{CAPEX_{trans}}{t_{dep}} + OPEX_{trans} \quad \textbf{(81)}$$

Using the previous expression, the annual cost due to transportation for the CO_2 EGR and Sequestration project is illustrated in Figure 49.

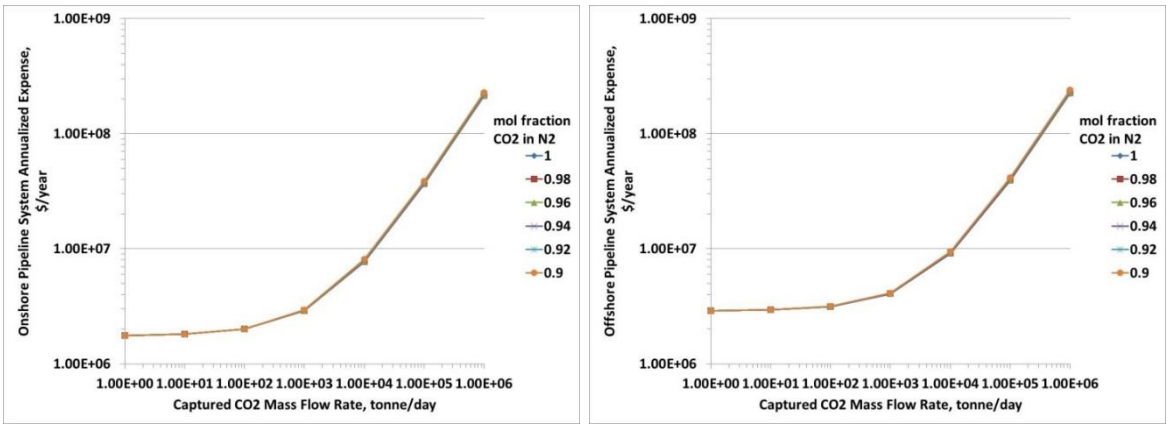

(a) (b)

Figure 49: Annualized Pipeline System Expense as Function of Captured CO_2 Mass Flow Rate and CO_2 Composition (a) Onshore (b) Offshore

The previous figure can be summarized into a simple correlation that takes into consideration CO_2 impurity, captured CO_2 mass flow rate, and whether the project is onshore or offshore. The following expression fits the annualized pipeline system expense.

$$\log(C_{trans}) = a_{trans}\log(m)^3 + b_{trans}\log(m)^2 + c_{trans}\log(m) + d_{trans} \quad \textbf{(82)}$$

The constants, a_{trans}, b_{trans}, c_{trans}, and d_{trans} are listed in Table 35 and Table 36 as a function of CO_2 impurity and whether the pipeline is offshore or onshore.

Table 35: Annualized Onshore Pipeline System Expense as Function of CO_2 Impurity

mol fraction CO_2 in N_2	a_{trans}	b_{trans}	c_{trans}	d_{trans}	R^2
1	0.0054	0.0403	-0.0884	6.2639	1.00
0.98	0.0053	0.0410	-0.0895	6.2640	1.00
0.96	0.0052	0.0419	-0.0907	6.2642	1.00
0.94	0.0051	0.0428	-0.0920	6.2644	1.00
0.92	0.0050	0.0438	-0.0934	6.2646	1.00
0.9	0.0049	0.0450	-0.0949	6.2648	1.00

Table 36: Annualized Offshore Pipeline System Expense as Function of CO_2 Impurity

mol fraction CO_2 in N_2	a_{trans}	b_{trans}	c_{trans}	d_{trans}	R^2
1	0.0084	0.0105	-0.0507	6.4747	1.00
0.98	0.0084	0.0112	-0.0518	6.4748	1.00
0.96	0.0083	0.0120	-0.0530	6.4750	1.00
0.94	0.0082	0.0128	-0.0543	6.4752	1.00
0.92	0.0081	0.0138	-0.0558	6.4754	1.00
0.9	0.0080	0.0149	-0.0574	6.4756	1.00

7.4 Storage Cost Module

The storage cost module uses the approach outlined by Algharaib and Al-Soof (2008). It consists of pricing the wells in a 5 spot pattern where the cost of one well is represented as the following relation where, DEPTH, is the total depth of the well

$$C_{well} = 106300 \times e^{0.0000244 \times DEPTH} \quad \textbf{(83)}$$

The total well cost for the wells in the 5 spot can be calculated using the following relationship.

$$C_{welltotal} = \sum_{i=1}^{Nwells} C_{well,i} \quad \textbf{(84)}$$

The total cost of developing surface facilities for the wells in the five spot pattern can be calculated using the following relationship developed by the Energy Information Administration (M. Algharaib and Al-Soof, 2008).

$$C_{pattern} = 10^6 + 310.36 \times DEPTH \quad \textbf{(85)}$$

Algharaib and Al-Soof (2008) recommend that the required cost, $CAP_{RECYCLE}$, for installing a CO_2 recycle plant be estimated as 4.8 MM$. The total cost for the storage cost module is represented in the following equation (M. Algharaib and Al-Soof, 2008).

$$CAP_{storage} = CAP_{RECYCLE} + (1-\alpha) \times N_{pattern} \times (C_{pattern} + 2C_{welltotal}) \quad \textbf{(86)}$$

Where $N_{pattern}$ represents the number of 5 spot patterns in the field and α represents the stage of field development for the field. For this work α was set to 0 indicating the initial planning stages of the project (a value of 1 is used if the field is already developed). The annualized cost can then be calculated assuming that the cost is divided up by the project length, t_{dep}. The annualized storage cost for the project can be calculated as the following expression (M. Algharaib and Al-Soof, 2008).

$$CAPEX_{storage} = \frac{CAP_{storage}}{t_{dep}} \quad \textbf{(87)}$$

The annual operating expense for the field is calculated as the following (M. Algharaib and Al-Soof, 2008).

$$FOPEX_{storage} = N_{pattern} \times [207800 + 47.407 \times DEPTH] \quad \textbf{(88)}$$

The total annual expenditure for the storage module is the sum of the annual capital and operating expenses that are associated with operating the 5 spot pattern(s). It can be calculated using the following relation (M. Algharaib and Al-Soof, 2008).

$$C_{storage} = CAPEX_{storage} + FOPEX_{storage} \quad \textbf{(89)}$$

The cost of recycling the produced CO_2 was assumed to be .38 USD per MSCF of separated CO_2. The recycle cost is then represented by the following expression.

$$C_{RECYCLE} = C_{CO2\_SEP} F_{PCO2} \quad \textbf{(90)}$$

C_{CO2_SEP} is .38 USD per MSCF (M. Algharaib and Al-Soof, 2008) and F_{PCO2} is the production rate of CO_2 from the 5 Spot patterns.

7.5 Injection Cost Module

Once the CO_2 reaches the well site it must be compressed for injection into the reservoir's pay zone. The required power to do this, $W_{INJ,i}$, to accomplish this can be found using the following expression.

$$W_{INJ,i} = \left(\frac{1000 \cdot 10}{24 \cdot 3600}\right)\left[\frac{m\left(P_{BHP} - P_{surf}\right)}{\rho_{INJ}\eta_{INJ}}\right] \quad \textbf{(91)}$$

Where P_{BHP} is the bottom hole pressure at the well site, η_{INJ} is the efficiency of the pump, and ρ_{INJ} is the density of the captured CO_2 at 356 K (181 F) and at the average pressure between the surface pressure P_{surf} (10.3 MPa) and P_{BHP}. Determination of the required power requires knowledge of the density as a function of pressure and CO_2 impurity. Figure 50, Equation 92, and Table 37 are the illustrated CO_2 density, polynomial fit of the CO2 density, and the listed coefficients for the best fit of the CO_2 density respectively. The presented equation is polynomial fit of the CO_2 density as a function of impurity and pressure.

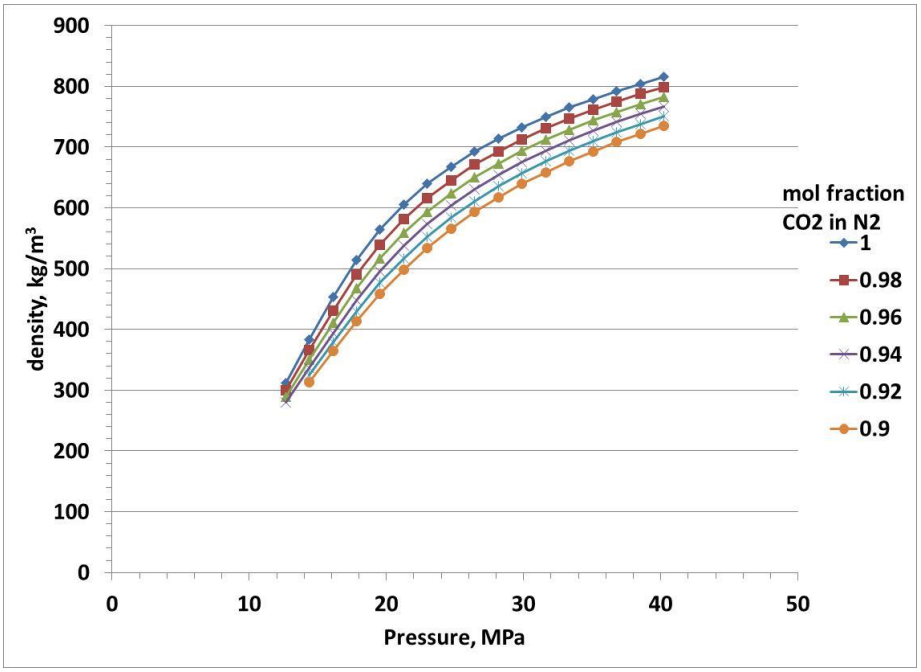

Figure 50: Captured CO_2 Density as Function of Pressure and Impurity

$$\rho_{INJ} = a_{INJ} P_{avg}^3 + b_{INJ} P_{avg}^2 + c_{INJ} P_{avg} + d_{INJ} \quad \textbf{(92)}$$

Table 37: Coefficients for CO_2 Density Determination as Function of Impurity at 356K

	a_{INJ}	b_{INJ}	c_{INJ}	d_{INJ}	R2
1	0.026	-2.7463	104.14	-619.6	1
0.98	0.0217	-2.3692	93.919	-555.36	1
0.96	0.0179	-2.0294	84.477	-494.17	1
0.94	0.0146	-1.7296	75.946	-437.66	1
0.92	0.0142	-1.6839	74.313	-439.19	1
0.9	0.0118	-1.4586	67.571	-393.16	1

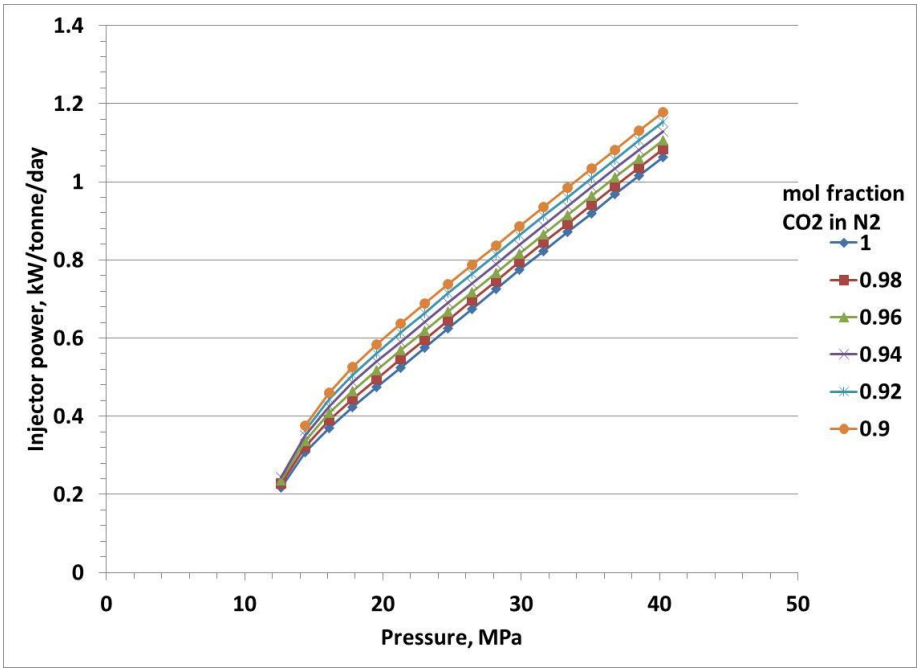

Figure 51: Injector Power Requirement as a Function of Pressure and CO_2 Impurity

Figure 51 illustrates the injector power requirements as a function of CO_2 impurity and pressure. To determine the injector's capital cost requires using the injector power expression and the following equation adapted from McCollum and Ogden (2006).

$$C_{INJ,i} = \left(1.11\times10^{6}\right)\left(\frac{W_{INJ,i}}{1000}\right) + 0.07\times10^{6} \quad \textbf{(93)}$$

The total capital of injectors for the 5 spot pattern(s) is the summation of all the injector cost in the field. This is expressed in the following equation where Ninj is the number of CO_2 injectors in the field.

$$CAP_{INJ} = \sum_{i=1}^{Ninj} C_{INJ,i} \quad \textbf{(94)}$$

The annualized cost of these injectors is the total capital of the injectors divided by the project length.

$$C_{INJ} = \frac{CAP_{INJ}}{t_{dep}} \quad \textbf{(95)}$$

The annual cost of electricity for the injectors in the 5 spot pattern can be found using a relation similar to the cost of electricity for the pumps described earlier. For this calculation the price of electricity for the four CO_2 capture with power generation technologies choices was used.

$$E_{INJ,i} = W_{INJ,i} P_e C_F \quad \textbf{(96)}$$

The cost of injecting CO_2 then as function of bottom hole pressure, CO_2 impurity, mass flow rate, and power generation technology can be found using the following expression.

$$w_{ICO2} = \frac{E_{INJ,i}}{m} \quad \textbf{(97)}$$

Using this expression the cost of injecting CO_2 is illustrated in Figure 52.

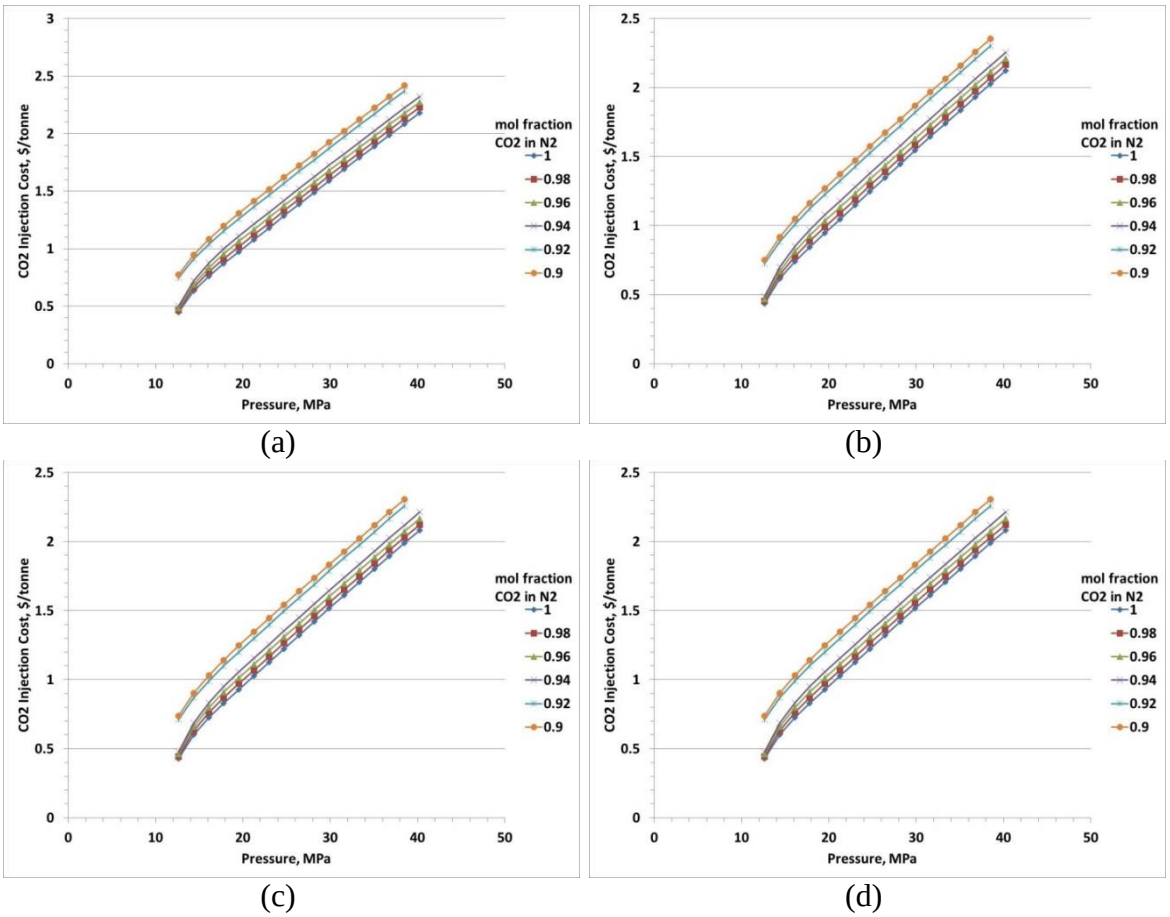

Figure 52: Injection Cost as Function of Pressure, Impurity and CO_2 Capture by Power Generation Technology (a) CFGA, (b) IGCC, (c) NGCC, and (d) OPC

7.6 Objective Function: NPV

The NPV of the CO_2 EGR and Sequestration project can be calculated using the Capturing Cost, Compression Cost, Transportation Cost, and Storage Cost, and Injection Cost Modules. The NPV is calculated for this work using the following equations.

$$\text{Revenue}_t = \left(w_{GP}F_{GP} + w_{OP}F_{OP}\right)\left(1 - r_{tax}\right) + w_{SCO2}F_{SCO2} \quad \textbf{(98)}$$

$$\text{Cost}_t = w_{WP}F_{WP} + w_{ICO2}F_{ICO2} + C_{cap}F_{cap} + C_{CO2\_SEP}F_{PCO2} + C_{capfacility} + C_{c-p} + C_{trans} + C_{storage} + C_{INJ} \quad \textbf{(99)}$$

$$NPV = \sum_{t=1}^{t_{dep}} \frac{\text{Revenue}_t - \text{Cost}_t}{\left(1 + IRR\right)^t} \quad \textbf{(100)}$$

Where w_{GP} represents gas price per MSCF, w_{OP} represents oil price per STB, $w_S CO_2$ represents CO_2 tax incentive per tonne, w_{WP} represents water disposal cost per STB, $w_I CO_2$ represents CO_2 injection cost per MSCF, $C CO_{2\_SEP}$ represents CO_2 separation cost per MSCF CO_2 separated, C_{CAP} represents CO_2 capture cost per MSCF of captured CO_2, F_{GP} represents gas production for time period *t*, F_{OP} represents oil production for time period *t*, $F_S CO_2$ represents CO_2 stored for time period *t*, F_{WP} represents water production for time period *t*, $F_I CO_2$ represent CO_2 injected for time period *t*, $F_P CO_2$ represent CO_2 separated from the total field production for time period *t*, t_{dep} is the total producing and accounting time for a field, F_{cap} represent CO_2 captured for time period *t*, *IRR* represents the interest rate, $C_{capfacility}$ is the annual CO_2 capture (from power generation) cost, $C_{c\text{-}p}$ is the annual compressor and pump cost from transporting the CO_2 to the injection site, C_{trans} is the annual cost of transporting CO_2 to the capture site, $C_{storage}$ is the annual cost of storing CO_2, C_{INJ} is the annual injector cost, $Revenue_t$ is the total revenue for time period *t*, $Cost_t$ is the total cost for time period *t*, and *NPV* is the net present value of the project. This objective function was programmed using a Microsoft J-script compiler. This code was then utilized in a subsequent optimization.

NPV is the primary objective function that quantifies the success of the CO_2 EGR and Sequestration project. The next chapter discusses the optimization of the CO_2 EGR and Sequestration process with respect to NPV.

8 CO_2 EGR OPTIMIZATION OF 5 SPOT MODEL

The previous chapter outlined the economic requirements necessary for the CO_2 EGR and Sequestration process. Considering these economic requirements, an optimization study was conducted on a 5 spot pattern field. CO_2 EGR and Sequestration is a complex process. It involves three primary goals which are storing CO_2, improving natural gas and condensate recovery, and meeting financial goals. These goals are contradictory. For example, CO_2 storage conflicts with the goal of improving natural gas and condensate recovery because the captured and injected CO_2 used to improve recovery is eventually produced. In another example, CO_2 storage conflicts with meeting financial goals because there is no substantial revenue involved in storing CO_2. Due to these contradictions, the CO_2 EGR and Sequestration process requires an objective function that can satisfy these primary goals. For this work, the NPV described in the last chapter is the primary objective function used to quantify the success of the CO_2 EGR and Sequestration project. NPV as the objective function helps mitigate the conflict between storing CO_2, improving natural gas and condensate recovery, and meeting financial goals. To maximize NPV requires having control of the process conditions that effect natural gas and condensate recovery. These primary controls are the bottom hole pressures of all the wells involved in the CO_2 EGR and Sequestration process.

Mathematically the goal of this work is to find a process vector, x, that maximizes the objective function. The process vector, *x*, represents the bottom hole

pressures of all the wells involved in the CO_2 Sequestration and EGR. This notion is illustrated in Figure 53 where the process vector, *x*, directly controls the total CO_2 injected.

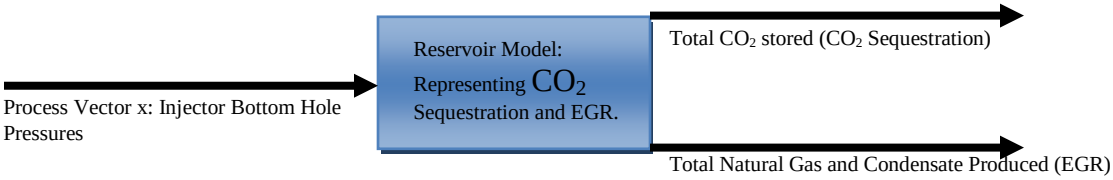

Figure 53: General CO_2 Sequestration and EGR Model

Figure 53 illustrates that finding the best process vector x for the CO_2 EGR and Sequestration process is an optimization problem. Specifically, the goal of this optimization is to find the best process vector that maximizes the objective function NPV. This can be written mathematically as the following:

$$\begin{aligned} &Max\ g(x) = NPV \\ &x \in \left(R^u\right) \end{aligned} \qquad \textbf{(101)}$$

Where R^u represents the space of possible user defined bottom hole pressures that can be applied to the CO_2 EGR and Sequestration process. With the problem defined, the task now is to choose an efficient algorithm that is able to consider the possible scenarios in the space R^u.

In this work a proprietary optimization method was applied to find the best possible process vector that maximizes the NPV. This method, Designed Exploration and Controlled Evolution (DECE), was created by the Computer Modeling Group (CMOST Studio, 2011) for history matching and optimization problems. It works by

using a Designed Exploration stage and Controlled Evolution stage on a user defined subspace R^u. The Designed Exploration stage involves searching the subspace R^u for possible experimental combinations that maximize the objective function. Experimental design is utilized in this stage to create the suitable combinations that represent the process vector x. These suitable combinations are used to determine the objective function. From there, the Controlled Exploration stage analyzes each of the resultant calculated objective functions to see if the current value for the objective function has improved since the last iteration. If a candidate process vector does not show an improved objective function value from the last iteration it removes the process vector from candidacy as a solution. If the candidate process vector does show improvement the process vector is kept as a possible solution. This optimization process is repeated until there is an optimal solution for the objective function (CMOST Studio, 2011).

To test the feasibility of using the CO_2 EGR and Sequestration process a 5 spot pattern was set up in a compositional reservoir simulation setting using the GEM Advanced Compositoinal and GHG Reservoir Simulator (2011). An optimization was conducted on this pattern model using the DECE optimization algorithm. The specifics of this pattern are listed in Table 38. The properties of the reservoir fluid used in the study are listed in Table 11 and initial aqueous component properties are listed in Table 16.

Table 38: Simulation Grid Properties for 5 Spot CO_2 EGR and Sequestration Optimization Study

Pattern Spacing	40 Acres	**Reservoir Temperature**	220 ^oF
Gridding of Radial Model	15 x 15 x 15	**Rock Compressibility**	5.00E-06 psi^{-1}
Δx	90.88ft	**Depth to top of formation**	9600 ft
Δy	90.88ft	**Initial Pressure**	5300 psia
Δz	43 ft	**Initial Water Saturation**	15%
Porosity	20%	**Critical Gas Saturation**	15%
Permeability	1 md	**Pay Zone**	645 ft
CO_2 Injector Constraint	.7 psi/ft of pay	**Producer Minimum Bottom Hole Pressure**	1000 psia

The field is located onshore on a desert terrain. Pipeline line system has the capacity to deliver up to 10,000 tonnes per day of captured CO_2 (100% pure CO_2) to a field that consists of 100 5 spot patterns which correlates to a maximum of 100 tonnes per day of CO_2 delivered per 5 spot pattern. Using this rating the calculated pipeline diameter was found to be 17.4 inches and the relevant annualized costs for each capture technology are illustrated in Figure 54. Economic parameters used for the study are listed in Table 39.

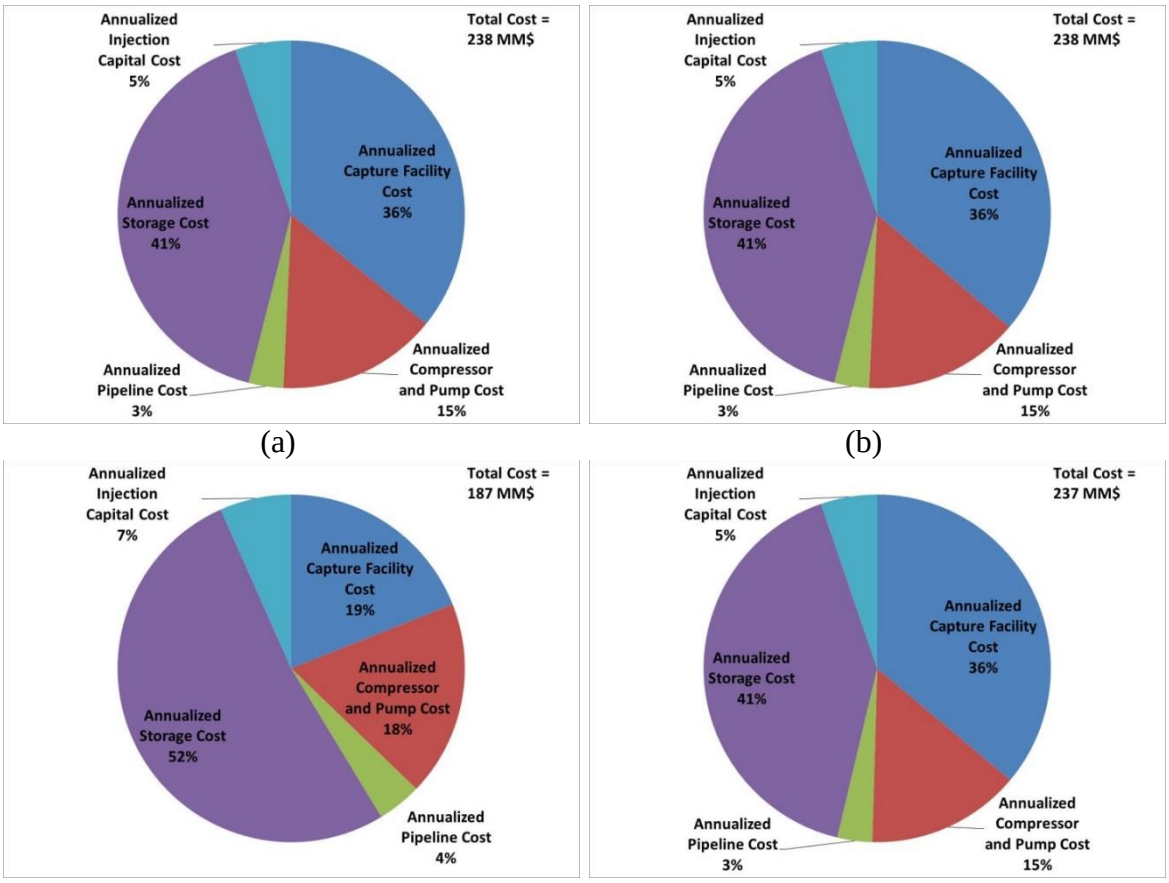

Figure 54: Annualized Cost for 5 Spot CO_2 EGR and Sequestration Study (a) CFGA, (b) IGCC, (c) NGCC, (d) OPC

Table 39: Constant Economic Parameters for 5 Spot CO_2 EGR and Sequestration Study

Internal Rate of Return	10%
Tax Rate	30%
Natural Gas Price	4.25 $/MSCF
Oil Price	80 $/bbl
Water Treatment Cost	1 $/bbl
CO_2 Storage credit	0 $/tonne
CO_2 Separation Cost	.38 $/MSCF

The process vector x for the 5 Spot optimization represents the CO_2 injector bottom hole pressure. For this optimization study each 5 spot consists of 1 injector in the middle and 4 producers in the corner. Because of this symmetry, only the injector are considered in the process vector through time. The optimization is for 20 years with the option of changing the injector and producer controls every 5 years. This process vector is represented in the following notation.

$$x = \left[CINJ_1, CINJ_2, CINJ_3, CINJ_4\right] \quad \textbf{(102)}$$

Where CINJ represents the controls for the injector for different periods (indicated by the subscripts 1, 2, 3, and etc.). For this work, a period corresponds to 5 years. For the optimization, the possible values chosen for injector were chosen based on the initial reservoir pressure, injector maximum bottom hole pressure, and the producers minimum bottomhole pressure. Specifically, the injector was constrained between the minimum bottomhole pressure (1000 psia) and the initial reservoir pressure (5300 psia). The initial reservoir pressure setting allows the injector to be operating in cases when the reservoir pressure falls below the initial reservoir pressure. Four realizations were chosen to represent the user defined range of values for both the injector and producer controls. Using these criteria Figure 55 illustrates the possible choke settings for the DECE optimization algorithm.

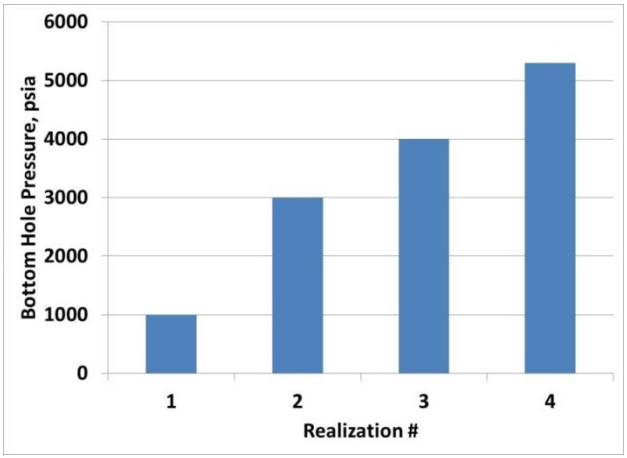

Figure 55: Candidate Injector Values for 5 Spot CO_2 EGR and Sequestration Optimization

The optimization was performed on the CFGA power generation option but the results from this optimization were applied to the other three power generation options. This was done because the main difference between each of the options is the annual capital investment. The necessary optimization iterations for the CFGA power generation choice are illustrated in Figure 56.

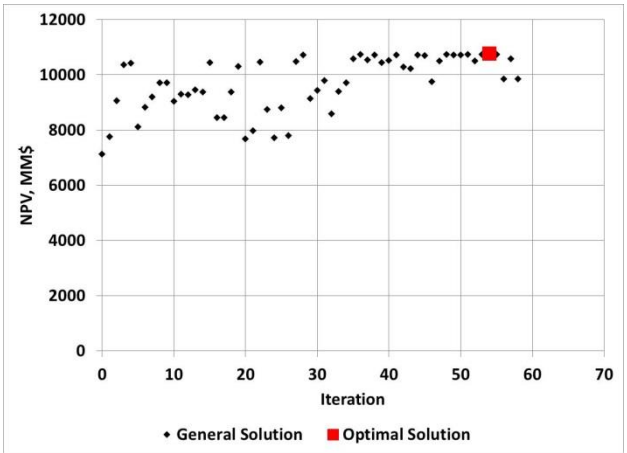

Figure 56: CFGA 5 Spot CO_2 EGR and Sequestration Optimization Iteration Using DECE

From the previous figure, it is illustrated that the CFGA power generation choice converged to a value indicative of profitability for the CO_2 EGR and Sequestration process. Applying the results of this optimization to the other three power generation options, it is illustrated by Figure 57 that the NGCC option was the most profitable when compared to the other options.

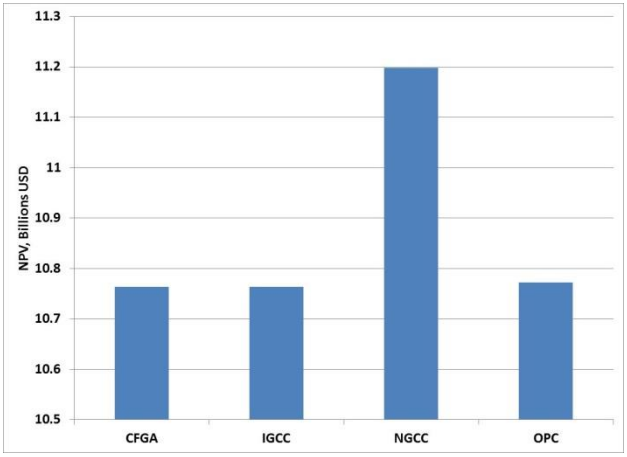

Figure 57: Optimal NPV for CO_2 EGR and Sequestration Process Options

Financially, this option had the least capital investment (see Figure 54) out of all the other options. The optimal control setting for the optimal NPVs is illustrated in Figure 58.

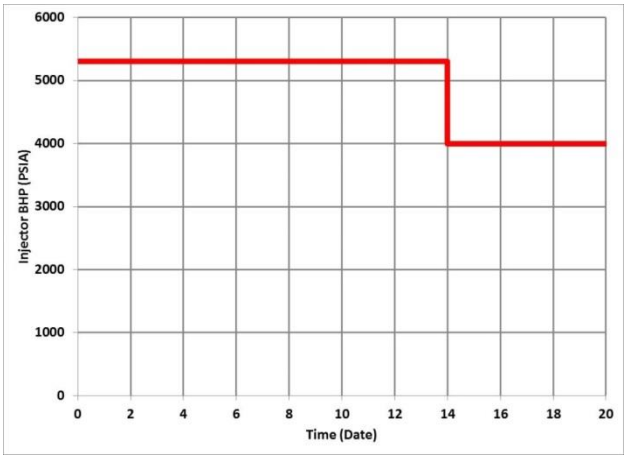

Figure 58: Optimal Injector Bottom Hole Pressures for CFGA 5 Spot CO_2 EGR and Sequestration Process

The optimization resulted in enhanced recovery of the field. This fact is illustrated in Figure 59 and Figure 60 which are comparisons between the optimal recovery and the recovery from primary depletion.

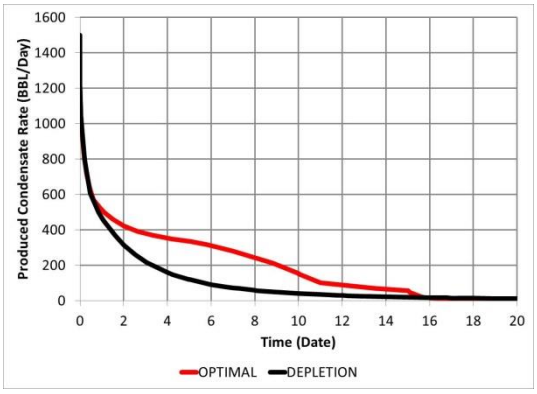

(a)

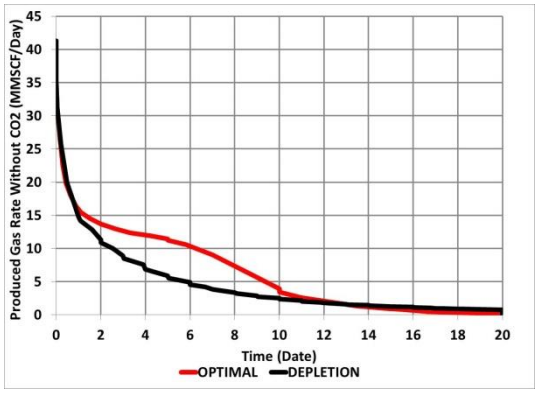

(b)

Figure 59: Production Rate Comparison Per Pattern (a) Condensate Production Rate (b) Natural Gas Production Rate Without CO_2

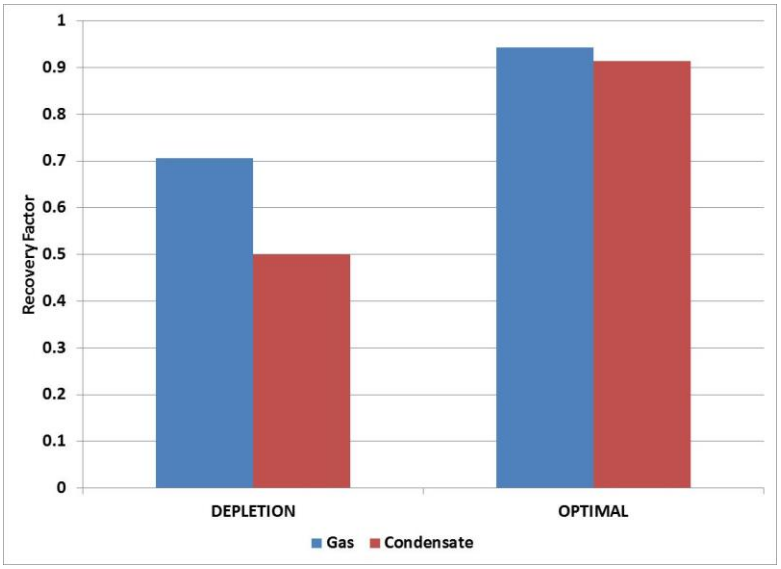

Figure 60: Recovery Factor Comparison for 5 Spot CO_2 EGR and Sequestration Process

In addition to favorable recovery, the optimization also resulted in substantial CO_2 being stored. A total of 40 BSCF of CO_2 per pattern was stored using the optimized controls. To get to this storage value and optimal recovery required injection of 79 BSCF of CO_2 per pattern. This large amount of CO_2 was necessary in enhancing the recovery of hydrocarbon from the field. One favorable aspect of these optimizations is the reduction of oil saturation in the near wellbore region of the producer well. This is illustrated in Figure 61.

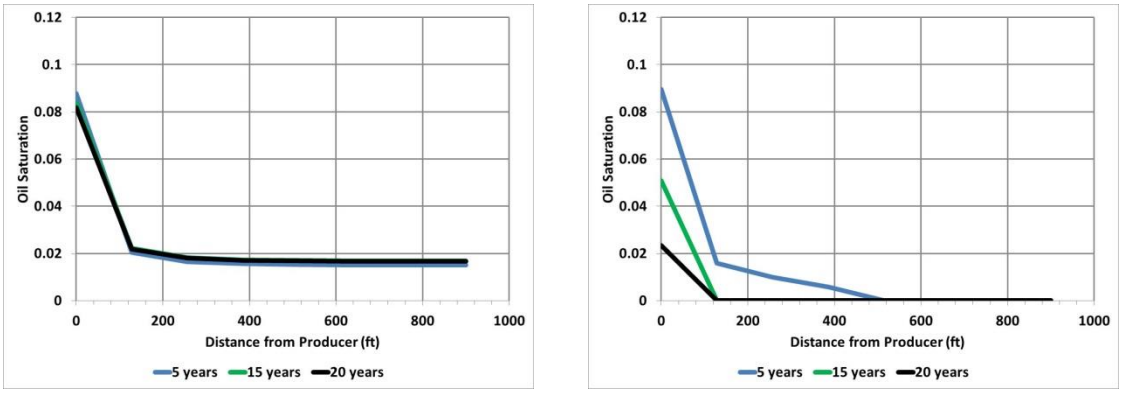

(a) (b)

Figure 61: Oil Saturation Profile (a) Depletion (b) Optimal

The optimal oil saturation profile shows that oil saturation is reduced as time progresses. This is an indication of vaporization of the condensate phase. The massive reduction in oil saturation exhibited by the optimal solution was made possible by the presence of CO_2 in the near wellbore region of the producing well as indicated by Figure 62.

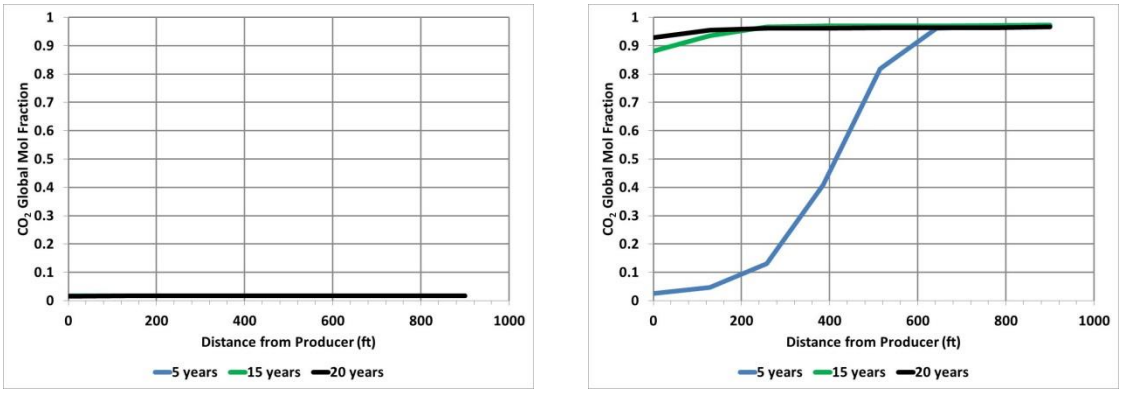

(a) (b)

Figure 62: CO_2 Composition Profile (a) Depletion (b) Optimal

From this figure it can be seen that this study was successful in illustrating the feasibility of using CO_2 to reduce condensate while improving the production of hydrocarbon from the wet gas reservoir. The next chapter discusses an additional study that illustrates the feasibility of using CO_2 EGR and Sequestration on a reservoir that has been studied in literature.

9 CO_2 EGR OPTIMIZATION OF PUNQ-S3 MODEL

So far it has been demonstrated that CO_2 has the ability to remove condensate banks through the ability of lowering the dew point pressure of the reservoir's wet gas. In this chapter a full field reservoir model is simulated to investigate the impact of using CO_2 in improving the productivity of realistic gas/condensate systems. The PUNQ-S3 reservoir model was utilized for this task. The PUNQ-S3 has been used by various research groups to study history matching and production optimization. Complete data-set and properties for the PUNQ-S3 reservoir are available in the public domain (Imperial College London Department of Earth Science and Engineering, 2011). For this study, structure and heterogeneity of the reservoir were kept the same, but carbonate geochemistry was added and the oil/gas compositions were changed to a wet gas composition listed in Table 11. In addition to this the relative permeability values that were used for simulations can be found in Figure 25. Compositional simulations were conducted for the production of this reservoir for 20 years under four alternate scenarios:

(a) Primary Depletion: The reservoir was allowed to undergo natural depletion.

(b) Continuous Injection: Injection of CO_2 for the entire production life.

(c) Delayed Injection: Delayed injection of CO_2.

(d) Preventative Injection: Setting the injector bottom hole pressure to the minimum reservoir pressure so as to inject CO_2 only when the reservoir pressure declines below the initial reservoir pressure.

These four scenarios were compared to understand the benefit of using CO_2 for repressurizing the reservoir and lowering the dew point pressure of the reservoir fluid. Specific details of the reservoir model are listed in Table 7. The structure of the reservoir, simulation grid, and location of various wells for three alternate scenarios are shown in Figure 63. Primary depletion includes production from six wells. One of the production wells, Pro-4, is converted to an injection well, Inj-4, for the three alternate CO_2 injection scenarios. Reservoir Properties are listed in Table 40.

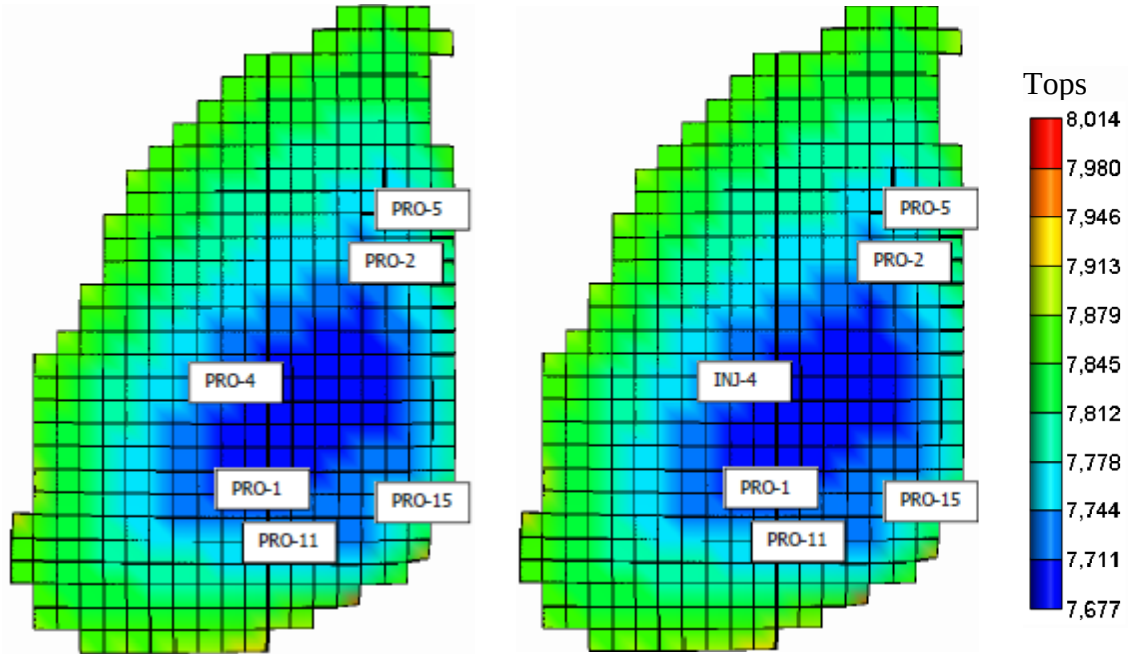

(a) (b)

Figure 63: Well Locations for PUNQ-S3 Reservoir Models; PRO=Producer and INJ=Injector (a) Primary Depletion (b) Pressure Maintenance and Delayed Pressure Maintenance

Table 40: Modified PUNQ-S3 Reservoir Model

Surface Area	4260 Acres	**Total Bulk Reservoir Volume**	1585 MMBBL
Gridding of Cartesian Model	19 x 28 x 5	**Total Pore Volume**	233 MMBBL
Producer(s) Bottomhole Pressure Constraint	1740 psia	**Total Hydrocarbon Pore Volume**	198 MMBBL
CO_2 **Injector Maximum Bottom Hole Pressure**	0.7 psi/ft	**Original Oil in Place, OOIP**	9.69 MMSTB
Reservoir Temperature	220 ^{o}F	**Original Gas in Place, OGIP**	278 BSCF
Initial Pressure, psia	5300 psia	**Original Water in Place, OWIP**	33.3 MMSTB
Initial Water Saturation	15%	**Critical Gas Saturation**	15%

For the primary depletion case each of the six wells were scheduled to produce 10 MMSCF/D of gas with a minimum bottomhole pressure constraint of 1740 psia. Figure 64 shows gas and condensate production rates for the primary depletion scenario. It is observed that target gas production rate of 60 MMSCF/D could be maintained for about six years after which it declined rapidly as each well lost productivity in succession, as shown in Figure 65. Clues about cause of predicted productivity decline can be obtained from steady decline in surface condensate production rate, and, condensate-gas-ratio, during the first eight years of production gas production rate was maintained. Given that overall composition of reservoir gas doesn't change, reducing condensate-gas-ratio suggested condensate dropout in the reservoir, most likely, in the near-wellbore region. This observation is supported by steady decrease in productivity of all wells, as illustrated in Figure 65. Net result of, productivity decline for the

candidate wet-gas reservoir may be that the production becomes hindered due to condensate blockage.

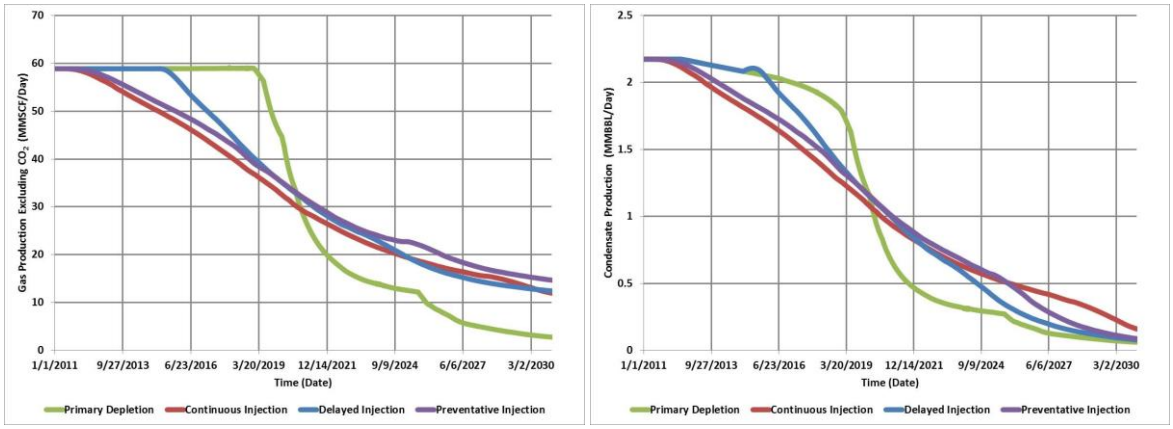

(a) (b)

Figure 64: PUNQ-S3 Production Rates for Different Scenarios (a) Gas Production (b) Condensate Production

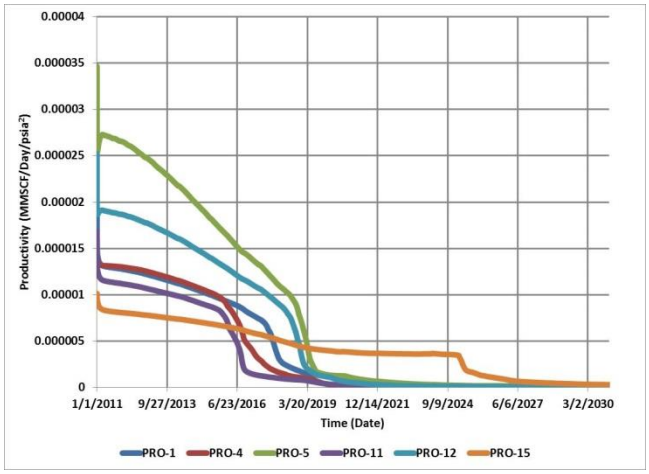

Figure 65: Productivity of PUNQ-S3 Reservoir (Primary Depletion)

To investigate if the production decline can be overcome, the continuous injection scenario was simulated. In this case, five wells were set at a total target gas

production rate of 60 MMSCF/D with a minimum bottomhole pressure constraint of 1740 psia. Well Pro-4 was converted to an injector that injected 60 MMSCF/D of CO_2 with a maximum bottomhole pressure gradient of 0.7 psi/ft to prevent fracturing of the reservoir. Predicted hydrocarbon production rates and gas productivity using pressure maintenance are shown in Figure 64 and Figure 66. As illustrated by Figure 66 and Figure 67, the targeted total field gas production rate was maintained for the entire production life while the gas productivity was maintained without significant production decline at each producer. This is in stark contrast with the depletion scenario, which showed a significant decline in total gas production rate. The recovery factor of the continuous injection scenario is competitive with the primary depletion scenario, as illustrated by Figure 68. The drawback to this scenario is that there is significant increase in field CO_2 production as illustrated by Figure 69. The increased CO_2 production is necessary to ensure that there is enough CO_2 in the near wellbore region of the producing wells. A high concentration of CO_2 in the near wellbore region reduces the amount of condensate blockage in the near wellbore region of all the producers.

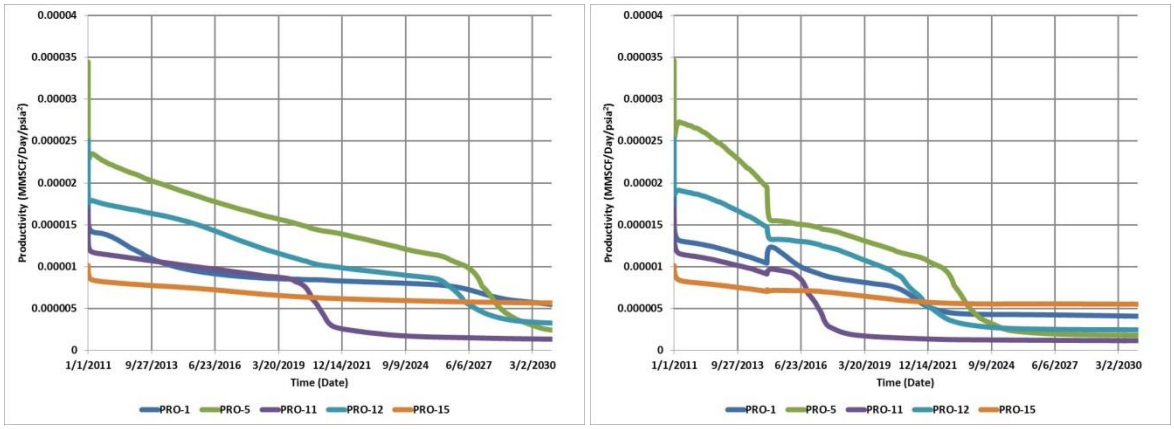

(a) (b)

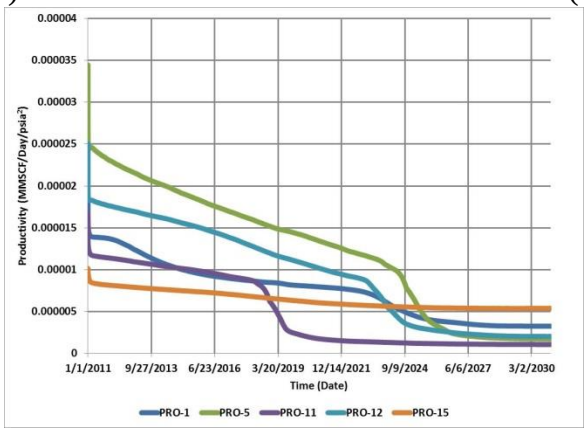

(c)

Figure 66: Productivity of CO_2 Injection Schemes (a) Continuous Injection (b) Delayed Injection (c) Preventative Injection

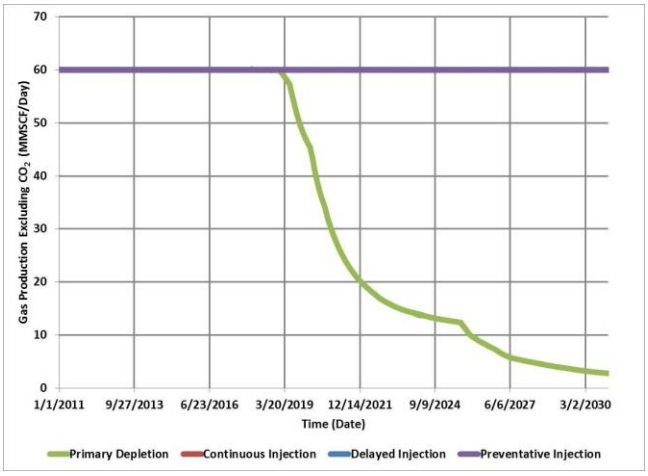

Figure 67: PUNQ-S3 Total Gas Production

The continuous injection scenario shows the benefit of injecting CO_2 to prevent total gas production decline. Figure 68 shows the condensate and gas recovery (excluding CO_2) in four different scenarios. It highlights that the continuous injection approach recovers more condensate than the depletion scenario. Figure 64 also shows that the continuous injection scenario had a gas recovery comparable to the depletion scenario. The main difference between these scenarios was the amount of CO_2 produced (revealed by Figure 69) and the condensate recovered (revealed by Figure 68). The improved condensate recovery suggests that CO_2 mobilizes and vaporizes near wellbore condensate at reservoir conditions. This suggests that the management of produced CO_2 in the continuous injection scheme may be justified by the added revenue from the condensate recovery.

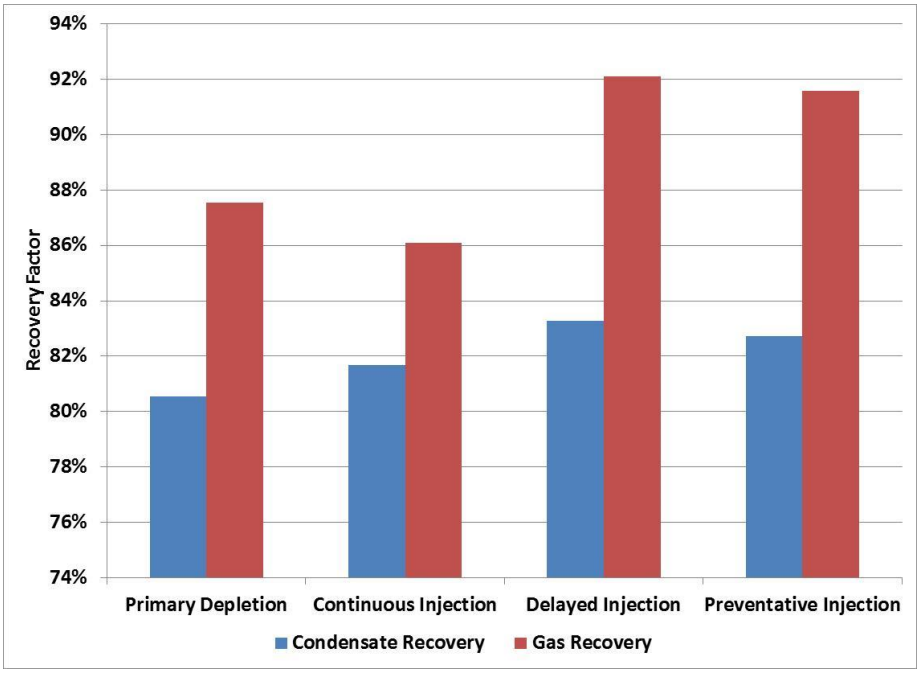

Figure 68: Recovery Factor of PUNQ-S3

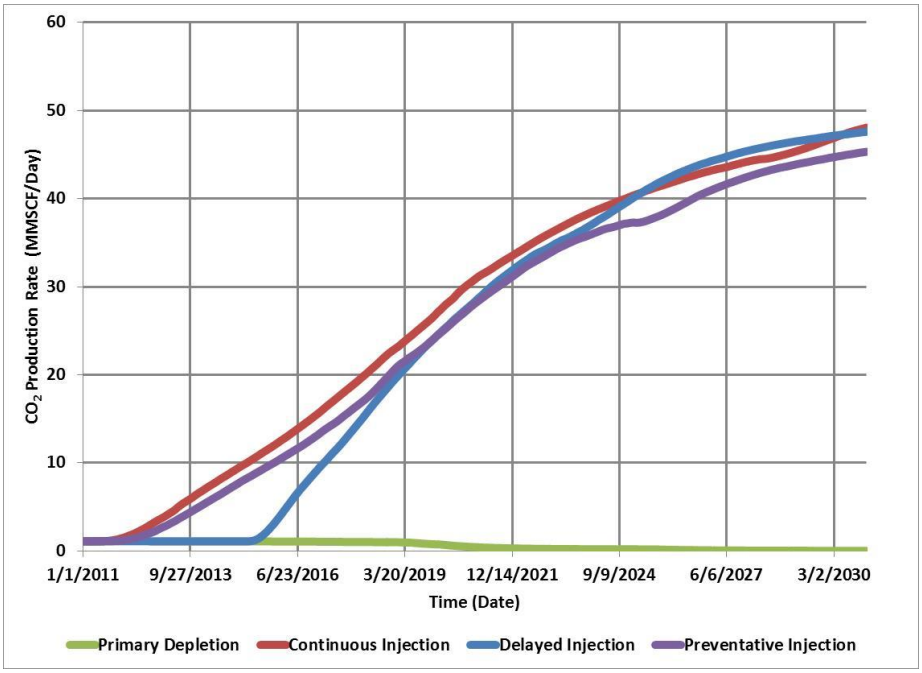

Figure 69: Field CO_2 Production Rate for PUNQ-S3

The benefit of increased condensate production may be nullified by the added cost associated with separating CO_2 from the produced gas stream. Thus, it may not be economical to inject CO_2 from the start of the project. Therefore a third scenario was investigated in which the CO_2 injection process was initiated to anticipate gas production decline. In this delayed injection scenario, the field was allowed to produce until 2015 using the depletion scenario production scheme. At the beginning of 2015, the wells were switched to produce using the continuous injection scenario production scheme. Predicted hydrocarbon production rates and gas productivity using the treatment scenario are shown in Figure 64, Figure 66, and Figure 67. For this scenario, these figures show that the total gas production is relatively constant for the entire production life. This scenario shows that improvements can be made over the depletion scenario

which showed significant decline. This delayed injection scenario compares favorably with the continuous injection scenario because both schemes were able to maintain the desired field total gas production rate. The added benefit of the delayed injection scenario is that it required less cumulative amount of CO_2 to maintain the same field gas production rates. The success of the delayed pressure maintenance scenario can be attributed to the initiated pressure maintenance scheme in year 2015 which re-pressurized the reservoir and helped lower the dew point near the producing wells. The re-pressurization of the reservoir is shown in Figure 70. It is clear that the CO_2 injection at the year 2015 initiated an increase in the average reservoir pressure and thus prevented a decline similar to the primary depletion case.

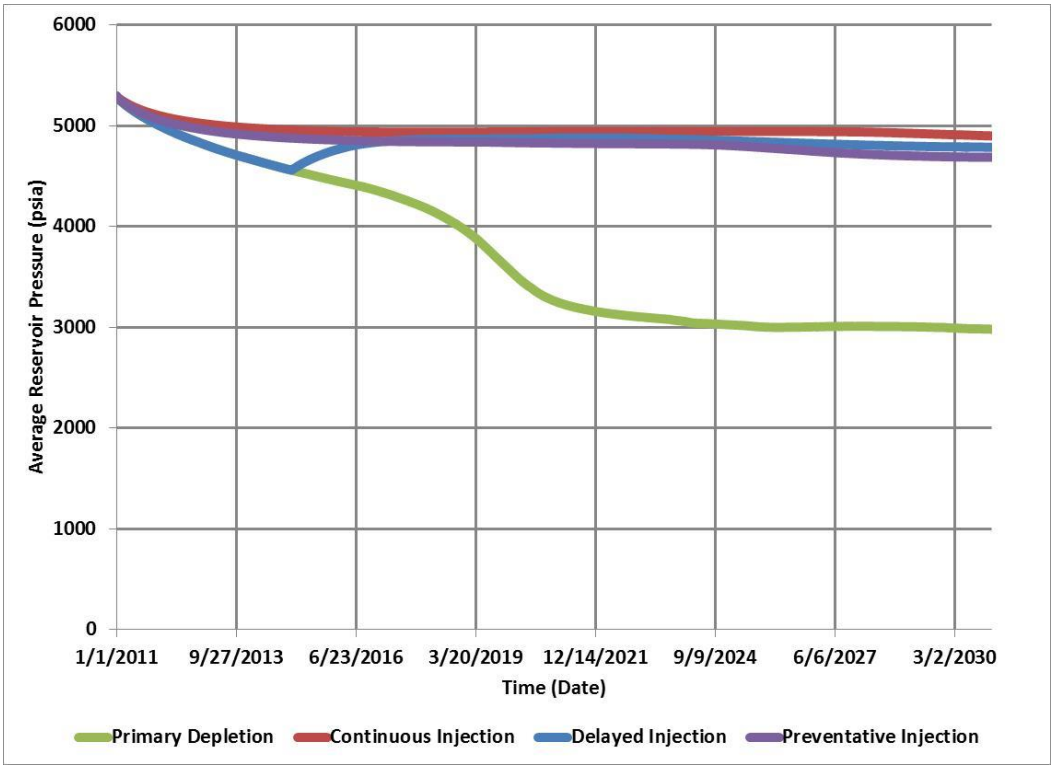

Figure 70: Average Reservoir Pressure for PUNQ-S3 Scenarios

The delayed injection scenario illustrated the potential of using a scheduled CO_2 injection to pressurize the reservoir and thus improve gas productivity and hydrocarbon recovery. To improve this scenario, the preventive injection scenario is investigated. This scenario injects CO_2 when the reservoir pressure declines below the initial reservoir pressure. This scenario insures that CO_2 refills the reservoir to counterbalance the reservoir pressure decline caused by hydrocarbon production from the producing wells. Observing Figure 68, it is clear that the preventive injection scheme has favorable recovery when compared to the other scenarios including. In addition, Figure 71 illustrates that the preventative injection option produces favorable condensate and natural gas yields when compared to the other injection scenarios while ensuring favorable storage of CO_2. Moreover, preventative injection provides an ideal reservoir management strategy for condensate blockage in the producing wells. This scenario injects enough CO_2 to maintain the reservoir pressure while ensuring that the dew point pressure is lowered in the near wellbore region of the producer due to the increased concentration of CO_2.

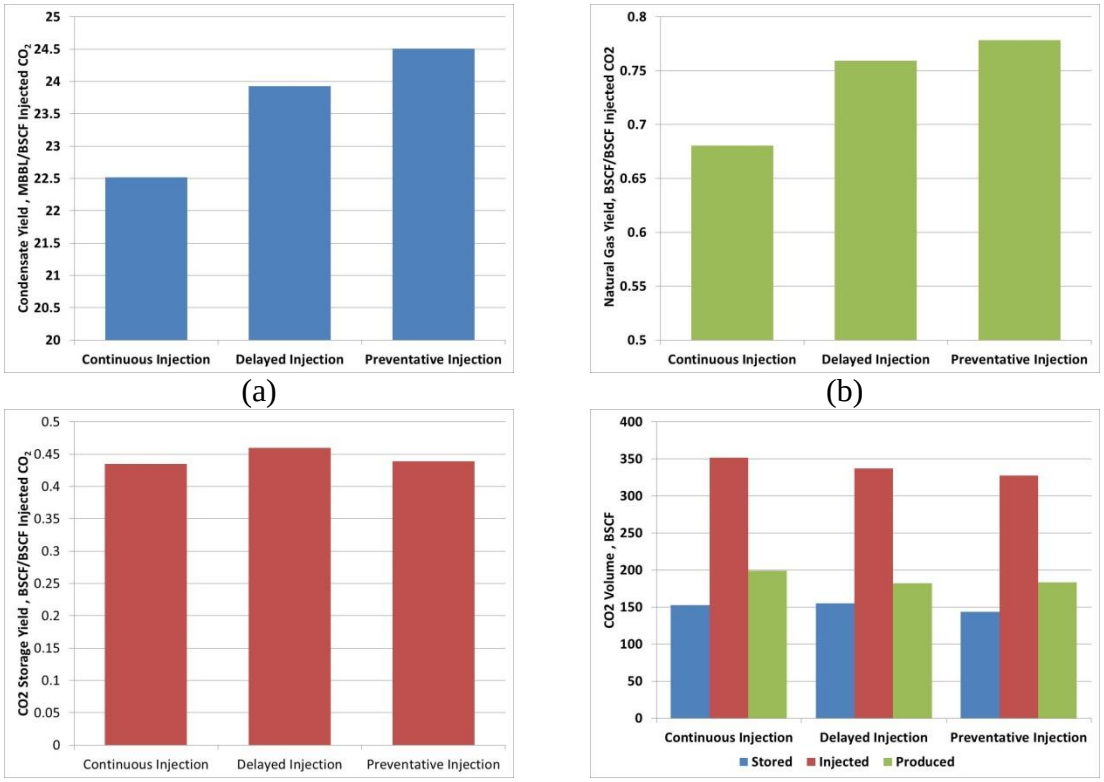

Figure 71: Injection Summary for the PUNQ-S3 Reservoir (a) Condensate Yield (b) Natural Gas Yield (c) CO_2 Storage Yield (d) CO_2 Volume Summary

To understand the impact of the different scenarios it is important to investigate the economics. Probabilistic analysis was completed by first assuming a triangular distribution for common parameters in the CO_2 EGR and Sequestration process. These parameters are listed in Table 41.

Table 41: Parameters for Monte Carlo Simulation of CO_2 EGR and Sequestration Economics for PUNQ-S3 Reservoir

	MIN	MODE	MAX
Operating Cost, $/year/well	12,000	36,000	1,000,000
Interest Rate	5%	10%	25%
Annual Capital Cost, $MM/year	1	5	100
Gas Price, $/MSCF	2	4.25	10
Oil Price , $/bbl	40	80	120
Water Treatment Cost, $/bbl	0.5	1	2
CO_2 **Separation Cost, $/MSCF**	.1	.3	1
CO_2 **Injection Cost, $/MSCF**	.1	.3	1
Tax Rate	10%	25%	50%
CO_2 **Storage Credit, $/tonne**	0	50	100
CO_2 **Storage Cost, $/tonne**	1	3	5
CO_2 **Capture Cost, $/MSCF**	.1	.5	1

These parameters represent the minimum (MIN), most likely (MODE), and maximum (MAX) values that can affect the economics of the CO_2 EGR process. A probability distribution of each of these parameters was created and a Monte Carlo simulation randomly sampled 1,000,000 values from each of these probability distributions. These values were then used to create a cumulative distribution of the net present value of the CO_2 EGR and Sequestration Process. From this cumulative distribution, shown in Figure 72, the results show all options are unprofitable at probabilities less than 5%. This means that at poor economic conditions the CO_2 EGR and Sequestration process can become unprofitable. Poor economic conditions include high operating cost per well, high interest rates, high annual capital cost, low natural gas price, low oil price, high water treatment cost, high CO_2 separation cost, high CO_2 injection cost, high tax rate, low storage credit, high storage cost, and high capture cost all relative to the parameters used for the Monte Carlo simulation.

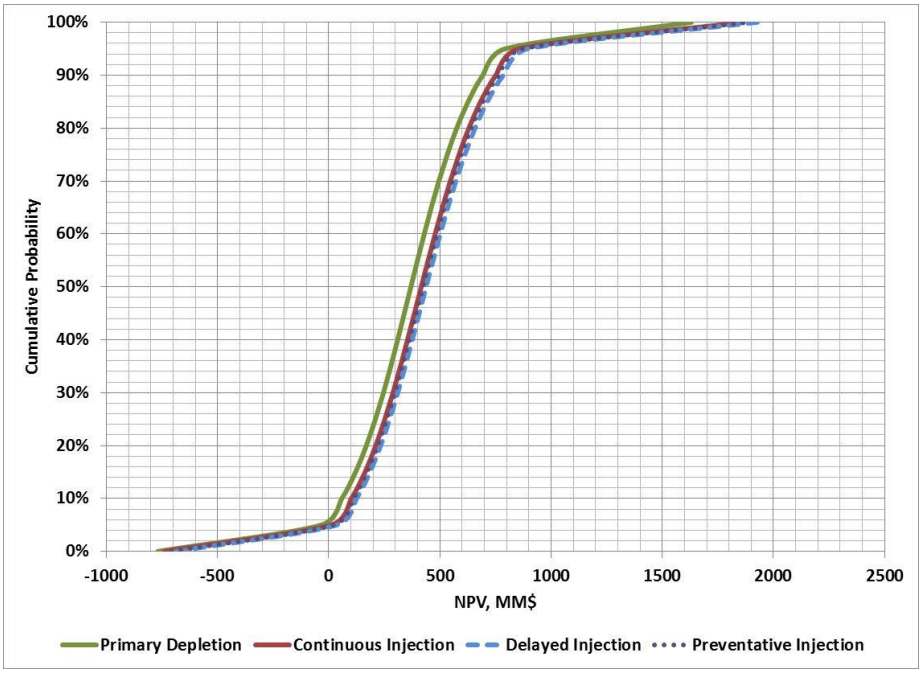

Figure 72: Monte Carlo Results for CO_2 EGR and Sequestration Economics for PUNQ-S3 Reservoir

Regardless of cumulative probabilities less than 5%, the injection scenarios illustrate profitability at probabilities greater than 5% when compared to the primary depletion scenario. Furthermore, all the injection scenarios are an indication of the benefit of using CO_2 to meet economic challenges while improving the hydrocarbon recovery and ensuring sufficient CO_2 Sequestration.

10 CONCLUSIONS

The impact of CO_2 EGR and Sequestration reveals the potential impact on wet gas reservoirs. Studies show the impact that CO_2 has on gas/condensate recovery and near wellbore condensate removal. Productivity models and evolution of skin factor show that condensate blockage can dramatically affect gas well performance. In addition to this, productivity models show that CO_2 can improve the productivity of gas wells affected by condensate blockage. The PUNQ-S3 model illustrated the field wide implications that CO_2 can have on gas/condensate recovery. The important conclusions of these studies are the following:

1. Distinct compressibility changes can be used to identify dew point pressures for a wet gas system.

2. CO_2 has the potential to form mixtures with reservoir fluids that have lower dew point pressure compared to the original reservoir fluid. As the concentration of CO_2 increases the dew point pressure is reduced and as a result of this liquid dropout is decreased. In addition, the heat of condensation increases as the amount of CO_2 increases in the reservoir fluid. The increase in CO_2 concentration results in wet gas fluid having a greater difficulty of having liquids dropout.

3. CO_2 has the ability to reduce condensate blockage skin by via two mechanisms which are reduction of dew point pressure and re-pressurization of the reservoir above the CO_2 controlled dew point pressure.

4. CO_2 EGR with CO_2 Sequestration can be profitable when there are favorable economic conditions.

5. Among the choices for CO_2 capture combined with power generation, NGCC is the best option when compared to CFGA, IGCC, and OPC. NGCC requires the least economic investment.

6. As an ideal strategy, it is best to set CO_2 injectors' bottom hole pressure to the initial reservoir pressure. This provides a preventive measure against condensate blockage in nearby producer wells. It also ensures profitable condensate yields and natural gas yields.

NOMENCLATURE

$\Delta h_{condensation}$ = heat of enthalpy due to condensation

μ_i = the chemical potential of component i

μ_g = gas viscosity

μ_o = oil viscosity

A = parameter in Standing correlation

A_c = capital cost without CO_2 capturing facilities in $/kWh

$a_{c\text{-}p}$ = parameter in correlation for compressor and pump annual expense

a_{INJ} = parameter in correlation for injected CO_2 at 356K

a_{trans} = parameter in correlation for pipeline annual expense

B = parameter in Standing correlation

$B^{(0)}$ = virial equation coefficient

$B^{(1)}$ = virial equation coefficient

B_c = fuel and operational cost to generate 1-kWh without CO_2 capturing facilities in $/kWh

$b_{c\text{-}p}$ = parameter in correlation for compressor and pump annual expense

B_g = gas formation volume factor

b_{INJ} = parameter in correlation for injected CO_2 at 356K

B_o = oil formation volume factor

B_r = virial equation parameter

b_{trans} = parameter in correlation for compressor and pump annual expense

C = parameter in Standing correlation

C_1 = Correlation Constant for Onshore and Offshore Pipeline System Capital Cost

C_2 = Correlation Constant for Onshore and Offshore Pipeline System Capital Cost

C_3 = Correlation Constant for Onshore and Offshore Pipeline System Capital Cost

C_4 = Correlation Constant for Onshore and Offshore Pipeline System Capital Cost

C_5 = Correlation Constant for Onshore and Offshore Pipeline System Capital Cost

C_6 = Correlation Constant for Onshore and Offshore Pipeline System Capital Cost

$CAP_{c\text{-}p}$ = total pump and capital cost

$CAPEX_{capfacility}$ = is the capital cost of the capture facility

$CAPEX_{c\text{-}p}$ = total annualized capital cost of the compressor and pump

$CAPEX_{storage}$ = annualized storage cost

$CAPEX_{trans}$ = total capital expense for the pipeline system

CAP_{INJ} = total capital expense for the CO_2 injectors

$CAP_{RECYCLE}$ = recycle plant cost

$CAP_{storage}$ = total storage cost

C_{cap} = CO_2 capture cost per amount of CO_2 captured

$C_{capfacility}$ = annual capture facility cost

C_{CCF} = capital cost factor of the pump and compressor

C_{CO2_SEP} = CO_2 separation cost

C_{comp} = capital cost for each compressor

$C_{c\text{-}p}$ = compressor and pump annual expense

$c_{c\text{-}p}$ = parameter in correlation for compressor and pump annual expense

C_F = capacity factor for the compressor and pumps

c_G = gas compressibility

c_{INJ} = parameter in correlation for injected CO_2 at 356K

$C_{INJ,i}$ = annual injector capital cost

$C_{INJ,i}$ = ith injector capital cost

$CINJ_i$ = controls for injector for time period i

c_L = liquid compressibility

COE = cost of generating power without CO_2 capture

COEW = cost of generating power with CO_2 capture

$Cost_t$ = total cost for time period *t*

$C_{pattern}$ = cost of developing 5 spot pattern

C_{pump} = pump capital cost

CR = compression ratio

$C_{RECYCLE}$ = recycle cost

$C_{storage}$ = annual storage cost

c_T = total isothermal compressibility

C_{trans} = annual capital expense for pipeline system

c_{trans} = parameter in correlation for compressor and pump annual expense

C_{well} = single well cost for 5 spot pattern

$C_{welltotal}$ = total well cost for single 5 spot pattern

$C_{\varepsilon\text{-}\$}$ = currency conversion factor from Euros to US dollars

D = parameter in Standing correlation

D_c = capital cost with CO_2 capturing facilities in $/kWh

$d_{c\text{-}p}$ = parameter in correlation for compressor and pump annual expense

DEPTH = total depth of the well

d_{INJ} = parameter in correlation for injected CO_2 at 356K

D_{pipe} = pipeline diameter

d_{trans} = parameter in correlation for compressor and pump annual expense

E_c = fuel and operational cost to generate 1-kWh with CO_2 capturing facilities in $/kWh

$E_{c\text{-}p}$ = annual electricity cost

$E_{INJ,i}$ = annual cost of electricity for the ith injector

F_{cap} = CO_2 captured for time period *t*

ff = fanning friction factor

f_G = gas saturation

F_{GP} = gas production for time period *t*

$F_I CO_2$ = CO_2 injected for time period *t*

f_L = liquid saturation

F_{OP} = oil production for time period *t*

$FOPEX_{storage}$ = annual operating expense for the field

$F_P CO_2$ = CO_2 separated from the total field production for time period *t*

F_{PCO2} = production rate of CO_2 from the 5 Spot pattern

$F_S CO_2$ = CO_2 stored for time period *t*

F_{WP} = water production for time period *t*

G = Gibbs free energy

g = molar gibbs free energy

G_c = tones of CO_2 emitted per 1 –kWh of electricity generated in tones/kWh

h = the net pay

InvBS = Investment correlation for booster stations for onshore and offshore pipeline

$InvBS_{norm}$ = normalized investment for the booster stations

InvPipe = pipeline capital investment

IRR = internal rate of return

J = parameter in Piper *et al* correlation

J = productivity of well without condensate blockage

J_0 = productivity of well undergoing condensate blockage

J_D= productivity ratio

k = absolute permeability

K = parameter in Piper *et al* correlation

k_{rg} = gas relative permeability

k_{ro} = oil relative permeability

k_s = permeability of damaged zone

k_{sc} = ratio of the specific heat at constant pressure to the specific heat at constant volume for each individual stage

l = subscript for liquid phase

m = mass rate of captured CO_2 in tonnes/day

m_G = mass of the gas phase of the PVT cell

m_L = mass of the liquid phase of the PVT cell

M_{sc} = molecular weight of the captured CO_2

m_{train} = mass rate through each compressor train

MW_i = i^{th} liquid component's molecular weight

n = moles

N_{inj} = number of CO_2 injectors in the field

$N_{pattern}$ = number of 5 spot patterns

NPV = Net Present Value of CO_2 EGR and Sequestration Process

N_{stage} = number of stages used for compression

N_{train} = number of compressor trains

N_{wells} = number of wells in 5 spot pattern

$OPEX_{c\text{-}p}$ = compressor and pump operating expense

$OPEX_{trans}$ = operational expense of pipeline system

p = pressure of the PVT cell

P_{avg} = average pressure between the surface pressure and bottom hole pressure

P_{BHP} = bottom hole pressure at the well site

$P_{cut\text{-}off}$ = cut off pressure of captured CO_2

P_{dew}= dew point pressure of the wet gas

$p_{dewpoint}$ = dewpoint pressure

P_e = cost of electricity

P_{final} = injection pressure at the injection site

P_i = loading or working pressure of the i^{th} component

$P_{initial}$ = inlet pressure into the compressor

P_{pc} = pseudo critical temperature

P_r = reduced pressure

p_s = pressure at end of damage zone

P_t = pressure larger than the dew point pressure

p_{wf} = bottom hole pressure

q_g = gas flow rate

R = ideal gas constant

r_c = condensate blockage radius

r_e = drainage radius

Re = Reynolds number

$Revenue_t$ = total revenue for time period t

r_s = radius of damage zone

R_s = solution gas oil ratio

R^u = space of possible user defined bottom hole pressures

r_w = wellbore radius

S = entropy

s = molar entropy

s_c = condensate blockage skin

s_m = total mechanical skin

s_t = the total skin factor

T = temperature

T = temperature in Rankin

t_{dep} = total length of CO_2 EGR and Sequestration project in years

T_F = terrain factor

T_{in} = inlet temperature to the compressor

T_{pc} = pseudo critical temperature

T_r = reduced temperature

T_t = temperature used for the CCE experiments

v = molar volume

v = subscript for vapor phase

V = volume

V_G = gas volume

V_i = i^{th} liquid component's feed liquid volume

V_i = loading volume of the i^{th} component

V_L = liquid volume

V_t = total volume of the PVT cell

w_{GP} = gas price per MSCF

$w_I CO_2$ = CO_2 injection cost per MSCF

w_{ICO2} = cost of injecting CO_2

$W_{INJ,i}$ = required power of CO_2 injector

w_{OP} = oil price per STB

W_p = pumping power

$W_{s,i}$ = power requirement for the ith stage of compression

$w_S CO_2$ = CO_2 tax incentive per tonne

$W_{s\text{-}total}$ = total compressor power

w_{WP} = water disposal cost per STB

x = process vector for CO_2 EGR and Sequestration Process

y_i = i^{th} component's mole fraction in the gas condensate mixture

z_G = compressibility factor of the gas phase

z_g = gas compressibility factor

z_i = compressibility factor of the i^{th} component

Z_{sc} = compressibility factor for the captured CO_2

z_t = total compressibility factor for condensate mixture

α = stage of field development

β_f = parameter in Piper *et al* correlation

γ_g, = specific gravity of the gas condensate sample

Δ = change

ΔL = pipeline distance between the CO_2 capture site and the CO_2 injection site

Δm = pseudo pressure

ΔP = pressure difference between the final pumping pressure and cut-off pressure

ε = pipeline roughness factor

η_f = parameter in Piper *et al* correlation

η_{INJ} = efficiency of the pump

η_{is} = isentropic efficiency of the compressor

η_p = efficiency of the pump

μ_{pipe} = viscosity of the captured CO_2 evaluated at the pumping temperature (356K) and average pressure between the cut-off pressure and final pumping pressure

ρ_G = gas density in the PVT cell

ρ_i = i^{th} liquid component's density at standard conditions

ρ_{INJ} = density of the captured CO_2 at 356 K (181 F) and at the average pressure between the surface pressure and bottom hole pressure

ρ_L = liquid density in the PVT cell

ρ_p = density of the captured CO_2 evaluated at 356 K (181 F) and at the average pressure between $P_{cut\text{-}off}$ and P_{final}

ρ_{pipe} = density of the captured CO_2 evaluated at the pumping temperature (356K) and average pressure between the cut-off pressure and final pumping pressure

ω = acentric factor of the component

REFERENCES

Algharaib, M. and Abu Al-Soof, N. 2008. Economic Modeling of CO_2 Capturing and Storage Projects. SPE 120815 first presented at the 2008 SPE Saudi Arabia Section Technical Symposium, Alkhobar, Saudi Arabia, 10-12 May. http://www.onepetro.org/mslib/app/Preview.do?paperNumber=SPE-120815-MS&societyCode=SPE.

American Petroleum Institute. 2008. Components-data.

Barrufet, M. 2013. Spreadsheet of PVT data for Cusiana field. Spreadsheet report. (unpublished report).

Barrufet, M., Bacquet, A., and Falcone, G. 2010. Analysis of the Storage Capacity for CO2 Sequestration of a Depleted Gas Condensate Reservoir and a Saline Aquifer (in English). *Journal of Canadian Petroleum Technology* **49** (8): pp.23-31. http://dx.doi.org/0.2118/139771-PA.

Carbon Dioxide Information Analysis Center. 2012a. Fossil Fuel CO_2 Emissions from Qatar. http://cdiac.ornl.gov/trends/emis/qat.html (accessed 2 Febuary 2012).

Carbon Dioxide Information Analysis Center. 2012b. Fossil Fuel CO_2 Emissions from the United States of America. http://cdiac.ornl.gov/trends/emis/usa.html accessed 2 Febuary 2012).

CMOST Studio, Version 2011 User Guide. 2011. Calgary, Aberta: CMG.

Cronquist, C. 2001. *Estimation and Classification of Reserves of Crude Oil, Natural Gas and Condensate*. Richardson, Texas: SPE book series, Society of Petroleum Engineers.

David, J. 2000. Economic Evaluation of Leading Technology Options for Sequestration of Carbon Dioxide. MS thesis, Massachusets Institute of Technology, Cambridge, MA (May 2000).

Economides, M.J., Hill, A. D., and Ehlig-Economides, C. 1994. *Petroleum Production Systems*. Englewood Cliffs, N.J., PTR Prentice Hall.

Fetkovich, M.J. 1973. "The Isochronal Testing of Oil Wells", paper SPE 4529 presented at the 1973 SPE Annual Fall Meeting, Las Vegas, Nevada, 30 September-3 October. http://dx.doi.org/10.2118/4529-MS.

Fevang, O. and Whitson, C.H. 1996. Modeling Gas-Condensate Well Deliverability. *SPE Reservoir Engineering* **11** (4): 221-230. http://dx.doi.org/10.2118/30714-PA.

Finkenrath, M. 2011. Cost and Performance of Carbon Dioxide Capture from Power Generation. International Energy Agency.

GEM Advanced Compositional and GHG Reservoir Simulator, Version 2011 User Guide. 2011. Calgary, Aberta: CMG.

Ghomian, Y., Sepehrnoori, K., and Pope, G.A. 2010. Efficient Investigation of Uncertainties in Flood Design Parameters for Coupled CO_2 Sequestration and Enhanced Oil Recovery. Paper SPE 139738 presented at the SPE International

Conference on CO_2 Capture, and Storage, and Utilization, New Orleans, LA, 10-12 November. http://dx.doi.org/10.2118/139738-MS.

Gupta, A. 2010. Development of Process for Enhancing Gas Recovery with Carbon Dioxide Sequestration in Carbonate Reservoirs. Report No. NPRP 4 – 007 – 002, Texas A&M University at Qatar, Doha, Qatar.

Heddle, G., Herzog, H., and Klett, M. 2003. The Economics of CO2 Storage. Report No. LFEE 2003-003 RP, Laboratory for Energy and the Environment, Massachusetts Institute of Technology, Cambridge, MA.

IEA Energy Technology Essentials. 2006. CO2 Capture & Storage, http://www.iea.org/techno/essentials1.pdf (downloaded January 29, 2011).

IEA Greenhouse Gas R&D Programme. 2005. Building The Cost Curves for CO_2 Storage: European Sector. Report No. 2005/2.

Imperial College London Department of Earth Science and Engineering. 2011. PUNQ-S3 Test Case. http://www3.imperial.ac.uk/earthscienceandengineering/research/perm/punq-s3model (downloaded 3 May 2011).

IPCC. 2005. IPCC Special Report on Carbon Dioxide Capture and Storage, Prepared by Working Group III of the Intergovernmental Panel on Climate Change [Metz, B., O. Davidson, H. C. de Coninck, M. Loos, and L. A. Meyer (eds.)], Cambridge, United Kingdom and New York, NY, USA.

Jones, J.R. and Raghavan., R. 1988. Interpretation of Flowing Well Response in Gas-Condensate Wells (includes associated papers 19014 and 19216) (in

English). *SPE Formation Evaluation* **3** (3): 578-594. http://dx.doi.org/10.2118/14204-PA.

Laidler, K.J., Meiser, J.H., and Sanctuary, B.C. 2003. *Physical Chemistry*, 4 edition. Boston, MA, Houghton Mifflin.

Lemmon, E.W., Huber, M.L., and McLinden, M.O. 2010. *NIST Standard Reference Database 23: Reference Fluid Thermodynamic and Transport Properties-REFPROP*, Version 9.0. Gaithersburg, Maryland: Standard Reference Data Program, National Institute of Standards and Technology.

Mamora, D.D. and Seo, J.G. 2002. Enhanced Gas Recovery by Carbon Dioxide Sequestration in Depleted Gas Reservoirs. Paper SPE 77347 presented at the SPE Annual Technical Conference and Exhibition. San Antonio, TX, 29 September- 2 October. http://dx.doi.org/10.2118/77347-MS.

McCain, William D. 1990. *The Properties of Petroleum Fluids, Second Edition*. Tulsa, OK, PennWell Books.

McCollum, D.L. and Ogden, J.M. 2006. Techno-Economic Models for Carbon Dioxide Compression, Transport, and Storage & Correlations for Estimating Carbon Dioxide Density and Viscosity. Report No. UCD-ITS-RR-06-14, Institute of Transportation Studies, University of California Davis.

Monger. T.G. and Khakoo, A. 1981. The Phase Behavior of CO_2- Appalachian Oil Systems. Paper SPE 10269 presented at the 56th Annual Fall Technical Conference and Exhibition. San Antonio, TX, 5-7 October. http://dx.doi.org/10.2118/10269-MS.

Muskat, M. 1981. *Physical Principles of Oil Production*, 2nd edition. Boston, MA, International Human Resources Development Corp.

Nghiem, L., Sammon, P., Grabenstetter, J., and Ohkuma, H. 2004. "Modeling CO_2 Storage in Aquifers with a Fully-Coupled Geochemical EOS Compostional Simulator" Paper SPE 89474 presented at the 2004 SPE/DOE Fourteenth Symposium on Improved Oil Recovery, Tulsa, Oklahoma, 17-21 April. http://dx.doi.org/10.2118/89474-MS.

O'Dell, H.G. and Miller, R.N. 1967. Successfully Cycling a Low Permeability, High-Yield Gas Condensate Reservoir. *Journal of Petroleum Technology* **19** (1): 41-47. SPE-1495-PA. http://dx.doi.org/10.2118/1495-PA.

Piper, L.D., McCain, W.D., and Holditch, S.A. 1993. Compressibility Factors for Naturally Occurring Petroleum Gases. Paper SPE 26668 presented at the 68th Annual Technical Conference and Exhibition of the Society of Petroleum Engineers, Houston, TX, 3-6 October. http://dx.doi.org/10.2118/26668-MS.

Poling, B.E., Prausnitz, J. M., and O'Connell, J. P. 2001. *The Properties of Gases and Liquids*, 5th edition. New York, NY, McGraw-Hill.

Potsch, K.T. and Braeuer, L. 1996. A Novel Graphical Method for Determining Dewpoint Pressures of Gas Condensates. Paper SPE 36919 presented at the European Petroleum Conference. Milan, Italy, 22-24 October 1996. http://dx.doi.org/10.2118/36919-MS.

Shamshiri, H. and Jafarpour, B. 2010. Optimization of Geologic CO_2 Storage in Heterogeneous Aquifers Through Improved Sweep Efficiency. Paper SPE

139643 presented at the SPE International Conference on CO_2 Capture, and Storage, and Utilization, New Orleans, LA, 10-12 November. http://dx.doi.org/10.2118/139643-MS.

Whitson, C.H. and Kuntadi, A. 2005. Khuff Gas Condensate Development. Paper IPTC 10692 presented at the International Petroleum Technology Conference. Doha, Qatar, 21-23 November 2005. http://dx.doi.org/10.2523/10692-MS.

Winnick, J. 1996. *Chemical Engineering Thermodynamics: An Introduction to Thermodynamics for Undergraduate Engineering Students*. New York, NY, Wiley.

WinProp Phase Property Program, Version 2011 User Guide. 2011. Calgary, Alberta: CMG.

Xu, S. and Lee, J. 1999. Gas Condensate Well Test Analysis Using a Single-Phase Analogy. Paper SPE 55992 presented at the 1999 SPE Western Regional Meeting, Anchorage, Alaska, 26-28 May. http://dx.doi.org/10.2118/55992-MS.

APPENDIX

Huff-n-Puff CMG GEM Data File

CMG's Gem was the compositional simulator used in this work. The following is the Base .dat file that was created to model the radial flow for the Huff-n-Puff Process.

```
** ----------------------------------------------------------------**
** Dr. Anuj Gupta CO2 EGR and Sequestrion Research Group            **
** ----------------------------------------------------------------**
** ----------------------------------------------------------------**
** **
** FILE:  K4_NORTHFIELDSIM.DAT                                      **
** **
** MODEL: RADIAL 25x1x145 GRID          CO2 INJECTION           **
** 24 COMPONENTS         Fluid Compositions based on K4 layer              **
** Whitson Fluid         Whitson Paper IPTC 10692                **
** SI UNITS              Geochemistry based on SPE 89341         **
** **
** ----------------------------------------------------------------**
** **
** **
** ----------------------------------------------------------------**
** CONTACT uchenna.odi@qatar.tamu.edu for questions                 **
** ----------------------------------------------------------------**
RESULTS SIMULATOR GEM 200900
** ------- Input/Output ---------------
FILENAMES OUTPUT SRFOUT RESTARTOUT INDEXOUT MAINRESULTSOUT
*INUNIT *SI
INTERRUPT INTERACTIVE
*XDR *ON

*MAXERROR  20
RANGECHECK ON
WPRN WELL TIME
WPRN GRID TIME
WPRN ITER BRIEF
WPRN ITER MATRIX
WSRF WELL 1
WSRF GRID TIME
OUTSRF WELL PSPLIT
DIARY WELL-INFO
DIM MDALP 100000000
DIM MDLU 10000000
DIM MDICLU 100000
*DIM *MDGRID 10000
OUTPRN WELL BRIEF
OUTPRN RES NONE
OUTPRN GRID KRG KRO KRW MINERAL 'CALCITE' MOLALITY 'CO2' MOLALITY 'H+' MOLALITY 'Ca++' MOLALITY
'OH-' MOLALITY 'CO3--' MOLALITY 'HCO3-' PRES
        RHOG RHOO SG SIG SO SW TEMP W 'CO2' X 'N2' X 'CO2' X 'H2S' X 'C1' X 'C2' X 'C3' X 'iC4' X 'nC4' X 'iC5' X 'nC5' X
'C6' X 'C7' X 'C8' X 'C9' X 'C10' X 'C11' X 'C12' X 'C13' X 'C14' X 'C15' X 'C16' X 'C17-19' X 'C20-29' X 'C30+'
        Y 'N2' Y 'CO2' Y 'H2S' Y 'C1' Y 'C2' Y 'C3' Y 'iC4' Y 'nC4' Y 'iC5' Y 'nC5' Y 'C6' Y 'C7' Y 'C8' Y 'C9' Y 'C10' Y 'C11' Y
'C12' Y 'C13' Y 'C14' Y 'C15' Y 'C16' Y 'C17-19' Y 'C20-29' Y 'C30+'
        Z 'N2' Z 'CO2' Z 'H2S' Z 'C1' Z 'C2' Z 'C3' Z 'iC4' Z 'nC4' Z 'iC5' Z 'nC5' Z 'C6' Z 'C7' Z 'C8' Z 'C9' Z 'C10' Z 'C11' Z 'C12' Z
'C13' Z 'C14' Z 'C15' Z 'C16' Z 'C17-19' Z 'C20-29' Z 'C30+'
```

```
OUTSRF GRID CAPN KRG KRO KRW MINERAL 'CALCITE' MOLALITY 'CO2' MOLALITY 'CO3--' MOLALITY 'Ca++'
MOLALITY 'H+' MOLALITY 'HCO3-' MOLALITY 'OH-'
        PRES RHOG RHOO SG SIG SO SW TEMP W 'CO2' X 'N2' X 'CO2' X 'H2S' X 'C1' X 'C2' X 'C3' X 'iC4' X 'nC4' X 'iC5' X
'nC5' X 'C6' X 'C7' X 'C8' X 'C9' X 'C10' X 'C11' X 'C12' X 'C13' X 'C14' X 'C15' X 'C16' X 'C17-19' X 'C20-29' X 'C30+'
        Y 'N2' Y 'CO2' Y 'H2S' Y 'C1' Y 'C2' Y 'C3' Y 'iC4' Y 'nC4' Y 'iC5' Y 'nC5' Y 'C6' Y 'C7' Y 'C8' Y 'C9' Y 'C10' Y 'C11' Y
'C12' Y 'C13' Y 'C14' Y 'C15' Y 'C16' Y 'C17-19' Y 'C20-29' Y 'C30+'
        Z 'N2' Z 'CO2' Z 'H2S' Z 'C1' Z 'C2' Z 'C3' Z 'iC4' Z 'nC4' Z 'iC5' Z 'nC5' Z 'C6' Z 'C7' Z 'C8' Z 'C9' Z 'C10' Z 'C11' Z 'C12' Z
'C13' Z 'C14' Z 'C15' Z 'C16' Z 'C17-19' Z 'C20-29' Z 'C30+'
OUTSRF RES
OUTSRF WELL GHGGAS
        GHGLIQ
        GHGTHY
        GHGSCRIT
        GHGSOL
        GHGAQU
        GHGMNR
        PAVG
**$  Distance units: m
RESULTS XOFFSET          0.0000
RESULTS YOFFSET          0.0000
RESULTS ROTATION          0.0000  **$  (DEGREES)
**$ *************************************************************************
**$ Definition of fundamental cartesian grid
**$ *************************************************************************
GRID RADIAL 15 1 15 *RW       0.099974
KDIR DOWN
DI IVAR       0.0677523       0.113656       0.190661       0.319838
      0.536536       0.900051        1.50986        2.53282        4.24887
       7.12757        11.9567        20.0576        33.6471        56.4438
       94.6858
DJ JVAR 360
DK ALL
 225*13.1064
DTOP
 15*2926.08
**$ Property: NULL Blocks  Max: 1  Min: 1
**$  0 = null block, 1 = active block
NULL CON           1
**$ Property: Porosity  Max: 0.1  Min: 0.1
POR CON         0.2
**$ Property: Permeability I (md)   Max: 500  Min: 5
PERMI KVAR
 7*1 1*1 7*1
PERMJ EQUALSI
PERMK EQUALSI
**$ Property: Pinchout Array  Max: 1  Min: 1
**$  0 = pinched block, 1 = active block
PINCHOUTARRAY CON           1
*CPOR  7.25189E-07
*PRPOR MATRIX   36645.6
** ---------- Fluid Model ----------
**$ Model and number of components
MODEL SRK
NC 24 24
***H2O_INCLUDED
COMPNAME 'N2' 'CO2' 'H2S' 'C1' 'C2' 'C3' 'iC4' 'nC4' 'iC5' 'nC5' 'C6' 'C7' 'C8' 'C9' 'C10' 'C11' 'C12' 'C13' 'C14' 'C15' 'C16' 'C17-19'
'C20-29' 'C30+'
HCFLAG
0 0 0 0 0 0 0 0 0 0 0 0 0 0 0 0 0 0 0 0 0 0 0 0
MW
28.01 44.01 34.08 16.04 30.07 44.1 58.12 58.12 72.15 72.15 82.32 95.36 108.77 121.9 134.78 147.59 160.3 172.91 185.42 197.82
210.11 233.39 299.51 477.34
AC
0.037 0.225 0.09 0.011 0.099 0.152 0.186 0.2 0.229 0.252 0.2373 0.2714 0.3094 0.35 0.39 0.4295 0.4684 0.5067 0.5444 0.5814
0.6178 0.6857 0.8712 1.0411
PCRIT
```

33.5330688 72.775197 88.4598 45.386682 48.0813036 41.9231406 35.9214834 37.4661276 33.3697584 33.2608848 33.4309998 31.1106312 28.7698488 26.53794 24.6122382 22.931502 21.4549038 20.1620298 19.0120524 17.998167 17.0863506 15.6029478 12.5612916 11.4045096

***VCRIT
TCRIT
125.8888889 303.7777778 373.0555556 190.2222222 305 369.5 407.5 424.7777778 460.0555556 469.3888889 513.1111111 548.7222222 579.6111111 607.5 632.2222222 654.6111111 675 693.7777778 711.1111111 727.1666667 742.0555556 768.0555556 829.5 897.9444444
BIN
0
0.12 0.12
0.02 0.12 0.07
0.06 0.15 0.06 0.06887
0.08 0.15 0.06 0.06887 0.06887
0.08 0.15 0.06 0.06887 0.06887 0.06887
0.08 0.15 0.06 0.06887 0.06887 0.06887 0.06887
0.08 0.15 0.06 0.06887 0.06887 0.06887 0.06887 0.06887
0.08 0.15 0.06 0.06887 0.06887 0.06887 0.06887 0.06887 0.06887
0.08 0.15 0.05 0.06887 0.06887 0.06887 0.06887 0.06887 0.06887 0.06887
0.08 0.15 0.03 0.06887 0.06887 0.06887 0.06887 0.06887 0.06887 0.06887 0.06887
0.08 0.15 0.03 0.06887 0.06887 0.06887 0.06887 0.06887 0.06887 0.06887 0.06887 0.06887
0.08 0.15 0.03 0.06887 0.06887 0.06887 0.06887 0.06887 0.06887 0.06887 0.06887 0.06887 0.06887
0.08 0.15 0.03 0.06887 0.06887 0.06887 0.06887 0.06887 0.06887 0.06887 0.06887 0.06887 0.06887 0.06887
0.08 0.15 0.03 0.06887 0.06887 0.06887 0.06887 0.06887 0.06887 0.06887 0.06887 0.06887 0.06887 0.06887 0.06887
0.08 0.15 0.03 0.06887 0.06887 0.06887 0.06887 0.06887 0.06887 0.06887 0.06887 0.06887 0.06887 0.06887 0.06887 0.06887
0.08 0.15 0.03 0.06887 0.06887 0.06887 0.06887 0.06887 0.06887 0.06887 0.06887 0.06887 0.06887 0.06887 0.06887 0.06887 0.06887
0.08 0.15 0.03 0.06887 0.06887 0.06887 0.06887 0.06887 0.06887 0.06887 0.06887 0.06887 0.06887 0.06887 0.06887 0.06887 0.06887 0.06887
0.08 0.15 0.03 0.06887 0.06887 0.06887 0.06887 0.06887 0.06887 0.06887 0.06887 0.06887 0.06887 0.06887 0.06887 0.06887 0.06887 0.06887 0.06887
0.08 0.15 0.03 0.06887 0.06887 0.06887 0.06887 0.06887 0.06887 0.06887 0.06887 0.06887 0.06887 0.06887 0.06887 0.06887 0.06887 0.06887 0.06887 0.06887
0.08 0.15 0.03 0.06887 0.06887 0.06887 0.06887 0.06887 0.06887 0.06887 0.06887 0.06887 0.06887 0.06887 0.06887 0.06887 0.06887 0.06887 0.06887 0.06887 0.06887
0.08 0.15 0.03 0.06887 0.06887 0.06887 0.06887 0.06887 0.06887 0.06887 0.06887 0.06887 0.06887 0.06887 0.06887 0.06887 0.06887 0.06887 0.06887 0.06887 0.06887 0.06887

TRES 104.4444
PHASEID DEN
CW 7.25188E-07
REFPW 36645.6
SOLUBILITY HENRY
FLASH-METHOD OUTER
DERIVATIVEMETHOD NUMERALL
DIFCOR-OIL SIGMUND
DIFCOR-GAS SIGMUND
**DIFFUSION COEFFICIENT IN CM2/S
DIFFC-AQU
0 2.00E-05 0 0 0 0 0 0 0 0 0 0 0 0 0 0 0 0 0 0 0 0 0 0

*HENRYC
0 1.9510547E+05 0 0 0 0 0 0 0 0 0 0 0 0 0 0 0 0 0 0 0 0 0 0

*REFPH
0 9.4000000E+03 0 0 0 0 0 0 0 0 0 0 0 0 0 0 0 0 0 0 0 0 0 0

*VINFINITY
0 3.5089333E-02 0 0 0 0 0 0 0 0 0 0 0 0 0 0 0 0 0 0 0 0 0 0

*YAQU-RATE-CUTOFF
100 0.0001 100 100 100 100 100 100 100 100 100 100
100 100 100 100 100 100 100 100 100 100 100 100

```
            100


*DER-CHEM-EQUIL *ANALYTICAL
*DER-REACT-RATE *ANALYTICAL

*ACTIVITY-MODEL *B-DOT
*SALINITY 0.1
*AQUEOUS-DENSITY *ROWE-CHOU
*AQUEOUS-VISCOSITY *KESTIN

*NC-AQUEOUS 5
*COMPNAME-AQUEOUS
'H+' 'Ca++' 'OH-' 'HCO3-' 'CO3--'
*MW-AQUEOUS
1.0079
40.0800
17.0073
61.0171
60.0092

*ION-SIZE-AQUEOUS
9.0 6.0 3.5 4.5 4.5
*CHARGE-AQUEOUS
1 2 -1 -1 -2

*NC-MINERAL 1
*COMPNAME-MINERAL
'CALCITE'
*MW-MINERAL
100.1

*MASSDENSITY-MINERAL
2710.00

*N-RATE-REACT 1
*N-CHEM-EQUIL 3

**REACTION NO. 1: H2O = H+ + OH-
*STOICHIOMETRY
0       0       0       0       0       0       0       0       0       0       0       0
        0       0       0       0       0       0       0       0       0       0       0
        0       -1      1       0       1       0       0       0
*LOG-CHEM-EQUIL-CONST
 -13.2631

**REACTION NO. 2: CO2 + H2O = H+ + HCO3--
*STOICHIOMETRY
0       -1      0       0       0       0       0       0       0       0       0       0
        0       0       0       0       0       0       0       0       0       0       0
        0       -1      1       0       0       1       0       0
*LOG-CHEM-EQUIL-CONST
 -6.3221

**REACTION NO. 3: CO2 + H2O = 2H+ + CO3--
*STOICHIOMETRY
0       -1      0       0       0       0       0       0       0       0       0       0
        0       0       0       0       0       0       0       0       0       0       0
        0       -1      2       0       0       0       1       0
*LOG-CHEM-EQUIL-CONST
 -16.5563

**REACTION NO. 1:  CALCITE + H+ = (Ca++) + (HCO3-)
*STOICHIOMETRY
0       0       0       0       0       0       0       0       0       0       0       0
        0       0       0       0       0       0       0       0       0       0       0
```

```
            0           0           -1          1           0           1           0           -1
*REACTIVE-SURFACE-AREA 88.0

*SPEC-REACT-SURFACE-AREA 1.0E+04
*MIN-REACT-SURFACE-AREA 1.0
*SUPER-SATURATION-INDEX 2.0

*ACTIVATION-ENERGY 41870.0
*REF-TEMP-RATE-CONST 25.0
*LOG-CHEM-EQUIL-CONST
 1.36
*LOG-TST-RATE-CONSTANT -8.8
***H2O_INCLUDED
***OGW_FLASH *ON
***SWR-H2OVAP 0
***SATWCUTOFF 0
**COMPONENT 1 IS A TRACE COMPONENT
*TRACE-COMP 1
*PERM-VS-POR 1

** ---------- Rock Fluid -----------
*ROCKFLUID
RPT 1


SWT
0.15        0                   0.9
0.2         0.000820562         0.736779008
0.25        0.004641802         0.592742192
0.3         0.012791302         0.467072318
0.35        0.026257997         0.358914003
0.4         0.045870834         0.267367796
0.45        0.072358532         0.191482562
0.5         0.106379201         0.130245358
0.55        0.148537664         0.082567501
0.6         0.199396668         0.047264395
0.65        0.259484621         0.023024344
0.7         0.329301218         0.008355244
0.8         0.5                 0
1           1                   0




SGT
0.1         0                   0.9
0.15        0.000449981         0.747791976
0.2         0.002545475         0.612174923
0.25        0.007014504         0.492497617
0.3         0.014399381         0.388081035
0.35        0.025154684         0.298214457
0.4         0.039680029         0.222150547
0.45        0.058336309         0.159099026
0.5         0.081455201         0.10821826
0.55        0.109345301         0.068603683
0.6         0.14229638          0.03927104
0.65        0.180582459         0.019130466
0.8         0.33                0
1           1                   0


** ---------- Initial ----------

*INITIAL
*VERTICAL *OFF
**$ Property: Pressure (kPa)   Max: 36542.2  Min: 36542.2
```

```
PRES CON      36542.2
**$ Property: Water Saturation  Max: 0.15  Min: 0.15
SW CON        0.15
**$ Property: Global Composition(N2)  Max: 3.349  Min: 3.349
ZGLOBALC 'N2' CON       3.349
**$ Property: Global Composition(CO2)  Max: 1.755  Min: 1.755
ZGLOBALC 'CO2' CON       1.755
**$ Property: Global Composition(H2S)  Max: 0.529  Min: 0.529
ZGLOBALC 'H2S' CON       0.529
**$ Property: Global Composition(C1)  Max: 83.265  Min: 83.265
ZGLOBALC 'C1' CON      83.265
**$ Property: Global Composition(C2)  Max: 5.158  Min: 5.158
ZGLOBALC 'C2' CON       5.158
**$ Property: Global Composition(C3)  Max: 1.907  Min: 1.907
ZGLOBALC 'C3' CON       1.907
**$ Property: Global Composition(iC4)  Max: 0.409  Min: 0.409
ZGLOBALC 'iC4' CON       0.409
**$ Property: Global Composition(nC4)  Max: 0.699  Min: 0.699
ZGLOBALC 'nC4' CON       0.699
**$ Property: Global Composition(iC5)  Max: 0.28  Min: 0.28
ZGLOBALC 'iC5' CON        0.28
**$ Property: Global Composition(nC5)  Max: 0.28  Min: 0.28
ZGLOBALC 'nC5' CON        0.28
**$ Property: Global Composition(C6)  Max: 0.39  Min: 0.39
ZGLOBALC 'C6' CON        0.39
**$ Property: Global Composition(C7)  Max: 0.486  Min: 0.486
ZGLOBALC 'C7' CON       0.486
**$ Property: Global Composition(C8)  Max: 0.361  Min: 0.361
ZGLOBALC 'C8' CON       0.361
**$ Property: Global Composition(C9)  Max: 0.266  Min: 0.266
ZGLOBALC 'C9' CON       0.266
**$ Property: Global Composition(C10)  Max: 0.201  Min: 0.201
ZGLOBALC 'C10' CON       0.201
**$ Property: Global Composition(C11)  Max: 0.153  Min: 0.153
ZGLOBALC 'C11' CON       0.153
**$ Property: Global Composition(C12)  Max: 0.116  Min: 0.116
ZGLOBALC 'C12' CON       0.116
**$ Property: Global Composition(C13)  Max: 0.089  Min: 0.089
ZGLOBALC 'C13' CON       0.089
**$ Property: Global Composition(C14)  Max: 0.068  Min: 0.068
ZGLOBALC 'C14' CON       0.068
**$ Property: Global Composition(C15)  Max: 0.052  Min: 0.052
ZGLOBALC 'C15' CON       0.052
**$ Property: Global Composition(C16)  Max: 0.04  Min: 0.04
ZGLOBALC 'C16' CON        0.04
**$ Property: Global Composition(C17-19)  Max: 0.073  Min: 0.073
ZGLOBALC 'C17-19' CON       0.073
**$ Property: Global Composition(C20-29)  Max: 0.063  Min: 0.063
ZGLOBALC 'C20-29' CON       0.063
**$ Property: Global Composition(C30+)  Max: 0.012  Min: 0.012
ZGLOBALC 'C30+' CON       0.012

*CALC-MOLALITYAQ-SECONDARY *OFF

*MOLALITY-AQUEOUS
  1.0E-07  9.12E-05   5.46E-07   1.17E-05   2.49E-02

*VOLUMEFRACTION-MINERAL
0.0088
***          Pressure    Temperature
*SEPARATOR    6894.76     26.6667
           2413.17     21.1111
           101.353     15.5556
** ---------- Numerical ----------

*NUMERICAL
```

```
NORM PRESS 102
MAXCHANGE PRESS 100000
MAXCHANGE SATUR 1
MAXCHANGE GMOLAR 1
NORM SATUR 0.01
NORM GMOLAR 0.01
AIM STAB 1
NORTH 100
ITERMAX 200
PIVOT ON
NEWTONCYC 1000


** ----------------- Recurrent ----------------------
*RUN

*DATE 2011 1 1
DTWELL 0.01
DTMAX 91.25
DTMIN .0001
**
** *WELL 1 'PRODUCER'
**$
WELL  'PRODUCER'
**$         rad  geofac  wfrac  skin
GEOMETRY  K  0.099974  0.5  1.  0.
PERF  GEO  'PRODUCER'
**$ UBA     ff  Status  Connection
   1 1 1   1.  OPEN    FLOW-TO  'SURFACE'
   1 1 2   1.  OPEN    FLOW-TO  1
   1 1 3   1.  OPEN    FLOW-TO  2
   1 1 4   1.  OPEN    FLOW-TO  3
   1 1 5   1.  OPEN    FLOW-TO  4
   1 1 6   1.  OPEN    FLOW-TO  5
   1 1 7   1.  OPEN    FLOW-TO  6
   1 1 8   1.  OPEN    FLOW-TO  7
   1 1 9   1.  OPEN    FLOW-TO  8
   1 1 10  1.  OPEN    FLOW-TO  9
   1 1 11  1.  OPEN    FLOW-TO  10
   1 1 12  1.  OPEN    FLOW-TO  11
   1 1 13  1.  OPEN    FLOW-TO  12
   1 1 14  1.  OPEN    FLOW-TO  13
   1 1 15  1.  OPEN    FLOW-TO  14  REFLAYER

*PRODUCER 'PRODUCER'
*OPERATE *MAX *STG 283168
*OPERATE *MIN *BHP 6894.76
** *WELL 2 'CO2-Injector'
**$
WELL  'CO2-Injector'
**$         rad  geofac  wfrac  skin
GEOMETRY  K  0.099974  0.5  1.  0.
PERF  GEO  'CO2-Injector'
**$ UBA     ff  Status  Connection
   1 1 1   1.  OPEN    FLOW-TO  'SURFACE'
   1 1 2   1.  OPEN    FLOW-TO  1
   1 1 3   1.  OPEN    FLOW-TO  2
   1 1 4   1.  OPEN    FLOW-TO  3
   1 1 5   1.  OPEN    FLOW-TO  4
   1 1 6   1.  OPEN    FLOW-TO  5
   1 1 7   1.  OPEN    FLOW-TO  6
   1 1 8   1.  OPEN    FLOW-TO  7
   1 1 9   1.  OPEN    FLOW-TO  8
   1 1 10  1.  OPEN    FLOW-TO  9
   1 1 11  1.  OPEN    FLOW-TO  10
   1 1 12  1.  OPEN    FLOW-TO  11
```

```
   1 1 13  1.  OPEN    FLOW-TO  12
   1 1 14  1.  OPEN    FLOW-TO  13
   1 1 15  1.  OPEN    FLOW-TO  14  REFLAYER

*INJECTOR 'CO2-Injector'
****       wdepth    wlength  rel_rough whtemp bhtemp    wradius
****IWELLBORE 3122.676  3122.676 0.00015     83   104.4444 .060325
*INCOMP  SOLVENT  0.  1.  0.  0.  0.  0.  0.  0.  0.  0.  0.  0.  0.  0.  0.  0.  0.  0.  0.  0.  0.  0.  0.
*OPERATE *MAX *STG 283168
*OPERATE *MAX *BHP 49444.5
****OPERATE *WHP *INITIALIZE 10300
*SHUTIN 'CO2-Injector'
AIMWELL WELLN



***STEP DOWN DRAWDOWN FOR 5 YEARS

*DATE 2012 1 1
*DATE 2013 1 1
*DATE 2014 1 1
*DATE 2015 1 1
*DATE 2016 1 1
*DATE 2017 1 1
*DATE 2018 1 1
*DATE 2019 1 1
*DATE 2020 1 1
*DATE 2021 1 1
*SHUTIN 'PRODUCER'
*OPEN 'CO2-Injector'
*DATE 2021 3 1
*SHUTIN 'CO2-Injector'
*DATE 2021 6 1
*OPEN 'PRODUCER'
*DATE 2022 1 1
*DATE 2023 1 1
*DATE 2024 1 1
*DATE 2025 1 1
*DATE 2026 1 1
*DATE 2027 1 1
*DATE 2028 1 1
*DATE 2029 1 1
*DATE 2030 1 1
*DATE 2031 1 1

*STOP

RESULTS SPEC 'Permeability I'
RESULTS SPEC SPECNOTCALCVAL -99999
RESULTS SPEC REGION 'Layer 1 - Whole layer'
RESULTS SPEC REGIONTYPE 'REGION_LAYER'
RESULTS SPEC LAYERNUMB 1
RESULTS SPEC PORTYPE 1
RESULTS SPEC CON 5
RESULTS SPEC REGION 'Layer 3 - Whole layer'
RESULTS SPEC REGIONTYPE 'REGION_LAYER'
RESULTS SPEC LAYERNUMB 3
RESULTS SPEC PORTYPE 1
RESULTS SPEC CON 5
RESULTS SPEC REGION 'Layer 2 - Whole layer'
RESULTS SPEC REGIONTYPE 'REGION_LAYER'
RESULTS SPEC LAYERNUMB 2
RESULTS SPEC PORTYPE 1
RESULTS SPEC CON 500
RESULTS SPEC STOP
```

```
RESULTS SPEC 'Permeability K'
RESULTS SPEC SPECNOTCALCVAL -99999
RESULTS SPEC REGION 'All Layers (Whole Grid)'
RESULTS SPEC REGIONTYPE 'REGION_WHOLEGRID'
RESULTS SPEC LAYERNUMB 0
RESULTS SPEC PORTYPE 1
RESULTS SPEC EQUALSI 0 1
RESULTS SPEC STOP


RESULTS SPEC 'Permeability J'
RESULTS SPEC SPECNOTCALCVAL -99999
RESULTS SPEC REGION 'All Layers (Whole Grid)'
RESULTS SPEC REGIONTYPE 'REGION_WHOLEGRID'
RESULTS SPEC LAYERNUMB 0
RESULTS SPEC PORTYPE 1
RESULTS SPEC EQUALSI 0 1
RESULTS SPEC STOP
```

5 SPOT EGR and Sequestration CMG GEM Data File

The following is the .dat file that was created to model 5SPOT CO_2 EGR and Sequestration Process. CMG's CMOST was used to optimize the chock setting of the injector.

```
** ------- Input/Output ----------------
FILENAMES OUTPUT SRFOUT RESTARTOUT INDEXOUT MAINRESULTSOUT
RANGECHECK ON
**CMG CMOST Dataset Generator 2011.10.4210.14420
**CMOST_PARAMETER   I_2011              36542
**CMOST_PARAMETER   I_2016              36542
**CMOST_PARAMETER   I_2021              36542
**CMOST_PARAMETER   I_2026              27578.9793

** ------------------------------------------------------------------**
** CONTACT uchenna.odi@qatar.tamu.edu for questions                 **
** ------------------------------------------------------------------**
** 2011-03-30, 10:01:01 AM, uchenna.odi
** 2011-03-30, 10:02:15 AM, uchenna.odi
** 2011-03-30, 11:19:48 AM, uchenna.odi
** 2011-03-30, 4:27:54 PM, uchenna.odi
** 2011-04-11, 10:48:13 AM, uchenna.odi
** 2011-04-17, 2:32:41 PM, uchenna.odi
** 2011-04-17, 2:48:10 PM, uchenna.odi
** 2011-04-17, 3:09:27 PM, uchenna.odi
** 2011-04-19, 8:42:37 AM, uchenna.odi
** 2011-04-20, 8:44:47 AM, uchenna.odi
** 2011-04-20, 9:03:18 AM, uchenna.odi
** 2011-04-20, 9:24:57 AM, uchenna.odi
** 2011-04-20, 11:24:27 AM, uchenna.odi
** 2011-04-21, 2:55:22 PM, uchenna.odi
** 2011-04-27, 2:47:00 PM, uchenna.odi
** 2011-04-27, 2:58:28 PM, uchenna.odi
** 2011-04-27, 3:02:12 PM, uchenna.odi
```

```
** 2011-04-27, 3:08:38 PM, uchenna.odi
RESULTS SIMULATOR GEM
*INUNIT *SI
INTERRUPT INTERACTIVE
*XDR *ON

*MAXERROR  20
WPRN WELL TIME
WPRN GRID TIME
WPRN ITER BRIEF
WPRN ITER MATRIX
WSRF WELL 5
WSRF GRID TIME
OUTSRF WELL PSPLIT
DIARY WELL-INFO
***DIM MDALP 100000000
***DIM MDLU 10000000
***DIM MDICLU 10000
*DIM *MDGRID 10000
OUTPRN WELL BRIEF
OUTPRN RES NONE
OUTPRN GRID KRG KRO KRW MINERAL 'CALCITE' MOLALITY 'CO2' MOLALITY 'H+' MOLALITY 'Ca++' MOLALITY
'OH-' MOLALITY 'CO3--' MOLALITY 'HCO3-' PRES
        RHOG RHOO SG SIG SO SW TEMP W 'CO2' X 'N2' X 'CO2' X 'H2S' X 'C1' X 'C2' X 'C3' X 'iC4' X 'nC4' X 'iC5' X 'nC5' X
'C6' X 'C7' X 'C8' X 'C9' X 'C10' X 'C11' X 'C12' X 'C13' X 'C14' X 'C15' X 'C16' X 'C17-19' X 'C20-29' X 'C30+'
        Y 'N2' Y 'CO2' Y 'H2S' Y 'C1' Y 'C2' Y 'C3' Y 'iC4' Y 'nC4' Y 'iC5' Y 'nC5' Y 'C6' Y 'C7' Y 'C8' Y 'C9' Y 'C10' Y 'C11' Y
'C12' Y 'C13' Y 'C14' Y 'C15' Y 'C16' Y 'C17-19' Y 'C20-29' Y 'C30+'
        Z 'N2' Z 'CO2' Z 'H2S' Z 'C1' Z 'C2' Z 'C3' Z 'iC4' Z 'nC4' Z 'iC5' Z 'nC5' Z 'C6' Z 'C7' Z 'C8' Z 'C9' Z 'C10' Z 'C11' Z 'C12' Z
'C13' Z 'C14' Z 'C15' Z 'C16' Z 'C17-19' Z 'C20-29' Z 'C30+'
OUTSRF GRID CAPN KRG KRO KRW MINERAL 'CALCITE' MOLALITY 'CO2' MOLALITY 'CO3--' MOLALITY 'Ca++'
MOLALITY 'H+' MOLALITY 'HCO3-' MOLALITY 'OH-'
        PRES RHOG RHOO SG SIG SO SW TEMP W 'CO2' X 'N2' X 'CO2' X 'H2S' X 'C1' X 'C2' X 'C3' X 'iC4' X 'nC4' X 'iC5' X
'nC5' X 'C6' X 'C7' X 'C8' X 'C9' X 'C10' X 'C11' X 'C12' X 'C13' X 'C14' X 'C15' X 'C16' X 'C17-19' X 'C20-29' X 'C30+'
        Y 'N2' Y 'CO2' Y 'H2S' Y 'C1' Y 'C2' Y 'C3' Y 'iC4' Y 'nC4' Y 'iC5' Y 'nC5' Y 'C6' Y 'C7' Y 'C8' Y 'C9' Y 'C10' Y 'C11' Y
'C12' Y 'C13' Y 'C14' Y 'C15' Y 'C16' Y 'C17-19' Y 'C20-29' Y 'C30+'
        Z 'N2' Z 'CO2' Z 'H2S' Z 'C1' Z 'C2' Z 'C3' Z 'iC4' Z 'nC4' Z 'iC5' Z 'nC5' Z 'C6' Z 'C7' Z 'C8' Z 'C9' Z 'C10' Z 'C11' Z 'C12' Z
'C13' Z 'C14' Z 'C15' Z 'C16' Z 'C17-19' Z 'C20-29' Z 'C30+'
OUTSRF RES
OUTSRF WELL GHGGAS
        GHGLIQ
        GHGTHY
        GHGSCRIT
        GHGSOL
        GHGAQU
        GHGMNR
        PAVG
**$  Distance units: m
RESULTS XOFFSET         0.0000
RESULTS YOFFSET         0.0000
RESULTS ROTATION          0.0000  **$  (DEGREES)
**$ *************************************************************************
**$ Definition of fundamental cartesian grid
**$ *************************************************************************
GRID VARI 15 15 15
KDIR DOWN
DI IVAR
 15*27.7021
DJ JVAR
 15*27.7021
DK ALL
 3375*13.1064
DTOP
 225*2926.08
**$ Property: NULL Blocks  Max: 1  Min: 1
**$  0 = null block, 1 = active block
NULL CON           1
```

```
**$ Property: Porosity  Max: 0.1  Min: 0.1
POR CON          0.2

*MOD

  1:1     2:14    1:15  = 0.1
  2:14    1:1     1:15  = 0.1
  2:14   15:15    1:15  = 0.1
 15:15    2:14    1:15  = 0.1
  1:1     1:1     1:15  = 0.05
  1:1    15:15    1:15  = 0.05
 15:15    1:1     1:15  = 0.05
 15:15   15:15    1:15  = 0.05
**$ Property: Permeability I (md)   Max: 500  Min: 5
PERMI CON 1

*MOD

  1:1     1:15    1:15  = 0.5
  1:15   15:15    1:15  = 0.5
 15:15    1:15    1:15  = 0.5
  1:15    1:1     1:15  = 0.5

PERMJ EQUALSI * 1
PERMK EQUALSI * 1

**$ Property: Pinchout Array  Max: 1  Min: 1
**$  0 = pinched block, 1 = active block
PINCHOUTARRAY CON            1
*CPOR  7.25189E-07
*PRPOR MATRIX   36645.6
** ---------- Fluid Model ----------
**$ Model and number of components
MODEL SRK
NC 24 24
***H2O_INCLUDED
COMPNAME 'N2' 'CO2' 'H2S' 'C1' 'C2' 'C3' 'iC4' 'nC4' 'iC5' 'nC5' 'C6' 'C7' 'C8' 'C9' 'C10' 'C11' 'C12' 'C13' 'C14' 'C15' 'C16' 'C17-19'
'C20-29' 'C30+'
HCFLAG
0 0 0 0 0 0 0 0 0 0 0 0 0 0 0 0 0 0 0 0 0 0 0 0
MW
28.01 44.01 34.08 16.04 30.07 44.1 58.12 58.12 72.15 72.15 82.32 95.36 108.77 121.9 134.78 147.59 160.3 172.91 185.42 197.82
210.11 233.39 299.51 477.34
AC
0.037 0.225 0.09 0.011 0.099 0.152 0.186 0.2 0.229 0.252 0.2373 0.2714 0.3094 0.35 0.39 0.4295 0.4684 0.5067 0.5444 0.5814
0.6178 0.6857 0.8712 1.0411
PCRIT
33.5330688 72.775197 88.4598 45.386682 48.0813036 41.9231406 35.9214834 37.4661276 33.3697584 33.2608848 33.4309998
31.1106312 28.7698488 26.53794 24.6122382 22.931502 21.4549038 20.1620298 19.0120524 17.998167 17.0863506 15.6029478
12.5612916 11.4045096

***VCRIT
TCRIT
125.8888889 303.7777778 373.0555556 190.2222222 305 369.5 407.5 424.7777778 460.0555556 469.3888889 513.1111111
548.7222222 579.6111111 607.5 632.2222222 654.6111111 675 693.7777778 711.1111111 727.1666667 742.0555556 768.0555556
829.5 897.9444444
BIN
0
0.12 0.12
0.02 0.12 0.07
0.06 0.15 0.06 0.06887
0.08 0.15 0.06 0.06887 0.06887
0.08 0.15 0.06 0.06887 0.06887 0.06887
0.08 0.15 0.06 0.06887 0.06887 0.06887 0.06887
0.08 0.15 0.06 0.06887 0.06887 0.06887 0.06887 0.06887
0.08 0.15 0.06 0.06887 0.06887 0.06887 0.06887 0.06887 0.06887
```

0.08 0.15 0.05 0.06887 0.06887 0.06887 0.06887 0.06887 0.06887 0.06887
0.08 0.15 0.03 0.06887 0.06887 0.06887 0.06887 0.06887 0.06887 0.06887 0.06887
0.08 0.15 0.03 0.06887 0.06887 0.06887 0.06887 0.06887 0.06887 0.06887 0.06887 0.06887
0.08 0.15 0.03 0.06887 0.06887 0.06887 0.06887 0.06887 0.06887 0.06887 0.06887 0.06887 0.06887
0.08 0.15 0.03 0.06887 0.06887 0.06887 0.06887 0.06887 0.06887 0.06887 0.06887 0.06887 0.06887 0.06887
0.08 0.15 0.03 0.06887 0.06887 0.06887 0.06887 0.06887 0.06887 0.06887 0.06887 0.06887 0.06887 0.06887 0.06887
0.08 0.15 0.03 0.06887 0.06887 0.06887 0.06887 0.06887 0.06887 0.06887 0.06887 0.06887 0.06887 0.06887 0.06887 0.06887
0.08 0.15 0.03 0.06887 0.06887 0.06887 0.06887 0.06887 0.06887 0.06887 0.06887 0.06887 0.06887 0.06887 0.06887 0.06887 0.06887
0.08 0.15 0.03 0.06887 0.06887 0.06887 0.06887 0.06887 0.06887 0.06887 0.06887 0.06887 0.06887 0.06887 0.06887 0.06887 0.06887 0.06887
0.08 0.15 0.03 0.06887 0.06887 0.06887 0.06887 0.06887 0.06887 0.06887 0.06887 0.06887 0.06887 0.06887 0.06887 0.06887 0.06887 0.06887 0.06887
0.08 0.15 0.03 0.06887 0.06887 0.06887 0.06887 0.06887 0.06887 0.06887 0.06887 0.06887 0.06887 0.06887 0.06887 0.06887 0.06887 0.06887 0.06887 0.06887
0.08 0.15 0.03 0.06887 0.06887 0.06887 0.06887 0.06887 0.06887 0.06887 0.06887 0.06887 0.06887 0.06887 0.06887 0.06887 0.06887 0.06887 0.06887 0.06887 0.06887

TRES 104.4444
PHASEID DEN
CW 7.25188E-07
REFPW 36645.6
SOLUBILITY HENRY
FLASH-METHOD OUTER
DERIVATIVEMETHOD NUMERALL
DIFCOR-OIL SIGMUND
DIFCOR-GAS SIGMUND
**DIFFUSION COEFFICIENT IN CM2/S
DIFFC-AQU
0 2.00E-05 0 0 0 0 0 0 0 0 0 0 0 0 0 0 0 0 0 0 0 0 0 0 0

*HENRYC
0 1.9510547E+05 0 0 0 0 0 0 0 0 0 0 0 0 0 0 0 0 0 0 0 0 0 0 0

*REFPH
0 9.4000000E+03 0 0 0 0 0 0 0 0 0 0 0 0 0 0 0 0 0 0 0 0 0 0 0

*VINFINITY
0 3.5089333E-02 0 0 0 0 0 0 0 0 0 0 0 0 0 0 0 0 0 0 0 0 0 0 0

*YAQU-RATE-CUTOFF
100 0.0001 100 100 100 100 100 100 100 100 100 100
100 100 100 100 100 100 100 100 100 100 100
100

*DER-CHEM-EQUIL *ANALYTICAL
*DER-REACT-RATE *ANALYTICAL

*ACTIVITY-MODEL *B-DOT
*SALINITY 0.1
*AQUEOUS-DENSITY *ROWE-CHOU
*AQUEOUS-VISCOSITY *KESTIN

*NC-AQUEOUS 5
*COMPNAME-AQUEOUS
'H+' 'Ca++' 'OH-' 'HCO3-' 'CO3--'
*MW-AQUEOUS
1.0079
40.0800
17.0073
61.0171

```
60.0092

*ION-SIZE-AQUEOUS
9.0 6.0 3.5 4.5 4.5
*CHARGE-AQUEOUS
1 2 -1 -1 -2

*NC-MINERAL 1
*COMPNAME-MINERAL
'CALCITE'
*MW-MINERAL
100.1

*MASSDENSITY-MINERAL
2710.00

*N-RATE-REACT 1
*N-CHEM-EQUIL 3

**REACTION NO. 1: H2O = H+ + OH-
*STOICHIOMETRY
0       0       0       0       0       0       0       0       0       0       0       0
        0       0       0       0       0       0       0       0       0       0       0
        0       -1      1       0       1       0       0       0
*LOG-CHEM-EQUIL-CONST
-13.2631

**REACTION NO. 2: CO2 + H2O = H+ + HCO3--
*STOICHIOMETRY
0       -1      0       0       0       0       0       0       0       0       0       0
        0       0       0       0       0       0       0       0       0       0       0
        0       -1      1       0       0       1       0       0
*LOG-CHEM-EQUIL-CONST
-6.3221

**REACTION NO. 3: CO2 + H2O = 2H+ + CO3--
*STOICHIOMETRY
0       -1      0       0       0       0       0       0       0       0       0       0
        0       0       0       0       0       0       0       0       0       0       0
        0       -1      2       0       0       0       1       0
*LOG-CHEM-EQUIL-CONST
-16.5563

**REACTION NO. 1:  CALCITE + H+ = (Ca++) + (HCO3-)
*STOICHIOMETRY
0       0       0       0       0       0       0       0       0       0       0       0
        0       0       0       0       0       0       0       0       0       0       0
        0       0       -1      1       0       1       0       -1
*REACTIVE-SURFACE-AREA 88.0

*SPEC-REACT-SURFACE-AREA 1.0E+04
*MIN-REACT-SURFACE-AREA 1.0
*SUPER-SATURATION-INDEX 2.0

*ACTIVATION-ENERGY 41870.0
*REF-TEMP-RATE-CONST 25.0
*LOG-CHEM-EQUIL-CONST
1.36
*LOG-TST-RATE-CONSTANT -8.8
***H2O_INCLUDED
***OGW_FLASH *ON
***SWR-H2OVAP 0
***SATWCUTOFF 0
**COMPONENT 1 IS A TRACE COMPONENT
*TRACE-COMP 1
*PERM-VS-POR 1
```

```
** ---------- Rock Fluid ----------
*ROCKFLUID
RPT 1


SWT
0.15        0                   0.9
0.2         0.000820562         0.736779008
0.25        0.004641802         0.592742192
0.3         0.012791302         0.467072318
0.35        0.026257997         0.358914003
0.4         0.045870834         0.267367796
0.45        0.072358532         0.191482562
0.5         0.106379201         0.130245358
0.55        0.148537664         0.082567501
0.6         0.199396668         0.047264395
0.65        0.259484621         0.023024344
0.7         0.329301218         0.008355244
0.8         0.5                 0
1           1                   0



SGT
0.1         0                   0.9
0.15        0.000449981         0.747791976
0.2         0.002545475         0.612174923
0.25        0.007014504         0.492497617
0.3         0.014399381         0.388081035
0.35        0.025154684         0.298214457
0.4         0.039680029         0.222150547
0.45        0.058336309         0.159099026
0.5         0.081455201         0.10821826
0.55        0.109345301         0.068603683
0.6         0.14229638          0.03927104
0.65        0.180582459         0.019130466
0.8         0.33                0
1           1                   0



** ---------- Initial ----------

*INITIAL
*VERTICAL *OFF
**$ Property: Pressure (kPa)   Max: 36542.2  Min: 36542.2
PRES CON      36542.2
**$ Property: Water Saturation  Max: 0.15  Min: 0.15
SW CON        0.15
**$ Property: Global Composition(N2)  Max: 3.349  Min: 3.349
ZGLOBALC 'N2' CON       3.349
**$ Property: Global Composition(CO2)  Max: 1.755  Min: 1.755
ZGLOBALC 'CO2' CON       1.755
**$ Property: Global Composition(H2S)  Max: 0.529  Min: 0.529
ZGLOBALC 'H2S' CON       0.529
**$ Property: Global Composition(C1)  Max: 83.265  Min: 83.265
ZGLOBALC 'C1' CON      83.265
**$ Property: Global Composition(C2)  Max: 5.158  Min: 5.158
ZGLOBALC 'C2' CON       5.158
**$ Property: Global Composition(C3)  Max: 1.907  Min: 1.907
ZGLOBALC 'C3' CON       1.907
**$ Property: Global Composition(iC4)  Max: 0.409  Min: 0.409
ZGLOBALC 'iC4' CON       0.409
**$ Property: Global Composition(nC4)  Max: 0.699  Min: 0.699
```

```
ZGLOBALC 'nC4' CON        0.699
**$ Property: Global Composition(iC5)  Max: 0.28  Min: 0.28
ZGLOBALC 'iC5' CON        0.28
**$ Property: Global Composition(nC5)  Max: 0.28  Min: 0.28
ZGLOBALC 'nC5' CON        0.28
**$ Property: Global Composition(C6)  Max: 0.39  Min: 0.39
ZGLOBALC 'C6' CON        0.39
**$ Property: Global Composition(C7)  Max: 0.486  Min: 0.486
ZGLOBALC 'C7' CON        0.486
**$ Property: Global Composition(C8)  Max: 0.361  Min: 0.361
ZGLOBALC 'C8' CON        0.361
**$ Property: Global Composition(C9)  Max: 0.266  Min: 0.266
ZGLOBALC 'C9' CON        0.266
**$ Property: Global Composition(C10)  Max: 0.201  Min: 0.201
ZGLOBALC 'C10' CON        0.201
**$ Property: Global Composition(C11)  Max: 0.153  Min: 0.153
ZGLOBALC 'C11' CON        0.153
**$ Property: Global Composition(C12)  Max: 0.116  Min: 0.116
ZGLOBALC 'C12' CON        0.116
**$ Property: Global Composition(C13)  Max: 0.089  Min: 0.089
ZGLOBALC 'C13' CON        0.089
**$ Property: Global Composition(C14)  Max: 0.068  Min: 0.068
ZGLOBALC 'C14' CON        0.068
**$ Property: Global Composition(C15)  Max: 0.052  Min: 0.052
ZGLOBALC 'C15' CON        0.052
**$ Property: Global Composition(C16)  Max: 0.04  Min: 0.04
ZGLOBALC 'C16' CON        0.04
**$ Property: Global Composition(C17-19)  Max: 0.073  Min: 0.073
ZGLOBALC 'C17-19' CON        0.073
**$ Property: Global Composition(C20-29)  Max: 0.063  Min: 0.063
ZGLOBALC 'C20-29' CON        0.063
**$ Property: Global Composition(C30+)  Max: 0.012  Min: 0.012
ZGLOBALC 'C30+' CON        0.012

*CALC-MOLALITYAQ-SECONDARY *OFF

*MOLALITY-AQUEOUS
  1.0E-07  9.12E-05   5.46E-07   1.17E-05   2.49E-02

*VOLUMEFRACTION-MINERAL
0.0088

***          Pressure    Temperature
*SEPARATOR    6894.76     26.6667
           2413.17     21.1111
           101.353     15.5556
** ----------------- Numerical ----------------------

*NUMERICAL
NORM PRESS 500
MAXCHANGE PRESS 100000
MAXCHANGE SATUR 1
MAXCHANGE GMOLAR 1
NORM SATUR 0.075
NORM GMOLAR 0.075
AIM STAB 1
NORTH 100
ITERMAX 200
PIVOT ON
NEWTONCYC 1000


** ----------------- Recurrent ----------------------
*RUN

*DATE 2011 1 1
```

```
DTWELL 0.01
DTMAX 36500
DTMIN .001
**
** *WELL 1 'P1'
**$
WELL  'P1'
**$         rad  geofac  wfrac  skin
GEOMETRY  K  0.099974  0.56  0.25  0.
PERF  GEO  'P1'
**$ UBA     ff  Status  Connection
   1 1 1   1.  OPEN    FLOW-TO  'SURFACE'
   1 1 2   1.  OPEN    FLOW-TO  1
   1 1 3   1.  OPEN    FLOW-TO  2
   1 1 4   1.  OPEN    FLOW-TO  3
   1 1 5   1.  OPEN    FLOW-TO  4
   1 1 6   1.  OPEN    FLOW-TO  5
   1 1 7   1.  OPEN    FLOW-TO  6
   1 1 8   1.  OPEN    FLOW-TO  7
   1 1 9   1.  OPEN    FLOW-TO  8
   1 1 10  1.  OPEN    FLOW-TO  9
   1 1 11  1.  OPEN    FLOW-TO  10
   1 1 12  1.  OPEN    FLOW-TO  11
   1 1 13  1.  OPEN    FLOW-TO  12
   1 1 14  1.  OPEN    FLOW-TO  13
   1 1 15  1.  OPEN    FLOW-TO  14  REFLAYER

*PRODUCER 'P1'
***OPERATE *MAX *STG 70792
*OPERATE *MIN *BHP 6894.76

** *WELL 2 'P2'
**$
WELL  'P2'
**$ UBA     ff  Status  Connection
**$         rad  geofac  wfrac  skin
GEOMETRY  K  0.099974  0.56  0.25  0.
PERF  GEO  'P2'
**$ UBA     ff  Status  Connection
   1 15 1   1.  OPEN    FLOW-TO  'SURFACE'
   1 15 2   1.  OPEN    FLOW-TO  1
   1 15 3   1.  OPEN    FLOW-TO  2
   1 15 4   1.  OPEN    FLOW-TO  3
   1 15 5   1.  OPEN    FLOW-TO  4
   1 15 6   1.  OPEN    FLOW-TO  5
   1 15 7   1.  OPEN    FLOW-TO  6
   1 15 8   1.  OPEN    FLOW-TO  7
   1 15 9   1.  OPEN    FLOW-TO  8
   1 15 10  1.  OPEN    FLOW-TO  9
   1 15 11  1.  OPEN    FLOW-TO  10
   1 15 12  1.  OPEN    FLOW-TO  11
   1 15 13  1.  OPEN    FLOW-TO  12
   1 15 14  1.  OPEN    FLOW-TO  13
   1 15 15  1.  OPEN    FLOW-TO  14  REFLAYER

*PRODUCER 'P2'
***OPERATE *MAX *STG 70792
*OPERATE *MIN *BHP 6894.76

** *WELL 3 'P3'
**$
WELL  'P3'
**$ UBA     ff  Status  Connection
**$         rad  geofac  wfrac  skin
GEOMETRY  K  0.099974  0.56  0.25  0.
PERF  GEO  'P3'
```

```
**$ UBA       ff  Status  Connection
   15 15 1   1.  OPEN    FLOW-TO  'SURFACE'
   15 15 2   1.  OPEN    FLOW-TO  1
   15 15 3   1.  OPEN    FLOW-TO  2
   15 15 4   1.  OPEN    FLOW-TO  3
   15 15 5   1.  OPEN    FLOW-TO  4
   15 15 6   1.  OPEN    FLOW-TO  5
   15 15 7   1.  OPEN    FLOW-TO  6
   15 15 8   1.  OPEN    FLOW-TO  7
   15 15 9   1.  OPEN    FLOW-TO  8
   15 15 10  1.  OPEN    FLOW-TO  9
   15 15 11  1.  OPEN    FLOW-TO  10
   15 15 12  1.  OPEN    FLOW-TO  11
   15 15 13  1.  OPEN    FLOW-TO  12
   15 15 14  1.  OPEN    FLOW-TO  13
   15 15 15  1.  OPEN    FLOW-TO  14  REFLAYER

*PRODUCER 'P3'
***OPERATE *MAX *STG 70792
*OPERATE *MIN *BHP 6894.76

** *WELL 4 'P4'
**$
WELL  'P4'
**$ UBA     ff  Status  Connection
**$         rad  geofac  wfrac  skin
GEOMETRY  K  0.099974  0.56  0.25  0.
PERF  GEO  'P4'
**$ UBA     ff  Status  Connection
   15 1 1   1.  OPEN    FLOW-TO  'SURFACE'
   15 1 2   1.  OPEN    FLOW-TO  1
   15 1 3   1.  OPEN    FLOW-TO  2
   15 1 4   1.  OPEN    FLOW-TO  3
   15 1 5   1.  OPEN    FLOW-TO  4
   15 1 6   1.  OPEN    FLOW-TO  5
   15 1 7   1.  OPEN    FLOW-TO  6
   15 1 8   1.  OPEN    FLOW-TO  7
   15 1 9   1.  OPEN    FLOW-TO  8
   15 1 10  1.  OPEN    FLOW-TO  9
   15 1 11  1.  OPEN    FLOW-TO  10
   15 1 12  1.  OPEN    FLOW-TO  11
   15 1 13  1.  OPEN    FLOW-TO  12
   15 1 14  1.  OPEN    FLOW-TO  13
   15 1 15  1.  OPEN    FLOW-TO  14  REFLAYER

*PRODUCER 'P4'
***OPERATE *MAX *STG 70792
*OPERATE *MIN *BHP 6894.76

** *WELL 5 'INJ-1'
**$
WELL  'INJ-1'
**$ UBA     ff  Status  Connection
**$         rad  geofac  wfrac  skin
GEOMETRY  K  0.099974  0.37  1.  0.
PERF  GEO  'INJ-1'
**$ UBA     ff  Status  Connection
   8 8 1   1.  OPEN    FLOW-TO  'SURFACE'
   8 8 2   1.  OPEN    FLOW-TO  1
   8 8 3   1.  OPEN    FLOW-TO  2
   8 8 4   1.  OPEN    FLOW-TO  3
   8 8 5   1.  OPEN    FLOW-TO  4
   8 8 6   1.  OPEN    FLOW-TO  5
   8 8 7   1.  OPEN    FLOW-TO  6
   8 8 8   1.  OPEN    FLOW-TO  7
   8 8 9   1.  OPEN    FLOW-TO  8
```

```
   8 8 10  1.  OPEN    FLOW-TO  9
   8 8 11  1.  OPEN    FLOW-TO  10
   8 8 12  1.  OPEN    FLOW-TO  11
   8 8 13  1.  OPEN    FLOW-TO  12
   8 8 14  1.  OPEN    FLOW-TO  13
   8 8 15  1.  OPEN    FLOW-TO  14  REFLAYER

*INJECTOR 'INJ-1'
****       wdepth    wlength  rel_rough whtemp bhtemp    wradius
*IWELLBORE 3122.676  3122.676 0.00015     83   104.4444 .060325
*INCOMP  SOLVENT  0.  1.  0.  0.  0.  0.  0.  0.  0.  0.  0.  0.  0.  0.  0.  0.  0.  0.  0.  0.  0.  0.  0.  0.
***OPERATE *MAX *STG 283168
*OPERATE *MAX *BHP 6894.76
AIMWELL WELLN

OPEN 'P1'
OPEN 'P2'
OPEN 'P3'
OPEN 'P4'
OPEN 'INJ-1'

TARGET BHP
'P1'
6894.76

TARGET BHP
'P2'
6894.76

TARGET BHP
'P3'
6894.76

TARGET BHP
'P4'
6894.76

TARGET BHP
'INJ-1'
36542


*DATE 2012 1 1

*DATE 2013 1 1

*DATE 2014 1 1

*DATE 2015 1 1

*DATE 2016 1 1

TARGET BHP
'P1'
6894.76

TARGET BHP
'P2'
6894.76

TARGET BHP
'P3'
6894.76

TARGET BHP
'P4'
```

```
6894.76

TARGET BHP
'INJ-1'
36542

*DATE 2017 1 1

*DATE 2018 1 1

*DATE 2019 1 1

*DATE 2020 1 1

*DATE 2021 1 1
TARGET BHP
'P1'
6894.76

TARGET BHP
'P2'
6894.76

TARGET BHP
'P3'
6894.76

TARGET BHP
'P4'
6894.76

TARGET BHP
'INJ-1'
36542


*DATE 2022 1 1

*DATE 2023 1 1

*DATE 2024 1 1

*DATE 2025 1 1

*DATE 2026 1 1
TARGET BHP
'P1'
6894.76

TARGET BHP
'P2'
6894.76

TARGET BHP
'P3'
6894.76

TARGET BHP
'P4'
6894.76

TARGET BHP
'INJ-1'
27578.9793
```

```
*DATE 2027 1 1

*DATE 2028 1 1

*DATE 2029 1 1

*DATE 2030 1 1

*DATE 2031 1 1

*DATE 2031 1 1.00001

SHUTIN 'P1'
SHUTIN 'P2'
SHUTIN 'P3'
SHUTIN 'P4'
SHUTIN 'INJ-1'

DATE 2081 1 1
DATE 2131 1 1
DATE 2181 1 1
DATE 2231 1 1
DATE 2281 1 1
DATE 2331 1 1
DATE 2381 1 1
DATE 2431 1 1
DATE 2481 1 1
DATE 2531 1 1
*STOP
RESULTS CMOST HEADER 0

RESULTS CMOST FOOTER 1274673845

RESULTS SPEC 'Permeability I'
RESULTS SPEC SPECNOTCALCVAL -99999
RESULTS SPEC REGION 'Layer 1 - Whole layer'
RESULTS SPEC REGIONTYPE 'REGION_LAYER'
RESULTS SPEC LAYERNUMB 1
RESULTS SPEC PORTYPE 1
RESULTS SPEC CON 5
RESULTS SPEC REGION 'Layer 3 - Whole layer'
RESULTS SPEC REGIONTYPE 'REGION_LAYER'
RESULTS SPEC LAYERNUMB 3
RESULTS SPEC PORTYPE 1
RESULTS SPEC CON 5
RESULTS SPEC REGION 'Layer 2 - Whole layer'
RESULTS SPEC REGIONTYPE 'REGION_LAYER'
RESULTS SPEC LAYERNUMB 2
RESULTS SPEC PORTYPE 1
RESULTS SPEC CON 500
RESULTS SPEC SPECKEEPMOD 'YES'
RESULTS SPEC STOP


RESULTS SPEC 'Permeability J'
RESULTS SPEC SPECNOTCALCVAL -99999
RESULTS SPEC REGION 'All Layers (Whole Grid)'
RESULTS SPEC REGIONTYPE 'REGION_WHOLEGRID'
RESULTS SPEC LAYERNUMB 0
RESULTS SPEC PORTYPE 1
RESULTS SPEC EQUALSI 1 1
RESULTS SPEC SPECKEEPMOD 'YES'
RESULTS SPEC STOP


RESULTS SPEC 'Permeability K'
```

```
RESULTS SPEC SPECNOTCALCVAL -99999
RESULTS SPEC REGION 'All Layers (Whole Grid)'
RESULTS SPEC REGIONTYPE 'REGION_WHOLEGRID'
RESULTS SPEC LAYERNUMB 0
RESULTS SPEC PORTYPE 1
RESULTS SPEC EQUALSI 1 1
RESULTS SPEC SPECKEEPMOD 'YES'
RESULTS SPEC STOP
```

J-script for CFGA 5 SPOT EGR and Sequestration NPV Optimization

J-scripts were used to create the optimization objective functions for the different power generation choices. This is the J-script that calculates the NPV for the 5 SPOT CFGA CO_2 EGR and Sequestration Process.

```
var dateTimes: Date[]=new Date[21];
//In JScript, the month is as an integer between 0 and 11 (January to December)
dateTimes[0]=new Date(2011,0,1);
dateTimes[1]=new Date(2012,0,1);
dateTimes[2]=new Date(2013,0,1);
dateTimes[3]=new Date(2014,0,1);
dateTimes[4]=new Date(2015,0,1);
dateTimes[5]=new Date(2016,0,1);
dateTimes[6]=new Date(2017,0,1);
dateTimes[7]=new Date(2018,0,1);
dateTimes[8]=new Date(2019,0,1);
dateTimes[9]=new Date(2020,0,1);
dateTimes[10]=new Date(2021,0,1);
dateTimes[11]=new Date(2022,0,1);
dateTimes[12]=new Date(2023,0,1);
dateTimes[13]=new Date(2024,0,1);
dateTimes[14]=new Date(2025,0,1);
dateTimes[15]=new Date(2026,0,1);
dateTimes[16]=new Date(2027,0,1);
dateTimes[17]=new Date(2028,0,1);
dateTimes[18]=new Date(2029,0,1);
dateTimes[19]=new Date(2030,0,1);
dateTimes[20]=new Date(2031,0,1);

//Declare arrays for time series values
var Years: double[]=[1, 2, 3, 4, 5, 6, 7, 8, 9, 10, 11, 12, 13, 14, 15, 16, 17, 18, 19, 20];

//CO2 produced for all years in MMSCF, FPCO2,cprd
var FPCO2: double[]=new double[Years.length];

//Gas produced without CO2 for all years in MMSCF, FGP, gprod
var FGP: double[]=new double[Years.length];

//Condensate produced for all years in bbls, FOP, oprod
var FOP: double[]=new double[Years.length];

//Water produced for all years in bbls, FWP, wprod
var FWP: double[]=new double[Years.length];

//CO2 injected for all years in MMSCF, FICO2
```

```
var FICO2: double[]=new double[Years.length];

// Cash flow for all years in $
var CF: double[]=new double[Years.length];

// Discounted Cash flow for all years in $
var DCF: double[]=new double[Years.length];

// Revenue for all years
var Revenuet: double[]=new double[Years.length];

// Cost for all years
var Costt: double[]=new double[Years.length];

//Declare economic parameters
// Internal Rate of Return
var IRR=0.10;

// Tax and Royalty
var RTAX=0.30;

// Gas Price $/MSCF
var wGP=4.25;

// Oil Price $/bbl
var wOP=80;

// Water Treatment Cost $/bbl
var wWP=1;

// CO2 Storage Credit $/tonne
var wSCO2=0;

// CO2 Seperation Cost $/MSCF
var CCO2_SEP=.38;

// CO2 Capture Cost, $/MSCF
var Ccap=11.14;

// Number of Patterns
var NPAT=100;

// Annualized Capture Facility Cost, $/year
var Ccapfacility=85428750;

// Annualized Compressor and Pump Cost, $/year
var Ccp=35497917;

// Annualized Transportation Cost, $/year
var Ctrans=7689148;

// Annualized Storage Cost, $/year
var Cstorage=97311110;

// Annualized Injection Capital Cost, $/year
var CINJ=124469;

//Cost of electricity produced by capture facility $/kWh
var Pe=.107;

// Efficiency of injector
var aeta_p=0.8;

// Injection Power requirement, kW
var Wpinj: double[]=new double[Years.length];
```

```
// Density of Captured CO2 at T=356K or 181 F for injector work calc, kg/m3
var rho_capCO2: double[]=new double[Years.length];
var rho_a=.026;
var rho_b=-2.7463;
var rho_c=104.14;
var rho_d=-619.6;

//Molecular weight of captured CO2
var MW_CCO2=44;

//Mass Rate of Injected Captured CO2, tonnes/day
var m_CCO2: double[]=new double[Years.length];

//Surface Injection Pressure in Injector, MPa
var PSINJ: double[]=new double[Years.length];

//Bottom Hole Pressure in Injector, MPa
var BHPINJ: double[]=new double[Years.length];

// CO2 Injection Energy Cost this is variable depending on the amount of CO2 injected,  $/year
var E_ICO2: double[]=new double[Years.length];

// CO2 Injection Cost this is variable depending on the amount of CO2 injected,  $/MSCF
var wICO2: double[]=new double[Years.length];

// CO2 Stored tonne
var CO2_CSTORED: double[]=new double[Years.length];

// CO2 Stored tonne/year
var CO2_STORED: double[]=new double[Years.length];

//Project Length
var STORAGEVLENGTH=0;
var PROJECTLENGTH=(Years.length)-STORAGEVLENGTH;

var dt=1;
//CO2 produced for all years in MMSCF/year
FPCO2[0]=(pCO2std_gmolcum.GetDoubleValueAt(dateTimes[1])-
pCO2std_gmolcum.GetDoubleValueAt(dateTimes[0]))*44/(0.1167*453.592*(1e6));
        for(var i=1; i<PROJECTLENGTH; i++)
        {
                FPCO2[i]=(pCO2std_gmolcum.GetDoubleValueAt(dateTimes[i+1])-
pCO2std_gmolcum.GetDoubleValueAt(dateTimes[i]))*44/(0.1167*453.592*(1e6));
        }
//Gas produced without CO2 for all years in MMSCF/year
FGP[0]=(pTotalgas_volcum.GetDoubleValueAt(dateTimes[1])-pTotalgas_volcum.GetDoubleValueAt(dateTimes[0]))*35.3147*(1e-
6)-FPCO2[0];
        for(var i=1; i<PROJECTLENGTH; i++)
        {
                FGP[i]=(pTotalgas_volcum.GetDoubleValueAt(dateTimes[i+1])-
pTotalgas_volcum.GetDoubleValueAt(dateTimes[i]))*35.3147*(1e-6)-FPCO2[i];
        }
//Condensate produced for all years in bbls/year
FOP[0]=(pOil_volcum.GetDoubleValueAt(dateTimes[1])-pOil_volcum.GetDoubleValueAt(dateTimes[0]))*35.3147/5.615;
        for(var i=1; i<PROJECTLENGTH; i++)
        {
                FOP[i]=(pOil_volcum.GetDoubleValueAt(dateTimes[i+1])-
pOil_volcum.GetDoubleValueAt(dateTimes[i]))*35.3147/5.615;
        }
//Water produced for all years in bbls/year
FWP[0]=(pWater_volcum.GetDoubleValueAt(dateTimes[1])-pWater_volcum.GetDoubleValueAt(dateTimes[0]))*35.3147/5.615;
        for(var i=1; i<PROJECTLENGTH; i++)
        {
                FWP[i]=(pWater_volcum.GetDoubleValueAt(dateTimes[i+1])-
pWater_volcum.GetDoubleValueAt(dateTimes[i]))*35.3147/5.615;
        }
```

```
//CO2 injected for all years in MMSCF/year
FICO2[0]=(iCO2std_volcum.GetDoubleValueAt(dateTimes[1])-
iCO2std_volcum.GetDoubleValueAt(dateTimes[0]))*35.3147/(1e6);
        for(var i=1; i<PROJECTLENGTH; i++)
        {
                FICO2[i]=(iCO2std_volcum.GetDoubleValueAt(dateTimes[i+1])-
iCO2std_volcum.GetDoubleValueAt(dateTimes[i]))*35.3147/(1e6);
        }

//Mass flow rate of Injected Captured CO2, tonnes/day
m_CCO2[0]=FICO2[0]*(1e6)*(MW_CCO2)*(.453592)*(1/1000)*(1/365)*(1/379.5061);
        for(var i=1; i<PROJECTLENGTH; i++)
        {
                m_CCO2[i]=FICO2[i]*(1e6)*(MW_CCO2)*(.453592)*(1/1000)*(1/365)*(1/379.5061);
        }

//Surface Injection Pressure in Injector, MPa
PSINJ[0]=(PS_INJ.GetDoubleValueAt(dateTimes[0]))*(1/1000);
        for(var i=1; i<PROJECTLENGTH; i++)
        {
                PSINJ[i]=(PS_INJ.GetDoubleValueAt(dateTimes[i]))*(1/1000);
        }

//Bottom Hole Injection Pressure in Injector, MPa
BHPINJ[0]=(BHP_INJ.GetDoubleValueAt(dateTimes[0]))*(1/1000);
        for(var i=1; i<PROJECTLENGTH; i++)
        {
                BHPINJ[i]=(BHP_INJ.GetDoubleValueAt(dateTimes[i]))*(1/1000);
        }

//Density for Injector calculations evaluated at average of BHP and PS of Injector, kg/m3
rho_capCO2[0]=rho_a*((POWER(BHPINJ[0]+PSINJ[0])/2),3)+rho_b*((POWER(BHPINJ[0]+PSINJ[0])/2),2)+rho_c*((POWER(B
HPINJ[0]+PSINJ[0])/2),1)+rho_d;
        for(var i=1; i<PROJECTLENGTH; i++)
        {

        rho_capCO2[i]=rho_a*((POWER(BHPINJ[i]+PSINJ[i])/2),3)+rho_b*((POWER(BHPINJ[i]+PSINJ[i])/2),2)+rho_c*((PO
WER(BHPINJ[i]+PSINJ[i])/2),1)+rho_d;
        }



// CO2 Injection Cost this is variable depending on the amount of CO2 injected,  $/MSCF
if(FICO2[0]=0)
{
Wpinj[0]=0;
}
if(FICO2[0]>0)
{
Wpinj[0]=(1000*10/(24*3600))*m_CCO2[0]*(BHPINJ[0]-PSINJ[0])*(1/rho_capCO2[0])*(1/aeta_p);
}

E_ICO2[0]=Wpinj[0]*24*365*aeta_p*Pe;
if(FICO2[0]=0)
{
 wICO2[0]=0;
}
if(FICO2[0]>0)
{
 wICO2[0]=(E_ICO2[0]/FICO2[0])*(1/1000);
}
        for(var i=1; i<PROJECTLENGTH; i++)
        {
      if(FICO2[i]=0)
      {
       Wpinj[i]=0;
```

```
    }
     if(FICO2[i]>0)
    {
     Wpinj[i]=(1000*10/(24*3600))*m_CCO2[i]*(BHPINJ[i]-PSINJ[i])*(1/rho_capCO2[i])*(1/aeta_p);
    }


        E_ICO2[i]=Wpinj[i]*24*365*aeta_p*Pe;
        if(FICO2[i]=0)
        {
         wICO2[i]=0;
        }
        if(FICO2[i]>0)
        {
         wICO2[i]=(E_ICO2[i]/FICO2[i])*(1/1000);
        }

            }


//CO2 Stored tonne/year
CO2_CSTORED[0]=(1e6)*(.453592/1000)*(1/379.5061)*(MW_CCO2)*(FICO2[0]-FPCO2[0]);
CO2_STORED[0]=(1e6)*(.453592/1000)*(1/379.5061)*(MW_CCO2)*(FICO2[0]-FPCO2[0]);
for(var i=1; i<PROJECTLENGTH; i++)
            {
        CO2_CSTORED[i]=(1e6)*(.453592/1000)*(1/379.5061)*(MW_CCO2)*(FICO2[i]-FPCO2[i])+CO2_CSTORED[i-1];
        CO2_STORED[i]=(1e6)*(.453592/1000)*(1/379.5061)*(MW_CCO2)*(FICO2[i]-FPCO2[i]);
            }




//Calculate Objective Function
            for(var i=0; i<PROJECTLENGTH; i++)
            {
        Revenuet[i]=NPAT*((FOP[i]*wOP+FGP[i]*wGP*1000)*(1-RTAX)+CO2_STORED[i]*wSCO2);

Costt[i]=NPAT*(FWP[i]*wWP+1000*FICO2[i]*wICO2[i]+Ccap*FICO2[i]*1000+CCO2_SEP*FPCO2[i]*1000+CINJ)+Ccapfacilit
y+Ccp+Ctrans+Cstorage;
        CF[i]=Revenuet[i]-Costt[i];
                    DCF[i]=CF[i]/POWER(1+IRR,dt*Years[i]);
            }
var NPV=0;
            for(var i=0; i<PROJECTLENGTH; i++)
            {
                    NPV=NPV+DCF[i];
            }

//Convert to million dollar
NPV=NPV*1e-6;
//The last line must specify only one variable, which is the result of objective function calculation
NPV;
```

PUNQ-S3 CMG GEM Data File for Delayed Injection Scenario

The following is the delayed injection case for the PUNQ-S3 reservoir model. This file was originally intended for use within Schlumberger's Eclipse software. It was

converted to a file suitable for CMG's GEM and its reservoir properties were changed to reflect a carbonate and wet gas reservoir.

```
** ----------------------------------------------------------------**
** Dr. Anuj Gupta CO2 EGR and Sequestrion Research Group            **
** ----------------------------------------------------------------**
** ----------------------------------------------------------------**
** **
** FILE:  K4_NORTHFIELDSIM.DAT                                      **
** **
** MODEL: PUNQ-S3            CO2 INJECTION                          **
** 24 COMPONENTS         Fluid Compositions based on K4 layer                  **
** Whitson Fluid         Whitson Paper IPTC 10692                 **
** SI UNITS              Geochemistry based on SPE 89341           **
** **
** ----------------------------------------------------------------**
** **
** **
** ----------------------------------------------------------------**
** CONTACT uchenna.odi@qatar.tamu.edu for questions                 **
** ----------------------------------------------------------------**

RESULTS SIMULATOR GEM 200900
** ------- Input/Output ---------------
FILENAMES OUTPUT SRFOUT RESTARTOUT INDEXOUT MAINRESULTSOUT
*INUNIT *SI
INTERRUPT INTERACTIVE
*XDR *ON

***DIM *MDLU 100000000

*MAXERROR  100
RANGECHECK ON
WPRN WELL TIME
WPRN GRID TIME
WPRN ITER BRIEF
WPRN ITER MATRIX
WSRF WELL 1
WSRF GRID TIME
OUTSRF WELL PSPLIT
DIARY WELL-INFO
***DIM MDALP 100000000
***DIM MDLU 10000000
***DIM MDICLU 10000
*DIM *MDGRID 100000
OUTPRN WELL BRIEF
OUTPRN RES NONE
OUTPRN GRID KRG KRO KRW MINERAL 'CALCITE' MOLALITY 'CO2' MOLALITY 'H+' MOLALITY 'Ca++' MOLALITY
'OH-' MOLALITY 'CO3--' MOLALITY 'HCO3-' PRES
        RHOG RHOO SG SIG SO SW TEMP W 'CO2' X 'N2' X 'CO2' X 'H2S' X 'C1' X 'C2' X 'C3' X 'iC4' X 'nC4' X 'iC5' X 'nC5' X
'C6' X 'C7' X 'C8' X 'C9' X 'C10' X 'C11' X 'C12' X 'C13' X 'C14' X 'C15' X 'C16' X 'C17-19' X 'C20-29' X 'C30+'
        Y 'N2' Y 'CO2' Y 'H2S' Y 'C1' Y 'C2' Y 'C3' Y 'iC4' Y 'nC4' Y 'iC5' Y 'nC5' Y 'C6' Y 'C7' Y 'C8' Y 'C9' Y 'C10' Y 'C11' Y
'C12' Y 'C13' Y 'C14' Y 'C15' Y 'C16' Y 'C17-19' Y 'C20-29' Y 'C30+'
        Z 'N2' Z 'CO2' Z 'H2S' Z 'C1' Z 'C2' Z 'C3' Z 'iC4' Z 'nC4' Z 'iC5' Z 'nC5' Z 'C6' Z 'C7' Z 'C8' Z 'C9' Z 'C10' Z 'C11' Z 'C12' Z
'C13' Z 'C14' Z 'C15' Z 'C16' Z 'C17-19' Z 'C20-29' Z 'C30+'
OUTSRF GRID CAPN KRG KRO KRW MINERAL 'CALCITE' MOLALITY 'CO2' MOLALITY 'CO3--' MOLALITY 'Ca++'
MOLALITY 'H+' MOLALITY 'HCO3-' MOLALITY 'OH-'
        PRES RHOG RHOO SG SIG SO SW TEMP W 'CO2' X 'N2' X 'CO2' X 'H2S' X 'C1' X 'C2' X 'C3' X 'iC4' X 'nC4' X 'iC5' X
'nC5' X 'C6' X 'C7' X 'C8' X 'C9' X 'C10' X 'C11' X 'C12' X 'C13' X 'C14' X 'C15' X 'C16' X 'C17-19' X 'C20-29' X 'C30+'
        Y 'N2' Y 'CO2' Y 'H2S' Y 'C1' Y 'C2' Y 'C3' Y 'iC4' Y 'nC4' Y 'iC5' Y 'nC5' Y 'C6' Y 'C7' Y 'C8' Y 'C9' Y 'C10' Y 'C11' Y
'C12' Y 'C13' Y 'C14' Y 'C15' Y 'C16' Y 'C17-19' Y 'C20-29' Y 'C30+'
        Z 'N2' Z 'CO2' Z 'H2S' Z 'C1' Z 'C2' Z 'C3' Z 'iC4' Z 'nC4' Z 'iC5' Z 'nC5' Z 'C6' Z 'C7' Z 'C8' Z 'C9' Z 'C10' Z 'C11' Z 'C12' Z
'C13' Z 'C14' Z 'C15' Z 'C16' Z 'C17-19' Z 'C20-29' Z 'C30+'
```

```
OUTSRF RES
OUTSRF WELL GHGGAS
        GHGLIQ
        GHGTHY
        GHGSCRIT
        GHGSOL
        GHGAQU
        GHGMNR
        PAVG
**$  Distance units: m
RESULTS XOFFSET         0.0000
RESULTS YOFFSET         0.0000
RESULTS ROTATION        0.0000  **$  (DEGREES)
**$ *************************************************************************
**$ Definition of fundamental cartesian grid
**$ *************************************************************************
*GRID  *CORNER 19 28 5
*KDIR *DOWN

*INCLUDE 'PUNQS3CMG_coord.GRDECL'
*INCLUDE 'PUNQS3CMG_zcorn.GRDECL'

*POR *ALL
0.26548    0.211005   0.204251   0.291204   0.163023   0.157237
0.083823   0.116185   0.017052   0.070381   0.124182   0.192789
0.277537   0.275535   0.245743   0.209113   0.197629   0.011654
0.010326   0.294386   0.260182   0.155488   0.275685   0.257884
0.1785     0.159943   0.107099   0.043849   0.011226   0.056972
0.248779   0.251793   0.297708   0.26898    0.19676    0.136161
0.120618   0.029067   0.296548   0.27093    0.217913   0.248845
0.267067   0.244027   0.068104   0.146204   0.104338   0.085187
0.015772   0.142013   0.278589   0.29265    0.263832   0.262329
0.168479   0.100576   0.046039   0.291542   0.294246   0.280916
0.199004   0.164365   0.224139   0.084604   0.125062   0.123027
0.112797   0.022471   0.14154    0.188543   0.285491   0.290016
0.228671   0.230794   0.060899   0.06377    0.293918   0.295812
0.289309   0.241585   0.216714   0.212809   0.188279   0.144323
0.132267   0.127482   0.126217   0.101368   0.148283   0.182185
0.294168   0.294342   0.224337   0.087585   0.018924   0.210741
0.297381   0.268685   0.280611   0.182669   0.255532   0.19973
0.176487   0.15441    0.194945   0.14836    0.105713   0.115899
0.153299   0.275508   0.295558   0.288848   0.255198   0.109739
0.124303   0.28062    0.296471   0.243301   0.291466   0.181888
0.198355   0.219343   0.254      0.259997   0.091501   0.074407
0.091292   0.115085   0.19709    0.28535    0.28524    0.230805
0.141463   0.062945   0.169348   0.288254   0.251088   0.287235
0.284685   0.280594   0.190325   0.230497   0.188334   0.208486
0.088102   0.052044   0.08511    0.146545   0.280564   0.292913
0.246304   0.105262   0.072768   0.129792   0.251099   0.287641
0.256824   0.29384    0.249263   0.269622   0.237823   0.173924
0.201754   0.094482   0.025544   0.044017   0.097166   0.196012
0.296178   0.286265   0.143564   0.018287   0.145731   0.241288
0.282866   0.203965   0.274373   0.288066   0.20017    0.200907
0.188631   0.250742   0.187498   0.070436   0.024595   0.060085
0.191821   0.272003   0.284799   0.271468   0.018613   0.085451
0.197816   0.167434   0.241618   0.140869   0.289549   0.28512
0.195077   0.161637   0.166059   0.211093   0.193724   0.078675
0.065024   0.149108   0.2346     0.284536   0.281207   0.017191
0.018535   0.088465   0.098442   0.123324   0.171229   0.289679
0.274569   0.257838   0.128582   0.150186   0.144422   0.203701
0.147931   0.0751     0.066916   0.17916    0.195099   0.268603
0.011499   0.016508   0.087475   0.190138   0.183439   0.136095
0.185936   0.282821   0.265842   0.159305   0.08016    0.17861
0.199092   0.165476   0.13846    0.137063   0.189819   0.243059
0.269076   0.01024    0.011769   0.036117   0.14319    0.141287
0.163441   0.149031   0.280666   0.287518   0.26883    0.140099
```

0.054783 0.151011 0.129517 0.117604 0.116911 0.180337
0.207969 0.186904 0.010642 0.010813 0.011991 0.050383
0.17179 0.183802 0.137448 0.243741 0.270172 0.288466
0.23196 0.175442 0.079269 0.167269 0.06509 0.088762
0.144499 0.184429 0.224359 0.033242 0.011273 0.021559
0.034155 0.067653 0.116504 0.174056 0.212578 0.281632
0.293125 0.273013 0.182328 0.150692 0.156302 0.14803
0.062703 0.129913 0.136766 0.239517 0.184638 0.010791
0.018819 0.018414 0.116438 0.108628 0.05618 0.179479
0.2192 0.222511 0.288705 0.267234 0.265487 0.177158
0.152782 0.062274 0.090555 0.173033 0.220828 0.155873
0.018493 0.010655 0.022358 0.02224 0.08775 0.01191
0.083493 0.207749 0.257127 0.262643 0.293177 0.264212
0.275357 0.168215 0.099014 0.103502 0.128505 0.236668
0.034002 0.056334 0.01619 0.017861 0.012795 0.022026
0.109486 0.029427 0.107 0.074902 0.272582 0.29278
0.2914 0.294545 0.227538 0.178445 0.139659 0.140627
0.17498 0.04335 0.040123 0.065959 0.024911 0.083669
0.021452 0.07818 0.066498 0.064463 0.077707 0.145181
0.232928 0.297941 0.292302 0.285028 0.270152 0.157655
0.142695 0.146611 0.011939 0.02171 0.051131 0.068742
0.045216 0.088014 0.028428 0.103513 0.018333 0.131838
0.048129 0.19577 0.287469 0.296058 0.299031 0.288735
0.280551 0.239066 0.199312 0.014197 0.014716 0.061603
0.085814 0.123478 0.148789 0.066234 0.077146 0.064023
0.0828 0.037883 0.076475 0.283811 0.292014 0.297687
0.298509 0.278328 0.272425 0.218617 0.028052 0.032463
0.018828 0.144389 0.032606 0.18213 0.139681 0.068929
0.030839 0.073516 0.079258 0.103953 0.230596 0.294713
0.298412 0.297674 0.293281 0.242047 0.235029 0.104635
0.032988 0.015698 0.122741 0.092513 0.156093 0.194241
0.035041 0.037112 0.016161 0.0828 0.063253 0.096385
0.294354 0.295347 0.296755 0.283312 0.202843 0.205329
0.055355 0.032193 0.016331 0.014662 0.080908 0.164827
0.124193 0.105031 0.051032 0.026843 0.021924 0.070821
0.149944 0.23427 0.279582 0.298451 0.265351 0.275893
0.182999 0.146644 0.014218 0.028745 0.031704 0.100114
0.029816 0.148811 0.112973 0.063088 0.038962 0.017621
0.027524 0.072427 0.239913 0.286798 0.291876 0.294659
0.284752 0.230321 0.059315 0.137107 0.077905 0.036632
0.024129 0.0289 0.066839 0.18653 0.190061 0.021684
0.044831 0.0176 0.064331 0.205637 0.225822 0.250775
0.279128 0.289613 0.268679 0.192756 0.154751 0.188092
0.09644 0.019585 0.014878 0.019177 0.111884 0.145808
0.184198 0.013898 0.019221 0.03672 0.141716 0.207397
0.236789 0.27613 0.231377 0.246788 0.077764 0.102304
0.151212 0.093236 0.115184 0.069112 0.07048 0.041988
0.054668 0.044492 0.045968 0.075192 0.066724 0.06808
0.109096 0.123822 0.05962 0.034172 0.05346 0.03122
0.096228 0.118316 0.052284 0.022878 0.053976 0.056344
0.021 0.06696 0.053528 0.051352 0.037276 0.058972
0.081048 0.059648 0.076852 0.066524 0.093544 0.124314
0.086076 0.116496 0.109184 0.028983 0.021009 0.018399
0.024637 0.057024 0.049488 0.059104 0.108604 0.077608
0.068384 0.056984 0.090096 0.070416 0.039516 0.037404
0.072612 0.105044 0.092552 0.08482 0.077832 0.05578
0.023236 0.015658 0.085564 0.094928 0.106388 0.150095
0.143633 0.138345 0.0944 0.088692 0.071608 0.032988
0.02689 0.03886 0.130136 0.132989 0.106184 0.084476
0.074528 0.081912 0.056816 0.092384 0.095236 0.141499
0.152738 0.137602 0.125863 0.126913 0.137783 0.075444
0.034688 0.042652 0.03776 0.128659 0.136315 0.13133
0.067216 0.070592 0.085932 0.102736 0.112304 0.113604
0.129652 0.154923 0.157126 0.155091 0.126563 0.12841
0.081628 0.084736 0.016313 0.03614 0.119216 0.138024
0.133231 0.084504 0.086132 0.130264 0.114204 0.126466

0.117936 0.136169 0.145349 0.162944 0.159822 0.150831
0.124982 0.07248 0.055464 0.032104 0.05802 0.134232
0.120644 0.12133 0.113512 0.123548 0.101856 0.15334
0.138787 0.140269 0.138126 0.137192 0.104064 0.132888
0.13013 0.117288 0.089668 0.041064 0.026549 0.016197
0.11166 0.091676 0.134309 0.0731 0.095156 0.10314
0.131451 0.153197 0.106184 0.113788 0.05238 0.08386
0.100076 0.158344 0.107704 0.07058 0.048412 0.043164
0.018468 0.079904 0.086636 0.070228 0.054776 0.095104
0.088788 0.092348 0.098436 0.065144 0.09932 0.0455
0.014907 0.06182 0.085116 0.037756 0.103048 0.066736
0.03462 0.039732 0.088592 0.08484 0.090584 0.10416
0.07538 0.042652 0.07784 0.068848 0.05234 0.09312
0.054696 0.087948 0.07786 0.08236 0.075456 0.095652
0.0708 0.034092 0.044916 0.075248 0.037712 0.05644
0.071564 0.075972 0.011765 0.011818 0.013361 0.021104
0.056076 0.051016 0.070416 0.09376 0.132897 0.1092
0.143954 0.092216 0.040532 0.023183 0.04488 0.034804
0.021655 0.034208 0.032724 0.025932 0.013702 0.017172
0.045948 0.035196 0.016604 0.034 0.107472 0.110356
0.090948 0.089624 0.07076 0.040584 0.05082 0.091584
0.070092 0.084816 0.081936 0.037724 0.037452 0.024396
0.017676 0.045164 0.028888 0.03074 0.024625 0.028581
0.077692 0.080632 0.079552 0.042776 0.058332 0.090352
0.088368 0.055564 0.051684 0.072888 0.061076 0.01777
0.0315 0.022801 0.03928 0.057884 0.012673 0.013799
0.021205 0.039632 0.068076 0.085656 0.060016 0.073072
0.111364 0.115804 0.081284 0.048036 0.077068 0.081984
0.016242 0.017292 0.025598 0.027349 0.051472 0.016384
0.020622 0.017753 0.015987 0.03018 0.053364 0.065132
0.073512 0.079068 0.074452 0.09322 0.031432 0.022801
0.071836 0.062476 0.039352 0.035824 0.0588 0.06132
0.045332 0.018514 0.062288 0.065468 0.021247 0.027579
0.045472 0.065724 0.04348 0.042048 0.050188 0.039988
0.013724 0.053376 0.075228 0.086164 0.096424 0.024834
0.058872 0.08502 0.030152 0.028915 0.065068 0.033912
0.028282 0.031664 0.038856 0.044344 0.01498 0.043828
0.028162 0.019318 0.043892 0.066672 0.08442 0.095588
0.023297 0.025179 0.018004 0.03736 0.022565 0.045932
0.089876 0.085484 0.049468 0.0708 0.09476 0.018773
0.022613 0.019714 0.016789 0.071256 0.069708 0.0555
0.055548 0.048432 0.04586 0.02339 0.050304 0.039344
0.08726 0.119188 0.069564 0.085652 0.086836 0.088216
0.016722 0.060752 0.017618 0.016375 0.056116 0.04366
0.109308 0.129269 0.09628 0.023784 0.015334 0.021082
0.066724 0.113432 0.1144 0.070316 0.09694 0.116484
0.108204 0.08126 0.115276 0.095956 0.068524 0.055
0.092764 0.13357 0.08262 0.082716 0.0616 0.035032
0.063212 0.042084 0.08744 0.102848 0.103576 0.0996
0.113888 0.048548 0.052544 0.1093 0.098252 0.05108
0.086788 0.131883 0.134443 0.110212 0.060428 0.098388
0.050156 0.05646 0.042096 0.052872 0.070604 0.089916
0.077248 0.059336 0.0165 0.087628 0.046216 0.040992
0.0952 0.132247 0.09684 0.1338 0.117336 0.086536
0.059812 0.088 0.073796 0.042092 0.075588 0.073684
0.08432 0.070196 0.045744 0.042868 0.09544 0.053784
0.03206 0.028873 0.096624 0.107816 0.089952 0.074728
0.087928 0.059336 0.039472 0.089896 0.09766 0.071256
0.107268 0.083536 0.096016 0.066368 0.09364 0.101232
0.073824 0.016723 0.014596 0.018351 0.062056 0.062848
0.069456 0.115256 0.084144 0.053976 0.130687 0.11352
0.08984 0.11862 0.147098 0.106664 0.127884 0.122503
0.092736 0.038612 0.03832 0.045464 0.05614 0.114816
0.136786 0.108444 0.095492 0.067604 0.108872 0.135158
0.12692 0.065228 0.065796 0.097332 0.05458 0.0621
0.098072 0.085484 0.047684 0.063424 0.126176 0.091856

0.141042 0.142557 0.132748 0.05136 0.064744 0.094928
0.132662 0.099756 0.079588 0.052084 0.062616 0.0302
0.075728 0.075708 0.135677 0.181459 0.209762 0.137074
0.123753 0.137899 0.180799 0.285295 0.285146 0.269815
0.291949 0.29004 0.297228 0.294869 0.289224 0.295808
0.297263 0.291574 0.266798 0.230915 0.203591 0.230717
0.167555 0.172373 0.124534 0.076189 0.204218 0.28028
0.214404 0.284041 0.289153 0.29372 0.297999 0.292754
0.290707 0.293885 0.295801 0.295299 0.265775 0.237493
0.245688 0.276809 0.17729 0.152639 0.127493 0.090247
0.203492 0.267435 0.24747 0.290484 0.290136 0.293482
0.298111 0.291499 0.286917 0.292086 0.293344 0.232103
0.240672 0.200302 0.216274 0.26936 0.198586 0.121003
0.070964 0.062604 0.177994 0.227725 0.199719 0.28687
0.285788 0.295539 0.298083 0.29041 0.292133 0.276742
0.16035 0.232026 0.203701 0.21942 0.22096 0.204064
0.246821 0.122587 0.107748 0.072702 0.212358 0.255679
0.265312 0.270904 0.293436 0.293388 0.296432 0.297785
0.283826 0.13637 0.175068 0.199829 0.264541 0.202535
0.205758 0.204812 0.169843 0.152518 0.084593 0.118286
0.128219 0.212974 0.238032 0.284607 0.294732 0.27787
0.292376 0.292776 0.162781 0.150252 0.150395 0.187058
0.27 0.199301 0.180227 0.204625 0.187212 0.17267
0.134423 0.12647 0.096649 0.141441 0.221488 0.282068
0.291068 0.288456 0.282855 0.209696 0.161241 0.096077
0.176091 0.230651 0.204988 0.207089 0.208783 0.181525
0.136029 0.172318 0.085198 0.168457 0.044073 0.191414
0.22921 0.259865 0.2874 0.283009 0.216263 0.200016
0.234886 0.180876 0.187311 0.256298 0.224271 0.235337
0.237801 0.175651 0.129132 0.13076 0.036471 0.098123
0.114689 0.168886 0.234941 0.263512 0.28293 0.135413
0.19885 0.148272 0.145291 0.159129 0.254262 0.254061
0.248647 0.232246 0.220399 0.154377 0.14429 0.082767
0.020169 0.134808 0.108199 0.174584 0.260094 0.268946
0.216274 0.159041 0.151891 0.087266 0.14363 0.125601
0.224095 0.259395 0.214965 0.236327 0.195704 0.171075
0.152782 0.054607 0.062098 0.142035 0.2115 0.173594
0.270801 0.175299 0.128989 0.159921 0.131541 0.079632
0.131222 0.090357 0.170877 0.231542 0.223831 0.246535
0.187168 0.200841 0.152287 0.1048 0.039769 0.139978
0.224843 0.176157 0.04544 0.141815 0.08115 0.121344
0.108221 0.07356 0.05673 0.110564 0.188642 0.211126
0.18653 0.206693 0.257475 0.244038 0.180216 0.109079
0.109365 0.203778 0.208849 0.039525 0.069622 0.108089
0.04835 0.134885 0.081656 0.141595 0.097672 0.108496
0.139351 0.182812 0.166939 0.18433 0.227505 0.27509
0.187036 0.138537 0.17256 0.2181 0.088047 0.074077
0.084637 0.082558 0.04991 0.113919 0.071767 0.163111
0.134071 0.208915 0.179809 0.206363 0.240012 0.13681
0.201281 0.262147 0.221158 0.16607 0.180282 0.174705
0.108958 0.146897 0.049235 0.075309 0.074385 0.102237
0.118198 0.15089 0.179292 0.19412 0.236723 0.23966
0.254272 0.228506 0.272248 0.236415 0.197893 0.126063
0.181745 0.130375 0.135897 0.155807 0.031668 0.048108
0.022253 0.127889 0.1114 0.129781 0.106648 0.16277
0.242707 0.277293 0.246084 0.264533 0.292195 0.250318
0.17366 0.164673 0.192954 0.147832 0.093448 0.097221
0.06564 0.02364 0.020603 0.048308 0.079379 0.135116
0.044611 0.150813 0.224931 0.23889 0.224744 0.269008
0.271449 0.210015 0.200951 0.199048 0.234248 0.148756
0.116119 0.081744 0.068665 0.015156 0.028202 0.023461
0.059029 0.15826 0.123544 0.195187 0.259856 0.203536
0.218925 0.243763 0.226064 0.177554 0.205549 0.270446
0.231861 0.102292 0.138702 0.088839 0.05783 0.021849
0.033759 0.016209 0.036153 0.197695 0.13131 0.204042
0.187058 0.208838 0.225129 0.243521 0.155158 0.227692

0.257549 0.245754 0.254061 0.150428 0.121366 0.107264
0.052517 0.039728 0.098442 0.02572 0.052418 0.176982
0.134115 0.191436 0.139417 0.241882 0.193218 0.141562
0.187366 0.280422 0.288642 0.219255 0.190303 0.113182
0.138603 0.187597 0.0982 0.030902 0.065475 0.033319
0.041539 0.154553 0.171988 0.1939 0.227197 0.206638
0.070656 0.163562 0.181063 0.290711 0.294304 0.271374
0.17729 0.206869 0.155389 0.207034 0.062835 0.049031
0.125766 0.086353 0.107077 0.102512 0.086342 0.145511
0.257099 0.028012 0.078444 0.213557 0.243697 0.287628
0.293386 0.285897 0.256985 0.228385 0.249252 0.2434
0.134918 0.079896 0.120871 0.103898 0.177829 0.090566
0.031585 0.149218 0.037578 0.030696 0.101731 0.196342
0.244181 0.28969 0.296781 0.289403 0.279261 0.260842
0.263367 0.208574 0.197266 0.085957 0.14165 0.139219
0.175882 0.198245 0.033545 0.014385 0.060591 0.067477
0.112038 0.238824 0.284819 0.290255 0.297109 0.292375
0.295838 0.28696 0.280637 0.197772 0.13692 0.08368
0.154399 0.172219 0.190402 0.124446 0.052935 0.031896
0.09061 0.127031 0.156808 0.236965 0.295051 0.29429
0.292082 0.296943 0.298689 0.294143 0.280228 0.193064
0.147326 0.113468 0.173726 0.249813 0.2137 0.014395
0.037412 0.030514 0.145544 0.155631 0.222203 0.254783
0.296317 0.295341 0.290949 0.296818 0.299206 0.29917
0.273349 0.231388 0.139054 0.108639 0.180579 0.253152
0.077038 0.078574 0.11356 0.156922 0.102088 0.088456
0.037894 0.096478 0.018008 0.082336 0.021379 0.030577
0.012132 0.016397 0.019014 0.027092 0.055282 0.098476
0.104506 0.043318 0.027694 0.12466 0.126292 0.090718
0.092266 0.061708 0.045532 0.027732 0.071446 0.086182
0.035971 0.060724 0.022848 0.025602 0.015884 0.06058
0.08404 0.077476 0.020338 0.046852 0.12598 0.109072
0.172987 0.112852 0.058696 0.072256 0.10612 0.08932
0.06658 0.133876 0.169162 0.057982 0.063994 0.084064
0.090916 0.107938 0.017768 0.053848 0.111136 0.177602
0.171182 0.160354 0.165496 0.131416 0.066988 0.134788
0.051388 0.084052 0.15913 0.147436 0.140482 0.103708
0.135652 0.111592 0.0832 0.026603 0.093436 0.153232
0.192787 0.178062 0.136432 0.111106 0.030098 0.029945
0.1387 0.062872 0.168502 0.173665 0.147088 0.117016
0.171642 0.126016 0.094762 0.1048 0.042376 0.095044
0.172081 0.200799 0.082342 0.085846 0.05779 0.013992
0.068302 0.163648 0.181427 0.142324 0.166804 0.174693
0.166438 0.186035 0.17061 0.157408 0.154048 0.053866
0.16549 0.191924 0.151072 0.073762 0.055564 0.013133
0.023645 0.082192 0.095836 0.121198 0.155584 0.189661
0.194099 0.166408 0.21155 0.184861 0.197721 0.141712
0.107338 0.161548 0.154042 0.127318 0.07126 0.015569
0.030033 0.091624 0.051376 0.086962 0.108964 0.12958
0.1843 0.2001 0.195452 0.202855 0.206768 0.198058
0.140134 0.116326 0.142174 0.093538 0.120004 0.081226
0.017602 0.058186 0.068008 0.064678 0.05446 0.116644
0.10882 0.12679 0.202079 0.203604 0.210599 0.2074
0.207004 0.196712 0.138394 0.066142 0.09424 0.102796
0.061888 0.027886 0.02701 0.015998 0.04087 0.077398
0.03375 0.138238 0.150598 0.211235 0.212172 0.202721
0.201982 0.165532 0.191273 0.173083 0.07276 0.077548
0.09586 0.028844 0.045586 0.019988 0.017006 0.025011
0.068074 0.066268 0.120484 0.174371 0.207776 0.190706
0.207346 0.13981 0.1498 0.149074 0.197581 0.140344
0.07093 0.1087 0.030178 0.039312 0.027058 0.072028
0.025462 0.107098 0.084388 0.125884 0.171549 0.198379
0.141598 0.180826 0.10027 0.126868 0.066802 0.14626
0.148852 0.079918 0.024664 0.093094 0.082684 0.05176
0.087328 0.047392 0.13969 0.184688 0.152092 0.19279
0.172806 0.089254 0.09808 0.106162 0.08758 0.092392

0.116572 0.084754 0.039982 0.10114 0.131638 0.046786
0.012218 0.02673 0.085822 0.182111 0.14536 0.152482
0.130084 0.131242 0.048724 0.014828 0.033247 0.070156
0.159682 0.09157 0.087064 0.067162 0.081394 0.123904
0.072766 0.015426 0.071272 0.168652 0.150772 0.172642
0.157708 0.108064 0.077626 0.0162 0.012822 0.115924
0.1285 0.0856 0.115024 0.100996 0.029445 0.083008
0.125542 0.049402 0.058984 0.109162 0.13279 0.134416
0.172767 0.1048 0.150172 0.10372 0.04402 0.040204
0.138862 0.07906 0.106132 0.116134 0.060592 0.070744
0.084682 0.060544 0.048664 0.105268 0.17889 0.124732
0.16 0.143662 0.144922 0.1513 0.061732 0.087598
0.134836 0.07879 0.101608 0.081562 0.100048 0.126262
0.051706 0.025705 0.082504 0.07234 0.138868 0.157768
0.178233 0.109972 0.166132 0.11539 0.105388 0.0667
0.060544 0.09136 0.065518 0.066448 0.147796 0.179297
0.122296 0.077824 0.060778 0.082846 0.066646 0.128512
0.190822 0.1246 0.15178 0.14305 0.13909 0.093868
0.090826 0.113968 0.109966 0.110812 0.089224 0.195529
0.184176 0.145012 0.109258 0.06028 0.088636 0.087538
0.158194 0.207739 0.194686 0.157468 0.196006 0.104332
0.134398 0.083932 0.142342 0.12904 0.082366 0.117928
0.184124 0.197045 0.091606 0.029037 0.025105 0.045058
0.11221 0.182111 0.207847 0.196431 0.12997 0.161338
0.052222 0.093856 0.06757 0.11668 0.11974 0.107908
0.189118 0.211285 0.183301 0.06772 0.031563 0.017671
0.067558 0.137194 0.136306 0.20158 0.195605 0.14146
0.1486 0.106828 0.130978 0.147376 0.135814 0.123298
0.150394 0.199508 0.147178 0.153028 0.071824 0.026171
0.056254 0.04513 0.11932 0.135406 0.157312 0.126466
0.164434 0.0733 0.124378 0.131944 0.120736 0.170032
0.159094 0.154684 0.193987 0.178278 0.11188 0.028489
0.07531 0.027044 0.054544 0.071272 0.114736 0.076726
0.155992 0.095602 0.102358 0.1342 0.114076 0.130864
0.150268 0.167752 0.158458 0.16867 0.12925 0.100384
0.05242 0.060748 0.019958 0.041566 0.035837 0.087904
0.122116 0.094312 0.150832 0.111406 0.143482 0.150064
0.178072 0.201415 0.15001 0.096958 0.13567 0.150118
0.184747 0.072478 0.027772 0.016147 0.026013 0.035179
0.102538 0.151348 0.121678 0.15196 0.082444 0.130672
0.10369 0.132382 0.098122 0.129412 0.087376 0.179273
0.126904 0.161638 0.031124 0.015245 0.022828 0.017553
0.084034 0.144694 0.158002 0.085102 0.069862 0.082654
0.087988 0.12556 0.110878 0.078472 0.079732 0.161296
0.098062 0.126976 0.131932 0.015525 0.015016 0.016132
0.018316 0.084112 0.117886 0.10558 0.053134 0.093946
0.07474 0.110782 0.108718 0.022231 0.042616 0.084982
0.116548 0.103264 0.127852 0.156184 0.250514 0.275155
0.292167 0.285061 0.236789 0.130848 0.05552 0.063836
0.085572 0.033351 0.061449 0.019662 0.024716 0.024075
0.036304 0.234303 0.284792 0.276067 0.285172 0.218991
0.253716 0.27989 0.266652 0.258991 0.227087 0.203877
0.074814 0.055124 0.113347 0.012649 0.015103 0.023413
0.0132 0.015134 0.027923 0.180997 0.23504 0.276386
0.191447 0.290679 0.287916 0.286334 0.294179 0.231575
0.235304 0.187663 0.139406 0.042258 0.020788 0.018514
0.010773 0.013306 0.023871 0.03029 0.088355 0.261601
0.245534 0.27004 0.278725 0.295995 0.274809 0.294717
0.29169 0.27993 0.231135 0.229826 0.18961 0.10546
0.092062 0.025942 0.011779 0.015055 0.088872 0.080611
0.082657 0.255747 0.287548 0.272083 0.286256 0.292554
0.290097 0.268024 0.280228 0.238065 0.179677 0.213381
0.165366 0.229485 0.133422 0.028494 0.016829 0.018933
0.102446 0.126998 0.254523 0.29487 0.296509 0.292929
0.293722 0.288831 0.287854 0.295679 0.292815 0.293765
0.245259 0.191931 0.164519 0.158953 0.086892 0.04594

0.037616 0.025612 0.133081 0.139769 0.27027 0.29321
0.284722 0.292617 0.271718 0.273883 0.286974 0.293934
0.291434 0.286667 0.276162 0.138812 0.07631 0.091809
0.112599 0.073769 0.050042 0.067488 0.065915 0.256634
0.283466 0.292991 0.27689 0.269521 0.203118 0.220091
0.273646 0.290915 0.298248 0.292289 0.286716 0.221598
0.088113 0.060404 0.081832 0.11019 0.06982 0.087849
0.261262 0.265541 0.279078 0.284968 0.288875 0.293724
0.269164 0.234666 0.231542 0.229848 0.268616 0.290274
0.283886 0.166994 0.097265 0.043895 0.100411 0.061625
0.130881 0.290012 0.22767 0.170569 0.137206 0.28423
0.297128 0.293003 0.286436 0.247745 0.276905 0.20864
0.267848 0.269542 0.264243 0.179083 0.17047 0.127768
0.126723 0.112973 0.252894 0.232631 0.213832 0.168094
0.144323 0.158337 0.28621 0.290374 0.284097 0.28384
0.292706 0.257801 0.272169 0.248735 0.208519 0.171097
0.0949 0.142244 0.125964 0.244896 0.266268 0.245589
0.192745 0.12075 0.072372 0.172043 0.252613 0.240232
0.270576 0.288965 0.260269 0.219013 0.231938 0.2401
0.243466 0.173814 0.061944 0.1488 0.232323 0.23724
0.203855 0.206902 0.195704 0.108188 0.090016 0.183384
0.231894 0.111081 0.188433 0.285894 0.276711 0.190072
0.269635 0.290565 0.220388 0.174815 0.076937 0.141375
0.216307 0.268108 0.200082 0.196441 0.146325 0.167918
0.114854 0.113336 0.156313 0.134764 0.16904 0.188697
0.21557 0.19456 0.251559 0.283751 0.279752 0.223655
0.169458 0.233159 0.236954 0.252717 0.2631 0.148778
0.212908 0.085462 0.041739 0.06047 0.099883 0.17102
0.211874 0.17058 0.183681 0.152617 0.262741 0.224634
0.238736 0.28559 0.234875 0.215515 0.278706 0.281253
0.242509 0.160812 0.231564 0.163518 0.035647 0.022173
0.086254 0.052924 0.129429 0.197684 0.164057 0.098332
0.235238 0.214976 0.241552 0.292176 0.29245 0.285615
0.297363 0.296361 0.292677 0.236866 0.2137 0.175728
0.090929 0.097716 0.041392 0.027923 0.096693 0.160548
0.083493 0.084142 0.190633 0.269448 0.263084 0.279859
0.29791 0.294847 0.292532 0.296887 0.292617 0.228836
0.205318 0.165586 0.164057 0.096077 0.068049 0.068445
0.030112 0.07895 0.054167 0.071371 0.157677 0.261305
0.277288 0.293982 0.2982 0.287771 0.292307 0.282953
0.281881 0.184627 0.174001 0.168259 0.153838 0.126371
0.047299 0.075947 0.087288 0.10414 0.087431 0.096594
0.060503 0.16134 0.288077 0.290285 0.292931 0.282143
0.271267 0.28726 0.245831 0.2071 0.220256 0.215823
0.222093 0.155059 0.180007 0.179996 0.085264 0.136392
0.064562 0.034255 0.034692 0.045694 0.129484 0.179556
0.199125 0.279881 0.277477 0.277885 0.272175 0.219211
0.178027 0.201083 0.240771 0.223512 0.201677 0.190677
0.13175 0.041074 0.045812 0.073219 0.021697 0.051703
0.075628 0.141023 0.277963 0.222786 0.2445 0.28667
0.272279 0.20776 0.266512 0.234072 0.276516 0.27527
0.229485 0.185265 0.042894 0.017349 0.019986 0.047941
0.047983 0.036676 0.098464 0.114238 0.236921 0.215999
0.207848 0.283925 0.260626 0.279406 0.282554 0.285018
0.295388 0.281624 0.21469 0.193152 0.147799 0.106802
0.052055 0.071756 0.109376 0.068841 0.075078 0.138372
0.128142 0.151 0.212721 0.24384 0.29226 0.291998
0.279156 0.274038 0.296188 0.293473 0.216956 0.203107
0.174584 0.11844 0.130254 0.090786 0.065112 0.099619
0.045792 0.161769 0.144081 0.194197 0.177576 0.156742
0.239352 0.22767 0.216406 0.257456 0.287958 0.233137
0.235766 0.18499 0.175354 0.121993 0.112423 0.156203
0.142783 0.177125 0.137206 0.193911 0.236943 0.246051
0.241244 0.208816 0.238648 0.23086 0.193878 0.25509
0.131442 0.190776 0.195638 0.222324 0.180172 0.129891
0.079071 0.202128 0.227428 0.222819 0.180282 0.204009

0.257193 0.242993 0.186519 0.268699 0.284935 0.267313
0.241277 0.12108 0.149009 0.182537 0.269468 0.176289
0.200797 0.220157 0.213359 0.240353 0.268402 0.238714
0.26509 0.227791 0.286702 0.290695 0.282982 0.209454
0.291933 0.28972

*PERMI *ALL
605.6267 790.7515 972.2367 944.5153 651.7725 662.43
22.69415 11.52076 8.613487 23.22373 48.96785 216.6512
996.8964 973.4485 833.9884 73.98965 80.77296 9.140143
2.92715 978.3945 767.9218 762.0544 996.7816 869.2586
711.0645 21.55778 5.189757 8.976334 3.483453 28.34458
546.5099 947.9338 931.4832 807.4246 63.68161 48.9595
24.20511 19.08987 990.0703 995.0479 958.4005 985.0902
986.5861 636.5243 127.5408 4.520547 9.452942 15.41477
7.016265 96.03532 883.086 985.6234 920.8842 814.9332
180.3882 16.89635 32.51839 961.2758 973.5135 987.8978
758.4361 882.7241 917.3329 285.7788 27.12339 2.74532
8.051708 10.23222 41.05027 497.9824 958.1511 937.9312
977.226 174.3464 40.08437 35.54528 927.921 996.6094
996.7265 927.7501 948.5495 950.0884 885.1013 61.7692
12.21485 17.74651 11.4296 31.79692 868.9544 573.5483
781.9086 991.7541 441.2462 34.59465 266.6539 749.9426
998.7527 997.5967 991.8797 975.1468 870.1558 963.2677
479.3514 38.87291 19.90458 25.69964 9.901409 156.0364
228.2123 681.3794 667.2169 775.0541 64.74706 209.1944
107.9295 922.8668 997.9321 982.6481 997.5439 807.7947
961.1828 511.312 743.2279 48.80968 2.978784 15.94278
32.68466 56.01521 637.485 828.3578 726.7549 87.18364
207.4512 29.83438 321.6637 985.7982 999.038 984.5891
994.4364 796.7352 370.1332 529.1636 55.53541 22.22824
4.785067 68.84399 20.5689 596.9075 429.0066 889.9795
832.5743 123.2688 96.88667 243.0592 895.5359 912.0969
986.2386 992.5834 996.5223 732.7823 337.0381 233.8541
98.37189 14.31901 7.689233 87.79969 258.4503 228.7937
861.7812 899.7275 712.9203 6.923457 50.13858 939.3772
550.5845 651.2474 922.0129 980.2029 944.1435 742.3505
591.3519 106.8641 26.96727 27.70027 5.000725 159.3496
473.3147 849.4523 566.7559 585.0527 35.5746 41.65604
610.0016 805.653 890.9596 886.7884 990.978 992.3914
787.5643 197.9046 641.929 108.9309 27.67146 7.460312
65.29712 904.3989 843.3755 953.4106 881.2314 11.82413
22.59571 26.6219 897.2325 298.2854 824.6734 993.3997
940.7192 610.7296 71.35756 245.5749 175.277 27.67521
14.78479 30.90295 153.8325 414.998 403.4753 600.0245
3.256207 20.81824 27.36598 770.6177 956.3261 717.5183
729.8372 951.5136 809.9403 611.1179 105.0159 723.7191
64.05175 18.96365 24.32484 238.4097 395.4895 170.8976
667.8701 4.647367 12.17649 18.65087 307.1899 455.5646
807.4562 428.8476 696.6602 973.3589 984.707 97.89939
213.011 269.4095 12.22892 30.2039 77.16458 967.5446
283.284 605.2712 1.328563 4.977715 6.037192 15.47437
340.5336 322.3636 467.0152 970.9167 319.2567 955.8021
253.7056 46.87961 234.7691 27.58989 13.24769 20.43878
276.7076 883.4216 904.9404 5.314018 6.083689 15.9208
3.934776 53.68179 48.77789 334.4067 554.7598 962.3765
939.9765 906.3835 294.7535 738.7543 84.52302 14.88329
17.04241 36.54946 842.5991 809.9421 14.82928 4.417749
7.81707 14.79606 24.95319 144.0038 39.55497 85.81358
666.816 486.6895 942.4233 910.6364 830.6824 497.6591
114.6318 16.07489 137.2341 132.6163 584.0378 63.64012
7.160148 2.783787 7.524004 1.488134 55.44227 60.34649
104.3484 120.5 408.5122 313.5884 983.5762 606.2364
452.4692 481.1317 29.5582 28.37749 286.1554 104.8429
59.27697 12.04315 6.544824 4.937146 2.204697 5.863609
4.825163 78.14478 57.52412 22.35486 441.9051 685.0464

949.3689	991.9459	921.2659	136.0993	18.92731	113.6967
166.6729	27.87494	2.084376	11.743	12.53407	12.67445
4.869036	2.756525	27.04992	32.25841	20.02419	61.90718
640.879	915.4971	984.2422	845.3489	912.3154	53.48771
113.0311	560.2128	12.15055	4.81615	3.935111	30.51919
18.09535	36.68234	2.185929	11.65617	16.63206	26.73794
33.14912	178.539	745.7942	840.9865	997.7483	981.9356
469.3221	205.0369	230.0928	12.91282	3.796601	2.194386
9.047842	11.53878	18.88265	6.199819	10.6586	13.24119
25.11886	24.54607	15.46454	914.3448	887.2357	895.5607
925.007	709.617	492.0713	302.0112	3.438436	5.078752
1.740171	4.68699	9.188466	36.405	16.68196	10.02561
1.912908	18.30189	9.906472	11.36952	185.2303	959.3697
986.2114	876.5183	677.0613	853.8351	524.0914	8.492137
4.747041	5.231509	4.234723	20.1984	83.13942	298.3706
19.18028	19.91297	10.76225	37.15352	12.11541	20.63227
952.8378	983.3181	311.9098	906.8115	292.5735	179.8465
39.75566	3.527232	1.575339	0.776408	21.59037	35.66638
92.89343	55.94973	12.5912	5.581308	16.3771	32.59357
125.0861	863.2827	927.0731	972.7674	91.40143	513.7952
157.1904	54.46769	6.717876	9.164062	3.46883	4.050839
42.11056	578.8646	549.5864	52.75662	18.46537	25.44023
9.284125	116.1796	937.5512	980.9006	822.7881	543.9425
840.429	693.8235	134.0069	68.58861	26.77978	11.64324
2.960943	11.12674	11.82437	770.4669	211.6669	34.59027
4.463782	16.36259	67.54482	442.9768	970.9011	973.7714
376.1985	910.6573	948.8772	609.5944	734.9114	73.8955
21.28786	17.79295	0.937294	12.77556	123.8879	166.099
95.81026	6.982244	14.02917	3.835279	78.6256	725.364
892.8469	621.4139	788.3517	712.9351	16.24464	42.12501
58.39195	12.86563	27.07622	71.88016	25.14792	13.16525
35.54504	11.25341	19.03439	39.24172	30.96335	10.70355
36.724	85.26485	52.96403	78.73249	25.06513	8.892011
71.14887	73.23505	16.65843	22.24155	18.18427	11.16925
18.39624	16.21791	10.72235	12.52769	9.690697	14.87123
16.99515	11.69906	23.93343	45.2884	43.08291	90.28363
34.81104	62.42751	34.04176	26.70023	3.905575	2.095174
2.787199	12.64792	12.47266	29.77536	71.22919	34.39838
17.40344	12.57072	28.2226	7.156159	25.02004	34.91805
13.44238	150.4032	108.4911	37.97205	6.517845	3.186787
5.061043	2.774502	62.43427	45.41988	103.188	160.639
157.8636	81.9802	20.55479	62.28737	29.35175	9.18817
2.58339	4.531646	170.4323	146.2366	61.77361	11.71041
18.8381	55.53771	70.47986	172.945	172.5703	181.6599
169.1438	83.83744	69.48931	24.37137	26.53371	25.32847
6.252087	5.56022	1.872152	157.2288	120.7589	115.1134
9.248621	18.06471	22.0209	140.4895	165.969	192.804
191.8412	197.2373	195.5699	154.9402	164.2446	131.0488
14.65507	14.28904	5.225947	2.848446	23.69933	62.77027
40.84181	26.30928	62.6647	52.12679	187.6364	161.4485
183.7858	177.6209	191.4631	198.1062	185.1979	189.9092
72.32676	23.90667	21.50349	3.548747	3.256994	126.9404
89.53709	51.68541	23.26752	24.5795	83.39864	172.0731
138.6401	178.0127	193.3521	171.3693	121.39	120.7425
108.3338	19.99922	25.88398	2.999984	4.150716	1.136203
171.2549	46.5225	125.7766	124.5028	39.4332	46.7928
180.692	176.6225	138.1698	184.1815	129.7424	95.38081
46.16204	183.6805	43.33602	10.10295	4.939079	4.239777
1.499008	62.25439	98.12982	33.7602	60.61373	53.72482
130.8679	69.16812	39.075	53.0596	160.2921	17.67018
4.300114	32.24876	35.62083	15.06486	47.59135	3.981283
6.563886	3.657573	33.59774	41.25162	18.92322	43.57426
19.06993	12.09066	100.6211	16.97407	22.93285	104.9388
31.5393	28.91778	31.81772	22.50448	29.80389	4.541183
16.36816	1.097511	2.218906	13.33654	10.8188	11.20885
7.9144	10.51465	1.351459	1.470229	3.109517	3.89775

4.17994	10.25716	12.919	73.69907	155.2634	72.77798
57.67638	18.58104	5.380678	4.435566	2.085778	6.709189
6.984527	7.908024	8.149651	2.839586	1.363343	2.450564
9.220448	7.750237	5.725705	7.218667	23.46	127.3606
72.65391	25.1886	14.95778	18.98834	3.59433	6.216973
2.006111	5.261372	29.59232	3.241642	5.819357	5.545223
2.565648	14.91829	5.722239	6.724934	5.155811	3.496206
44.12614	42.41818	71.42644	9.059245	10.26403	18.89252
12.37958	16.95708	4.782754	11.4242	4.228049	2.966019
7.31001	3.612302	10.63078	36.21071	3.238762	0.507259
0.710461	5.807203	42.15907	22.01157	56.07458	12.79614
16.14634	31.17138	95.16034	7.07861	20.8535	16.83658
9.170774	6.071905	3.056258	8.466814	18.4468	2.979202
1.840683	0.784856	1.810615	8.925057	3.474249	14.8071
11.23531	16.59728	14.05035	38.23402	8.562232	5.090753
27.13651	11.30334	4.869193	2.486652	13.122	33.65333
5.65136	5.127752	5.392523	17.75833	4.119979	6.103276
4.058215	7.565977	4.436291	14.96315	10.67763	5.336838
16.32841	12.68981	50.03305	28.72301	30.91527	15.36909
12.39978	11.87173	7.206361	8.223108	16.57609	1.917317
8.678667	8.420211	6.429438	15.35161	11.49646	11.44242
5.015347	3.505702	13.71387	35.54627	67.41492	38.14433
8.528173	4.566937	1.646698	3.895704	5.046369	2.066955
14.44907	5.248776	2.232323	5.736077	25.42963	7.887657
2.689459	2.263117	3.962771	37.68617	37.70014	16.34798
22.95858	18.02034	8.470733	2.534206	3.22118	2.45294
19.98596	14.35833	9.531516	6.675933	12.24938	61.1505
5.77931	5.653208	3.942321	12.1432	21.37509	32.53389
39.86089	143.0899	19.58322	16.83445	1.967343	3.035988
9.148713	20.88378	101.5956	46.48288	18.91873	12.0578
17.88451	21.99455	118.8645	77.31362	11.06894	52.42302
114.2097	148.9073	97.29556	25.62477	13.86756	10.63891
17.79381	5.712247	20.5815	96.38512	18.83467	55.20774
15.98873	12.52608	17.04814	46.75144	23.94181	9.22854
17.54272	160.2932	146.069	169.6153	26.73216	20.10379
21.80033	18.47481	9.165328	7.452603	17.49565	10.76646
11.57148	6.933476	6.272707	48.12048	3.189914	16.22135
20.08505	71.84706	48.42749	147.3798	92.18665	60.28663
29.09176	31.76874	17.49657	4.403622	12.41538	25.95165
48.06976	17.14537	3.318968	7.588746	11.60713	5.942607
3.257054	2.424761	5.488643	5.464985	67.2766	31.68466
47.46965	13.69298	22.27148	77.00856	62.06532	38.66215
26.03772	41.8043	22.44089	14.21105	61.94225	20.54618
6.165623	1.972246	2.224221	0.509311	3.717141	6.147761
24.36273	58.2425	24.54409	70.00193	26.81112	52.62438
113.5939	55.11959	93.27602	50.71799	96.4353	23.6906
24.82561	10.74942	2.206119	4.277549	11.3067	30.23305
30.51357	20.18278	37.98761	31.78974	125.238	170.5548
36.2404	63.55109	16.65839	36.96477	22.29975	7.63108
15.58411	36.86014	3.462757	3.71786	49.12697	12.70726
146.2928	161.9269	23.1264	19.27538	5.512315	69.14647
33.32077	28.45424	92.74276	35.44688	7.14995	8.25517
33.30773	31.16442	754.1435	594.6262	891.4623	239.7778
462.0692	109.6632	203.685	784.7313	949.0891	963.8912
885.2766	991.9688	960.2206	838.8668	845.9701	940.2969
458.4004	268.8258	426.9972	319.7607	696.819	901.3262
683.002	157.4077	126.7328	36.08685	137.3843	719.4904
871.8785	821.673	778.0814	995.8777	991.9916	577.4987
875.1228	835.0491	180.6746	338.5096	60.129	87.11762
265.4208	964.906	483.061	130.3392	56.92722	127.7833
621.8534	966.6227	954.2035	951.6473	969.2259	988.7876
981.5626	758.5706	842.4012	751.2872	290.4404	517.9454
120.108	34.5714	254.5025	845.8104	451.2093	122.6097
126.7739	643.3732	856.8445	962.3011	915.7037	855.5984
981.0519	948.1477	859.7952	881.0895	419.4421	660.1248
116.7855	271.1484	91.34441	109.8841	231.6253	775.7611

739.9664	357.6803	88.84582	377.1447	750.7442	951.9102
938.0651	899.4251	978.3405	852.2951	810.3134	444.9139
17.85196	140.7055	205.4878	243.2809	88.43293	75.57358
86.15788	569.7706	657.7654	447.7556	48.34516	411.9732
739.5065	834.4839	552.0787	682.6687	968.0594	866.3054
263.6331	477.0754	160.2983	67.71845	271.1808	229.6503
247.1582	154.235	128.5124	529.4379	349.8775	572.5455
88.18485	85.72885	350.8335	427.8672	610.0704	427.1663
873.0337	725.6547	120.9893	57.5379	114.7329	119.8439
254.3197	328.888	299.4077	126.9431	178.4584	532.7776
160.9374	247.4121	89.34536	101.4047	208.7426	105.7747
328.9289	799.4071	840.5644	802.6921	35.75699	103.2569
98.79319	142.7743	746.5983	381.3405	168.2031	86.56812
146.1161	417.364	266.63	242.0656	206.5461	181.0944
36.55577	220.8051	110.5684	304.8028	729.9095	55.38511
99.31458	239.9247	74.39796	197.6496	727.3325	483.818
217.1321	256.7273	363.3624	337.5849	547.5869	127.1818
181.7929	88.42213	200.2673	451.5876	220.3307	333.4433
848.26	108.7264	68.5534	116.4145	103.9303	393.812
708.1496	582.4545	176.5989	384.3908	262.527	209.0056
302.6635	45.31782	52.71692	56.18637	717.6423	300.841
237.9984	385.8789	576.059	72.15111	19.74099	45.47189
176.1039	304.8639	368.1629	593.525	220.9938	377.3975
173.8357	221.8033	163.3676	46.77351	84.29446	70.57518
216.4108	72.96171	4.134034	73.28279	225.1143	63.31374
27.95883	31.78725	94.59823	78.00204	265.9714	454.8456
116.0462	211.7859	237.3215	118.1814	42.24273	19.7369
40.80863	253.7535	327.6755	37.50516	28.95176	51.58851
80.23355	43.66827	46.42875	86.58188	65.92877	41.84292
110.7077	142.678	171.6714	310.5997	232.8145	51.21215
113.1684	57.97303	50.27221	391.9485	78.75842	49.16375
23.74504	66.77779	65.41118	119.0351	24.59348	68.68391
135.4213	222.5471	106.3994	340.8725	566.478	472.6776
97.40898	130.8796	105.5745	61.61536	94.87221	623.3055
247.7433	87.32327	25.35695	13.75365	105.3584	64.00074
45.55311	196.3374	65.26871	220.8391	95.82261	484.3909
796.97	889.0067	675.3937	667.2629	67.60114	62.87326
863.6843	624.3124	116.6442	76.48213	37.2108	14.58754
30.19076	68.47531	67.6083	151.5629	188.0338	206.0137
160.8126	581.8754	334.5022	335.3675	306.0187	901.9158
87.69887	854.7281	887.4318	764.559	46.04378	72.8687
42.65118	21.20699	37.30714	26.13551	138.5884	136.7688
104.3528	208.8503	108.7319	554.0284	135.7929	633.7136
826.1026	754.9393	917.5421	943.6957	841.6335	566.7989
71.90068	129.3615	98.73202	5.947056	23.0646	35.99565
91.54993	139.6912	160.6934	127.0428	358.5932	749.6473
186.8551	233.0671	666.2896	868.6464	891.8298	966.3334
944.3413	351.0751	158.9366	119.7769	19.99056	8.100895
23.97143	18.69334	125.7625	193.6801	400.8824	416.4367
879.5692	724.5928	133.6857	273.0593	719.5716	958.4953
984.4644	987.5748	924.8941	316.3115	363.2235	310.4674
35.3999	7.379246	93.61383	30.69241	86.0314	146.4108
658.878	274.1593	331.6477	947.9229	429.5542	337.4155
774.1926	990.3347	988.0479	930.6106	460.8133	446.5869
457.3851	572.5376	44.66836	17.15703	21.97465	36.63161
186.7244	137.8145	222.8994	239.8833	356.0918	633.257
210.1905	566.4205	867.7248	992.8577	997.6381	957.3506
845.8026	285.6538	707.527	397.4166	70.49462	58.04396
42.20443	95.26031	231.8414	163.8925	238.244	47.57535
228.1172	110.3431	103.0258	320.9963	845.6273	998.8057
998.4883	989.8469	784.7657	378.9082	960.3311	684.4741
83.59898	185.0223	178.2966	251.595	166.1629	123.5378
123.9615	43.1092	8.217013	20.80497	127.2457	296.2027
861.1107	995.316	999.1116	985.088	928.6649	879.5226
856.7932	402.552	57.23082	141.8042	160.7334	98.54849
135.8316	93.0782	365.946	33.47973	14.64408	59.95412

104.6625	675.2491	985.1514	998.6217	998.7344	933.1812
993.1892	954.7463	991.2358	325.0686	39.1612	110.9257
360.8436	566.1937	131.3119	105.1182	3.472826	46.05969
32.22976	115.7697	250.9499	926.5567	997.0134	978.3157
999.0334	998.0057	990.6472	983.8729	982.6436	418.9518
191.2115	106.2383	369.5907	520.2463	147.9923	2.615345
3.081534	22.6295	32.77714	164.0945	267.5703	961.3024
983.1007	978.0139	987.2656	999.0173	993.9122	992.9811
944.6436	364.403	94.58298	129.2978	599.3424	246.3667
57.59344	9.157375	157.3483	126.311	23.49492	18.36648
10.47307	122.6013	23.66007	6.443399	11.74381	3.63385
1.415533	2.20026	0.987918	3.097904	5.358361	106.5433
59.47329	20.96549	3.895077	16.39933	24.7926	19.47032
89.14685	107.9021	8.564421	22.98444	13.27715	25.70212
3.900767	2.427828	3.524812	0.847555	2.007747	5.690114
60.5981	27.61239	2.936169	3.266066	89.29806	24.42334
467.8719	335.1359	62.61653	50.71145	11.93249	12.30257
11.76224	37.49747	94.96838	1.792702	5.936234	8.191605
17.48868	59.83592	29.65227	3.342997	36.06575	484.0642
468.3268	474.8222	359.8322	313.3805	49.50636	40.85733
29.72802	159.9591	146.7135	54.55505	46.41443	40.71158
35.68552	29.75631	69.0146	15.56231	10.75241	401.3692
485.6373	495.8987	145.5506	173.8593	11.7695	20.24576
391.1254	151.4726	289.661	398.1714	218.4369	61.37747
435.4818	45.06216	114.8188	105.514	29.41575	132.4043
482.0466	498.3231	384.9178	75.23882	7.759719	4.496007
124.9051	298.7955	174.6807	154.3484	443.0207	276.5037
483.2201	493.7067	419.5348	134.869	312.6266	29.1411
368.2655	497.2926	264.2086	48.85016	56.99923	0.544275
6.694374	10.60367	33.92244	156.6098	88.95636	300.8528
488.3453	212.7189	498.8523	498.672	497.1232	203.3036
177.8918	478.3657	138.5122	138.4016	30.81158	4.984769
1.182331	10.65244	2.275931	36.13516	32.76649	15.47826
369.7873	487.9261	491.9772	498.7765	498.4941	490.43
85.88039	62.22444	164.6255	59.93217	83.28427	35.88277
3.006422	9.696567	2.439389	11.90014	24.05215	18.41145
15.99381	400.2635	494.3949	491.4553	498.8672	496.8989
492.5542	343.8959	33.75103	207.0647	406.0869	48.63714
5.46008	3.307737	0.808643	2.202161	2.80411	18.49132
30.64771	47.36778	172.5437	450.989	457.6147	488.1294
388.415	272.5198	457.2977	67.79848	301.9882	79.89618
39.7857	5.510538	13.47811	9.24215	1.710504	3.589864
3.518795	22.52911	79.09918	213.5492	261.1367	39.87953
467.7793	143.8153	212.8139	372.7632	415.1012	153.8112
17.00161	15.82804	5.42769	2.793045	1.5072	3.839282
0.897191	9.159442	110.3123	106.0506	241.5288	281.597
32.86548	418.2029	36.31332	198.6081	79.59357	93.64336
61.59862	92.60278	9.34039	5.576863	2.641721	3.010981
2.891166	6.729395	106.0264	161.3162	133.0798	207.9012
115.4099	64.48222	39.10686	76.21948	87.112	32.70876
49.91591	21.49275	34.40377	8.868047	23.59837	0.518443
0.736782	4.565486	24.19937	267.9026	159.2099	245.8584
61.04274	288.5061	18.9044	6.609902	13.17489	38.61153
40.55935	46.51671	34.0405	40.4684	17.70557	6.403332
7.842942	1.419796	24.74241	221.4869	435.4667	77.87679
30.61526	24.63576	12.79104	11.80535	6.630206	62.44304
35.57173	27.21692	50.65508	54.10694	13.44513	15.60357
16.22079	1.831041	28.79844	44.69984	275.5859	133.3365
288.0753	59.80342	60.77878	35.1329	57.77102	26.03353
40.12075	52.5262	33.40673	77.87571	42.13898	64.39112
37.60313	8.530981	10.20495	88.30291	78.95652	138.5294
441.3092	174.9653	77.42354	21.46293	22.66715	126.347
68.93615	22.79807	37.18177	20.75726	68.85825	71.17213
26.81649	16.03061	5.985081	36.63178	203.3462	33.33696
385.2627	45.17176	235.3781	384.0811	28.29509	43.71868
15.59111	53.41165	31.97452	124.2136	43.15081	466.2018

76.39624	38.92665	17.77813	4.269372	79.08206	25.01347
212.6919	256.8077	176.5294	420.0132	205.9596	35.90459
9.059892	91.60749	28.69789	18.33868	103.4304	455.6192
493.1659	85.91955	44.40879	24.66573	5.623595	22.30103
21.62335	362.621	491.4971	275.6811	304.3365	105.103
18.72294	17.33381	17.23769	17.79459	87.19629	254.2436
498.6743	496.5854	34.62597	8.307819	6.135162	16.93718
11.89701	199.8987	489.8251	483.8937	481.1184	129.9377
27.67356	19.56451	54.6637	93.30588	149.4425	266.4545
498.33	496.765	463.9263	21.4041	47.84031	19.71446
7.243325	18.23278	124.9505	445.3372	484.5705	487.6093
265.4605	98.72633	32.1298	49.75835	30.75311	122.0442
287.0774	497.8093	468.6785	124.5782	49.64643	12.02541
5.385896	9.317684	15.11113	16.04697	240.5127	347.7955
487.3848	64.06163	214.2945	92.18792	224.6187	409.5265
223.6192	492.0237	481.0077	491.6341	105.3033	9.304114
5.860626	6.809559	2.520032	11.81082	56.40752	32.38441
69.26455	46.90844	196.3672	152.7566	209.6583	97.77797
431.6115	457.4314	493.1182	411.0163	95.55249	46.85878
9.570596	10.0698	2.561439	15.03038	10.51081	13.11677
39.61238	38.93068	201.7446	66.89151	287.2678	468.1812
140.2165	438.0544	270.2384	254.6238	45.20297	192.8719
48.99796	6.118655	1.555941	0.717188	2.211923	1.129593
16.50133	137.7381	45.37357	95.55623	35.70705	172.3765
378.4321	106.9456	76.39272	425.8631	31.53211	26.54716
84.63754	31.31785	2.741101	1.488483	2.214716	0.4967
3.521948	12.27391	27.86699	42.89059	12.95588	13.00418
52.04033	188.3849	23.72652	30.99538	73.14017	22.42018
4.604972	86.15927	64.11063	2.607264	0.523902	2.022335
0.845526	4.99197	14.41883	15.1444	9.100055	20.23485
10.65114	14.72902	34.10484	18.68082	76.21352	114.9593
16.45341	5.610854	191.7869	412.8298	992.7091	995.6415
994.0358	933.6949	194.1909	55.10221	58.54476	20.84813
20.39591	10.65666	17.30394	12.74134	16.466	20.42359
114.4672	263.6046	579.1659	731.9426	152.1483	960.7447
970.4809	986.2999	995.3825	962.0995	260.8303	139.0337
41.4976	6.111629	8.955256	8.804405	3.827771	10.39382
15.51869	49.71518	88.54071	210.1798	358.6171	204.5145
812.911	933.1254	995.3137	987.6271	974.9852	955.9496
616.2302	670.8911	255.2378	10.42147	18.48507	9.669989
3.981998	6.531561	14.27266	49.93568	493.0444	392.6214
626.8303	924.5875	742.6959	913.0215	929.2894	994.1914
990.0247	849.0554	557.7659	676.1048	152.2804	11.88401
10.94662	1.446499	1.104221	12.98548	43.2253	40.80008
367.2823	757.3611	937.2382	720.7672	938.4173	975.8678
946.0106	806.4901	635.7231	936.4897	865.8586	324.5062
125.0086	3.394447	10.06939	0.922435	1.33203	3.636001
35.27354	50.39263	620.4017	994.954	994.1021	985.9298
987.7249	967.068	997.4589	994.8853	973.2603	862.2635
492.2435	191.5107	33.49731	27.9569	10.66162	9.405871
3.954231	13.07365	93.72253	35.55986	972.1359	999.1369
998.7804	997.5117	903.0671	946.0651	969.8956	996.0703
965.0637	566.9608	763.4402	205.1167	4.064293	39.98794
14.07032	13.04172	50.28506	10.3815	76.25845	986.9088
983.6486	997.661	997.9712	993.665	946.4681	408.3175
887.0662	882.9132	925.8465	595.0014	752.1717	299.3857
7.750826	33.42497	28.08109	53.22921	24.39181	12.8982
647.3602	960.7845	989.9335	996.1758	999.1829	995.9648
949.8784	736.9008	900.3347	892.5982	732.4416	458.4258
30.38988	140.7515	35.66654	21.55693	90.81028	288.2511
94.77112	761.0409	947.9622	908.4939	488.6456	945.8407
997.9872	996.0267	998.6999	980.7944	661.0784	686.9799
812.6302	714.4848	333.0842	85.68327	31.53189	141.4298
591.796	292.5459	276.763	843.0106	321.946	365.3642
609.4288	938.467	994.2051	995.1625	995.009	980.0021
942.0262	939.3642	919.3354	723.201	543.8073	88.71806

34.67368 194.6547 290.7335 907.9982 777.4384 707.224
718.0654 570.5609 133.6993 638.0695 695.5815 965.715
997.7277 984.902 954.5991 952.5461 911.1125 768.9445
586.3649 180.8111 181.1286 73.29494 876.6374 920.5004
727.6273 457.795 281.7007 122.108 142.7247 482.4919
313.8434 182.5408 234.1154 955.7031 977.9215 982.3947
725.5762 991.4413 971.3998 566.4049 344.2786 367.1758
787.131 989.7967 923.7256 866.1238 799.1053 384.5546
28.2163 53.22382 95.34941 298.3699 578.0135 349.5103
892.6187 895.0865 962.9617 968.5098 981.4541 942.8769
118.174 262.4853 836.8661 959.0516 990.6472 885.2644
942.1086 841.5792 112.7943 41.36919 46.90455 457.3809
794.0411 590.1359 739.59 864.3408 415.3412 883.0515
950.2744 738.4362 877.1563 796.6343 632.6332 951.334
970.1904 914.0038 946.1979 671.2743 704.1513 18.77842
32.63097 39.29841 870.6087 892.9209 760.0339 583.601
833.3108 920.1826 856.8879 965.6973 974.9807 627.5004
808.3287 426.2045 885.3052 827.5153 316.2278 375.0922
253.9885 157.39 74.79732 258.2224 102.1718 404.8471
279.5503 357.3683 233.6501 717.9761 971.6839 949.3077
967.8409 944.5197 991.6376 983.5739 971.6168 759.6613
917.9034 361.3591 186.3528 166.3489 21.36874 34.94886
84.10503 810.3227 614.1706 290.1904 176.0832 297.7885
599.497 973.9777 637.2209 419.643 961.8581 962.8021
981.7524 775.1915 592.3072 756.9078 408.6354 91.53454
9.052802 43.7365 60.21394 571.5747 696.9346 25.64785
49.16511 80.91351 299.2423 257.4785 90.23624 913.4799
951.1916 915.1557 741.8157 333.5362 695.0227 271.0841
597.7148 538.8898 184.1968 130.0526 22.26871 353.0222
35.45969 18.74843 10.71783 19.43663 131.5007 11.51179
51.24907 608.7458 981.809 785.9393 711.1857 915.0335
845.6974 684.1715 757.792 694.2454 740.7386 242.6281
32.39023 37.71933 33.05164 30.44087 2.111514 10.47109
50.16999 85.16203 165.6136 624.426 869.8232 803.6002
949.6619 865.6693 944.7698 985.4827 922.8859 865.7211
700.4078 82.79498 164.907 52.08132 32.28226 15.47904
10.45064 10.62155 17.68618 17.72687 661.5795 582.704
650.3782 908.5336 950.6573 990.6494 966.5493 990.7521
993.0543 955.5887 864.3726 243.9355 602.0617 206.814
76.86861 33.94111 42.77076 16.67063 8.401194 129.338
199.0889 128.825 814.2261 872.3424 984.7205 994.2006
975.9802 989.6691 973.8655 941.3064 135.8658 339.1252
174.4102 103.7144 201.6694 350.9102 115.8049 85.36208
107.0062 125.2587 115.049 265.2394 157.9465 148.3915
804.8594 989.9608 942.0783 897.0776 995.7699 331.1754
195.3057 113.5288 104.9062 149.6784 117.5563 219.7328
82.51217 235.5055 184.3296 242.7348 739.1524 688.0627
480.9922 169.4849 321.503 648.2612 455.119 796.0916
194.2008 103.8831 281.0302 130.404 161.4132 475.782
167.2623 181.2984 577.4163 320.6882 519.6094 430.3264
911.8156 460.1421 306.4573 103.3513 468.5252 350.6978
609.586 42.99768 141.536 86.81205 200.747 343.3998
366.3692 123.8566 257.5847 119.5099 183.3344 567.2715
812.9559 858.5231 894.8454 599.7952 805.575 388.7281
441.8634 708.4529

*PERMK *ALL
479.1671 484.0564 446.9861 455.8669 193.4751 295.742
52.77825 26.70902 11.27273 6.942694 192.9652 240.3378
482.7697 480.8272 183.126 14.35572 41.86142 4.714558
0.285949 483.426 474.7292 487.6992 488.8864 158.4703
119.7237 88.87078 20.32174 4.103704 13.95626 12.86045
334.8621 458.3097 483.5061 413.9206 23.87982 9.360671
41.64914 0.864452 461.6183 485.9158 486.0378 465.1382
480.2253 20.06412 59.79667 10.35192 2.855795 7.628603
5.11352 28.20324 341.523 465.5486 460.2693 263.7357

8.840911	22.61658	1.912269	455.8039	492.9138	493.3055
473.9658	251.4734	207.2163	69.30251	9.725927	7.354819
5.144486	81.09723	41.40369	281.3494	376.657	451.8611
466.9184	9.023167	3.149931	11.87263	447.4505	445.7763
492.1664	478.5585	244.3099	63.81165	82.25684	49.56099
8.229397	10.45796	6.870716	8.163962	117.3143	262.135
418.5082	480.3204	98.55984	1.902339	22.62622	46.10617
476.9666	481.6716	495.5734	460.6107	136.322	276.6094
220.3703	3.231454	4.71496	7.064038	5.659226	25.50774
167.6803	405.9598	406.4283	426.3429	19.23512	17.9285
70.24558	402.4019	465.511	489.1263	475.6254	316.2132
44.43242	157.9752	100.5947	4.794496	1.190817	11.98505
1.530375	148.4192	90.58431	425.5631	460.0373	425.049
61.12572	23.31358	295.3201	466.9732	439.0056	493.4055
496.8966	348.9073	90.68114	93.85491	25.91481	1.27212
6.99668	7.884316	9.187598	292.062	250.0224	467.1292
148.8528	107.8388	20.1747	32.09032	345.9553	472.3218
477.5952	493.0603	452.6161	38.01649	148.4086	27.28733
4.935578	0.926567	15.83139	12.73864	39.63446	303.7484
435.0759	307.7592	362.3464	9.293237	76.42175	182.9422
366.7245	390.4137	495.0305	492.6608	234.874	101.4283
251.0556	33.59835	8.800858	11.21414	22.77655	10.12428
287.2798	331.8998	244.0602	308.0825	7.894707	14.63511
158.2031	170.2798	214.8874	493.9261	497.6064	487.1313
139.5652	124.3303	19.99401	14.91451	5.522287	10.11917
19.679	233.146	344.2825	395.5424	462.6505	6.071556
27.51921	50.31054	385.1244	435.5901	332.6718	493.8875
489.168	220.4159	12.67564	28.45136	13.97784	4.037876
13.19812	13.80384	43.32584	69.56968	225.7428	305.1736
3.785951	2.509817	17.53485	341.7685	312.2526	292.7534
387.8832	495.2072	460.1061	121.8426	29.81412	19.17397
44.35494	12.76139	25.07339	78.7713	71.20049	145.4015
427.2745	0.379234	1.140762	9.784396	18.49367	443.2737
200.3983	330.5316	478.9928	483.9862	460.5184	110.5256
73.81574	45.2859	6.601916	6.617089	30.9799	434.2802
30.96863	445.7291	0.401819	4.792686	8.843924	2.259368
371.7312	408.1427	402.5557	466.2588	449.986	454.2741
230.747	79.75355	28.18221	12.89636	2.919127	31.41427
135.0508	405.3825	222.2056	4.116707	1.077663	2.173832
7.717151	7.5006	90.52593	205.7349	290.6176	409.5595
432.9931	445.7004	135.0806	427.8997	95.02634	18.41611
17.77428	24.17687	207.1052	324.6871	0.811518	1.682674
2.09651	6.326711	7.250951	45.46194	159.3555	61.96593
257.5746	418.7049	415.8828	372.0566	242.5029	354.118
71.663	15.52605	53.83045	123.502	439.6844	6.588522
3.926793	4.78315	6.11905	3.398678	9.775928	56.04424
180.9281	96.18825	376.5737	101.5051	437.9212	460.8165
252.2394	172.6863	24.16829	28.82425	199.1544	260.6268
0.927135	9.103974	5.111296	5.340685	9.071205	23.05006
14.8414	46.43474	80.42591	136.691	114.7881	301.4054
481.818	478.5981	311.9737	328.9274	66.85425	220.9347
339.6159	11.28774	0.90659	2.300504	3.150359	6.976025
3.558082	10.03116	144.9249	13.85894	18.12133	415.6627
158.1547	360.4516	474.3578	414.3859	443.1615	307.0457
212.7874	135.3415	2.086138	0.46417	3.091819	6.401312
2.64986	19.6732	3.216422	41.55727	36.98631	13.93888
36.59055	204.0601	99.45257	419.2171	472.989	453.0081
313.0192	92.37065	53.15694	2.248356	1.050768	0.315561
3.731015	2.319578	17.05851	1.841035	41.9445	30.67892
12.30269	1.739803	63.10184	66.38654	451.2861	391.8339
475.1798	389.2593	168.5683	20.52948	13.96307	1.277144
0.996984	0.439482	3.837806	8.464474	4.175928	1.736681
3.192876	5.271109	4.221483	2.327068	78.68664	25.39815
395.343	435.138	336.8054	373.2759	79.87742	17.40127
3.419542	0.845902	0.791777	1.835689	24.85776	50.01324
1.940524	61.19783	27.78011	14.12537	2.153188	11.1313

189.434	202.4865	305.6849	379.1779	157.0413	156.7751
16.99143	31.61382	3.022338	0.431954	2.752067	12.66068
66.85902	16.991	5.847739	25.1741	6.585428	6.566471
13.05762	77.20653	223.4853	457.9236	456.5696	82.4252
66.29626	12.10147	3.444633	6.156941	0.51065	0.697925
11.63625	46.54617	32.53419	21.58654	8.947362	19.24873
1.86828	9.905856	130.8215	226.406	454.2856	454.0671
432.2639	164.7324	82.36961	12.58186	4.318371	1.668411
1.573269	2.75111	15.86792	69.8435	42.64135	28.79102
5.59044	0.698829	2.426442	141.6368	234.0001	404.6504
360.6932	477.0611	410.1144	109.7903	45.43411	4.572935
2.142057	1.632409	2.036653	13.26951	61.45426	221.3192
121.0944	38.50313	4.529184	1.062236	9.52772	269.2868
188.8209	449.8109	428.2072	243.4389	2.796327	1.976938
6.86934	2.228558	6.268982	6.557058	6.039361	5.795475
11.68119	11.05333	19.72659	2.843047	2.292831	1.190836
11.7168	9.404311	31.1548	42.2331	8.685704	2.252532
9.901044	25.47364	11.46128	8.337868	3.036925	3.405179
4.514815	5.979006	6.80116	8.693787	2.893224	4.101238
4.84969	4.074863	11.56008	14.61501	5.076764	18.59512
4.612443	14.85641	17.76049	6.382708	0.660745	0.641217
1.190674	13.30136	5.317347	4.713049	12.21546	21.29899
5.693194	7.619211	10.44783	10.8362	24.05459	7.986233
1.809585	11.39714	11.99684	30.79775	2.563333	1.184955
1.851527	1.470466	6.20789	30.55955	40.9551	45.99938
39.44591	30.02624	3.974825	6.49111	16.29795	7.360749
1.159258	1.026777	24.21029	45.90532	10.20044	5.769777
4.307944	9.035226	5.560182	19.93485	41.89633	48.05095
49.08186	35.23035	25.1857	29.16084	5.147437	12.3955
1.059146	0.808463	0.440614	35.62993	13.11505	7.188346
2.18061	10.68336	36.65718	35.40283	41.14537	48.90396
48.36476	49.06197	49.62597	48.00694	33.09032	23.40669
1.511193	1.831399	1.073873	0.601192	10.89326	14.28753
13.29018	7.063485	12.16208	38.19662	40.60289	37.78644
42.56445	27.09474	48.86996	49.38715	48.40186	47.74831
21.35969	5.165496	3.553522	2.162081	3.258442	13.08121
13.65951	6.528298	10.44297	7.700998	36.08311	45.04463
43.69432	45.86961	41.84311	30.19743	48.03016	45.32794
21.78522	3.593064	5.127457	0.896817	1.921383	0.607052
14.04931	14.96522	18.29132	28.07282	15.73704	5.895301
48.95161	45.30415	31.43041	8.258078	20.26007	32.20209
15.96824	17.23646	5.605934	0.617884	0.714164	0.904272
0.316697	9.049134	11.07037	4.311268	32.87699	32.04026
22.36428	9.765826	4.08452	20.36587	38.66295	3.808386
2.545148	8.071161	1.315961	1.315891	1.853365	0.873474
1.128234	0.758785	25.01866	9.764635	1.287757	12.72093
15.46799	1.420516	11.61093	5.362138	6.706424	43.86377
9.39864	21.54076	17.26335	12.07124	5.600077	1.675024
3.837072	0.284845	0.431679	6.946275	4.043561	3.768591
2.257798	1.25936	0.232709	1.15127	0.757286	1.319727
1.577938	3.327561	26.1995	45.74062	39.96686	26.14996
5.893238	2.512401	0.87225	2.317672	0.942849	2.382407
0.656744	2.556154	2.178352	0.332031	0.614653	2.258375
3.394447	1.465538	2.111067	3.631466	6.852531	21.73317
41.91882	34.73002	8.456663	0.748409	0.844007	0.734287
0.321926	0.461168	3.745545	0.277342	0.579848	0.600066
0.864546	1.925134	1.693605	2.50269	0.87095	1.069486
6.466808	13.17249	24.00844	4.675607	0.964186	1.039827
1.155338	2.230468	0.385202	0.880913	0.404944	0.882275
0.38791	0.42876	1.040382	4.493875	1.46402	0.231081
0.525551	1.506683	6.813888	3.520562	10.03552	4.343822
2.695709	1.942665	3.170473	0.692628	3.331294	2.780078
0.458335	0.562328	0.410292	2.046873	13.85623	2.382967
0.664915	0.41069	0.655858	0.653966	0.530557	7.841949
0.970186	4.683915	1.782592	5.514714	1.652068	3.231119
9.017538	1.231816	1.179666	1.061434	3.388442	2.035415

0.750869	0.970233	4.806224	5.000967	0.404044	0.289238
0.477931	0.910561	3.11553	1.95148	1.233252	0.548559
3.927833	24.83253	9.233854	7.054577	8.498866	3.404356
5.797717	0.956095	3.647657	4.687594	1.027167	0.363615
0.394265	0.494643	1.834742	4.51283	1.493448	1.430507
1.708394	1.415777	2.930542	32.37658	20.84582	3.762158
1.252567	1.892867	0.91817	0.632552	0.431952	0.845859
1.645091	1.872199	0.294272	0.947609	2.940614	2.236331
0.785585	0.778356	1.049658	7.930581	7.029525	7.022666
16.86235	1.235848	3.654366	0.425001	0.781817	0.661007
3.231343	1.37267	9.719614	1.795982	1.590911	7.181514
6.590601	2.425001	1.252037	7.961355	3.10805	6.581335
19.24957	34.51628	1.761514	2.112526	1.347994	1.494301
3.149416	4.984252	16.65724	7.616282	8.107165	10.86228
3.938102	4.278662	25.97222	6.859287	6.467002	12.40384
36.58677	43.60387	39.72007	7.119967	3.630781	1.589948
2.722049	1.385323	9.127882	12.16228	3.930991	14.06048
6.872156	1.801242	5.267251	3.752667	26.31601	5.231256
5.921231	15.48057	15.29829	41.15902	13.6274	1.496584
1.161529	2.56436	1.099659	1.629082	2.564484	6.56697
4.030417	0.868011	0.504636	7.159505	2.932561	6.362005
4.743556	12.84101	28.73803	31.40169	36.37391	9.149492
4.37891	7.979947	4.100889	4.767481	0.876076	4.644864
7.815954	8.371263	0.821058	0.498333	2.964019	1.936293
0.757351	0.251922	1.278945	4.721935	14.64044	17.57244
15.88397	3.985942	7.766512	4.932397	5.781812	3.089242
8.831917	7.903765	8.167892	4.750256	12.0312	4.915707
2.043121	0.918887	0.330181	0.438559	2.069369	3.081109
7.990188	14.13973	25.02367	9.260832	9.263562	9.433742
31.40928	11.97187	18.17775	33.12082	17.72385	8.807892
1.329652	3.180094	0.741336	0.821548	0.410085	3.175653
8.980076	4.085526	3.535705	14.55466	12.20475	43.52272
41.33767	37.65581	35.84132	23.73553	8.080831	3.418283
4.621862	3.118954	0.477189	1.989793	6.439157	2.664219
10.88168	5.967054	8.448761	4.405325	3.424948	11.26027
7.293937	19.77398	41.57488	13.48314	5.49756	8.050095
5.636896	3.908805	238.0061	16.39491	185.9474	301.0496
448.4882	322.9394	324.8456	267.401	429.6017	481.3589
478.7293	495.205	452.2932	382.7384	274.2976	230.9261
51.45316	43.68879	59.67632	86.35232	153.6211	111.6128
274.9717	158.3766	428.8051	391.3695	404.9804	414.8891
481.1805	470.5264	471.2322	496.797	491.8571	365.8997
404.6262	218.6497	15.02215	14.14901	157.9072	67.00404
159.5604	128.8757	52.30787	239.2638	186.5026	450.9143
475.3889	470.8385	453.9531	466.0473	450.0513	488.6355
492.9218	380.2288	324.8284	177.5894	25.24166	69.81777
62.72794	44.65252	56.18974	101.9431	47.23403	342.9557
290.6217	373.9392	425.3564	469.774	466.145	383.5933
462.9958	494.2105	492.5689	397.8194	309.8817	64.3231
36.08311	65.44357	71.38155	40.1518	89.96136	101.2533
121.7253	378.6788	425.8543	442.1402	380.4153	459.4085
462.2448	406.565	451.3693	482.2797	493.0603	297.2624
246.5097	113.3872	64.31096	44.24467	97.40158	63.41091
116.0756	108.1085	232.4599	362.7279	261.0586	381.2984
188.3818	376.6786	381.9662	432.6104	399.9991	492.6982
490.4187	339.2235	52.301	84.97105	109.0933	51.44024
56.05044	96.41842	126.8358	142.82	202.2181	306.2683
260.5841	126.9013	67.91207	179.7103	469.5523	388.6306
473.9309	486.8083	476.5001	15.52694	71.09695	81.82462
51.85994	56.33444	86.90424	162.0623	88.98996	24.24242
222.7117	223.6928	150.7447	102.1316	116.1229	210.6663
396.0965	446.2426	448.5512	492.4408	56.87337	48.44556
75.50957	37.48349	101.4297	132.9689	154.1903	238.1727
16.72396	86.04705	252.9828	121.0264	71.96777	92.92295
72.49532	232.2405	331.5454	371.0035	474.2027	52.82396
53.36998	60.77444	111.8814	68.13904	270.122	53.592

54.19397	347.181	57.00947	117.836	62.33113	63.40332
161.7402	272.5022	289.5363	239.8297	468.2675	440.126
98.82391	54.15019	28.77266	29.22658	153.3953	181.6264
334.2412	67.82847	73.87951	318.6677	196.2239	181.1907
59.20536	39.26657	61.05103	96.01233	231.3076	286.6322
431.2787	124.3887	101.4374	67.31549	36.30079	18.03383
38.57581	56.04192	64.42894	95.4254	98.70473	109.1408
85.73971	128.6349	31.61979	22.38721	39.89367	177.1251
336.8767	366.6182	15.18424	53.27347	96.21084	29.2288
27.54343	15.47084	28.5094	47.79836	44.40092	29.36852
43.68839	99.54077	38.11606	68.69182	13.62564	38.5576
18.08202	390.2788	322.7335	137.6439	39.91958	24.47462
54.45842	29.28694	29.35236	28.55801	15.92652	20.32179
26.51917	15.42922	26.21893	132.9554	22.31218	34.80896
44.95862	82.27578	27.28689	137.8996	436.2686	93.28289
76.32626	45.4542	25.83259	63.14529	33.4359	28.82179
22.32606	51.80957	48.17437	25.64065	37.78331	81.12113
39.51691	27.8734	52.67881	33.21567	61.65666	475.1393
422.8487	76.84224	79.53733	108.2109	15.74878	23.04873
45.35603	77.02576	26.07672	23.81552	50.92148	111.2725
119.7107	144.1299	105.7226	285.7038	53.72445	49.52688
480.013	472.2174	311.0613	151.505	20.77433	66.19284
12.35447	20.41752	27.54229	84.88267	14.04284	30.05716
20.99771	143.3366	243.2333	101.2672	90.55095	281.7585
50.50856	491.3863	476.488	363.4586	372.8653	95.45485
30.47453	33.08149	7.805757	9.426056	48.60724	35.61008
19.37033	51.09319	35.14674	161.3355	218.0721	118.1435
322.9424	284.3315	477.6304	481.7825	461.1254	302.4023
309.8525	82.23411	17.1234	12.7426	10.55356	29.65364
39.79605	34.29083	24.13498	38.53151	39.39789	47.97732
72.98927	120.4046	137.7844	470.3553	492.7504	481.0497
459.8403	289.4196	211.9044	68.69735	28.93603	10.89264
5.985563	41.90627	93.50956	29.06337	24.7805	31.20951
51.52524	60.84235	12.74371	118.4265	435.541	472.112
490.4458	472.1294	456.3909	409.6378	172.9267	87.3645
16.53488	15.92883	7.150329	21.76993	197.4522	206.4829
81.60391	161.0408	102.6885	116.2626	20.56696	484.739
449.3968	469.9287	457.8983	453.6271	461.1923	469.7697
394.3865	34.34124	17.37801	28.0187	10.38061	30.29396
81.76417	36.5775	109.1981	123.0269	163.3436	66.32099
387.387	484.873	442.6862	475.5443	479.2333	446.1943
486.889	478.9222	380.8527	157.5535	65.56544	25.87546
52.00379	54.5959	68.03682	58.95315	59.07599	30.4551
77.85168	50.85352	230.5722	431.9605	266.2827	470.3488
480.1434	457.8002	479.2775	464.6436	470.3477	320.5826
79.19523	13.38255	23.70697	63.42361	68.4791	27.06724
26.02346	29.10047	30.13506	28.38873	403.4335	424.7252
449.4237	491.6273	492.1109	450.0544	488.6479	493.3055
466.9292	359.616	87.90873	26.65852	45.43275	35.78195
122.3114	107.705	12.57179	14.1876	24.73011	73.90027
356.6506	379.4644	466.51	482.6063	490.2482	469.1244
491.2867	493.0001	470.8158	354.6247	98.71815	69.45795
40.40648	55.93556	286.2734	76.61574	1.342493	6.549784
18.80763	170.3605	308.7841	433.1347	375.9984	483.7957
491.1521	490.2335	496.1843	494.2697	436.2375	183.7943
148.9323	54.37735	66.32282	203.776	360.1638	0.757907
2.012983	9.813976	24.61546	92.82907	223.7747	317.2861
240.5282	478.2214	489.3527	495.4707	492.0226	491.229
410.7542	354.0234	22.25138	98.66248	125.4163	275.2048
17.53307	1.163328	4.297788	5.399928	5.409361	17.61282
16.3728	10.36611	10.90144	2.031164	0.901635	0.250195
0.424292	0.370073	0.214789	0.261522	0.978951	19.3349
73.34863	2.998845	1.26575	9.418419	11.42265	11.66836
33.06359	18.80815	2.997761	5.167459	0.725539	1.201606
1.276774	1.347408	0.331998	0.242042	0.778578	2.324524
16.51772	25.62943	0.727776	2.249345	4.092399	25.9326

90.76094	46.24534	18.04825	1.115645	3.864506	1.587914
5.439863	27.54121	9.288894	0.327126	0.541659	6.196065
12.26154	6.798702	9.77962	8.036797	8.567261	62.36946
94.796	64.92919	10.05963	19.77903	1.723971	20.95521
20.47392	92.30772	81.65392	3.391439	1.681508	5.596107
22.86641	3.046597	36.31015	7.319308	10.0619	19.38769
95.90208	95.35665	83.43168	9.546144	2.02928	2.869882
37.22786	43.89611	70.74846	13.85674	10.61938	14.57357
77.30151	24.5812	10.63484	32.15977	8.125311	26.3949
72.1345	79.94624	86.03101	40.25187	5.61715	2.111218
7.025561	32.186	8.435562	11.92016	56.51503	35.47252
88.85994	83.84033	14.26869	67.32122	68.29627	6.418625
85.23186	92.83612	64.62894	67.99751	23.24224	2.047486
3.965975	0.858025	1.941306	20.35242	10.21048	53.63311
93.49319	84.68217	85.71582	76.38586	99.68343	71.41821
51.46133	82.1064	74.25932	55.19109	8.667663	1.058381
0.519836	1.935477	1.25	2.360386	35.00088	10.03878
18.63391	76.74039	44.68297	96.78543	99.76196	98.67747
56.53222	52.1514	88.70498	57.6983	12.11108	41.33482
0.626813	3.278189	2.361691	0.463305	3.524609	12.45165
3.293169	47.63838	31.95781	98.4487	99.39785	99.66668
95.45529	92.78249	83.96262	59.8763	15.49273	11.70359
2.332754	1.685986	1.690959	1.233341	0.629838	1.496852
14.10522	26.85443	57.41151	81.09554	88.00027	94.90891
96.52905	90.3997	98.52966	97.41817	92.15502	20.76338
7.133226	2.044212	1.443823	3.716696	1.442076	0.765694
1.1735	4.811207	36.69095	32.8251	47.63476	13.4257
97.83405	94.27076	81.21608	96.46861	98.6836	86.18307
16.11718	10.32355	1.159615	1.518333	8.28562	0.571055
0.586486	2.945629	9.585704	32.16325	56.13891	79.9166
77.54682	76.21281	64.45224	96.7039	49.57629	60.60787
14.61578	21.67425	16.37529	1.611978	1.356763	4.10619
1.736769	1.95335	22.59915	38.66847	12.09266	49.80742
83.71668	47.7105	80.42776	71.86013	29.0018	55.18283
47.19087	14.01797	79.16532	14.30494	3.827525	0.565738
0.427408	0.588238	2.751706	37.51086	13.23016	62.09391
45.65738	75.35551	5.102606	4.184649	14.08916	26.31837
67.29379	67.14861	20.32947	35.2134	6.156615	12.16757
52.28463	1.467473	0.505222	35.41588	24.37328	44.11934
41.31055	8.813005	6.386604	11.04541	3.211234	8.886321
15.73555	65.49242	46.95123	28.28968	7.299918	8.604923
2.460764	1.387149	0.936265	19.61201	61.79638	50.57746
59.4996	12.82726	36.12085	5.188681	6.848209	5.970105
9.513953	20.72779	29.87913	58.48587	87.51873	9.718629
14.89063	3.151258	11.34935	14.02785	44.46006	77.07899
89.86881	41.8918	17.52476	22.09836	2.687955	10.66933
39.67583	15.57586	25.70301	52.64244	92.38745	45.29059
8.122898	2.498492	1.947525	12.84787	31.40234	27.44568
91.12489	19.74445	22.65056	55.21372	81.69058	13.93985
6.965896	33.28028	47.37268	56.85413	71.84657	99.51671
5.451575	7.028004	4.026994	7.019287	6.914902	6.824047
81.01361	51.1696	38.81602	96.54149	52.60875	32.14193
4.077585	15.02689	21.449	59.4985	89.57648	98.5957
99.27753	3.724089	3.901791	3.088802	1.994775	1.703288
12.43114	83.3234	86.2468	79.00762	85.97595	50.63654
15.55561	26.60168	14.8116	43.914	95.2147	88.29945
97.89285	99.33653	12.89223	0.832785	2.527621	0.654654
5.770933	73.61494	98.01172	98.36282	98.7468	95.19344
16.69744	10.58859	28.1036	20.3952	76.43407	97.37916
98.6761	92.3932	92.10432	5.247543	0.541066	3.624791
3.582399	1.05793	46.24726	98.73884	98.77272	96.99738
67.39645	39.15255	8.092729	8.527741	12.50918	82.95164
83.36697	89.6097	83.11703	53.82673	1.409396	1.587698
2.093312	2.09256	1.23304	36.83435	76.44446	89.94913
99.09802	63.94874	86.86063	18.06866	56.79721	84.81545
84.05683	97.94065	88.77077	64.30282	48.66425	1.259175

0.991026	4.04766	0.533395	4.634352	18.76783	17.50113
62.28092	83.14995	96.95317	40.17908	62.30114	54.20109
84.73055	96.0727	97.14669	65.01746	5.840634	17.66058
3.128708	0.383784	1.269913	2.311463	3.778	4.070924
12.12288	59.68552	86.12872	85.90669	94.85648	51.48847
48.04354	83.37925	85.13517	44.0772	11.09461	26.9956
5.766642	1.061388	0.462092	0.707824	0.433756	0.736846
4.665541	7.598047	25.12124	26.94052	43.68245	94.07408
93.61922	14.78264	21.67195	62.75481	7.340776	6.157565
15.98873	4.442526	0.517254	0.225383	0.271271	0.423796
1.008486	3.099431	8.812071	37.88096	17.55788	29.44706
39.39399	66.04577	7.350942	4.251107	11.02945	3.303893
1.202422	10.01516	20.89864	0.310119	0.147798	0.200185
0.283927	1.415106	5.643961	1.129694	6.392151	40.15568
17.73565	22.86478	76.1516	2.202997	10.1396	3.774244
2.860652	2.340852	22.75045	55.25085	404.9319	471.8892
478.1685	456.7599	197.6997	18.40997	16.8061	2.679224
1.19538	2.284389	0.544155	1.771871	1.61301	3.989266
3.769181	2.929814	21.72201	36.61424	29.67461	449.1134
429.5809	458.676	473.0096	412.088	210.3192	56.78897
24.03638	1.61668	0.500898	1.34472	0.319569	0.499473
1.254949	2.072879	10.59732	17.36625	38.50853	43.66968
338.0469	308.7913	446.2518	448.6328	455.2616	475.8127
439.8656	353.1328	39.54695	1.845793	0.506041	0.573642
0.808545	0.22884	0.675464	2.742654	17.37309	13.4887
41.72516	461.5173	376.3553	456.558	397.5411	232.0401
441.5755	333.2192	459.3492	112.6761	27.51661	6.59101
1.762175	2.242183	1.199323	1.705038	3.665211	14.63602
17.72573	61.49375	480.4852	447.8989	394.1704	408.9696
452.3744	352.1146	270.5927	406.771	389.9106	153.2343
36.06575	2.524068	0.822387	1.665831	3.152485	1.217814
8.125292	7.273091	72.10062	490.3577	481.8435	494.8915
461.5896	479.4585	482.1298	479.3624	281.909	363.2696
315.2514	44.63875	7.432792	2.436868	0.879622	3.186765
10.13487	2.395505	12.83539	42.10455	495.804	493.9091
493.4896	492.9785	486.5573	483.6821	491.7224	454.5943
393.9354	300.7814	178.694	141.8646	11.13425	5.635663
5.105579	6.342566	15.32848	8.733091	11.45241	433.2474
493.376	495.2905	497.7806	494.879	486.0926	417.7236
452.2442	421.8208	451.4088	346.0374	419.9939	267.041
13.16976	6.168762	7.042146	9.650971	20.16527	26.91498
451.6646	438.2622	490.4717	497.8987	498.4011	496.5031
465.226	239.7933	283.7534	394.5799	371.6268	399.1416
90.62437	31.35025	33.64682	23.85371	7.387968	35.96806
88.14507	352.6347	427.8554	405.9186	479.3326	488.0182
497.3109	498.1579	495.075	477.0161	317.4944	238.2989
280.5085	360.5936	25.45921	25.53295	22.39608	28.34007
96.7529	37.50343	213.2009	409.9397	428.6778	340.1167
476.713	478.5695	492.3546	492.7901	493.8545	473.2962
478.4053	403.6194	361.6971	374.9445	134.2845	32.21885
13.80384	14.84281	47.21478	318.0497	119.1909	268.1446
431.2509	312.1145	94.09618	378.6544	460.8982	488.6366
494.9781	491.6783	487.4948	484.285	370.0514	257.5746
432.7868	351.7451	97.80408	22.79812	390.3202	280.2528
367.5818	312.2389	333.4172	463.1312	430.6337	385.4056
292.461	448.8446	422.1599	461.8936	467.1765	479.7556
396.2662	387.5359	486.7007	459.1991	87.50764	480.8039
401.8935	473.2166	202.7856	279.475	316.5775	434.8215
72.2873	27.29147	60.33426	368.8782	208.3977	458.9337
300.2292	414.4613	408.53	483.4928	494.7263	482.0455
383.4723	462.282	461.5386	396.5354	172.2789	397.6537
411.0399	322.3629	216.1539	20.72975	143.3115	386.0753
348.1024	156.2126	215.6026	371.643	387.3495	479.8439
470.4831	259.2502	463.1109	482.3386	431.9704	372.6748
343.8056	278.9279	358.6716	313.6707	426.9136	218.1835
47.93724	73.78345	105.2209	282.501	339.6167	361.3683

```
416.4894   472.3686   122.6755   341.9188   464.9358   457.2882
432.1992   427.4477   371.1197   91.78527   169.8244   380.3383
438.1199   267.2945   91.84362   170.43     191.0729   189.6413
203.4094   49.89327   133.2883   18.12137   387.3727   352.6858
360.8527   428.8101   470.5123   481.3589   473.9156   411.6148
310.3416   223.2518   393.4676   132.1749   21.41657   121.2506
357.3831   334.2789   198.9716   83.0061    18.12972   10.87219
92.36193   235.156    127.1774   147.1364   452.1734   440.3074
473.2875   477.0677   371.7475   354.5831   314.7205   297.5329
24.44601   363.4327   257.6588   70.01369   228.412    15.98188
9.999171   6.532539   19.85354   21.55247   78.53278   433.0201
410.6823   427.7805   356.5989   368.5318   398.6484   401.3396
391.2173   484.3229   60.76689   114.0725   37.73732   52.00906
30.78988   8.697912   6.391665   13.51431   5.66688    3.540022
81.70733   265.0971   402.9137   465.7512   475.5049   481.0775
468.3354   437.3066   451.4524   460.7157   287.3155   48.33781
27.11559   16.84783   83.27469   21.44939   11.88324   9.255843
38.92324   27.76905   74.84521   384.5262   305.9384   328.3568
458.846    479.1351   493.9966   482.9198   477.571    386.8094
210.8779   57.89819   15.03118   4.849322   21.76497   17.20731
4.648812   6.970951   22.69306   10.70883   31.8019    20.95024
182.7036   288.9156   484.2604   491.7507   493.8613   484.9846
474.1928   399.8425   249.5485   249.2516   54.25578   11.28275
8.270923   43.31667   10.49124   27.43317   20.23811   15.26416
117.2584   46.77351   141.3328   358.8897   479.3073   485.2751
490.8322   488.3104   490.3712   485.7111   82.72904   108.9429
29.39436   13.61426   5.872865   11.86615   3.188666   34.62079
90.78645   76.26548   131.8354   45.03633   43.67119   401.1142
465.0236   485.9203   457.7106   461.4089   494.1616   41.96527
64.7314    138.1857   112.6178   27.31593   3.670414   16.52456
93.72404   86.29646   264.0584   132.1691   166.2371   152.5123
114.5484   75.80223   333.0504   450.101    475.2148   476.0691
189.7593   60.27067   129.0093   236.6394   222.3151   188.4413
19.03084   21.50909   44.80928   49.11532   298.1714   255.6313
94.46197   253.2731   207.3495   171.2482   55.55536   435.9554
431.4495   26.15929   61.38511   21.93461   43.11179   137.2221
41.26549   27.5499    18.42875   18.99954   27.43829   51.33281
277.8849   297.2419   320.2845   327.1561   209.8172   81.39205
56.92211   415.9336
**$ Property: Pinchout Array  Max: 1  Min: 1
**$  0 = pinched block, 1 = active block
PINCHOUTARRAY CON          1

*PERMJ *ALL
605.6267   790.7515   972.2367   944.5153   651.7725   662.43
22.69415   11.52076   8.613487   23.22373   48.96785   216.6512
996.8964   973.4485   833.9884   73.98965   80.77296   9.140143
2.92715    978.3945   767.9218   762.0544   996.7816   869.2586
711.0645   21.55778   5.189757   8.976334   3.483453   28.34458
546.5099   947.9338   931.4832   807.4246   63.68161   48.9595
24.20511   19.08987   990.0703   995.0479   958.4005   985.0902
986.5861   636.5243   127.5408   4.520547   9.452942   15.41477
7.016265   96.03532   883.086    985.6234   920.8842   814.9332
180.3882   16.89635   32.51839   961.2758   973.5135   987.8978
758.4361   882.7241   917.3329   285.7788   27.12339   2.74532
8.051708   10.23222   41.05027   497.9824   958.1511   937.9312
977.226    174.3464   40.08437   35.54528   927.921    996.6094
996.7265   927.7501   948.5495   950.0884   885.1013   61.7692
12.21485   17.74651   11.4296    31.79692   868.9544   573.5483
781.9086   991.7541   441.2462   34.59465   266.6539   749.9426
998.7527   997.5967   991.8797   975.1468   870.1558   963.2677
479.3514   38.87291   19.90458   25.69964   9.901409   156.0364
228.2123   681.3794   667.2169   775.0541   64.74706   209.1944
107.9295   922.8668   997.9321   982.6481   997.5439   807.7947
961.1828   511.312    743.2279   48.80968   2.978784   15.94278
32.68466   56.01521   637.485    828.3578   726.7549   87.18364
```

207.4512	29.83438	321.6637	985.7982	999.038	984.5891
994.4364	796.7352	370.1332	529.1636	55.53541	22.22824
4.785067	68.84399	20.5689	596.9075	429.0066	889.9795
832.5743	123.2688	96.88667	243.0592	895.5359	912.0969
986.2386	992.5834	996.5223	732.7823	337.0381	233.8541
98.37189	14.31901	7.689233	87.79969	258.4503	228.7937
861.7812	899.7275	712.9203	6.923457	50.13858	939.3772
550.5845	651.2474	922.0129	980.2029	944.1435	742.3505
591.3519	106.8641	26.96727	27.70027	5.000725	159.3496
473.3147	849.4523	566.7559	585.0527	35.5746	41.65604
610.0016	805.653	890.9596	886.7884	990.978	992.3914
787.5643	197.9046	641.929	108.9309	27.67146	7.460312
65.29712	904.3989	843.3755	953.4106	881.2314	11.82413
22.59571	26.6219	897.2325	298.2854	824.6734	993.3997
940.7192	610.7296	71.35756	245.5749	175.277	27.67521
14.78479	30.90295	153.8325	414.998	403.4753	600.0245
3.256207	20.81824	27.36598	770.6177	956.3261	717.5183
729.8372	951.5136	809.9403	611.1179	105.0159	723.7191
64.05175	18.96365	24.32484	238.4097	395.4895	170.8976
667.8701	4.647367	12.17649	18.65087	307.1899	455.5646
807.4562	428.8476	696.6602	973.3589	984.707	97.89939
213.011	269.4095	12.22892	30.2039	77.16458	967.5446
283.284	605.2712	1.328563	4.977715	6.037192	15.47437
340.5336	322.3636	467.0152	970.9167	319.2567	955.8021
253.7056	46.87961	234.7691	27.58989	13.24769	20.43878
276.7076	883.4216	904.9404	5.314018	6.083689	15.9208
3.934776	53.68179	48.77789	334.4067	554.7598	962.3765
939.9765	906.3835	294.7535	738.7543	84.52302	14.88329
17.04241	36.54946	842.5991	809.9421	14.82928	4.417749
7.81707	14.79606	24.95319	144.0038	39.55497	85.81358
666.816	486.6895	942.4233	910.6364	830.6824	497.6591
114.6318	16.07489	137.2341	132.6163	584.0378	63.64012
7.160148	2.783787	7.524004	1.488134	55.44227	60.34649
104.3484	120.5	408.5122	313.5884	983.5762	606.2364
452.4692	481.1317	29.5582	28.37749	286.1554	104.8429
59.27697	12.04315	6.544824	4.937146	2.204697	5.863609
4.825163	78.14478	57.52412	22.35486	441.9051	685.0464
949.3689	991.9459	921.2659	136.0993	18.92731	113.6967
166.6729	27.87494	2.084376	11.743	12.53407	12.67445
4.869036	2.756525	27.04992	32.25841	20.02419	61.90718
640.879	915.4971	984.2422	845.3489	912.3154	53.48771
113.0311	560.2128	12.15055	4.81615	3.935111	30.51919
18.09535	36.68234	2.185929	11.65617	16.63206	26.73794
33.14912	178.539	745.7942	840.9865	997.7483	981.9356
469.3221	205.0369	230.0928	12.91282	3.796601	2.194386
9.047842	11.53878	18.88265	6.199819	10.6586	13.24119
25.11886	24.54607	15.46454	914.3448	887.2357	895.5607
925.007	709.617	492.0713	302.0112	3.438436	5.078752
1.740171	4.68699	9.188466	36.405	16.68196	10.02561
1.912908	18.30189	9.906472	11.36952	185.2303	959.3697
986.2114	876.5183	677.0613	853.8351	524.0914	8.492137
4.747041	5.231509	4.234723	20.1984	83.13942	298.3706
19.18028	19.91297	10.76225	37.15352	12.11541	20.63227
952.8378	983.3181	311.9098	906.8115	292.5735	179.8465
39.75566	3.527232	1.575339	0.776408	21.59037	35.66638
92.89343	55.94973	12.5912	5.581308	16.3771	32.59357
125.0861	863.2827	927.0731	972.7674	91.40143	513.7952
157.1904	54.46769	6.717876	9.164062	3.46883	4.050839
42.11056	578.8646	549.5864	52.75662	18.46537	25.44023
9.284125	116.1796	937.5512	980.9006	822.7881	543.9425
840.429	693.8235	134.0069	68.58861	26.77978	11.64324
2.960943	11.12674	11.82437	770.4669	211.6669	34.59027
4.463782	16.36259	67.54482	442.9768	970.9011	973.7714
376.1985	910.6573	948.8772	609.5944	734.9114	73.8955
21.28786	17.79295	0.937294	12.77556	123.8879	166.099
95.81026	6.982244	14.02917	3.835279	78.6256	725.364

892.8469	621.4139	788.3517	712.9351	16.24464	42.12501
58.39195	12.86563	27.07622	71.88016	25.14792	13.16525
35.54504	11.25341	19.03439	39.24172	30.96335	10.70355
36.724	85.26485	52.96403	78.73249	25.06513	8.892011
71.14887	73.23505	16.65843	22.24155	18.18427	11.16925
18.39624	16.21791	10.72235	12.52769	9.690697	14.87123
16.99515	11.69906	23.93343	45.2884	43.08291	90.28363
34.81104	62.42751	34.04176	26.70023	3.905575	2.095174
2.787199	12.64792	12.47266	29.77536	71.22919	34.39838
17.40344	12.57072	28.2226	7.156159	25.02004	34.91805
13.44238	150.4032	108.4911	37.97205	6.517845	3.186787
5.061043	2.774502	62.43427	45.41988	103.188	160.639
157.8636	81.9802	20.55479	62.28737	29.35175	9.18817
2.58339	4.531646	170.4323	146.2366	61.77361	11.71041
18.8381	55.53771	70.47986	172.945	172.5703	181.6599
169.1438	83.83744	69.48931	24.37137	26.53371	25.32847
6.252087	5.56022	1.872152	157.2288	120.7589	115.1134
9.248621	18.06471	22.0209	140.4895	165.969	192.804
191.8412	197.2373	195.5699	154.9402	164.2446	131.0488
14.65507	14.28904	5.225947	2.848446	23.69933	62.77027
40.84181	26.30928	62.6647	52.12679	187.6364	161.4485
183.7858	177.6209	191.4631	198.1062	185.1979	189.9092
72.32676	23.90667	21.50349	3.548747	3.256994	126.9404
89.53709	51.68541	23.26752	24.5795	83.39864	172.0731
138.6401	178.0127	193.3521	171.3693	121.39	120.7425
108.3338	19.99922	25.88398	2.999984	4.150716	1.136203
171.2549	46.5225	125.7766	124.5028	39.4332	46.7928
180.692	176.6225	138.1698	184.1815	129.7424	95.38081
46.16204	183.6805	43.33602	10.10295	4.939079	4.239777
1.499008	62.25439	98.12982	33.7602	60.61373	53.72482
130.8679	69.16812	39.075	53.0596	160.2921	17.67018
4.300114	32.24876	35.62083	15.06486	47.59135	3.981283
6.563886	3.657573	33.59774	41.25162	18.92322	43.57426
19.06993	12.09066	100.6211	16.97407	22.93285	104.9388
31.5393	28.91778	31.81772	22.50448	29.80389	4.541183
16.36816	1.097511	2.218906	13.33654	10.8188	11.20885
7.9144	10.51465	1.351459	1.470229	3.109517	3.89775
4.17994	10.25716	12.919	73.69907	155.2634	72.77798
57.67638	18.58104	5.380678	4.435566	2.085778	6.709189
6.984527	7.908024	8.149651	2.839586	1.363343	2.450564
9.220448	7.750237	5.725705	7.218667	23.46	127.3606
72.65391	25.1886	14.95778	18.98834	3.59433	6.216973
2.006111	5.261372	29.59232	3.241642	5.819357	5.545223
2.565648	14.91829	5.722239	6.724934	5.155811	3.496206
44.12614	42.41818	71.42644	9.059245	10.26403	18.89252
12.37958	16.95708	4.782754	11.4242	4.228049	2.966019
7.31001	3.612302	10.63078	36.21071	3.238762	0.507259
0.710461	5.807203	42.15907	22.01157	56.07458	12.79614
16.14634	31.17138	95.16034	7.07861	20.8535	16.83658
9.170774	6.071905	3.056258	8.466814	18.4468	2.979202
1.840683	0.784856	1.810615	8.925057	3.474249	14.8071
11.23531	16.59728	14.05035	38.23402	8.562232	5.090753
27.13651	11.30334	4.869193	2.486652	13.122	33.65333
5.65136	5.127752	5.392523	17.75833	4.119979	6.103276
4.058215	7.565977	4.436291	14.96315	10.67763	5.336838
16.32841	12.68981	50.03305	28.72301	30.91527	15.36909
12.39978	11.87173	7.206361	8.223108	16.57609	1.917317
8.678667	8.420211	6.429438	15.35161	11.49646	11.44242
5.015347	3.505702	13.71387	35.54627	67.41492	38.14433
8.528173	4.566937	1.646698	3.895704	5.046369	2.066955
14.44907	5.248776	2.232323	5.736077	25.42963	7.887657
2.689459	2.263117	3.962771	37.68617	37.70014	16.34798
22.95858	18.02034	8.470733	2.534206	3.22118	2.45294
19.98596	14.35833	9.531516	6.675933	12.24938	61.1505
5.77931	5.653208	3.942321	12.1432	21.37509	32.53389
39.86089	143.0899	19.58322	16.83445	1.967343	3.035988

9.148713	20.88378	101.5956	46.48288	18.91873	12.0578
17.88451	21.99455	118.8645	77.31362	11.06894	52.42302
114.2097	148.9073	97.29556	25.62477	13.86756	10.63891
17.79381	5.712247	20.5815	96.38512	18.83467	55.20774
15.98873	12.52608	17.04814	46.75144	23.94181	9.22854
17.54272	160.2932	146.069	169.6153	26.73216	20.10379
21.80033	18.47481	9.165328	7.452603	17.49565	10.76646
11.57148	6.933476	6.272707	48.12048	3.189914	16.22135
20.08505	71.84706	48.42749	147.3798	92.18665	60.28663
29.09176	31.76874	17.49657	4.403622	12.41538	25.95165
48.06976	17.14537	3.318968	7.588746	11.60713	5.942607
3.257054	2.424761	5.488643	5.464985	67.2766	31.68466
47.46965	13.69298	22.27148	77.00856	62.06532	38.66215
26.03772	41.8043	22.44089	14.21105	61.94225	20.54618
6.165623	1.972246	2.224221	0.509311	3.717141	6.147761
24.36273	58.2425	24.54409	70.00193	26.81112	52.62438
113.5939	55.11959	93.27602	50.71799	96.4353	23.6906
24.82561	10.74942	2.206119	4.277549	11.3067	30.23305
30.51357	20.18278	37.98761	31.78974	125.238	170.5548
36.2404	63.55109	16.65839	36.96477	22.29975	7.63108
15.58411	36.86014	3.462757	3.71786	49.12697	12.70726
146.2928	161.9269	23.1264	19.27538	5.512315	69.14647
33.32077	28.45424	92.74276	35.44688	7.14995	8.25517
33.30773	31.16442	754.1435	594.6262	891.4623	239.7778
462.0692	109.6632	203.685	784.7313	949.0891	963.8912
885.2766	991.9688	960.2206	838.8668	845.9701	940.2969
458.4004	268.8258	426.9972	319.7607	696.819	901.3262
683.002	157.4077	126.7328	36.08685	137.3843	719.4904
871.8785	821.673	778.0814	995.8777	991.9916	577.4987
875.1228	835.0491	180.6746	338.5096	60.129	87.11762
265.4208	964.906	483.061	130.3392	56.92722	127.7833
621.8534	966.6227	954.2035	951.6473	969.2259	988.7876
981.5626	758.5706	842.4012	751.2872	290.4404	517.9454
120.108	34.5714	254.5025	845.8104	451.2093	122.6097
126.7739	643.3732	856.8445	962.3011	915.7037	855.5984
981.0519	948.1477	859.7952	881.0895	419.4421	660.1248
116.7855	271.1484	91.34441	109.8841	231.6253	775.7611
739.9664	357.6803	88.84582	377.1447	750.7442	951.9102
938.0651	899.4251	978.3405	852.2951	810.3134	444.9139
17.85196	140.7055	205.4878	243.2809	88.43293	75.57358
86.15788	569.7706	657.7654	447.7556	48.34516	411.9732
739.5065	834.4839	552.0787	682.6687	968.0594	866.3054
263.6331	477.0754	160.2983	67.71845	271.1808	229.6503
247.1582	154.235	128.5124	529.4379	349.8775	572.5455
88.18485	85.72885	350.8335	427.8672	610.0704	427.1663
873.0337	725.6547	120.9893	57.5379	114.7329	119.8439
254.3197	328.888	299.4077	126.9431	178.4584	532.7776
160.9374	247.4121	89.34536	101.4047	208.7426	105.7747
328.9289	799.4071	840.5644	802.6921	35.75699	103.2569
98.79319	142.7743	746.5983	381.3405	168.2031	86.56812
146.1161	417.364	266.63	242.0656	206.5461	181.0944
36.55577	220.8051	110.5684	304.8028	729.9095	55.38511
99.31458	239.9247	74.39796	197.6496	727.3325	483.818
217.1321	256.7273	363.3624	337.5849	547.5869	127.1818
181.7929	88.42213	200.2673	451.5876	220.3307	333.4433
848.26	108.7264	68.5534	116.4145	103.9303	393.812
708.1496	582.4545	176.5989	384.3908	262.527	209.0056
302.6635	45.31782	52.71692	56.18637	717.6423	300.841
237.9984	385.8789	576.059	72.15111	19.74099	45.47189
176.1039	304.8639	368.1629	593.525	220.9938	377.3975
173.8357	221.8033	163.3676	46.77351	84.29446	70.57518
216.4108	72.96171	4.134034	73.28279	225.1143	63.31374
27.95883	31.78725	94.59823	78.00204	265.9714	454.8456
116.0462	211.7859	237.3215	118.1814	42.24273	19.7369
40.80863	253.7535	327.6755	37.50516	28.95176	51.58851
80.23355	43.66827	46.42875	86.58188	65.92877	41.84292

110.7077	142.678	171.6714	310.5997	232.8145	51.21215
113.1684	57.97303	50.27221	391.9485	78.75842	49.16375
23.74504	66.77779	65.41118	119.0351	24.59348	68.68391
135.4213	222.5471	106.3994	340.8725	566.478	472.6776
97.40898	130.8796	105.5745	61.61536	94.87221	623.3055
247.7433	87.32327	25.35695	13.75365	105.3584	64.00074
45.55311	196.3374	65.26871	220.8391	95.82261	484.3909
796.97	889.0067	675.3937	667.2629	67.60114	62.87326
863.6843	624.3124	116.6442	76.48213	37.2108	14.58754
30.19076	68.47531	67.6083	151.5629	188.0338	206.0137
160.8126	581.8754	334.5022	335.3675	306.0187	901.9158
87.69887	854.7281	887.4318	764.559	46.04378	72.8687
42.65118	21.20699	37.30714	26.13551	138.5884	136.7688
104.3528	208.8503	108.7319	554.0284	135.7929	633.7136
826.1026	754.9393	917.5421	943.6957	841.6335	566.7989
71.90068	129.3615	98.73202	5.947056	23.0646	35.99565
91.54993	139.6912	160.6934	127.0428	358.5932	749.6473
186.8551	233.0671	666.2896	868.6464	891.8298	966.3334
944.3413	351.0751	158.9366	119.7769	19.99056	8.100895
23.97143	18.69334	125.7625	193.6801	400.8824	416.4367
879.5692	724.5928	133.6857	273.0593	719.5716	958.4953
984.4644	987.5748	924.8941	316.3115	363.2235	310.4674
35.3999	7.379246	93.61383	30.69241	86.0314	146.4108
658.878	274.1593	331.6477	947.9229	429.5542	337.4155
774.1926	990.3347	988.0479	930.6106	460.8133	446.5869
457.3851	572.5376	44.66836	17.15703	21.97465	36.63161
186.7244	137.8145	222.8994	239.8833	356.0918	633.257
210.1905	566.4205	867.7248	992.8577	997.6381	957.3506
845.8026	285.6538	707.527	397.4166	70.49462	58.04396
42.20443	95.26031	231.8414	163.8925	238.244	47.57535
228.1172	110.3431	103.0258	320.9963	845.6273	998.8057
998.4883	989.8469	784.7657	378.9082	960.3311	684.4741
83.59898	185.0223	178.2966	251.595	166.1629	123.5378
123.9615	43.1092	8.217013	20.80497	127.2457	296.2027
861.1107	995.316	999.1116	985.088	928.6649	879.5226
856.7932	402.552	57.23082	141.8042	160.7334	98.54849
135.8316	93.0782	365.946	33.47973	14.64408	59.95412
104.6625	675.2491	985.1514	998.6217	998.7344	933.1812
993.1892	954.7463	991.2358	325.0686	39.1612	110.9257
360.8436	566.1937	131.3119	105.1182	3.472826	46.05969
32.22976	115.7697	250.9499	926.5567	997.0134	978.3157
999.0334	998.0057	990.6472	983.8729	982.6436	418.9518
191.2115	106.2383	369.5907	520.2463	147.9923	2.615345
3.081534	22.6295	32.77714	164.0945	267.5703	961.3024
983.1007	978.0139	987.2656	999.0173	993.9122	992.9811
944.6436	364.403	94.58298	129.2978	599.3424	246.3667
57.59344	9.157375	157.3483	126.311	23.49492	18.36648
10.47307	122.6013	23.66007	6.443399	11.74381	3.63385
1.415533	2.20026	0.987918	3.097904	5.358361	106.5433
59.47329	20.96549	3.895077	16.39933	24.7926	19.47032
89.14685	107.9021	8.564421	22.98444	13.27715	25.70212
3.900767	2.427828	3.524812	0.847555	2.007747	5.690114
60.5981	27.61239	2.936169	3.266066	89.29806	24.42334
467.8719	335.1359	62.61653	50.71145	11.93249	12.30257
11.76224	37.49747	94.96838	1.792702	5.936234	8.191605
17.48868	59.83592	29.65227	3.342997	36.06575	484.0642
468.3268	474.8222	359.8322	313.3805	49.50636	40.85733
29.72802	159.9591	146.7135	54.55505	46.41443	40.71158
35.68552	29.75631	69.0146	15.56231	10.75241	401.3692
485.6373	495.8987	145.5506	173.8593	11.7695	20.24576
391.1254	151.4726	289.661	398.1714	218.4369	61.37747
435.4818	45.06216	114.8188	105.514	29.41575	132.4043
482.0466	498.3231	384.9178	75.23882	7.759719	4.496007
124.9051	298.7955	174.6807	154.3484	443.0207	276.5037
483.2201	493.7067	419.5348	134.869	312.6266	29.1411
368.2655	497.2926	264.2086	48.85016	56.99923	0.544275

6.694374	10.60367	33.92244	156.6098	88.95636	300.8528
488.3453	212.7189	498.8523	498.672	497.1232	203.3036
177.8918	478.3657	138.5122	138.4016	30.81158	4.984769
1.182331	10.65244	2.275931	36.13516	32.76649	15.47826
369.7873	487.9261	491.9772	498.7765	498.4941	490.43
85.88039	62.22444	164.6255	59.93217	83.28427	35.88277
3.006422	9.696567	2.439389	11.90014	24.05215	18.41145
15.99381	400.2635	494.3949	491.4553	498.8672	496.8989
492.5542	343.8959	33.75103	207.0647	406.0869	48.63714
5.46008	3.307737	0.808643	2.202161	2.80411	18.49132
30.64771	47.36778	172.5437	450.989	457.6147	488.1294
388.415	272.5198	457.2977	67.79848	301.9882	79.89618
39.7857	5.510538	13.47811	9.24215	1.710504	3.589864
3.518795	22.52911	79.09918	213.5492	261.1367	39.87953
467.7793	143.8153	212.8139	372.7632	415.1012	153.8112
17.00161	15.82804	5.42769	2.793045	1.5072	3.839282
0.897191	9.159442	110.3123	106.0506	241.5288	281.597
32.86548	418.2029	36.31332	198.6081	79.59357	93.64336
61.59862	92.60278	9.34039	5.576863	2.641721	3.010981
2.891166	6.729395	106.0264	161.3162	133.0798	207.9012
115.4099	64.48222	39.10686	76.21948	87.112	32.70876
49.91591	21.49275	34.40377	8.868047	23.59837	0.518443
0.736782	4.565486	24.19937	267.9026	159.2099	245.8584
61.04274	288.5061	18.9044	6.609902	13.17489	38.61153
40.55935	46.51671	34.0405	40.4684	17.70557	6.403332
7.842942	1.419796	24.74241	221.4869	435.4667	77.87679
30.61526	24.63576	12.79104	11.80535	6.630206	62.44304
35.57173	27.21692	50.65508	54.10694	13.44513	15.60357
16.22079	1.831041	28.79844	44.69984	275.5859	133.3365
288.0753	59.80342	60.77878	35.1329	57.77102	26.03353
40.12075	52.5262	33.40673	77.87571	42.13898	64.39112
37.60313	8.530981	10.20495	88.30291	78.95652	138.5294
441.3092	174.9653	77.42354	21.46293	22.66715	126.347
68.93615	22.79807	37.18177	20.75726	68.85825	71.17213
26.81649	16.03061	5.985081	36.63178	203.3462	33.33696
385.2627	45.17176	235.3781	384.0811	28.29509	43.71868
15.59111	53.41165	31.97452	124.2136	43.15081	466.2018
76.39624	38.92665	17.77813	4.269372	79.08206	25.01347
212.6919	256.8077	176.5294	420.0132	205.9596	35.90459
9.059892	91.60749	28.69789	18.33868	103.4304	455.6192
493.1659	85.91955	44.40879	24.66573	5.623595	22.30103
21.62335	362.621	491.4971	275.6811	304.3365	105.103
18.72294	17.33381	17.23769	17.79459	87.19629	254.2436
498.6743	496.5854	34.62597	8.307819	6.135162	16.93718
11.89701	199.8987	489.8251	483.8937	481.1184	129.9377
27.67356	19.56451	54.6637	93.30588	149.4425	266.4545
498.33	496.765	463.9263	21.4041	47.84031	19.71446
7.243325	18.23278	124.9505	445.3372	484.5705	487.6093
265.4605	98.72633	32.1298	49.75835	30.75311	122.0442
287.0774	497.8093	468.6785	124.5782	49.64643	12.02541
5.385896	9.317684	15.11113	16.04697	240.5127	347.7955
487.3848	64.06163	214.2945	92.18792	224.6187	409.5265
223.6192	492.0237	481.0077	491.6341	105.3033	9.304114
5.860626	6.809559	2.520032	11.81082	56.40752	32.38441
69.26455	46.90844	196.3672	152.7566	209.6583	97.77797
431.6115	457.4314	493.1182	411.0163	95.55249	46.85878
9.570596	10.0698	2.561439	15.03038	10.51081	13.11677
39.61238	38.93068	201.7446	66.89151	287.2678	468.1812
140.2165	438.0544	270.2384	254.6238	45.20297	192.8719
48.99796	6.118655	1.555941	0.717188	2.211923	1.129593
16.50133	137.7381	45.37357	95.55623	35.70705	172.3765
378.4321	106.9456	76.39272	425.8631	31.53211	26.54716
84.63754	31.31785	2.741101	1.488483	2.214716	0.4967
3.521948	12.27391	27.86699	42.89059	12.95588	13.00418
52.04033	188.3849	23.72652	30.99538	73.14017	22.42018
4.604972	86.15927	64.11063	2.607264	0.523902	2.022335

0.845526	4.99197	14.41883	15.1444	9.100055	20.23485
10.65114	14.72902	34.10484	18.68082	76.21352	114.9593
16.45341	5.610854	191.7869	412.8298	992.7091	995.6415
994.0358	933.6949	194.1909	55.10221	58.54476	20.84813
20.39591	10.65666	17.30394	12.74134	16.466	20.42359
114.4672	263.6046	579.1659	731.9426	152.1483	960.7447
970.4809	986.2999	995.3825	962.0995	260.8303	139.0337
41.4976	6.111629	8.955256	8.804405	3.827771	10.39382
15.51869	49.71518	88.54071	210.1798	358.6171	204.5145
812.911	933.1254	995.3137	987.6271	974.9852	955.9496
616.2302	670.8911	255.2378	10.42147	18.48507	9.669989
3.981998	6.531561	14.27266	49.93568	493.0444	392.6214
626.8303	924.5875	742.6959	913.0215	929.2894	994.1914
990.0247	849.0554	557.7659	676.1048	152.2804	11.88401
10.94662	1.446499	1.104221	12.98548	43.2253	40.80008
367.2823	757.3611	937.2382	720.7672	938.4173	975.8678
946.0106	806.4901	635.7231	936.4897	865.8586	324.5062
125.0086	3.394447	10.06939	0.922435	1.33203	3.636001
35.27354	50.39263	620.4017	994.954	994.1021	985.9298
987.7249	967.068	997.4589	994.8853	973.2603	862.2635
492.2435	191.5107	33.49731	27.9569	10.66162	9.405871
3.954231	13.07365	93.72253	35.55986	972.1359	999.1369
998.7804	997.5117	903.0671	946.0651	969.8956	996.0703
965.0637	566.9608	763.4402	205.1167	4.064293	39.98794
14.07032	13.04172	50.28506	10.3815	76.25845	986.9088
983.6486	997.661	997.9712	993.665	946.4681	408.3175
887.0662	882.9132	925.8465	595.0014	752.1717	299.3857
7.750826	33.42497	28.08109	53.22921	24.39181	12.8982
647.3602	960.7845	989.9335	996.1758	999.1829	995.9648
949.8784	736.9008	900.3347	892.5982	732.4416	458.4258
30.38988	140.7515	35.66654	21.55693	90.81028	288.2511
94.77112	761.0409	947.9622	908.4939	488.6456	945.8407
997.9872	996.0267	998.6999	980.7944	661.0784	686.9799
812.6302	714.4848	333.0842	85.68327	31.53189	141.4298
591.796	292.5459	276.763	843.0106	321.946	365.3642
609.4288	938.467	994.2051	995.1625	995.009	980.0021
942.0262	939.3642	919.3354	723.201	543.8073	88.71806
34.67368	194.6547	290.7335	907.9982	777.4384	707.224
718.0654	570.5609	133.6993	638.0695	695.5815	965.715
997.7277	984.902	954.5991	952.5461	911.1125	768.9445
586.3649	180.8111	181.1286	73.29494	876.6374	920.5004
727.6273	457.795	281.7007	122.108	142.7247	482.4919
313.8434	182.5408	234.1154	955.7031	977.9215	982.3947
725.5762	991.4413	971.3998	566.4049	344.2786	367.1758
787.131	989.7967	923.7256	866.1238	799.1053	384.5546
28.2163	53.22382	95.34941	298.3699	578.0135	349.5103
892.6187	895.0865	962.9617	968.5098	981.4541	942.8769
118.174	262.4853	836.8661	959.0516	990.6472	885.2644
942.1086	841.5792	112.7943	41.36919	46.90455	457.3809
794.0411	590.1359	739.59	864.3408	415.3412	883.0515
950.2744	738.4362	877.1563	796.6343	632.6332	951.334
970.1904	914.0038	946.1979	671.2743	704.1513	18.77842
32.63097	39.29841	870.6087	892.9209	760.0339	583.601
833.3108	920.1826	856.8879	965.6973	974.9807	627.5004
808.3287	426.2045	885.3052	827.5153	316.2278	375.0922
253.9885	157.39	74.79732	258.2224	102.1718	404.8471
279.5503	357.3683	233.6501	717.9761	971.6839	949.3077
967.8409	944.5197	991.6376	983.5739	971.6168	759.6613
917.9034	361.3591	186.3528	166.3489	21.36874	34.94886
84.10503	810.3227	614.1706	290.1904	176.0832	297.7885
599.497	973.9777	637.2209	419.643	961.8581	962.8021
981.7524	775.1915	592.3072	756.9078	408.6354	91.53454
9.052802	43.7365	60.21394	571.5747	696.9346	25.64785
49.16511	80.91351	299.2423	257.4785	90.23624	913.4799
951.1916	915.1557	741.8157	333.5362	695.0227	271.0841
597.7148	538.8898	184.1968	130.0526	22.26871	353.0222

35.45969 18.74843 10.71783 19.43663 131.5007 11.51179
51.24907 608.7458 981.809 785.9393 711.1857 915.0335
845.6974 684.1715 757.792 694.2454 740.7386 242.6281
32.39023 37.71933 33.05164 30.44087 2.111514 10.47109
50.16999 85.16203 165.6136 624.426 869.8232 803.6002
949.6619 865.6693 944.7698 985.4827 922.8859 865.7211
700.4078 82.79498 164.907 52.08132 32.28226 15.47904
10.45064 10.62155 17.68618 17.72687 661.5795 582.704
650.3782 908.5336 950.6573 990.6494 966.5493 990.7521
993.0543 955.5887 864.3726 243.9355 602.0617 206.814
76.86861 33.94111 42.77076 16.67063 8.401194 129.338
199.0889 128.825 814.2261 872.3424 984.7205 994.2006
975.9802 989.6691 973.8655 941.3064 135.8658 339.1252
174.4102 103.7144 201.6694 350.9102 115.8049 85.36208
107.0062 125.2587 115.049 265.2394 157.9465 148.3915
804.8594 989.9608 942.0783 897.0776 995.7699 331.1754
195.3057 113.5288 104.9062 149.6784 117.5563 219.7328
82.51217 235.5055 184.3296 242.7348 739.1524 688.0627
480.9922 169.4849 321.503 648.2612 455.119 796.0916
194.2008 103.8831 281.0302 130.404 161.4132 475.782
167.2623 181.2984 577.4163 320.6882 519.6094 430.3264
911.8156 460.1421 306.4573 103.3513 468.5252 350.6978
609.586 42.99768 141.536 86.81205 200.747 343.3998
366.3692 123.8566 257.5847 119.5099 183.3344 567.2715
812.9559 858.5231 894.8454 599.7952 805.575 388.7281
441.8634 708.4529

*NULL *ALL
14*0 4*1 14*0 6*1 10*0 8*1
10*0 9*1 9*0 10*1 8*0 11*1
7*0 13*1 5*0 14*1 5*0 14*1
4*0 15*1 4*0 15*1 4*0 15*1
3*0 16*1 3*0 16*1 2*0 17*1
0 18*1 0 18*1 0 18*1
0 18*1 0 18*1 0 18*1
0 36*1 0 18*1 0 17*1
3*0 14*1 5*0 12*1 9*0 8*1
22*0 4*1 14*0 6*1 10*0 8*1
10*0 9*1 9*0 10*1 8*0 11*1
7*0 13*1 5*0 14*1 5*0 14*1
4*0 15*1 4*0 15*1 4*0 15*1
3*0 16*1 3*0 16*1 2*0 17*1
0 18*1 0 18*1 0 18*1
0 18*1 0 18*1 0 18*1
0 36*1 0 18*1 0 17*1
3*0 14*1 5*0 12*1 9*0 8*1
78*0 5*1 12*0 7*1 11*0 8*1
10*0 9*1 9*0 10*1 8*0 12*1
6*0 13*1 5*0 14*1 5*0 14*1
4*0 15*1 4*0 15*1 3*0 16*1
3*0 16*1 2*0 17*1 2*0 17*1
2*0 17*1 2*0 17*1 2*0 17*1
2*0 17*1 2*0 16*1 3*0 16*1
3*0 15*1 5*0 12*1 9*0 8*1
95*0 5*1 12*0 7*1 11*0 8*1
10*0 9*1 9*0 10*1 8*0 12*1
6*0 13*1 5*0 14*1 5*0 14*1
4*0 15*1 4*0 15*1 3*0 16*1
3*0 16*1 2*0 17*1 2*0 17*1
2*0 17*1 2*0 17*1 2*0 17*1
2*0 17*1 2*0 16*1 3*0 16*1
3*0 15*1 5*0 12*1 9*0 8*1
95*0 5*1 12*0 7*1 11*0 8*1
10*0 9*1 9*0 10*1 8*0 12*1
6*0 13*1 5*0 14*1 5*0 14*1
4*0 15*1 4*0 15*1 3*0 16*1

```
3*0     16*1    2*0     17*1    2*0     17*1
2*0     17*1    2*0     17*1    2*0     17*1
2*0     17*1    2*0     16*1    3*0     16*1
3*0     15*1    5*0     12*1    9*0     8*1
25*0


*CPOR 4.5E-06
*PRPOR 23500
**C WARNING: UNTRANSLATED ARGUMENTS FOR THIS KEYWORD
*AQUIFER *REGION 14 4 5 *IDIR
**C WARNING: UNTRANSLATED ARGUMENTS FOR THIS KEYWORD
      *REGION 15 4 5 *JDIR
**C WARNING: UNTRANSLATED ARGUMENTS FOR THIS KEYWORD
      *REGION 16 4 5 *JDIR
**C WARNING: UNTRANSLATED ARGUMENTS FOR THIS KEYWORD
      *REGION 17 4 5 *JDIR
**C WARNING: UNTRANSLATED ARGUMENTS FOR THIS KEYWORD
      *REGION 18 4 5 *IDIR
**C WARNING: UNTRANSLATED ARGUMENTS FOR THIS KEYWORD
      *REGION 12 5 5 *IDIR
**C WARNING: UNTRANSLATED ARGUMENTS FOR THIS KEYWORD
      *REGION 13 5 5 *IDIR
**C WARNING: UNTRANSLATED ARGUMENTS FOR THIS KEYWORD
      *REGION 11 6 5 *JDIR
**C WARNING: UNTRANSLATED ARGUMENTS FOR THIS KEYWORD
      *REGION 10 7 5 *IDIR
**C WARNING: UNTRANSLATED ARGUMENTS FOR THIS KEYWORD
      *REGION 9 8 5 *IDIR
**C WARNING: UNTRANSLATED ARGUMENTS FOR THIS KEYWORD
      *REGION 8 9 5 *IDIR
**C WARNING: UNTRANSLATED ARGUMENTS FOR THIS KEYWORD
      *REGION 7 10 5 *IDIR
**C WARNING: UNTRANSLATED ARGUMENTS FOR THIS KEYWORD
      *REGION 6 11 5 *IDIR
**C WARNING: UNTRANSLATED ARGUMENTS FOR THIS KEYWORD
      *REGION 6 12 5 *IDIR
**C WARNING: UNTRANSLATED ARGUMENTS FOR THIS KEYWORD
      *REGION 5 13 5 *IDIR
**C WARNING: UNTRANSLATED ARGUMENTS FOR THIS KEYWORD
      *REGION 5 14 5 *IDIR
**C WARNING: UNTRANSLATED ARGUMENTS FOR THIS KEYWORD
      *REGION 4 15 5 *IDIR
**C WARNING: UNTRANSLATED ARGUMENTS FOR THIS KEYWORD
      *REGION 4 16 5 *IDIR
**C WARNING: UNTRANSLATED ARGUMENTS FOR THIS KEYWORD
      *REGION 3 17 5 *IDIR
**C WARNING: UNTRANSLATED ARGUMENTS FOR THIS KEYWORD
      *REGION 3 18 5 *IDIR
**C WARNING: UNTRANSLATED ARGUMENTS FOR THIS KEYWORD
      *REGION 3 19 5 *IDIR
**C WARNING: UNTRANSLATED ARGUMENTS FOR THIS KEYWORD
      *REGION 3 20 5 *IDIR
**C WARNING: UNTRANSLATED ARGUMENTS FOR THIS KEYWORD
      *REGION 3 21 5 *IDIR
**C WARNING: UNTRANSLATED ARGUMENTS FOR THIS KEYWORD
      *REGION 3 22 5 *IDIR
**C WARNING: UNTRANSLATED ARGUMENTS FOR THIS KEYWORD
      *REGION 3 23 5 *IDIR
**C WARNING: UNTRANSLATED ARGUMENTS FOR THIS KEYWORD
      *REGION 3 24 5 *IDIR
**C WARNING: UNTRANSLATED ARGUMENTS FOR THIS KEYWORD
      *REGION 3 25 5 *IDIR
**C WARNING: UNTRANSLATED ARGUMENTS FOR THIS KEYWORD
      *REGION 4 26 5 *IDIR
**C WARNING: UNTRANSLATED ARGUMENTS FOR THIS KEYWORD
```

```
      *REGION 5 26 5 *JDIR
**C WARNING: UNTRANSLATED ARGUMENTS FOR THIS KEYWORD
      *REGION 6 27 5 *IDIR
**C WARNING: UNTRANSLATED ARGUMENTS FOR THIS KEYWORD
      *REGION 7 27 5 *JDIR
**C WARNING: UNTRANSLATED ARGUMENTS FOR THIS KEYWORD
      *REGION 8 27 5 *JDIR
**C WARNING: UNTRANSLATED ARGUMENTS FOR THIS KEYWORD
      *REGION 9 27 5 *JDIR
**C WARNING: UNTRANSLATED ARGUMENTS FOR THIS KEYWORD
      *REGION 10 27 5 *JDIR
**C WARNING: UNTRANSLATED ARGUMENTS FOR THIS KEYWORD
      *REGION 11 27 5 *JDIR
**C WARNING: UNTRANSLATED ARGUMENTS FOR THIS KEYWORD
      *REGION 12 27 5 *IDIR
**C WARNING: UNTRANSLATED ARGUMENTS FOR THIS KEYWORD
      *REGION 14 4 4 *IDIR
**C WARNING: UNTRANSLATED ARGUMENTS FOR THIS KEYWORD
      *REGION 15 4 4 *JDIR
**C WARNING: UNTRANSLATED ARGUMENTS FOR THIS KEYWORD
      *REGION 16 4 4 *JDIR
**C WARNING: UNTRANSLATED ARGUMENTS FOR THIS KEYWORD
      *REGION 17 4 4 *JDIR
**C WARNING: UNTRANSLATED ARGUMENTS FOR THIS KEYWORD
      *REGION 18 4 4 *IDIR
**C WARNING: UNTRANSLATED ARGUMENTS FOR THIS KEYWORD
      *REGION 12 5 4 *IDIR
**C WARNING: UNTRANSLATED ARGUMENTS FOR THIS KEYWORD
      *REGION 13 5 4 *IDIR
**C WARNING: UNTRANSLATED ARGUMENTS FOR THIS KEYWORD
      *REGION 11 6 4 *JDIR
**C WARNING: UNTRANSLATED ARGUMENTS FOR THIS KEYWORD
      *REGION 10 7 4 *IDIR
**C WARNING: UNTRANSLATED ARGUMENTS FOR THIS KEYWORD
      *REGION 9 8 4 *IDIR
**C WARNING: UNTRANSLATED ARGUMENTS FOR THIS KEYWORD
      *REGION 8 9 4 *IDIR
**C WARNING: UNTRANSLATED ARGUMENTS FOR THIS KEYWORD
      *REGION 7 10 4 *IDIR
**C WARNING: UNTRANSLATED ARGUMENTS FOR THIS KEYWORD
      *REGION 6 11 4 *IDIR
**C WARNING: UNTRANSLATED ARGUMENTS FOR THIS KEYWORD
      *REGION 6 12 4 *IDIR
**C WARNING: UNTRANSLATED ARGUMENTS FOR THIS KEYWORD
      *REGION 5 13 4 *IDIR
**C WARNING: UNTRANSLATED ARGUMENTS FOR THIS KEYWORD
      *REGION 5 14 4 *IDIR
**C WARNING: UNTRANSLATED ARGUMENTS FOR THIS KEYWORD
      *REGION 4 15 4 *IDIR
**C WARNING: UNTRANSLATED ARGUMENTS FOR THIS KEYWORD
      *REGION 4 16 4 *IDIR
**C WARNING: UNTRANSLATED ARGUMENTS FOR THIS KEYWORD
      *REGION 3 17 4 *IDIR
**C WARNING: UNTRANSLATED ARGUMENTS FOR THIS KEYWORD
      *REGION 3 18 4 *IDIR
**C WARNING: UNTRANSLATED ARGUMENTS FOR THIS KEYWORD
      *REGION 3 19 4 *IDIR
**C WARNING: UNTRANSLATED ARGUMENTS FOR THIS KEYWORD
      *REGION 3 20 4 *IDIR
**C WARNING: UNTRANSLATED ARGUMENTS FOR THIS KEYWORD
      *REGION 3 21 4 *IDIR
**C WARNING: UNTRANSLATED ARGUMENTS FOR THIS KEYWORD
      *REGION 3 22 4 *IDIR
**C WARNING: UNTRANSLATED ARGUMENTS FOR THIS KEYWORD
      *REGION 3 23 4 *IDIR
**C WARNING: UNTRANSLATED ARGUMENTS FOR THIS KEYWORD
```

```
      *REGION 3 24 4 *IDIR
**C WARNING: UNTRANSLATED ARGUMENTS FOR THIS KEYWORD
      *REGION 3 25 4 *IDIR
**C WARNING: UNTRANSLATED ARGUMENTS FOR THIS KEYWORD
      *REGION 4 26 4 *IDIR
**C WARNING: UNTRANSLATED ARGUMENTS FOR THIS KEYWORD
      *REGION 5 26 4 *JDIR
**C WARNING: UNTRANSLATED ARGUMENTS FOR THIS KEYWORD
      *REGION 6 27 4 *IDIR
**C WARNING: UNTRANSLATED ARGUMENTS FOR THIS KEYWORD
      *REGION 7 27 4 *JDIR
**C WARNING: UNTRANSLATED ARGUMENTS FOR THIS KEYWORD
      *REGION 8 27 4 *JDIR
**C WARNING: UNTRANSLATED ARGUMENTS FOR THIS KEYWORD
      *REGION 9 27 4 *JDIR
**C WARNING: UNTRANSLATED ARGUMENTS FOR THIS KEYWORD
      *REGION 10 27 4 *JDIR
**C WARNING: UNTRANSLATED ARGUMENTS FOR THIS KEYWORD
      *REGION 11 27 4 *JDIR
**C WARNING: UNTRANSLATED ARGUMENTS FOR THIS KEYWORD
      *REGION 12 27 4 *IDIR
**C WARNING: UNTRANSLATED ARGUMENTS FOR THIS KEYWORD
      *REGION 14 4 3 *IDIR
**C WARNING: UNTRANSLATED ARGUMENTS FOR THIS KEYWORD
      *REGION 15 4 3 *JDIR
**C WARNING: UNTRANSLATED ARGUMENTS FOR THIS KEYWORD
      *REGION 16 4 3 *JDIR
**C WARNING: UNTRANSLATED ARGUMENTS FOR THIS KEYWORD
      *REGION 17 4 3 *JDIR
**C WARNING: UNTRANSLATED ARGUMENTS FOR THIS KEYWORD
      *REGION 18 4 3 *IDIR
**C WARNING: UNTRANSLATED ARGUMENTS FOR THIS KEYWORD
      *REGION 12 5 3 *IDIR
**C WARNING: UNTRANSLATED ARGUMENTS FOR THIS KEYWORD
      *REGION 13 5 3 *IDIR
**C WARNING: UNTRANSLATED ARGUMENTS FOR THIS KEYWORD
      *REGION 11 6 3 *JDIR
**C WARNING: UNTRANSLATED ARGUMENTS FOR THIS KEYWORD
      *REGION 10 7 3 *IDIR
**C WARNING: UNTRANSLATED ARGUMENTS FOR THIS KEYWORD
      *REGION 9 8 3 *IDIR
**C WARNING: UNTRANSLATED ARGUMENTS FOR THIS KEYWORD
      *REGION 8 9 3 *IDIR
**C WARNING: UNTRANSLATED ARGUMENTS FOR THIS KEYWORD
      *REGION 7 10 3 *IDIR
**C WARNING: UNTRANSLATED ARGUMENTS FOR THIS KEYWORD
      *REGION 6 11 3 *IDIR
**C WARNING: UNTRANSLATED ARGUMENTS FOR THIS KEYWORD
      *REGION 6 12 3 *IDIR
**C WARNING: UNTRANSLATED ARGUMENTS FOR THIS KEYWORD
      *REGION 5 13 3 *IDIR
**C WARNING: UNTRANSLATED ARGUMENTS FOR THIS KEYWORD
      *REGION 5 14 3 *IDIR
**C WARNING: UNTRANSLATED ARGUMENTS FOR THIS KEYWORD
      *REGION 4 15 3 *IDIR
**C WARNING: UNTRANSLATED ARGUMENTS FOR THIS KEYWORD
      *REGION 4 16 3 *IDIR
**C WARNING: UNTRANSLATED ARGUMENTS FOR THIS KEYWORD
      *REGION 3 17 3 *IDIR
**C WARNING: UNTRANSLATED ARGUMENTS FOR THIS KEYWORD
      *REGION 3 18 3 *IDIR
**C WARNING: UNTRANSLATED ARGUMENTS FOR THIS KEYWORD
      *REGION 3 19 3 *IDIR
**C WARNING: UNTRANSLATED ARGUMENTS FOR THIS KEYWORD
      *REGION 3 20 3 *IDIR
**C WARNING: UNTRANSLATED ARGUMENTS FOR THIS KEYWORD
```

```
      *REGION 3 21 3 *IDIR
**C WARNING: UNTRANSLATED ARGUMENTS FOR THIS KEYWORD
      *REGION 3 22 3 *IDIR
**C WARNING: UNTRANSLATED ARGUMENTS FOR THIS KEYWORD
      *REGION 3 23 3 *IDIR
**C WARNING: UNTRANSLATED ARGUMENTS FOR THIS KEYWORD
      *REGION 3 24 3 *IDIR
**C WARNING: UNTRANSLATED ARGUMENTS FOR THIS KEYWORD
      *REGION 3 25 3 *IDIR
**C WARNING: UNTRANSLATED ARGUMENTS FOR THIS KEYWORD
      *REGION 4 26 3 *IDIR
**C WARNING: UNTRANSLATED ARGUMENTS FOR THIS KEYWORD
      *REGION 5 26 3 *JDIR
**C WARNING: UNTRANSLATED ARGUMENTS FOR THIS KEYWORD
      *REGION 6 27 3 *IDIR
**C WARNING: UNTRANSLATED ARGUMENTS FOR THIS KEYWORD
      *REGION 7 27 3 *JDIR
**C WARNING: UNTRANSLATED ARGUMENTS FOR THIS KEYWORD
      *REGION 8 27 3 *JDIR
**C WARNING: UNTRANSLATED ARGUMENTS FOR THIS KEYWORD
      *REGION 9 27 3 *JDIR
**C WARNING: UNTRANSLATED ARGUMENTS FOR THIS KEYWORD
      *REGION 10 27 3 *JDIR
**C WARNING: UNTRANSLATED ARGUMENTS FOR THIS KEYWORD
      *REGION 11 27 3 *JDIR
**C WARNING: UNTRANSLATED ARGUMENTS FOR THIS KEYWORD
      *REGION 12 27 3 *IDIR
**C WARNING: UNTRANSLATED ARGUMENTS FOR THIS KEYWORD
*AQPROP
19.6 0.2125 137.5 3000 0.2638889
**C WARNING: UNTRANSLATED ARGUMENTS FOR THIS KEYWORD
*AQUIFER *REGION 15 1 2 *IDIR
**C WARNING: UNTRANSLATED ARGUMENTS FOR THIS KEYWORD
      *REGION 16 1 2 *JDIR
**C WARNING: UNTRANSLATED ARGUMENTS FOR THIS KEYWORD
      *REGION 17 1 2 *JDIR
**C WARNING: UNTRANSLATED ARGUMENTS FOR THIS KEYWORD
      *REGION 18 1 2 *IDIR
**C WARNING: UNTRANSLATED ARGUMENTS FOR THIS KEYWORD
      *REGION 14 2 2 *IDIR
**C WARNING: UNTRANSLATED ARGUMENTS FOR THIS KEYWORD
      *REGION 11 3 2 *IDIR
**C WARNING: UNTRANSLATED ARGUMENTS FOR THIS KEYWORD
      *REGION 12 3 2 *JDIR
**C WARNING: UNTRANSLATED ARGUMENTS FOR THIS KEYWORD
      *REGION 13 3 2 *JDIR
**C WARNING: UNTRANSLATED ARGUMENTS FOR THIS KEYWORD
      *REGION 10 4 2 *IDIR
**C WARNING: UNTRANSLATED ARGUMENTS FOR THIS KEYWORD
      *REGION 9 5 2 *IDIR
**C WARNING: UNTRANSLATED ARGUMENTS FOR THIS KEYWORD
      *REGION 8 6 2 *IDIR
**C WARNING: UNTRANSLATED ARGUMENTS FOR THIS KEYWORD
      *REGION 7 7 2 *IDIR
**C WARNING: UNTRANSLATED ARGUMENTS FOR THIS KEYWORD
      *REGION 6 8 2 *IDIR
**C WARNING: UNTRANSLATED ARGUMENTS FOR THIS KEYWORD
      *REGION 6 9 2 *IDIR
**C WARNING: UNTRANSLATED ARGUMENTS FOR THIS KEYWORD
      *REGION 5 10 2 *IDIR
**C WARNING: UNTRANSLATED ARGUMENTS FOR THIS KEYWORD
      *REGION 5 11 2 *IDIR
**C WARNING: UNTRANSLATED ARGUMENTS FOR THIS KEYWORD
      *REGION 5 12 2 *IDIR
**C WARNING: UNTRANSLATED ARGUMENTS FOR THIS KEYWORD
      *REGION 4 13 2 *IDIR
```

```
**C WARNING: UNTRANSLATED ARGUMENTS FOR THIS KEYWORD
      *REGION 4 14 2 *IDIR
**C WARNING: UNTRANSLATED ARGUMENTS FOR THIS KEYWORD
      *REGION 3 15 2 *IDIR
**C WARNING: UNTRANSLATED ARGUMENTS FOR THIS KEYWORD
      *REGION 2 16 2 *IDIR
**C WARNING: UNTRANSLATED ARGUMENTS FOR THIS KEYWORD
      *REGION 2 17 2 *IDIR
**C WARNING: UNTRANSLATED ARGUMENTS FOR THIS KEYWORD
      *REGION 2 18 2 *IDIR
**C WARNING: UNTRANSLATED ARGUMENTS FOR THIS KEYWORD
      *REGION 1 23 2 *IDIR
**C WARNING: UNTRANSLATED ARGUMENTS FOR THIS KEYWORD
      *REGION 1 24 2 *IDIR
**C WARNING: UNTRANSLATED ARGUMENTS FOR THIS KEYWORD
      *REGION 1 25 2 *IDIR
**C WARNING: UNTRANSLATED ARGUMENTS FOR THIS KEYWORD
      *REGION 2 26 2 *IDIR
**C WARNING: UNTRANSLATED ARGUMENTS FOR THIS KEYWORD
      *REGION 3 27 2 *IDIR
**C WARNING: UNTRANSLATED ARGUMENTS FOR THIS KEYWORD
      *REGION 4 28 2 *IDIR
**C WARNING: UNTRANSLATED ARGUMENTS FOR THIS KEYWORD
      *REGION 5 28 2 *JDIR
**C WARNING: UNTRANSLATED ARGUMENTS FOR THIS KEYWORD
      *REGION 15 1 1 *IDIR
**C WARNING: UNTRANSLATED ARGUMENTS FOR THIS KEYWORD
      *REGION 16 1 1 *JDIR
**C WARNING: UNTRANSLATED ARGUMENTS FOR THIS KEYWORD
      *REGION 17 1 1 *JDIR
**C WARNING: UNTRANSLATED ARGUMENTS FOR THIS KEYWORD
      *REGION 18 1 1 *IDIR
**C WARNING: UNTRANSLATED ARGUMENTS FOR THIS KEYWORD
      *REGION 14 2 1 *IDIR
**C WARNING: UNTRANSLATED ARGUMENTS FOR THIS KEYWORD
      *REGION 11 3 1 *IDIR
**C WARNING: UNTRANSLATED ARGUMENTS FOR THIS KEYWORD
      *REGION 12 3 1 *JDIR
**C WARNING: UNTRANSLATED ARGUMENTS FOR THIS KEYWORD
      *REGION 13 3 1 *JDIR
**C WARNING: UNTRANSLATED ARGUMENTS FOR THIS KEYWORD
      *REGION 10 4 1 *IDIR
**C WARNING: UNTRANSLATED ARGUMENTS FOR THIS KEYWORD
      *REGION 9 5 1 *IDIR
**C WARNING: UNTRANSLATED ARGUMENTS FOR THIS KEYWORD
      *REGION 8 6 1 *IDIR
**C WARNING: UNTRANSLATED ARGUMENTS FOR THIS KEYWORD
      *REGION 7 7 1 *IDIR
**C WARNING: UNTRANSLATED ARGUMENTS FOR THIS KEYWORD
      *REGION 6 8 1 *IDIR
**C WARNING: UNTRANSLATED ARGUMENTS FOR THIS KEYWORD
      *REGION 6 9 1 *IDIR
**C WARNING: UNTRANSLATED ARGUMENTS FOR THIS KEYWORD
      *REGION 5 10 1 *IDIR
**C WARNING: UNTRANSLATED ARGUMENTS FOR THIS KEYWORD
      *REGION 5 11 1 *IDIR
**C WARNING: UNTRANSLATED ARGUMENTS FOR THIS KEYWORD
      *REGION 5 12 1 *IDIR
**C WARNING: UNTRANSLATED ARGUMENTS FOR THIS KEYWORD
      *REGION 4 13 1 *IDIR
**C WARNING: UNTRANSLATED ARGUMENTS FOR THIS KEYWORD
      *REGION 4 14 1 *IDIR
**C WARNING: UNTRANSLATED ARGUMENTS FOR THIS KEYWORD
      *REGION 3 15 1 *IDIR
**C WARNING: UNTRANSLATED ARGUMENTS FOR THIS KEYWORD
      *REGION 2 16 1 *IDIR
```

```
**C WARNING: UNTRANSLATED ARGUMENTS FOR THIS KEYWORD
        *REGION 2 17 1 *IDIR
**C WARNING: UNTRANSLATED ARGUMENTS FOR THIS KEYWORD
        *REGION 2 18 1 *IDIR
**C WARNING: UNTRANSLATED ARGUMENTS FOR THIS KEYWORD
        *REGION 1 23 1 *IDIR
**C WARNING: UNTRANSLATED ARGUMENTS FOR THIS KEYWORD
        *REGION 1 24 1 *IDIR
**C WARNING: UNTRANSLATED ARGUMENTS FOR THIS KEYWORD
        *REGION 1 25 1 *IDIR
**C WARNING: UNTRANSLATED ARGUMENTS FOR THIS KEYWORD
        *REGION 2 26 1 *IDIR
**C WARNING: UNTRANSLATED ARGUMENTS FOR THIS KEYWORD
        *REGION 3 27 1 *IDIR
**C WARNING: UNTRANSLATED ARGUMENTS FOR THIS KEYWORD
        *REGION 4 28 1 *IDIR
**C WARNING: UNTRANSLATED ARGUMENTS FOR THIS KEYWORD
        *REGION 5 28 1 *JDIR
**C WARNING: UNTRANSLATED ARGUMENTS FOR THIS KEYWORD
*AQPROP
6.0 0.2125 137.5 3200 0.2638889


** ---------- Fluid Model ----------
**$ Model and number of components
MODEL SRK
NC 24 24
***H2O_INCLUDED
COMPNAME 'N2' 'CO2' 'H2S' 'C1' 'C2' 'C3' 'iC4' 'nC4' 'iC5' 'nC5' 'C6' 'C7' 'C8' 'C9' 'C10' 'C11' 'C12' 'C13' 'C14' 'C15' 'C16' 'C17-19'
'C20-29' 'C30+'
HCFLAG
0 0 0 0 0 0 0 0 0 0 0 0 0 0 0 0 0 0 0 0 0 0 0 0
MW
28.01 44.01 34.08 16.04 30.07 44.1 58.12 58.12 72.15 72.15 82.32 95.36 108.77 121.9 134.78 147.59 160.3 172.91 185.42 197.82
210.11 233.39 299.51 477.34
AC
0.037 0.225 0.09 0.011 0.099 0.152 0.186 0.2 0.229 0.252 0.2373 0.2714 0.3094 0.35 0.39 0.4295 0.4684 0.5067 0.5444 0.5814
0.6178 0.6857 0.8712 1.0411
PCRIT
33.5330688 72.775197 88.4598 45.386682 48.0813036 41.9231406 35.9214834 37.4661276 33.3697584 33.2608848 33.4309998
31.1106312 28.7698488 26.53794 24.6122382 22.931502 21.4549038 20.1620298 19.0120524 17.998167 17.0863506 15.6029478
12.5612916 11.4045096

***VCRIT
TCRIT
125.8888889 303.7777778 373.0555556 190.2222222 305 369.5 407.5 424.7777778 460.0555556 469.3888889 513.1111111
548.7222222 579.6111111 607.5 632.2222222 654.6111111 675 693.7777778 711.1111111 727.1666667 742.0555556 768.0555556
829.5 897.9444444
BIN
0
0.12 0.12
0.02 0.12 0.07
0.06 0.15 0.06 0.06887
0.08 0.15 0.06 0.06887 0.06887
0.08 0.15 0.06 0.06887 0.06887 0.06887
0.08 0.15 0.06 0.06887 0.06887 0.06887
0.08 0.15 0.06 0.06887 0.06887 0.06887 0.06887 0.06887
0.08 0.15 0.06 0.06887 0.06887 0.06887 0.06887 0.06887 0.06887
0.08 0.15 0.05 0.06887 0.06887 0.06887 0.06887 0.06887 0.06887 0.06887
0.08 0.15 0.03 0.06887 0.06887 0.06887 0.06887 0.06887 0.06887 0.06887 0.06887
0.08 0.15 0.03 0.06887 0.06887 0.06887 0.06887 0.06887 0.06887 0.06887 0.06887 0.06887
0.08 0.15 0.03 0.06887 0.06887 0.06887 0.06887 0.06887 0.06887 0.06887 0.06887 0.06887 0.06887
0.08 0.15 0.03 0.06887 0.06887 0.06887 0.06887 0.06887 0.06887 0.06887 0.06887 0.06887 0.06887 0.06887
0.08 0.15 0.03 0.06887 0.06887 0.06887 0.06887 0.06887 0.06887 0.06887 0.06887 0.06887 0.06887 0.06887 0.06887
0.08 0.15 0.03 0.06887 0.06887 0.06887 0.06887 0.06887 0.06887 0.06887 0.06887 0.06887 0.06887 0.06887 0.06887 0.06887
```

```
0.06887
0.08 0.15 0.03 0.06887 0.06887 0.06887 0.06887 0.06887 0.06887 0.06887 0.06887 0.06887 0.06887 0.06887 0.06887
0.06887 0.06887
0.08 0.15 0.03 0.06887 0.06887 0.06887 0.06887 0.06887 0.06887 0.06887 0.06887 0.06887 0.06887 0.06887 0.06887
0.06887 0.06887 0.06887
0.08 0.15 0.03 0.06887 0.06887 0.06887 0.06887 0.06887 0.06887 0.06887 0.06887 0.06887 0.06887 0.06887 0.06887
0.06887 0.06887 0.06887 0.06887
0.08 0.15 0.03 0.06887 0.06887 0.06887 0.06887 0.06887 0.06887 0.06887 0.06887 0.06887 0.06887 0.06887 0.06887
0.06887 0.06887 0.06887 0.06887 0.06887
0.08 0.15 0.03 0.06887 0.06887 0.06887 0.06887 0.06887 0.06887 0.06887 0.06887 0.06887 0.06887 0.06887 0.06887
0.06887 0.06887 0.06887 0.06887 0.06887 0.06887
0.08 0.15 0.03 0.06887 0.06887 0.06887 0.06887 0.06887 0.06887 0.06887 0.06887 0.06887 0.06887 0.06887 0.06887
0.06887 0.06887 0.06887 0.06887 0.06887 0.06887 0.06887

TRES 104.4444
PHASEID DEN
CW 7.25188E-07
REFPW 36645.6
SOLUBILITY HENRY
FLASH-METHOD OUTER
DERIVATIVEMETHOD NUMERALL
DIFCOR-OIL SIGMUND
DIFCOR-GAS SIGMUND
**DIFFUSION COEFFICIENT IN CM2/S
DIFFC-AQU
0 2.00E-05 0 0 0 0 0 0 0 0 0 0 0 0 0 0 0 0 0 0 0 0 0 0 0
*HENRYC
0 1.9510547E+05 0 0 0 0 0 0 0 0 0 0 0 0 0 0 0 0 0 0 0 0 0 0 0

*REFPH
0 9.4000000E+03 0 0 0 0 0 0 0 0 0 0 0 0 0 0 0 0 0 0 0 0 0 0 0

*VINFINITY
0 3.5089333E-02 0 0 0 0 0 0 0 0 0 0 0 0 0 0 0 0 0 0 0 0 0 0 0

*YAQU-RATE-CUTOFF
100     0.0001  100     100     100     100     100     100     100     100     100     100
        100     100     100     100     100     100     100     100     100     100     100
        100


*DER-CHEM-EQUIL *ANALYTICAL
*DER-REACT-RATE *ANALYTICAL

*ACTIVITY-MODEL *B-DOT
*SALINITY 0.1
*AQUEOUS-DENSITY *ROWE-CHOU
*AQUEOUS-VISCOSITY *KESTIN

*NC-AQUEOUS 5
*COMPNAME-AQUEOUS
'H+' 'Ca++' 'OH-' 'HCO3-' 'CO3--'
*MW-AQUEOUS
1.0079
40.0800
17.0073
61.0171
60.0092

*ION-SIZE-AQUEOUS
9.0 6.0 3.5 4.5 4.5
*CHARGE-AQUEOUS
1 2 -1 -1 -2

*NC-MINERAL 1
*COMPNAME-MINERAL
```

```
'CALCITE'
*MW-MINERAL
100.1

*MASSDENSITY-MINERAL
2710.00

*N-RATE-REACT 1
*N-CHEM-EQUIL 3

**REACTION NO. 1: H2O = H+ + OH-
*STOICHIOMETRY
0          0          0          0          0          0          0          0          0          0          0          0
           0          0          0          0          0          0          0          0          0          0          0
           0          -1         1          0          1          0          0          0
*LOG-CHEM-EQUIL-CONST
 -13.2631

**REACTION NO. 2: CO2 + H2O = H+ + HCO3--
*STOICHIOMETRY
0          -1         0          0          0          0          0          0          0          0          0          0
           0          0          0          0          0          0          0          0          0          0          0
           0          -1         1          0          0          1          0          0
*LOG-CHEM-EQUIL-CONST
 -6.3221

**REACTION NO. 3: CO2 + H2O = 2H+ + CO3--
*STOICHIOMETRY
0          -1         0          0          0          0          0          0          0          0          0          0
           0          0          0          0          0          0          0          0          0          0          0
           0          -1         2          0          0          0          1          0
*LOG-CHEM-EQUIL-CONST
 -16.5563

**REACTION NO. 1:  CALCITE + H+ = (Ca++) + (HCO3-)
*STOICHIOMETRY
0          0          0          0          0          0          0          0          0          0          0          0
           0          0          0          0          0          0          0          0          0          0          0
           0          0          -1         1          0          1          0          -1
*REACTIVE-SURFACE-AREA 88.0

*SPEC-REACT-SURFACE-AREA 1.0E+04
*MIN-REACT-SURFACE-AREA 1.0
*SUPER-SATURATION-INDEX 2.0

*ACTIVATION-ENERGY 41870.0
*REF-TEMP-RATE-CONST 25.0
*LOG-CHEM-EQUIL-CONST
 1.36
*LOG-TST-RATE-CONSTANT -8.8
***H2O_INCLUDED
***OGW_FLASH *ON
***SWR-H2OVAP 0
***SATWCUTOFF 0
**COMPONENT 1 IS A TRACE COMPONENT
*TRACE-COMP 1
*PERM-VS-POR 1

** ---------- Rock Fluid ----------
*ROCKFLUID
RPT 1


SWT
0.15       0                  0.9
0.2        0.000820562        0.736779008
```

```
0.25        0.004641802         0.592742192
0.3         0.012791302         0.467072318
0.35        0.026257997         0.358914003
0.4         0.045870834         0.267367796
0.45        0.072358532         0.191482562
0.5         0.106379201         0.130245358
0.55        0.148537664         0.082567501
0.6         0.199396668         0.047264395
0.65        0.259484621         0.023024344
0.7         0.329301218         0.008355244
0.8         0.5                 0
1           1                   0



SGT
0.1         0                   0.9
0.15        0.000449981         0.747791976
0.2         0.002545475         0.612174923
0.25        0.007014504         0.492497617
0.3         0.014399381         0.388081035
0.35        0.025154684         0.298214457
0.4         0.039680029         0.222150547
0.45        0.058336309         0.159099026
0.5         0.081455201         0.10821826
0.55        0.109345301         0.068603683
0.6         0.14229638          0.03927104
0.65        0.180582459         0.019130466
0.8         0.33                0
1           1                   0



** ---------- Initial ----------

*INITIAL
*VERTICAL *OFF
****REFDEPTH 2355.00
****REFPRES 23446
****DWOC 2395.0
****DGOC 2355.0
**$ Property: Pressure (kPa)   Max: 36542.2  Min: 36542.2
PRES CON 36542.2
**$ Property: Water Saturation  Max: 0.15  Min: 0.15
SW CON .15
**$ Property: Global Composition(N2)  Max: 3.349  Min: 3.349
ZGLOBALC 'N2' CON       3.349
**$ Property: Global Composition(CO2)  Max: 1.755  Min: 1.755
ZGLOBALC 'CO2' CON       1.755
**$ Property: Global Composition(H2S)  Max: 0.529  Min: 0.529
ZGLOBALC 'H2S' CON       0.529
**$ Property: Global Composition(C1)  Max: 83.265  Min: 83.265
ZGLOBALC 'C1' CON      83.265
**$ Property: Global Composition(C2)  Max: 5.158  Min: 5.158
ZGLOBALC 'C2' CON       5.158
**$ Property: Global Composition(C3)  Max: 1.907  Min: 1.907
ZGLOBALC 'C3' CON       1.907
**$ Property: Global Composition(iC4)  Max: 0.409  Min: 0.409
ZGLOBALC 'iC4' CON       0.409
**$ Property: Global Composition(nC4)  Max: 0.699  Min: 0.699
ZGLOBALC 'nC4' CON       0.699
**$ Property: Global Composition(iC5)  Max: 0.28  Min: 0.28
ZGLOBALC 'iC5' CON       0.28
**$ Property: Global Composition(nC5)  Max: 0.28  Min: 0.28
ZGLOBALC 'nC5' CON       0.28
```

```
**$ Property: Global Composition(C6)  Max: 0.39  Min: 0.39
ZGLOBALC 'C6' CON         0.39
**$ Property: Global Composition(C7)  Max: 0.486  Min: 0.486
ZGLOBALC 'C7' CON        0.486
**$ Property: Global Composition(C8)  Max: 0.361  Min: 0.361
ZGLOBALC 'C8' CON        0.361
**$ Property: Global Composition(C9)  Max: 0.266  Min: 0.266
ZGLOBALC 'C9' CON        0.266
**$ Property: Global Composition(C10)  Max: 0.201  Min: 0.201
ZGLOBALC 'C10' CON        0.201
**$ Property: Global Composition(C11)  Max: 0.153  Min: 0.153
ZGLOBALC 'C11' CON        0.153
**$ Property: Global Composition(C12)  Max: 0.116  Min: 0.116
ZGLOBALC 'C12' CON        0.116
**$ Property: Global Composition(C13)  Max: 0.089  Min: 0.089
ZGLOBALC 'C13' CON        0.089
**$ Property: Global Composition(C14)  Max: 0.068  Min: 0.068
ZGLOBALC 'C14' CON        0.068
**$ Property: Global Composition(C15)  Max: 0.052  Min: 0.052
ZGLOBALC 'C15' CON        0.052
**$ Property: Global Composition(C16)  Max: 0.04  Min: 0.04
ZGLOBALC 'C16' CON         0.04
**$ Property: Global Composition(C17-19)  Max: 0.073  Min: 0.073
ZGLOBALC 'C17-19' CON        0.073
**$ Property: Global Composition(C20-29)  Max: 0.063  Min: 0.063
ZGLOBALC 'C20-29' CON        0.063
**$ Property: Global Composition(C30+)  Max: 0.012  Min: 0.012
ZGLOBALC 'C30+' CON        0.012

*CALC-MOLALITYAQ-SECONDARY *ON

*MOLALITY-AQUEOUS
  1.0D-07  9.12D-05   5.46D-07   1.17D-05   2.49D-02

*VOLUMEFRACTION-MINERAL
0.0088
***          Pressure    Temperature
*SEPARATOR    6894.76     26.6667
           2413.17     21.1111
           101.353     15.5556
** ----------------- Numerical ----------------------

*NUMERICAL
***NORM *UNKNOWN
*NORM PRESS 10000
MAXCHANGE PRESS 1000000
MAXCHANGE SATUR 1
MAXCHANGE GMOLAR 1
*NORM SATUR 0.05
*NORM GMOLAR 0.05
AIM STAB 1
NORTH 10000
ITERMAX 200
PIVOT ON
NEWTONCYC 10000
****CONVERGE PRESS 100

** ----------------- Recurrent ----------------------
*RUN

DATE 2011 1 1
DTWELL 1e-5
DTMAX 36500
DTMIN 1e-10
GROUP 'G1' ATTACHTO 'FIELD'
*** Producers
```

```
*WELL 'PRO-1' *ATTACHTO 'G1'
*BHPDEPTH 'PRO-1' 2362.2
*XFLOW-MODEL 'PRO-1' *FULLY-MIXED
*WELL 'PRO-4' *ATTACHTO 'G1'
*BHPDEPTH 'PRO-4' 2373.0
*XFLOW-MODEL 'PRO-4' *FULLY-MIXED
*WELL 'PRO-5' *ATTACHTO 'G1'
*BHPDEPTH 'PRO-5' 2381.7
*XFLOW-MODEL 'PRO-5' *FULLY-MIXED
*WELL 'PRO-11' *ATTACHTO 'G1'
*BHPDEPTH 'PRO-11' 2386.0
*XFLOW-MODEL 'PRO-11' *FULLY-MIXED
*WELL 'PRO-12' *ATTACHTO 'G1'
*BHPDEPTH 'PRO-12' 2380.5
*XFLOW-MODEL 'PRO-12' *FULLY-MIXED
*WELL 'PRO-15' *ATTACHTO 'G1'
*BHPDEPTH 'PRO-15' 2381.0
*XFLOW-MODEL 'PRO-15' *FULLY-MIXED


*** Injectors
*WELL 'INJ-1' *ATTACHTO 'G1'
*BHPDEPTH 'INJ-1' 2362.2
*XFLOW-MODEL 'INJ-1' *FULLY-MIXED
*WELL 'INJ-4' *ATTACHTO 'G1'
*BHPDEPTH 'INJ-4' 2373.0
*XFLOW-MODEL 'INJ-4' *FULLY-MIXED
*WELL 'INJ-5' *ATTACHTO 'G1'
*BHPDEPTH 'INJ-5' 2381.7
*XFLOW-MODEL 'INJ-5' *FULLY-MIXED
*WELL 'INJ-11' *ATTACHTO 'G1'
*BHPDEPTH 'INJ-11' 2386.0
*XFLOW-MODEL 'INJ-11' *FULLY-MIXED
*WELL 'INJ-12' *ATTACHTO 'G1'
*BHPDEPTH 'INJ-12' 2380.5
*XFLOW-MODEL 'INJ-12' *FULLY-MIXED
*WELL 'INJ-15' *ATTACHTO 'G1'
*BHPDEPTH 'INJ-15' 2381.0
*XFLOW-MODEL 'INJ-15' *FULLY-MIXED


*** Producers
*PRODUCER 'PRO-1'
*OPERATE *MIN *BHP 12000
*SHUTIN 'PRO-1'

*PRODUCER 'PRO-4'
*OPERATE *MIN *BHP 12000
*SHUTIN 'PRO-4'

*PRODUCER 'PRO-5'
*OPERATE *MIN *BHP 12000
*SHUTIN 'PRO-5'

*PRODUCER 'PRO-11'
*OPERATE *MIN *BHP 12000
*SHUTIN 'PRO-11'

*PRODUCER 'PRO-12'
*OPERATE *MIN *BHP 12000
*SHUTIN 'PRO-12'

*PRODUCER 'PRO-15'
*OPERATE *MIN *BHP 12000
*SHUTIN 'PRO-15'
```

```
*** Injectors CO2 max pressure is .7 psi/ft or 15.8344 kPa/m
*INJECTOR 'INJ-1'
*INCOMP  SOLVENT  0. 1. 0. 0. 0. 0. 0. 0. 0. 0. 0. 0. 0. 0. 0. 0. 0. 0. 0. 0. 0. 0. 0. 0.
*OPERATE *MAX *BHP 37404.1
*SHUTIN 'INJ-1'

*INJECTOR 'INJ-4'
****       wdepth    wlength  rel_rough whtemp bhtemp    wradius
****IWELLBORE 2373.0  2373.0 0.00015     83   104.4444 .060325
*INCOMP  SOLVENT  0. 1. 0. 0. 0. 0. 0. 0. 0. 0. 0. 0. 0. 0. 0. 0. 0. 0. 0. 0. 0. 0. 0. 0.
*OPERATE *MAX *BHP 37575.1
****OPERATE *WHP *INITIALIZE 10300
*SHUTIN 'INJ-4'

*INJECTOR 'INJ-5'
*INCOMP  SOLVENT  0. 1. 0. 0. 0. 0. 0. 0. 0. 0. 0. 0. 0. 0. 0. 0. 0. 0. 0. 0. 0. 0. 0. 0.
*OPERATE *MAX *BHP 37712.8
*SHUTIN 'INJ-5'

*INJECTOR 'INJ-11'
*INCOMP  SOLVENT  0. 1. 0. 0. 0. 0. 0. 0. 0. 0. 0. 0. 0. 0. 0. 0. 0. 0. 0. 0. 0. 0. 0. 0.
*OPERATE *MAX *BHP 37780.9
*SHUTIN 'INJ-11'

*INJECTOR 'INJ-12'
*INCOMP  SOLVENT  0. 1. 0. 0. 0. 0. 0. 0. 0. 0. 0. 0. 0. 0. 0. 0. 0. 0. 0. 0. 0. 0. 0. 0.
*OPERATE *MAX *BHP 37693.8
*SHUTIN 'INJ-12'

*INJECTOR 'INJ-15'
*INCOMP  SOLVENT  0. 1. 0. 0. 0. 0. 0. 0. 0. 0. 0. 0. 0. 0. 0. 0. 0. 0. 0. 0. 0. 0. 0. 0.
*OPERATE *MAX *BHP 37701.8
*SHUTIN 'INJ-15'

**$         rad  geofac  wfrac  skin
***Producers
GEOMETRY  K  0.075  0.37  1.  5.
PERF  GEOA  'PRO-1'
**$ UBA     ff  Status  Connection
   10 22 5  1.  OPEN    FLOW-TO  'SURFACE'  REFLAYER
   10 22 4  1.  OPEN    FLOW-TO  1
**$         rad  geofac  wfrac  skin
GEOMETRY  K  0.075  0.37  1.  5.
PERF  GEOA  'PRO-4'
**$ UBA     ff  Status  Connection
   9 17 5  1.  OPEN    FLOW-TO  'SURFACE'  REFLAYER
   9 17 4  1.  OPEN    FLOW-TO  1
**$         rad  geofac  wfrac  skin
GEOMETRY  K  0.075  0.37  1.  5.
PERF  GEOA  'PRO-5'
**$ UBA     ff  Status  Connection
   17 11 4  1.  OPEN    FLOW-TO  'SURFACE'  REFLAYER
   17 11 3  1.  OPEN    FLOW-TO  1
**$         rad  geofac  wfrac  skin
GEOMETRY  K  0.075  0.37  1.  5.
PERF  GEOA  'PRO-11'
**$ UBA     ff  Status  Connection
   11 24 4  1.  OPEN    FLOW-TO  'SURFACE'  REFLAYER
   11 24 3  1.  OPEN    FLOW-TO  1
**$         rad  geofac  wfrac  skin
GEOMETRY  K  0.075  0.37  1.  5.
PERF  GEOA  'PRO-12'
**$ UBA     ff  Status  Connection
   15 12 5  1.  OPEN    FLOW-TO  'SURFACE'  REFLAYER
   15 12 4  1.  OPEN    FLOW-TO  1
```

```
**$         rad  geofac  wfrac  skin
GEOMETRY  K  0.075  0.37  1.  5.
PERF  GEOA  'PRO-15'
**$ UBA      ff  Status  Connection
   17 22 4  1.  OPEN    FLOW-TO  'SURFACE'

***Injectors
GEOMETRY  K  0.075  0.37  1.  5.
PERF  GEOA  'INJ-1'
**$ UBA      ff  Status  Connection
   10 22 5  1.  OPEN    FLOW-TO  'SURFACE'  REFLAYER
   10 22 4  1.  OPEN    FLOW-TO  1
**$         rad  geofac  wfrac  skin
GEOMETRY  K  0.075  0.37  1.  5.
PERF  GEOA  'INJ-4'
**$ UBA      ff  Status  Connection
   9 17 5  1.  OPEN    FLOW-TO  'SURFACE'  REFLAYER
   9 17 4  1.  OPEN    FLOW-TO  1
**$         rad  geofac  wfrac  skin
GEOMETRY  K  0.075  0.37  1.  5.
PERF  GEOA  'INJ-5'
**$ UBA      ff  Status  Connection
   17 11 4  1.  OPEN    FLOW-TO  'SURFACE'  REFLAYER
   17 11 3  1.  OPEN    FLOW-TO  1
**$         rad  geofac  wfrac  skin
GEOMETRY  K  0.075  0.37  1.  5.
PERF  GEOA  'INJ-11'
**$ UBA      ff  Status  Connection
   11 24 4  1.  OPEN    FLOW-TO  'SURFACE'  REFLAYER
   11 24 3  1.  OPEN    FLOW-TO  1
**$         rad  geofac  wfrac  skin
GEOMETRY  K  0.075  0.37  1.  5.
PERF  GEOA  'INJ-12'
**$ UBA      ff  Status  Connection
   15 12 5  1.  OPEN    FLOW-TO  'SURFACE'  REFLAYER
   15 12 4  1.  OPEN    FLOW-TO  1
**$         rad  geofac  wfrac  skin
GEOMETRY  K  0.075  0.37  1.  5.
PERF  GEOA  'INJ-15'
**$ UBA      ff  Status  Connection
   17 22 4  1.  OPEN    FLOW-TO  'SURFACE'

****AIMWELL WELLN

***INCLUDE FILE FOR PRODUCTION/INJECTION and STORAGE

OPEN 'PRO-1'
OPEN 'PRO-4'
OPEN 'PRO-5'
OPEN 'PRO-11'
OPEN 'PRO-12'
OPEN 'PRO-15'

TARGET STG
'PRO-1'
283168
TARGET STG
'PRO-4'
283168
TARGET STG
'PRO-5'
283168
TARGET STG
'PRO-11'
283168
TARGET STG
```

```
'PRO-12'
283168
TARGET STG
'PRO-15'
283168

*DATE 2012 1 1
*DATE 2013 1 1
*DATE 2014 1 1
*DATE 2015 1 1

SHUTIN 'PRO-4'
OPEN 'INJ-4'

TARGET STG
'PRO-1'
339802
TARGET STG
'INJ-4'
1.69901E6
TARGET STG
'PRO-5'
339802
TARGET STG
'PRO-11'
339802
TARGET STG
'PRO-12'
339802
TARGET STG
'PRO-15'
339802

*DATE 2016 1 1
*DATE 2017 1 1
*DATE 2018 1 1
*DATE 2019 1 1
*DATE 2020 1 1



*DATE 2021 1 1
*DATE 2022 1 1
*DATE 2023 1 1
*DATE 2024 1 1
*DATE 2025 1 1



*DATE 2026 1 1
*DATE 2027 1 1
*DATE 2028 1 1
*DATE 2029 1 1
*DATE 2030 1 1
*DATE 2031 1 1



*STOP
```